New Variety of Pyridine and Pyrazine-Based Arginine Mimics : Synthesis, Structural Study and Preliminary Biological Evaluation

Olga Ovdiichuk

Doctoral School RP2E
Science and Engineering, Resources, Processes, Products and Environment

New Variety of Pyridine and Pyrazine-Based Arginine Mimics: Synthesis, Structural Study and Preliminary Biological Evaluation

A dissertation presented to

the Université de Lorraine

and the Taras Shevchenko National University of Kyiv

To obtain the degree

Doctor of Philosophy

Olga OVDIICHUK

Jury members

Florine CAVELIER *DR, IBMM, Université de Montpellier, Reviewer*
Claude TAILLEFUMIER *Prof., Université Clermont-Ferrand, Reviewer*
Marc LE BORGNE *Prof., Université Claude Bernard Lyon 1, Examinator*
Zoia VOITENKO *Prof., Taras Shevchenko National University of Kyiv, Examinator*
Alain DURAND, *Prof., Université de Lorraine, Examinator*
Marie-Christine AVERLANT-PETIT *CR, LCPM, Université de Lorraine, Director*
Olga HORDIYENKO *Dr., Taras Shevchenko National University of Kyiv, Co-director*
Axelle ARRAULT, *MCF, Université de Lorraine, guest member, Co-director*

November 28, 2016

ABSTRACT

Heterocycle-containing amino acids have become important precursors in the design of peptidomimetics. The pyridine and pyrazine rings can improve the binding affinity and bioavailability of potential drugs. Moreover, an enzymatic degradation resistance is known to be more pronounced in peptidomimetics with heterocyclic cores as non-peptidic fragments. In addition, an amidoxime group introduced into the structure represents potent pharmacophore due to the ability for its *in vivo* oxidation to amide with a subsequent release of NO (antiaggregatory activity) or their reduction to amidine, an excellent mimic of the arginine side chain. The use of amidoximes as amidine prodrugs allows to overcome unfavorable physicochemical and pharmacokinetic properties.

This work hence describes the synthesis, structural study and preliminary biologycal evaluation of new variety of pyridine and pyrazine-based peptidomimetics. The first part of the thesis is devoted to the design and convenient synthesis of novel peptidomimetics bearing amidoxime function. Moreover, the introduction of an additional amino acid through different linkage like hydrazide, ester or heterocyclic unit (1,2,4-oxadiazole, 1,2,4-triazole) was of our great interest. 1,2,4-oxadiazole and 1,2,4-triazole rings are known as isosteric replacement of the amide and/or ester group due to its high resistance to metabolic degradation that has been widely used in peptide mimicry. Thus, several chemical functionalization of new scaffolds were studied. We have developed the acylation of amidoximes with further microwave-assisted condensation into amino acid derived 1,2,4-oxadiazoles. The synthesis of 1,2,4-triazoles was performed *via N*-acylamidrazones. The latter were synthesized in mild conditions using a new approach from the pyrrolopyridines(pyrazines) precursors in good to excellent yields. On further developing constrained peptidomimetics, we also synthesized hydrazide modified turn mimics derived from amidoximes.

The second section describes structural analysis of the prepared compounds by NMR, IR spectroscopic studies and molecular modelling. Crystal structures of some compounds were analyzed by X-Ray diffraction study. Conformational preferences and thermodynamic studies of proline-containing peptidomimetics were investigated and both series – pyridine and pyrazine ones were compared. Examination of a new ProPhe pyrazine-based pseudotripeptide revealed the hydrogen bond formation between the proton of the OH and the carbonyl oxygen of the *C*-terminal phenylalanine and the hydrogen bond that adopts a seven-membered γ-turn conformation. Therefore, a dramatic increase of the *trans* rotamer up to 98%

was observed in weakly polar solvent, which is $CHCl_3$. Hydrazide modified peptidomimetics adopt a turn structure in solution also stabilized by the hydrogen bond forming C_{10}-pseudocycle. Conformational studies confirmed that these heterocyclic moieties can be used to increase rigidity and the pyrazine core could stronger effect on conformation stabilization.

The third part of the thesis is dedicated to the preliminary results of the NO release assay on amidoximes. All compounds revealed release NO in concentration sufficient for pharmacological effects (≥1 μM). A tentative correlation between structure and activity was performed.

DEDICATION

To my family

ACKNOWLEDGMENTS

I would like to thank everybody who contributed to the success of this work. First and foremost, I would like to thank Dr. Olga V. HORDIYENKO, Dr. Axelle ARRAULT and Dr. Marie-Christine AVERLANT-PETIT for the opportunity to work on these interesting project. Their mentorship and the insightful discussions have been a major encouragement during my studies.

I would also like to thank the members of the jury Prof. Claude TAILLEFUMIER, Dr. Florine CAVELIER, Prof. Marc LE BORGNE and Prof. Zoia VOITENKO for accepting the invitation to serve on my committee.

Additionally, I thank Dr. Caroline GAUCHER at the Faculty of Pharmacy of the Université de Lorraine for the collaboration on the NO-donors project and the biological testing of my compounds.

I also thank the Taras Shevchenko National University of Kyiv and the Campus France for financial support of this work and the Université de Lorraine for ATER position which gave me the opportunity to finish my thesis in four years.

My thanks also go to the members of LCPM for their suggestions and a pleasant working atmosphere: Prof. Alain DURAND, Dr. Jacques BODIGUEL, Dr. Regis VANDERESSE, Dr. Guillaume PICKAERT, Dr. Samir ACHERAR, Dr. Olivier FABRE and Mme Mathilde ACHARD. Furthermore, I would like to thank Dr. Emmanuel WENGER (CRM2), Dr. Volodymyr MEDVIEDIEV and Prof. Oleg SHISHKIN (Institute for Single Crystals, NASU) for their X-ray diffraction measurements.

I am especially thankful for Tanya SAHYOUN and Mohamed IBRAHIM with whom I shared the lab and to Amirah GAZZALI, they always made me looking forward to come here and were always willing to show support.

Most importantly, I am extremely grateful for my parents, who have always supported me and encouraged me in my education. Equally important was the emotional support from my sister Alina and my friends Viktoriia, Iulia, Anastasiia, Vika and Larisa; I deeply appreciate your friendship.

Thank you / Merci beaucoup / Щиро дякую!

Olga

TABLE OF CONTENTS

Abstract 2
Dedication 4
Acknowledgments 5
Table of Contents 6
Abbreviations 8
Chapter 1: Introduction 11

1. Introduction 12
2. Pyridine and pyrazine heterocycles as scaffolds for peptidomimetics 12
3. Amidoximes and masked amidoximes as prodrugs of amidines, an arginine mimics 13
4. Amidoximes as NO donors 19

Chapter 2: Synthesis of Pyridine and Pyrazine-based Peptidomimetics 23

1. Introduction 24
2. Synthetic plan 24
3. Synthesis of starting 2-cyanonicotinic and 3-cyanopyrazine-2-carboxylic acids 25
4. Synthesis of peptidomimetics bearing amidoxime function 26
   4.1 Synthesis of amidoximes 26
   4.2 Synthesis of pyridine based amidoximes 27
   4.3 Synthesis of pyrazine based amidoximes 35
5. Studies towards the synthesis of 1,2,4-oxadiazoles *via* amidoxime ester units 42
   5.1 Overview of synthetic approaches to 3,5-disubstituted 1,2,4-oxadiazoles *via* amidoxime esters 43
   5.2 Acylation of amidoximes with further conversion into amino acid derived 1,2,4-oxadiazoles 53
6. Studies towards the synthesis of 1,2,4-triazoles *via N*-acylamidrazones 56
   6.1 Overview of synthetic approaches *via N*-acylamidrazones 57
   6.2 Synthesis of pyridine(pyrazine)-based *N*-acylamidrazones with further conversion into amino acid derived 1,2,4-triazoles 63
7. Synthesis of hydrazide modified turn mimics 66
8. Conclusions 68

Chapter 3: Structural Analysis 70

1. Introduction 71
2. Methods and techniques of conformational study 71
2.1 Infrared absorption spectroscopy (IR) 71
2.2 Nuclear Magnetic Resonance spectroscopy (NMR) 71
2.2.1 One dimensional NMR 72
2.2.2 Two dimensional NMR 72
2.3 Molecular modeling 73
3. Structural and thermodynamic studies of proline-containing peptidomimetics 74
3.1 Conformational preferences and thermodynamic studies of proline derivatives 74
3.2 Stuctural and thermodynamic analysis of pseudotripeptide methyl (2*S*)-2-({[(2*S*)-1-({3-[(*Z*)-(hydroxyamino)(imino)methyl]pyrazin-2-yl}carbonyl)pyrrolidin-2-yl]carbonyl}amino)-3-phenylpropanoate **7'd** 80
3.2.1 FT-IR and NMR investigations 81
3.2.2 Molecular modeling 84
3.2.3 *cis-trans* isomerization study 88
3.2.4 A tentative correlation between toxicity and structure 90
4. Stuctural analysis of esterified amidoximes and oxadiazoles **8**, **8'** and **9**, **9'** 91
4.1 Conformational analysis of alanine and phenylalanine derivatives **8**, **8'** (**a,b**) and **9**, **9'** (**a,b**) 91
4.2 Conformational analysis of the proline derivatives **8c**, **8'c** and **9c**, **9'c** 95
5. Structural and thermodynamic studies of acylamidrazones **10**, **10'** 98
6. Stuctural analysis of hydrazide modified peptidomimetics **12**, **12'** 104
7. Conclusions 113

Chapter 4: Preliminary Biologycal Evaluation of Amidoximes as NO Donors 115
General conclusions and perspectives 121
Chapter 5: Experimental 122

1. General Methods 123
2. Experimental procedures 126

References 171
Appendix 180
Résumé de these 187

Abbreviations

1D	One dimensional
2D	Two dimensional
Å	Angstrom
AA	Amino acid
Ac	acyl
Ada	adamantyl
Aib	alpha-aminoisobutyric
Ala	alanine
Alk	alkyl
Ar	aryl
a.u.	Hartree atomic units
BEMP	2-*tert*-butylimino-2-diethylamino-1,3-dimethylperhydro-1,3,2-diazaphosphorine
Boc	*tert*-butyloxycarbonyl
BOP	(benzotriazol-1-yloxy)tris(dimethylamino)phosphonium hexafluorophosphate
Bu	butyl
Bz, Bn	benzyl
BZA	benzamidoximes
Cbz	carboxybenzyl
CDI	1,1'-carbonyldiimidazole
CDMT	2-chloro-4,6-dimethoxy-1,3,5-triazine
cGMP	cyclic guanosine-3′,5′-monophosphate
COSY	Correlated SpectroscopY
CysTr	cysteine-S-trityl
DBU	1,8-diazabicyclo[5.4.0]undec-7-ene
DCC	dicyclohexylcarbodiimide
DCM	dichloromethane
DIC	*N,N′*-diisopropylcarbodiimide
DIPEA	*N*,*N*-diisopropylethylamine
DMAP	4-dimethylaminopyridine
DME	dimethoxyethane
DMF	*N,N*-dimethylformamide
DMSO	dimethyl sulfoxide
DPP-4	dipeptidyl peptidase IV
EDCI	*N*-ethyl-*N'*-(3-dimethylaminopropyl)carbodiimide hydrochloride
EDRF	endothelium-derived relaxing factor
ESI	electrospray ionization
Et	ethyl
Fmoc	9-fluorenylmethyl
g	gram
Gln	glutamine
Glu	glutamic acid

Gly	glycine
h	hour
HATU	1-[bis(dimethylamino)methylene]-1*H*-1,2,3-triazolo[4,5-*b*]pyridinium 3-oxid hexafluorophosphate
HBTU	*N,N,N′,N′*-tetramethyl-*O*-(1*H*-benzotriazol-1-yl)uronium hexafluorophosphate
HCTU	O-(6-chlorobenzotriazol-1-yl)-*N,N,N′,N′*-tetramethyluronium hexafluorophosphate
Het	heteroaryl
HMBC	Heteronuclear multiple-bond correlation spectroscopy
HMPA	hexamethylphosphoramide
HOBt	1-hydroxybenzotriazole
HPLC	high-performance liquid chromatography
HSQC	Heteronuclear single-quantum correlation spectroscopy
ILP	ionic liquid-phase
ppm	parts per million
PS	polystyrene
Py	pyridyl
Hz	Herz
IoLiPOS	ionic liquid-phase organic synthesis
IOP	intraocular pressure
IR	Infrared
L	litre
LC/MS	Liquid chromatography–mass spectrometry
Leu	leucine
M	mole
mARC	mitochondrial amidoxime reducing component
Me	methyl
MHz	megaHerz
mM	millimole
mp	melting point
MTT	3-(4,5-dimethylthiazol-2-yl)-2,5-diphenyltetrazolium bromide
MW	microwave
NAD	nicotinamide adenine dinucleotide
NADP	nicotinamide adenine dinucleotide phosphate
NED	*N*-(1-naphthyl)-ethylenediamine dihydrochloride
NMM	4-methylmorpholine
NMR	Nuclear Magnetic Resonance
NOE	Nuclear Overhauser Effect
NOESY	Nuclear Overhauser Effect SpectroscopY
NOHA	N^{ω}-hydroxy-L-arginine
NOS	nitric oxide synthase
NP	normal phase
Pg	protecting group
Ph	phenyl
Phe	phenylalanine

Pro	proline
ROESY	Rotating frame Overhauser Effect SpectroscopY
SOD	superoxide dismutase
Su	succinimidyl
TBAF	tetrabutylammonium fluoride
TBAH	tetrabutylammonium hydroxide
t-Bu	*tert*-butyl
TFA	trifluoroacetic acid
THF	tetrahydrofuran
TMS	tetramethylsilan
TOCSY	Totally Correlated SpectroscopY
Tol	tolyl
Trp	tryptophan
Ts	tosyl
TSIL	task-specific ionic liquid
UV	ultraviolet
Val	valine

Chapter 1: Introduction

1. Introduction

This work is a continuation of joint research on the synthesis of heterocycle-based peptidomimetics that mimic β-turn, which had begun between Dr. Olga Hordiyenko (Taras Shevchenko National University of Kyiv) and Dr. Axelle Arrault (LCPM, ENSIC, Universite de Lorraine, Nancy). The previous study was focused on the synthesis of pseudopeptides where turn structure was determined by central 1*H*-isoindole unit that was connected at 1 and 3 positions with peptide chains. Several key molecules were synthesized from mono to pentapeptide, and it was shown that intramolecular hydrogen bonding could provide turn structures (Biitseva A. V., Rudenko I. V., Hordiyenko O. V., Jamart-Grégoire B., Arrault A., *Eur. J. Org. Chem.*, **2012**, *23*, 4387).

In order to continue joint research on combining amino acids with heterocyclic core as a turn guiding factor, the introduction of pyridine and pyrazine 2,3-cyano acids into peptide chain was suggested to give promissing peptidomimetics. This study became the aim of the PhD theses in co-tutelle between the Taras Shevchenko National University of Kyiv and the LCPM, Universite de Lorraine. The bibliography search, editing of articles and some analyses (elemental analysis, LC-MS and IR for some products) were performed at the Taras Shevchenko National University of Kyiv while the synthesis and conformational analysis of peptidomimetics have been done in the Laboratoire de Chimie-Physique Macromoléculaire, Universite de Lorraine.

2. Pyridine and pyrazine heterocycles as scaffolds for peptidomimetics

The combination of aromatic or heterocyclic rings with a peptide motif represents one of the possible strategies towards peptidomimetics. Heterocycle-containing amino acids have become important precursors in the design of peptidomimetics. This approach is advanced for introduction of conformational restrictions which leads to a more stable and bioavailable product, hence favoring recognition and pharmacological properties of peptide-based drugs and decreasing toxicity. Moreover, a resistance to peptidase degradation is known to be more pronounced in peptidomimetics with heterocyclic cores as non-peptidic fragments. In this thesis we describe, the study of new pyridine and pyrazine-based peptidomimetics: synthesis, conformational behaviour and preliminary biological evaluation.

The pyridine ring, naturally occurring in the vitamins, nicotinic acid (vitamin B_3/niacin) and pyridoxine (vitamin B_6), a number of alkaloids, such as nicotine, pyridine, is therefore

notable for a wide range of biological activities (Figure 1.1). Moreover, niacin and nicotinamide, are precursors of the coenzymes nicotinamide adenine dinucleotide (NAD) and nicotinamide adenine dinucleotide phosphate (NADP) *in vivo.*[1]

The pyrazine ring can improve the binding affinity and bioavailability of potential drugs. A number of compounds containing a pyrazine moiety are in late stage clinical trials (VE-821 – an ATR inhibitor) or have reached the market such as, bortezomib - the first therapeutic proteasome inhibitor, eszopiclone - a nonbenzodiazepine sedative hypnotic etc (Figure 1).[2]

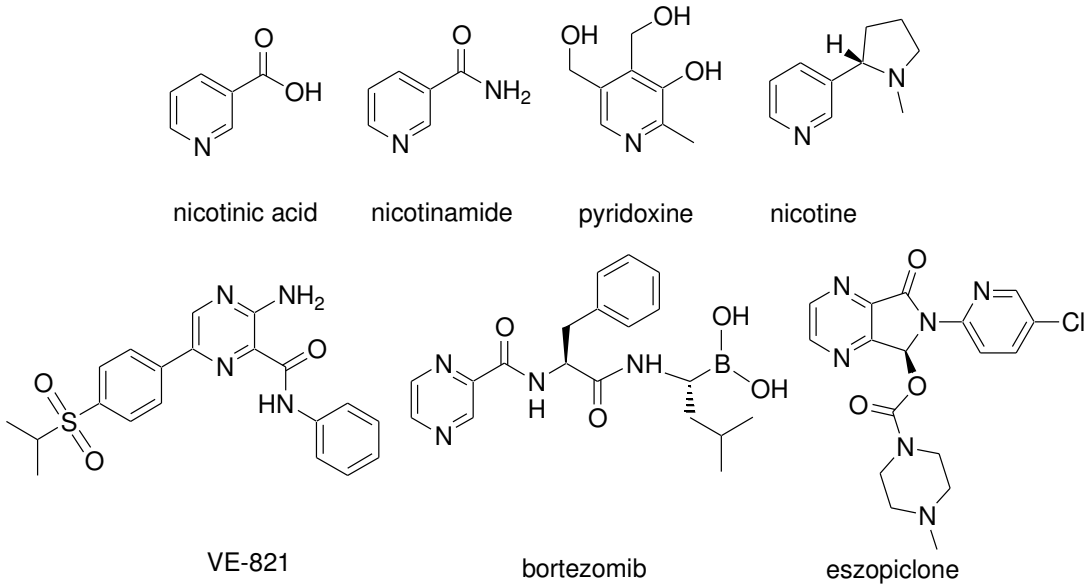

Figure 1.1 Selected examples of biologically active pyridine and pyrazine compounds

Consequently, the six-member pyridine and pyrazine heterocycles are utilized in many pharmaceutical actives and thus they have been chosen as scaffolds of the corresponding peptidomimetics.

The benefits of the amidoxime group and modified amidoxime moieties (amidoxime esters and oxadiazoles) are further emphasized in Chapter 1 of the manuscript.

3. Amidoximes and masked amidoximes as prodrugs of amidines, an arginine mimics

Investigations in the chemistry as well as in the biological applications of amidoximes up to 2008 are summerized in the reviews [3-5]. However, a number of publications and patents appeared to date, in particular concerning the use of amidoximes and its derivatives as prodrugs of amidines in drug design and the way of their activation.

Amidoximes are compounds bearing both a hydroxyimino and an amino group at the same carbon atom which makes them structurally close to amidines, amides and hydroxamic acids. Amidines are often used as mimetics of the guanidine side chain of arginine which is responsible for pharmacological effects. Variety of drugs and drug candidates possesses the amidine moiety, such as thrombine inhibitors, factor Xa and VIIa inhibitors, glycoprotein IIb/IIIa receptor antagonists, and in other drugs. [6-8] However, due to their high hydrophilicity they are protonated at sp^2 nitrogen atom, forming a highly mesomerically stabilized cation under physiological conditions (Scheme 1.1). The cations formed are essential for interactions with the negatively charged carboxylates or targeted molecules, but prevent an absorption from the gastrointestinal tract.[9]

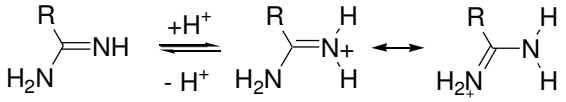

Scheme 1.1 Protonation of amidines

This problem can be solved by using prodrugs - bioreversible derivatives of drug molecules that undergo an enzymatic and/or chemical transformation *in vivo* to release the pharmacologically active agent with the promoiety being non-toxic (Figure 1.2).[10,11] The development of prodrugs have become a tool for improving physicochemical, biopharmaceutical or pharmacokinetic properties of active parent drugs.

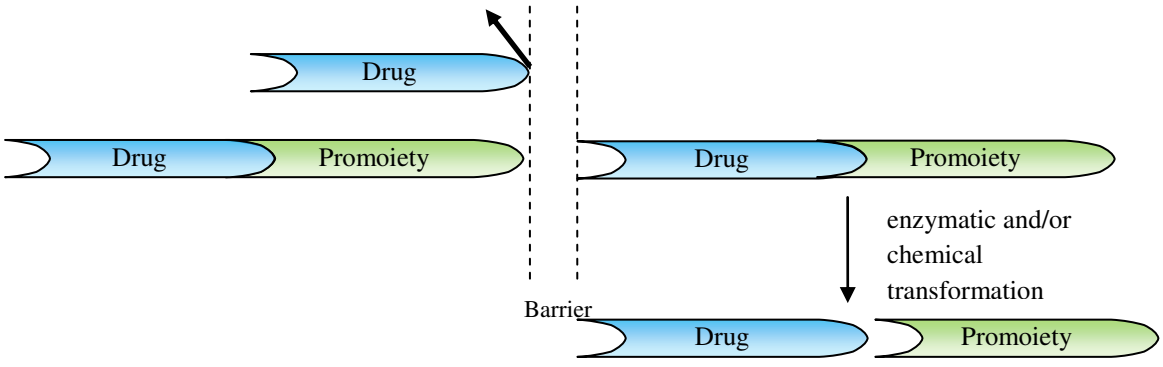

Figure 1.2 Prodrug concept

An amidoxime group introduced into the structure is not protonated under physiological conditions, thus it can be employed as an amidine replacement. The prodrug approach "Amidoximes instead of amidines" has a growing interest due to improved physicochemical properties and oral bioavailabilities.[5]

Recently it has been shown that the *N*-reductive enzyme system is responsible for the activation of amidoxime prodrugs in mitochondries.[12,13] This enzyme system is able to reduce a variety of *N*-hydroxylated derivatives (including amidoximes) in the presence of NADH. It consist of the «mitochondrial amidoxime reducing component» (mARC) and the two electron transport proteins cytochrome b_5 type B and NADH cytochrome b_5 reductase (Figure 1.3).

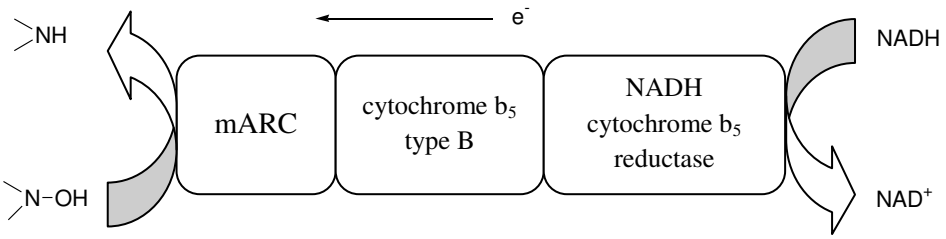

Figure 1.3 A simplified illustration of *N*-reductive enzyme system

This prodrug strategy has been successfully applied to a wide range of drug molecules. Firstly it was developed for the aromatic diamidine pentamidine, an antiprotozoal drug (Scheme 1.2).[14,15] The replacement of amidine functionalities into amidoxime led to improved bioavailability and solubility. To optimize the pharmacokinetic profile, many studies have been devoted to new pentamidine analogues. Although, *N,N*-bis(acetoxy)pentamidine showed a clearly increased lipophilicity and oral bioavailability in animal studies it has very low water solubility.[16] Further prodrug principles were transferred to pentamidine (hydroxylation, conjugation with amino acids etc.)[17,18], however *N,N'*-bis(succinyloxy)pentamidine exhibited clearly superior solubility and pharmacokinetic behavior as compared to the other prodrugs of pentamidine.[19] The activation of the prodrug proceeds *via* hydrolysis by esterases and the mARC enzyme system reduction and is hence the double prodrug strategy.

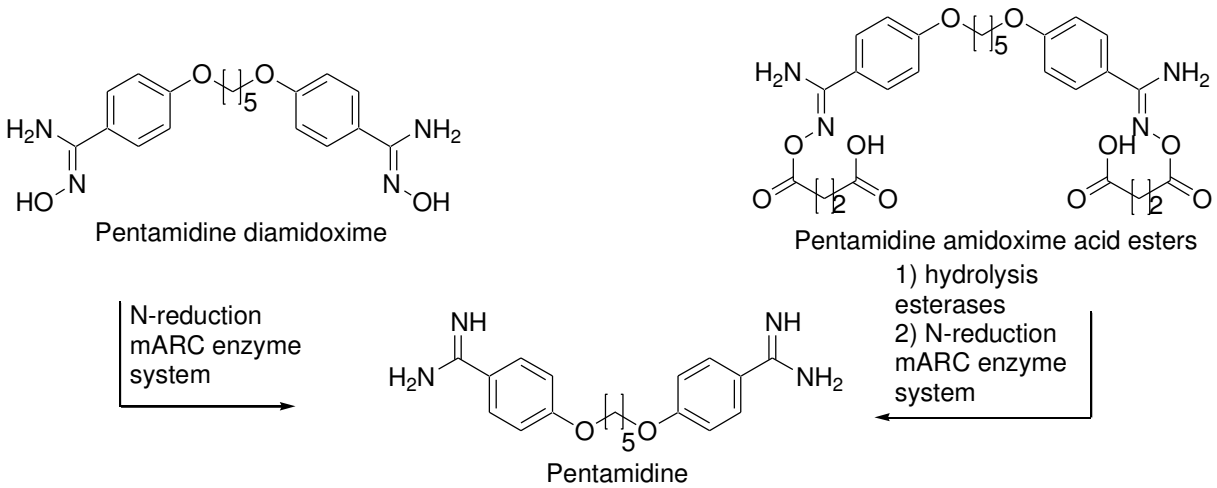

Scheme 1.2 The activation of the pentamidine-prodrugs

Amidoximes have widely been studied as antitrombotic agents. A known example is ximelagatran (Exanta®, Astra Zeneca), which was the first approved direct thrombin inhibitor for oral application (Figure 1.4).[20,21] This pharmacologically inactive molecule is transformed *in vivo* in two steps into the active form melagatran.[22] Ximelagatran showed a significant improvement of oral bioavailability in human (about 20%), compare with melagatran with oral bioavailability of only 5%. Unfortunately, a hepatotoxicity that forced the market withdrawal in 2006 has been reported.

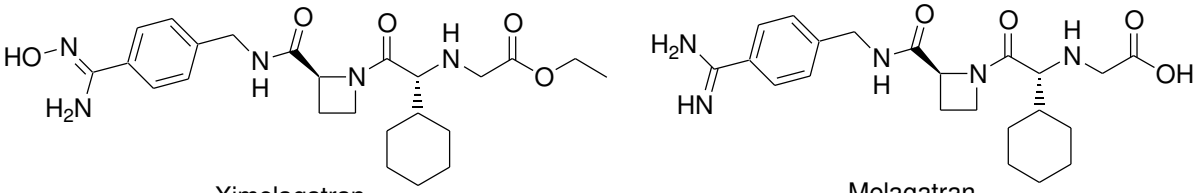

Figure 1.4 Antitrombotic amidoxime prodrug and its active drug

Dabigatran etexilate (Pradaxa®) – the only available oral thrombin inhibitor, is prodrug of the actual active substance dabigatran (Figure 1.5).[23] To overcome some disadvantages of Pradaxa, dabigatran amidoxime succinic acid ester has been patented as prodrug with excellent solubility, appropriate stability, and good oral bioavailability.[24]

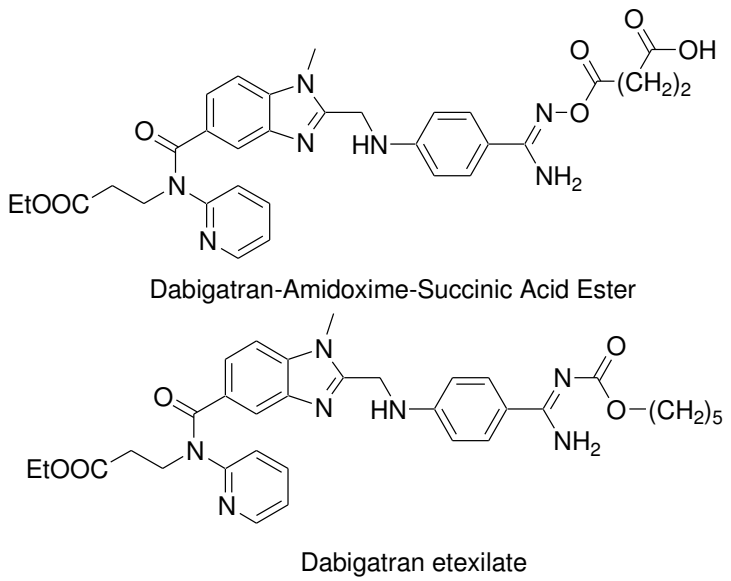

Figure 1.5 Prodrugs of dabigatran thrombin inhibitor

Recently, the amidoxime prodrug strategy was applied to another serine protease inhibitor upamostat (Mesupron®, WX-671), which has passed clinical phase II trials (Figure

1.6).[25,26] It is the orally available prodrug of an active form WX-UK1, the urokinase inhibitor. The bioactivation by the mARC-containing N-reductive enzyme system has also been studied.

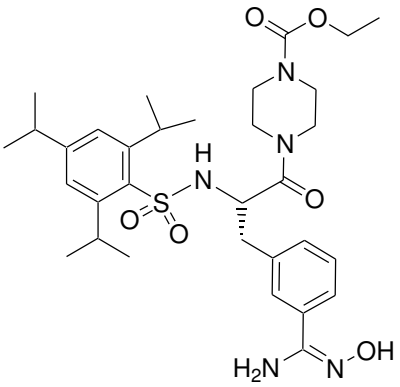

Figure 1.6 Prodrug of the urokinase inhibitor

The development of new antiviral agents can solve both major problems of known neuraminidase inhibitors (NAIs), a drug resistance and unfavorable pharmacokinetic (PK) properties. Oseltamivir (Tamiflu®) - the first orally available NAI that was marketed in 2000 (Scheme 1.3).[27] Its amidoxime prodrug was shown to possess a better PK profile with comparable oral bioavailability (31% versus 36% for oseltamivir).

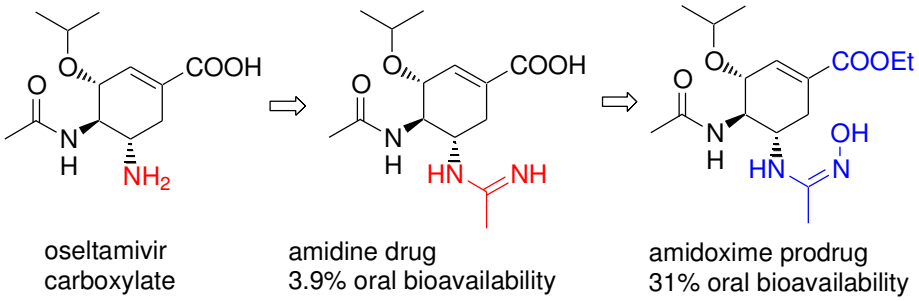

Scheme 1.3 Development of oseltamivir derivatives

A new class of potential prodrugs was reported recentely by Schwarz *et al.* (Scheme 1.4).[28] It includes hydroxylation the functional group at both nitrogen atoms of amidines to further reduce its basic character (the pK_a from 11.6 in case of amidines and 4.8 for amidoximes to 3.8 for *N*,*N*-dihydroxybenzamidines) and increase lipophilicity. The additional reaction step necessary for *in vivo* reduction of an additional hydroxy group delays the degradation to amidines leading to extended bioavailability.

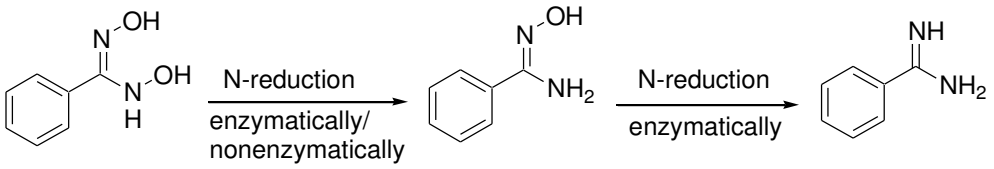

Scheme 1.4 Metabolic reduction of *N*,*N*-dihydroxybenzamidines as double prodrugs

Another strategy to amidoxime prodrugs is the use of 1,2,4-oxadiazol-5-ones and 1,2,4-oxadiazoles with the masked amidine functionality in order to reduce basic character and improve bioavailability. This method was applied for the synthesis of double prodrugs of the potent GPIIb/IIIa antagonists with a fast onset and prolonged duration of action after oral administration (Figure 1.7).[29]

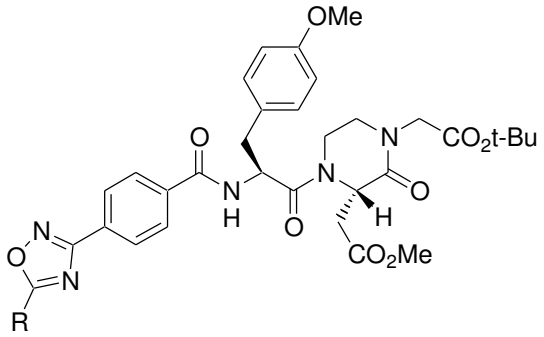

Figure 1.7 1,2,4-Oxadiazole-based double prodrugs of the potent GPIIb/IIIa antagonists

Bis-oxadiazolone derivative was evaluated by Ouattara *et al.*[30] as potent oral antimalarial prodrug of 1,12-bis-(*N,N'*-acetamidinyl)dodecane M64 (Figure 1.8). New modified amidine was validated as the best prodrug acting on *Plasmodium in vivo* after oral administration.

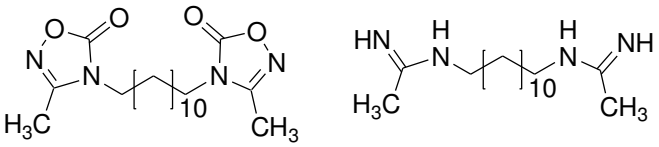

Figure 1.8 Bis-oxadiazolone prodrug of potent antimalarial M64

This concept was also developed for masked bis-amidine prodrugs of a promising N^1,N^5-bis[4-(*N'*-(carbamimidoyl)phenyl]glutaramide antifungal lead TH-701 (Figure 1.9). [31]

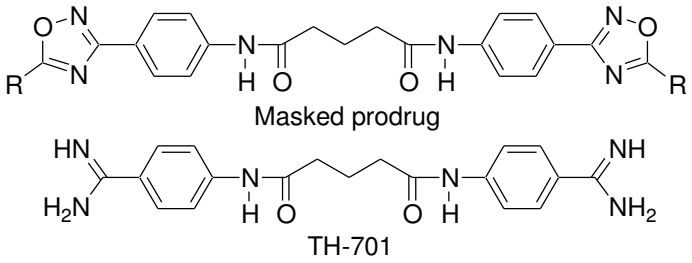

Figure 1.9 Masked prodrugs of potent antifungal lead TH-701

4. Amidoximes as NO donors

Nitric oxide (NO) is an endothelium-derived relaxing factor (EDRF) that plays a key role in many bioregulatory systems including cardiovascular through platelet aggregation inhibition and vascular relaxation, nervous system by neurotransmission and immune stimulation.[32,33] Owing to the properties highlighted, there is great interest in the molecules called nitric oxide donors (NO-donors).

NO is mainly biosynthesized endogenously from L-arginine by O_2 and NADPH catalyzed by various nitric oxide synthase (NOS) enzymes with the intermediate formation of N^{ω}-hydroxy-L-arginine (NOHA) (Scheme 1.5).

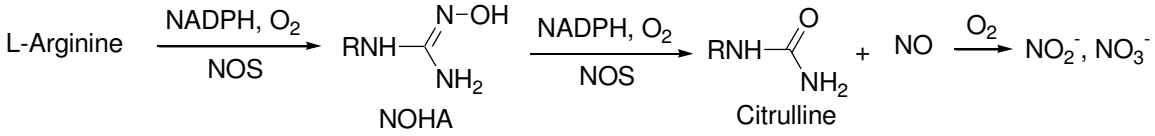

Scheme 1.5 Biosynthesis of NO

The oxidative cleavage of the C=N(OH) bond of NOHA has been found to be also catalyzed by liver microsomal cytochromes P450 with formation of citrulline and nitrogen oxides (NO, NO_2^-...).[34] Similarly, NO is formed *in vivo* by rat liver microsomal oxidation of exogenous compounds containing an amidoxime or a related function. Firstly it was shown for *p*-hexyloxy-benzamidoxime which is transformed to the corresponding arylamide and nitrogen oxides by a cytochromes P450-dependent oxidation with NADPH and O_2 (Scheme 1.6).[35]

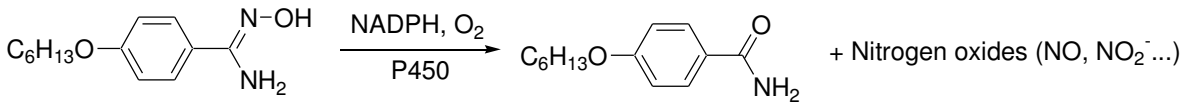

Scheme 1.6 Reaction of amidoxime with liver microsomal cytochromes P450

Clement *et al.* showed that *N*-hydroxy pentamidine undergo the P450-dependent oxidative conversion to the respective amide derivative and nitrogen oxides.[36] The formation of NO was confirmed by the formation of the cytochromes P450 Fe(II) – NO complex detected in visible spectroscopy.

More detailed study of the oxidation of C=N(OH) bond was reported by Jousserandot *et al.*[37,38] Variety of aldoximes, ketoximes, amidoximes and hydroxyguanidines were studied for the formation of NO_2^- upon microsomal oxidation in the presence of the cofactors of cytochromes P450, NADPH and O_2. It was found that the rate of the reaction depends on the number of nitrogen-containing electron-donating substituents on the C=N(OH) carbon atom in the order *N,N*-disubstituted *N'*-hydroxyguanidines>N-substituted *N'*-hydroxyguanidines>*N,N*-disubstituted amidoximes>amidoximes>ketoximes. A mechanism of the reaction was studied and oxidation appeared to be mainly due to $O_2^{\cdot-}$ derived from the oxidase function of cytochrome P450, which was suggested from inhibitory effect of superoxide dismutase (SOD). On the contrary, the formation of the sideproducts nitriles was not inhibited by SOD thus was due to a cytochrome-P450-iron active species.

NO release and antithrombotic effects of several arylazoamidoximes were investigated by Rehse and co-workers (Figure 1.10).[39]

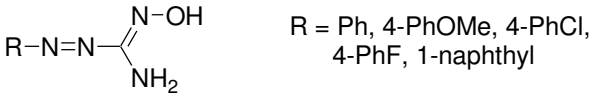

Figure 1.10 Azoamidoximes testet for NO release

Antithrombotic effects showed phenyl-, 4-chlorophenyl- and 1-naphthyl substituted azoamidoximes whereas compounds with the strongest electron donating (4-methoxyphenylazo-methanamidoxime) and electron withdrawing (4-fluorophenylazo-methanamidoxime) properties did not influence the thrombus formation in arterioles. In addition, the effect of SOD on the formation of NO was tested and revealed no influence in case of phenylazomethaneamidoxime indicating the oxidation by a P450-Fe(III)-$OO^{\cdot}$ species. In contrast the formation of NO from 4-methoxyphenylazo-methanamidoxime was significantly suppressed by the addition of superoxide dismutase and hence the release of $O_2^{\cdot-}$ is responsible for the oxidation.

A fast preliminary screening of potential NO precursors was carried out by Koikov *et al.* in order to reveal the unknown NO generating potential of the well-known oximes, amidoximes and hydroxamic acids (Figure 1.11).[40]

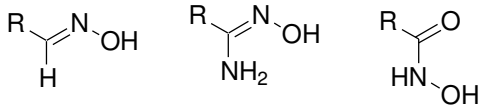

R = Me, Ph, 2-HOPh, 2-MeOPh, 4-HOPh, 4-MeOPh, 4-HOBn, 2-Py, 4-Py, 2,6-Py

Figure 1.11 Oximes, amidoximes and hydroxamic acids tested as nitric oxide donors

NO formation was performed by oxidation of the above compounds with $K_3[Fe(CN)_6]$ and further detection of $[Fe(CN)_5NO]^{2-}$ (nitroprusside) anion. The substitution of a benzene ring for pyridine ring led to an essential leap in amidoxime activity. Preliminary tests on the activation of soluble guanylate cyclase from human platelets was achieved and comparison of values showed the pronounced *ortho*-effect in derivatives studied either due to superior stabilisation of the intermediates (or the released NO) or higher complementarity to the active site.

Other scientists exemined some *p*-substituted aromatic amidoximes on their ability to produce endothelium-independent vasorelaxation in the rat aorta (Figure 1.12).[41]

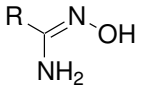

R = H, NH_2, Ph, 4-ClPh, 4-C_6H_{13}OPh, 4-NO_2Ph, 4-MeOPh

Figure 1.12 Amidoximes tested for relaxant activity in the rat aorta

The order of relaxant activity of amidoxime, ketoxime and *N*-hydroxyguanidine derivatives has been shown to be opposite to the order of reactivity of the same compounds for P450-dependent oxidative cleavage of the C=NOH bond. The substituted benzamidoximes (BZA) were all active, the electron-poor 4-chloro- and 4-nitro- being more potent than the unsubstituted BZA and substituted by the electron-rich groups *N*-cyclohexyl and 4-methoxy derivatives. The most active studied compound, 4-chlorobenzamidoxime has shown to cause endothelium-independent relaxation in the rat aorta through activation of guanylyl cyclase by NO. Failure of P450 and NO synthase inhibitors to blunt relaxation lend no support to the hypothesis of the involvement of a P450 or NO synthase in the relaxant effect of compounds with a C=NOH function in the rat aorta. Therefore, it was indicated that non α-amino acid-

substituted benzamidoximes can act as efficient NO synthase-independent activators of the cyclic guanosine-3′,5′-monophosphate (cGMP) pathway in the rat aorta.

Chalupsky *et al.* demonstrated that in the isolated rat aorta, formamidoxime and other oxime derivatives increased NO levels and induced the relaxant effect.[42] The NO-cyclic GMP pathway was shown to be involved in the relaxant properties of oxime derivatives. In the later study, these substances were evaluated on their vasodilator properties on rats, however, only 3 out of 5 derivatives active *in vitro* were also active *in vivo*.[43] Formamidoxime surpassed the effects of both other efficient substances and induced pronounced dose-dependent blood pressure reduction. Nitric oxide was shown to be responsible for a considerable part of blood pressure changes elicited by amidoxime compound.

Amidoximes with the imidazole scaffold were prepared and tested for their ability to donate NO and for their intraocular pressure (IOP) lowering *via* the activation of guanylate cyclase (Figure 1.13).[44]

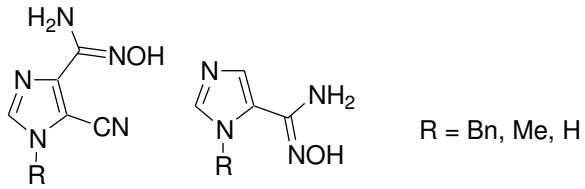

Figure 1.13 Tested imidazole amidoximes

NO formation of these compounds was studied by following the production of cGMP in the incubation of porcine iris-ciliary body. Imidazole amidoximes elevated NO_x and cGMP concentrations *in vitro*, however derivatives with cyano group at the imidazole ring appeared to abolish the activity. Unfortunately tested amidoximes had no significant effect on IOP *in vivo*.

The ability of amidoximes and 1,2,4-oxadiazoles to release NO in the presence of a thiol co-factor in order to design new anti-inflammatory agents was investigated by Ispikoudi *et al.*[45] NO donation with simultaneous production of nitrile, was tested *in vitro* by acting of reducing agents like L-cysteine or thiophenol. Although the amidoximes tested did not release NO in the presence of a thiol factor, acetylated 5-amino-1,2,4-oxadiazole derivatives exhibited high NO release.

Chapter 2: Synthesis of Pyridine and Pyrazine-Based Peptidomimetics

1. Introduction

The purpose of this project is the synthesis of pyridine and pyrazine-based peptidomimetics possessing *o*-substitution in non-peptidic fragment which can promote turn-like structure thus providing additional conformational rigidity. In order to achieve this goal, compounds bearing amino acid substuent and amidoxime function as a replacement of amidine one have been investigated. Moreover, the introduction of an additional amino acid through different linkage like hydrazide, ester or heterocyclic unit (1,2,4-oxadiazole, 1,2,4-triazole) is of our great interest.

Compounds of pyrine series were numbered like **1** – **12** while the corresponding pyrazine analogues as **2'** – **12'**. Difference in amino acid residues was indicated using letters **a-h** for pyridine derivatives and **a-d** in case of pyrazine counterparts.

2. Synthetic plan

A synthetic route to desired pyridine and pyrazine-based peptidomimetics is shown in Scheme 2.1. We decided to employ 2-cyanonicotinic and 3-cyanopyrazine-2-carboxylic acids as starting products. The corresponding amidoximes can be synthesized in two steps to give different pyridine and pyrazine-bazed pseudodipeptides. Additionally, the same intermediates can be utilized for the reaction with amino acid hydrazides in order to obtain *N*-acylamidrazones that can be used to produce 1,2,4-triazole-containing scaffolds. Esterification of amidoximes either with amino acid or with hydrazide of amino acid displays a way towards pseudotripeptides or double prodrugs of amidines. The cyclization of the latter can give pharmaceutically important 1,2,4-oxadiazole derivatives.

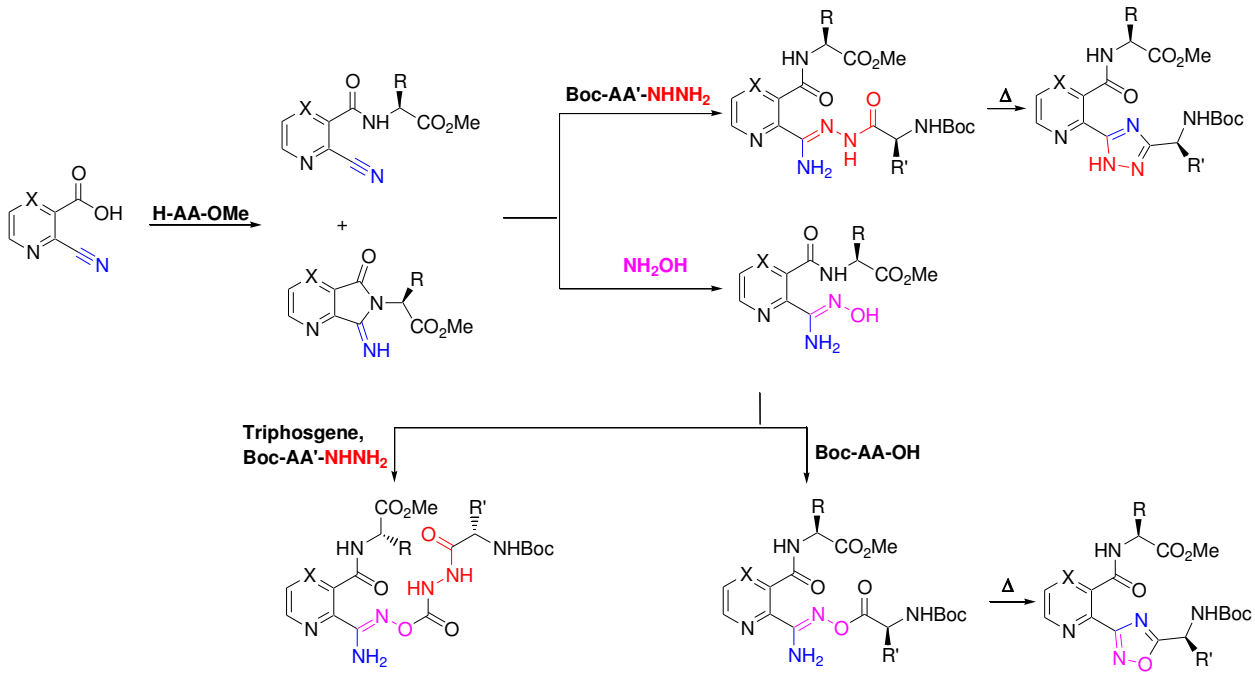

X = C, N; **R**, **R'** = side chain of amino acid (**AA**) residue

Scheme 2.1 Synthetic strategy to obtain target peptidomimetics

3. Synthesis of starting 2-cyanonicotinic and 3-cyanopyrazine-2-carboxylic acids

Preparation of the starting acid **4** was perfomed according to a known literature procedure;[46-48] the synthetic route is depicted in Scheme 2.2. Thus, commercialy available quinolinic anhydride **1** was first quickly hydrolyzed with aqueous ammonia (28%), similar to the method developed for phthalamic acid[46] and used later in the synthesis of the pyridine analogue by Spiessens and Anteunis,[48] to give 2-carbamoylnicotinic acid (**2**). The reaction proceeds selectively with formation of the product **2** and no isomeric 3-carbamoylpicolinic acid was obtained. It can be explained by the effect of the electronegative nitrogen atom that favors electrophilic character of the carbon of the closer carbonyl group thus promoting the attack on this carbon. We also suggested the hydrogen bonding between the proton of ammonia molecule and the pyridine nitrogen lone pair which can support the attack giving the acid **2** (Scheme 2.2). Then, ester **3** was obtained by treatment of acid **2** with methyl chloroformate, which was followed by hydrolysis with sodium hydroxide (1M) to give the corresponding 2-cyanonicotinic acid (**4**) in 28% overall yield.[47,48]

Starting 3-cyanopyrazine-2-carboxylic acid **4'** was synthesized from readily available 3-carbamoylpyrazine-2-carboxylic acid **2'**, which was treated with methyl chloroformate[49]

followed by selective hydrolysis of ester group with 1M NaOH to give the corresponding acid **4'** in 71% total yield (Scheme 2.2).

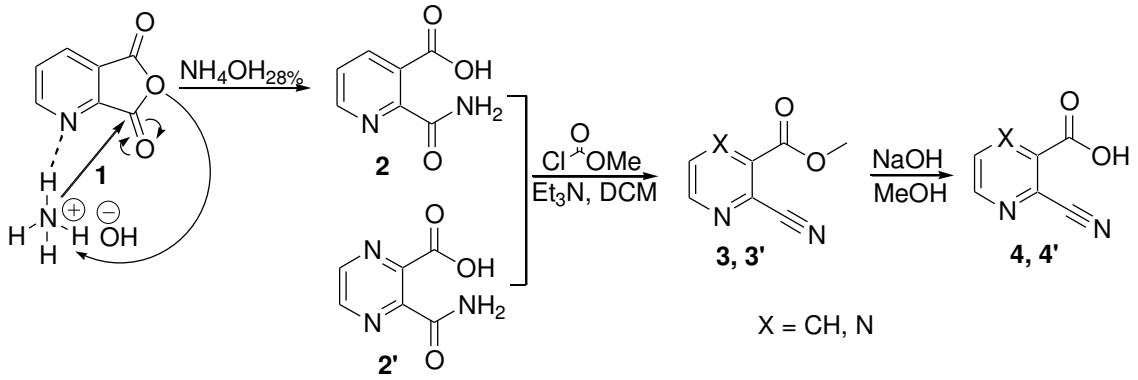

Scheme 2.2 Synthesis of 2-cyanonicotinic and 3-cyanopyrazine-2-carboxylic acids

4. Synthesis of peptidomimetics bearing amidoxime function

4.1 Synthesis of amidoximes

The most commonly used method for the synthesis of amidoximes involve condensation of nitriles with hydroxylamine hydrochloride (Scheme 2.3).[4,5]

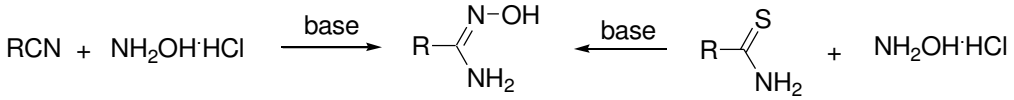

Scheme 2.3 Synthesis of amidoximes

The experimental procedure consists of liberating the hydroxylamine from its hydrochloride by means of sodium carbonate, adding the appropriate nitrile and alcohol and finally keeping the mixture at 60-80 °C for several hours to obtain amidoximes in high yields. Potassium or sodium hydroxide, sodium methoxide or ethoxide in place of sodium carbonate can lead to considerable reduced yields. Action of an excess of hydroxylamine may ameliorate the percentage in case of aromatic amidoximes. This reaction is also very useful, since nitriles are compounds readily available.

The development of new technologies and techniques enabled the attachement of amidoximes on a solid support. The reaction proceed by treating resin-bound nitriles with hydroxylamine, and the resulting resin bounded amidoximes can be further used for library generation and screening in drug discovery.[50,51] Moreover, amidoximes can be synthesized

using ionic liquid-phase organic synthesis (IoLiPOS) methodology that has several advantages over solid support.[52]

The reaction of hydroxylamine with thioamides can be used in case if they are more accessible that the corresponding nitriles or to afford amidoximes containing electron-withdrawing groups (Scheme 2.3).

The reaction of hydroxamoyl chlorides with ammonia leads to amidoximes *via* dehydrohalogenation step and formation of the nitrile oxide (Scheme 6, R^1, R^2 = H). Treatment of amines with ammonia affords *N*-unsubstituted amidoximes respectively (Scheme 2.4).

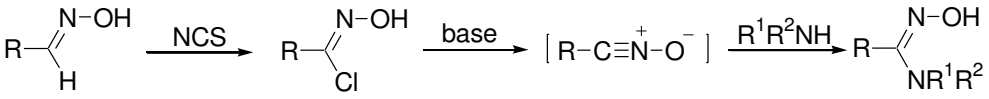

Scheme 2.4 Synthesis of amidoximes from hydroxamoyl chlorides

Other syntheses of amidoximes, involve the amidoxime-derived starting materials, thus are less general, can be realized by reactions: a) reduction of nitrosolic acid RC(=NOH)-NO with H_2S and nitrolic acid RC(=NOH)-NO_2 by a reduction with Pt; reduction of hydroxyamidoximes like PhC(=NOH)-NHOH with SO_2; b) action of hydroxylamine on amidine hydrochlorides RC(=NH)NH_2·HCl, amidrazones RC(=NH)-$NHNH_2$, iminoethers RC(=NH)-OR' and on imidoyl chlorides RC(=NH)-Cl; c) action of ammonia and amines on oximinoethers RC(=NHOH)-OR'; d) a reductive ring opening of 1,2,4-oxadiazoles or 1,2,4-oxadiazolin-5-ones upon reduction with $LiAlH_4$ and 1,2,5-oxadiazoles with H_2 on a Pd/C catalyst.[4]

4.2 Synthesis of pyridine based amidoximes

In our attempts to develop a new variety of arginine peptidomimetics with an amidinoheteroaroyl motif in a peptide chain, we elaborated the synthesis of nicotinic acid based amino acid units bearing an amidoxime function on the pyridine ring as precursors of the corresponding amidine-containing pseudopeptides.

We envisioned that the coupling of 2-cyanonicotinic acid **4** with methyl esters of L-α-amino acids with further conversion of the cyano residue into amidoxime group might be employed as a basic strategy for the synthesis of the target pyridine-based peptidomimetics.

The amination reaction in the series of α-cyanopyridinecarboxylic acids was studied earlier,[48,53] and it was shown that conversion of the methyl or ethyl esters of 2-cyanonicotinic acid **4** into the corresponding cyano amide was unsuccessful, and produced only cyclic 7-imino-6,7-dihydro-5*H*-pyrrolo[3,4-*b*]pyridin-5-one upon reaction with ammonia. Similar bicyclic imines were obtained by treatment of cyano esters with primary amines.[53]

To investigate the scope of this novel method, the coupling of 2-cyanonicotinic acid (**4**) with several commercially available methyl esters of L-α-amino acids (such as Ala, Phe, Pro, Gly, Val, Leu, Trp and CysTr) was examined (Scheme 2.5). As activating agent, *N*-ethyl-*N'*-(3-dimethylaminopropyl)carbodiimide hydrochloride (EDCI) in the presence of 1-hydroxybenzotriazole (HOBt) and triethylamine was used.[54]

^{1}H NMR analysis of the reaction products confirmed that, in most cases, the formation of open chain methyl esters of (2*S*)-*N*-(2-cyanopyridin-3-yl)carbonyl substituted amino acids **5** was followed by further intramolecular cyclization and giving a pyrrolidine ring and production of the tautomeric methyl esters of (2*S*)-2-(7-imino-5-oxo-5,6-dihydro-6*H*-pyrrolo[3,4-*b*]pyridin-6-yl)alkanoic acids **6** (Scheme 2.5). The reaction proceeds with nucleophilic attack by the amide nitrogen lone pair on the the sp carbon and further transfer of a proton.

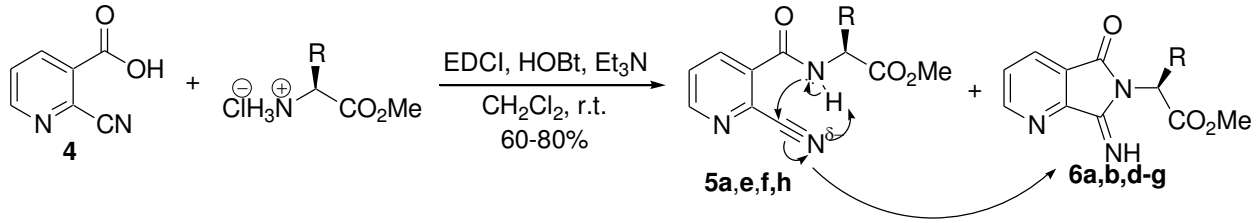

Scheme 2.5 Synthesis of methyl esters of (2*S*)-(2-cyanopyridin-3-yl)carbonyl substituted amino acids **5a**,**e**,**f**,**h** and methyl esters of (2*S*)-2-(7-imino-5-oxo-5,6-dihydro-6*H*-pyrrolo[3,4-*b*] pyridin-6-yl) alkanoic acids **6a,b,d-g**

When the alanine, valine and leucine methyl esters were used, the formation of both products **5** and **6** in different ratios, with an increasing amount of the cyclic form **6**, was observed while in the case of phenylalanine, glycine, tryptophan, the individual cyclic esters **6b**,**d**,**g** were exclusively isolated. The total yield of the amino acid derivatives **5** and **6** was 60-80% after purification by column chromatography (Table 2.1).

Table 2.1 Yield and 1H NMR data for compounds **5a**,**e**,**f**,**h** and **6a,b,d-g**

Ester	R	δ, ppm (J, Hz)				Yield, (%)[a]
		H^2, d (J=4.8 Hz)	H^3, dd (J, Hz)	H^4, d (J, Hz)	NH	
5a	Me (Ala)	8.79	7.61 (8.1, 4.8)	8.15 (8.1)	7.15[b]	15
6a		8.86	7.57 (8.1, 4.8)	8.14 (8.1)	9.34	58
6b	Bn (Phe)	8.81	7.51 (7.8, 4.8)	8.06 (7.8)	9.29	76
5c	Side chain of Pro-residue				-	87
6d	H (Gly)	8.87	7.58 (7.8, 4.8)	8.17 (7.8)	9.33	58
5e	*i*-Pr (Val)	8.81	7.62 (9.0, 4.8)	8.18 (9.0)	6.97	37
6e		8.87	7.58 (9.0, 4.8)	8.15 (9.0)	9.33	34
5f	*i*-Bu (Leu)	8.78	7.61 (8.1, 4.8)	8.15 (8.1)	7.06[c]	9
6f		8.81	7.54	8.09 (6.6)	9.37	76
6g	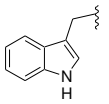 (Trp)	8.69	7.36 (7.8, 4.8)	7.91 (7.8)	9.33	83
5h	CH_2STr (CysTr)	8.77	7.46 (7.8, 4.8)	8.04 (7.8)	7.36 - 7.02	60

[a]Isolated yeald.
[b]d, j = 5.7 Hz.
[c]d, j = 6.9 Hz.

We also succeeded in separation of the open **5** and cyclic **6** forms of the alanine, valine and leucine derivatives by flash column chromatography, and in identification and characterization of the individual components by means of LC/MS and ^{1}H NMR, ^{13}C NMR

and IR spectroscopy. The assignment of the synthesized compounds to open-chain or closed structure was possible on the basis of comparative analysis of their ^{1}H NMR spectra (Table 2.1) and X-ray crystallography data.

The only product formed from the reaction of methyl glycinate with acid **4** was analysed by single-crystal X-ray diffraction. It was shown that this product has the cyclic structure **6d** (Figure 2.1).

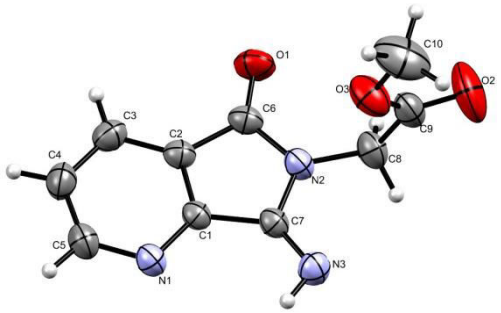

Figure 2.1 Molecular structure of compound **6d** according to results of the X-ray diffraction study, with the atom numbering used in the crystallographic analysis; thermal ellipsoids are shown at 50% probability level

In the ^{1}H NMR spectrum of this cyclic glycine derivative **6d**, the NH proton resonance appeared at δ = 9.33 ppm. The individual phenylalanine **6b** and tryptophan **6g** derivatives also displayed NH signals in the same region (Table 2.1). Thus, the NH proton peaks at δ = 6.97-7.15 ppm should correspond to derivative **5** with an open chain. Correspondingly, the open **5** or closed **6** structures in other cases were assigned based on the NH proton chemical shifts in their ^{1}H NMR spectra.

As follows from the X-ray crystallography data, compound **6d** adopts the *E* configuration at the C=N bond and *syn* orientation of the NH proton to the aromatic ring, for steric reasons. The substituent at the N2 atom is almost planar and has orthogonal orientation with respect to the rings (the C6-N2-C8-C9 and N2-C8-C9-O3 torsion angles are 91.93(16)° and 3.24(19)°, respectively; atom numbering as used in the crystallographic analysis). The structures of other compounds of this series were assigned by analogy with **6d**.

In the isolated pyrrolopyridines **6a**-**g** the amino acid residue is attached to the endocyclic nitrogen atom, and not to the exocyclic imine nitrogen atom as was assumed for the structure of the major products in the similar reaction of ester **3** with ethyl or benzyl

amines.[53] Two products were also isolated when ester **3** was reacted with benzylhydrazine, and their structures were assigned as isomeric pyrrolopyridines possessing a benzylamino substituent at either the imino or the pyrrole nitrogen atom.[55] Along with tryptophan derivative **6g**, a very small amount of crystals of the unexpected substance **A** was isolated from the reaction mixture (Figure 2.2).[56] In contrast to the major cyclic product **6g**, this unexpected material has an open structure that is regioisomeric to the nonisolated open form of **6g**. Even though the starting acid **4** was obtained as individual compound of 100% purity (according to LC/MS data), the presence of the isomeric ester **A** could result from an undetected 3-cyanopicolinic acid impurity in the 2-cyanonicotinic acid (**4**).

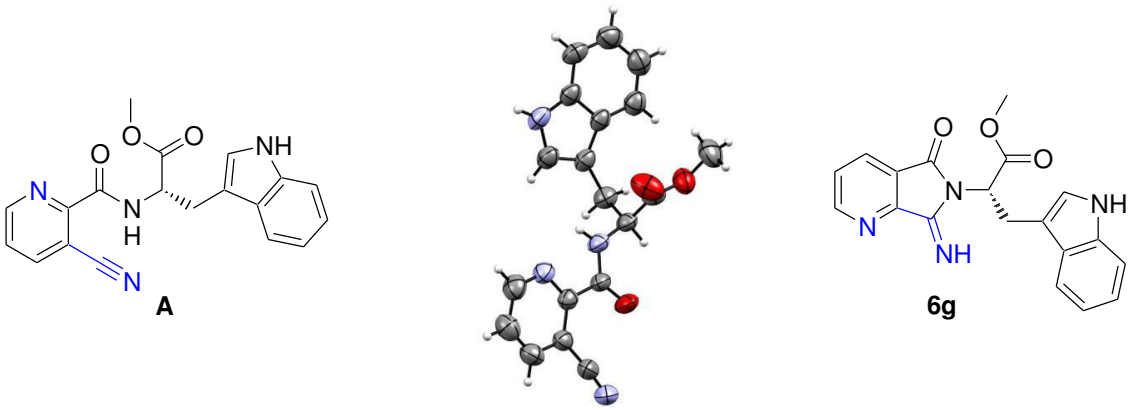

Figure 2.2 Structures of **A** and **6g**

Under LC/MS analysis conditions (gradient elution of H_2O + 0.1% formic acid and MeCN + 0.1% formic acid), each of the individual samples **5a**,**e**,**f** and **6a**,**b**,**d**,**e**,**g** (according to ^1H, ^{13}C NMR spectra) yielded two peaks in variable ratios, which corresponded to the same molecular ions (Table 2.2). It was found that these major and minor peaks appear as a result of reversible intramolecular cyclization/recyclization of compounds **5** and **6** during analysis. For each compound, the major peak value was around 70-100% and the minor peak was less than 30%.

Table 2.2 LC/MS data for esters **5a**,**e**,**f** and **6a**,**b**,**d**,**e**,**g**[a]

Entry	[M+1]	Major peak (%)	Minor peak (%)
5a	234	68 - 96	4 - 32
6a	234	74 - 100	0 - 26
6b	310	87	13
6d	220	78 – 94	6 – 22

5e	262	78-100	0 - 22
6e	262	87 - 98	2 - 13
5f	276	73	27
6g	349	80 - 88	12 - 20

[a]The values were determined on the basis of three LC/MS analyses for each of the compounds **5a**,**e** and **6a**,**d**,**e**,**g**, and one LC/MS analysis each for **5f**, **6b**.

The proline derivative **5c** was prepared similarly from acid **4** in 87% yield. Unlike other amino acids, in the case of L-proline the formation of only the open-chain product, methyl (2*S*)-1-[(2-cyanopyridin-3-yl)carbonyl]pyrrolidine-2-carboxylate (**5c**), was possible (Scheme 2.6).

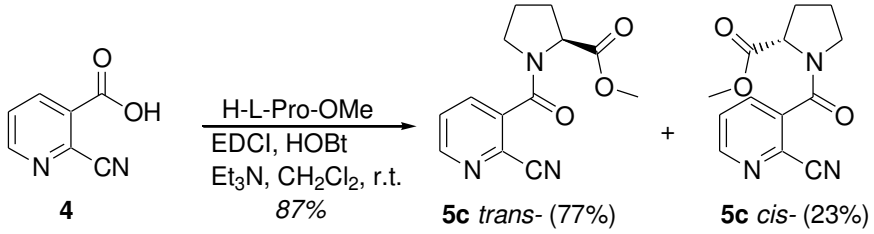

Scheme 2.6 Synthesis of methyl (2*S*)-1-[(2-cyanopyridin-3-yl)carbonyl]pyrrolidine-2-carboxylate (**5c**)

Most amide bonds in peptides exist almost exclusively in the *trans* configuration. The *cis* form is energetically unfavorable, largely due to steric hindrance. The cyclic structure of proline lowers the steric hindrance, making both the *cis* and *trans* forms nearly equally energetically stable.[57,58] Due to this fact, two sets of signals were observed in the ^{1}H NMR spectrum of proline derivative **5c**. In this context, structural and thermodynamic studies of proline-containing pseudopeptides were performed (see Chapter 3).

The open-chain methyl esters of (2*S*)-*N*-(2-cyanopyridin-3-yl)carbonyl-substituted amino acids **5a**,**c**,**e**,**f** exhibited a characteristic cyano group IR absorption band at around 2237 cm^{-1}. The band intensity was weak, similar to the almost undetectable absorption of the reference compound, 2-cyanonicotinic acid (**4**).[48]

The next step in the synthesis of amidine prodrugs consisted of transformation of the cyano group into an amidoxime function. Methyl esters of (2*S*)-*N*-[2-(*N*′-hydroxycarbamimidoyl)pyridin-3-yl]carbonyl-substituted amino acids (**7**) were obtained as individual products in 67-79% yield from the corresponding methyl esters **5a**,**e**,**f**,**h** and/or

methyl esters **6a**,**b**,**e-g** by treatment with hydroxylamine hydrochloride in methanol (Table 2.3).[4]

Table 2.3 Synthesis of the methyl esters of (2*S*)-*N*-[2-(*N'*-hydroxycarbamimidoyl)pyridin-3-yl]carbonyl-substituted amino acids **7a**,**b**,**e-h**

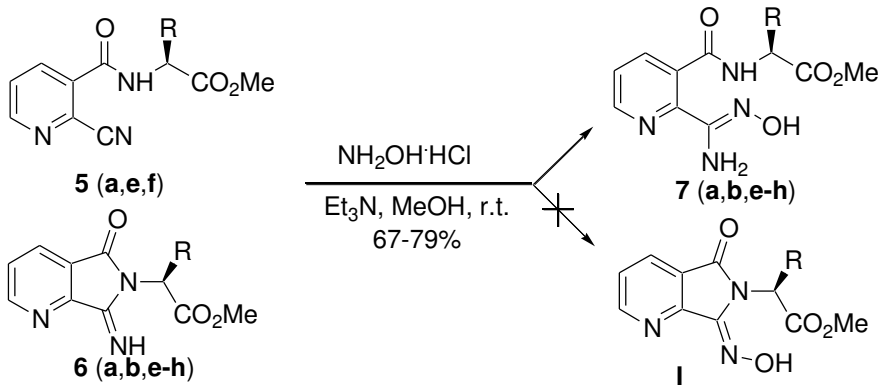

5, 6	R	7	Isolated yield (%)
5a, **6a**	Me	**7a**	68
6b	Bn	**7b**	77
5e, **6e**	*i*-Pr	**7e**	79
5f, **6f**	*i*-Bu	**7f**	70
6g		**7g**	67
6h	CH_2STr	**7h**	94

The corresponding proline analogue **7c** was synthesized similarly from the cyano derivative **5c** in 70% yield (Scheme 2.7). The cyano transformation reaction proceeded upon stirring the mixture at room temperature overnight, and the crude products were purified by flash column chromatography.

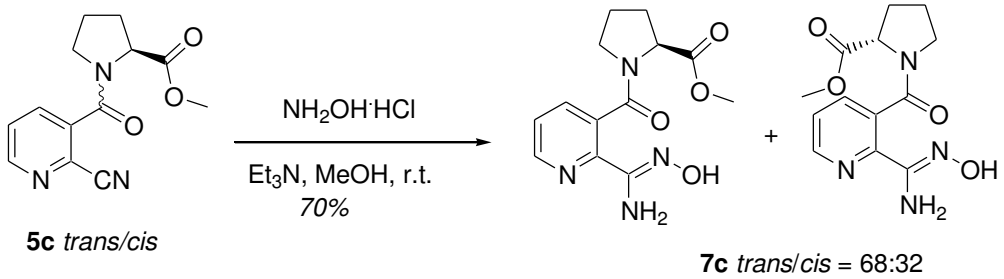

Scheme 2.7 Synthesis of methyl (2*S*)-1-{[2-(*N'*-hydroxycarbamimidoyl)pyridine-3-yl]carbonyl}pyrrolidine-2-carboxylate **7c**

NMR and X-ray diffraction analysis of the representative pseudopeptide **7b** (Figure 2.3) confirmed that it consisted of only one open-chain structural isomer of nicotinic acid. Thus, the reaction of ester **6b** with hydroxylamine proceeded with unexpected selective ring opening at the C–N bond closest to the imino group moiety. The same regiochemistry has been generalized for all other products **7a**,**b**,**e**-**h** formed from this reaction.

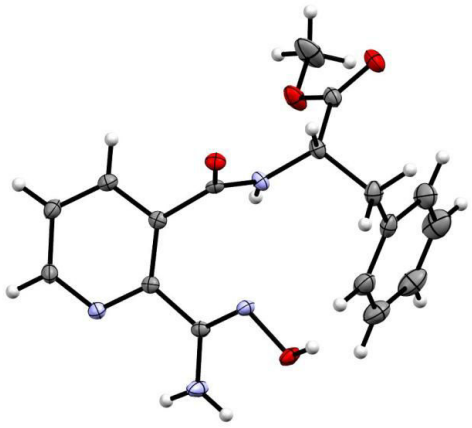

Figure 2.3 Molecular structure of compound **7b** according to results of the X-ray diffraction study; thermal ellipsoids are shown at 50% probability level

The ^{1}H NMR spectrum of the phenylalanine derivative **7b** revealed a chemical shift of δ = 5.49 ppm for the NH_2 protons. The other amidoximes **7a**,**e-h** and Pro derivative **7c** also gave amino group protons with a signal in the same region, at δ = 5.46-5.50 ppm.

A predominance of the *trans* form for the proline-containing amodoxime **7c** was observed. The ^{1}H NMR and ^{13}C NMR spectra displayed two sets of resonance signals, indicating a *trans*/*cis* isomeric ratio of about 68:32 (Scheme 2.7).

Both open-chain **5** and the corresponding cyclic **6** amino acid derivatives gave the same open-chain amidoximes **7** as the sole product. No cyclic amidoximes of type **I**, the formation of which could be expected according to a previously reported condensation of the benzene analogue 3-imino-1-oxoisoindoline with hydroxylamine that led to 3-(hydroxyimino)-1-oxoisoindole (**II**),[59] were found (Table 2.3, Figure 2.4).

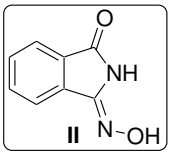

II

Figure 2.4

The formation of pseudopeptides **7** from esters of type **6** proceeds *via* pyrrolidine ring opening by hydroxylamine to afford the same open-chain amidoximes as those obtained from the corresponding cyano esters **5** (Scheme 2.8). However, a formation of small amount of (7*Z*)-7-(hydroxyimino)-6,7-dihydro-5*H*-pyrrolo[3,4-*b*]pyridin-5-one (Scheme 2.8, **III**) as a side product was observed during the workup and/or further column purification of the corresponding amidoximes.

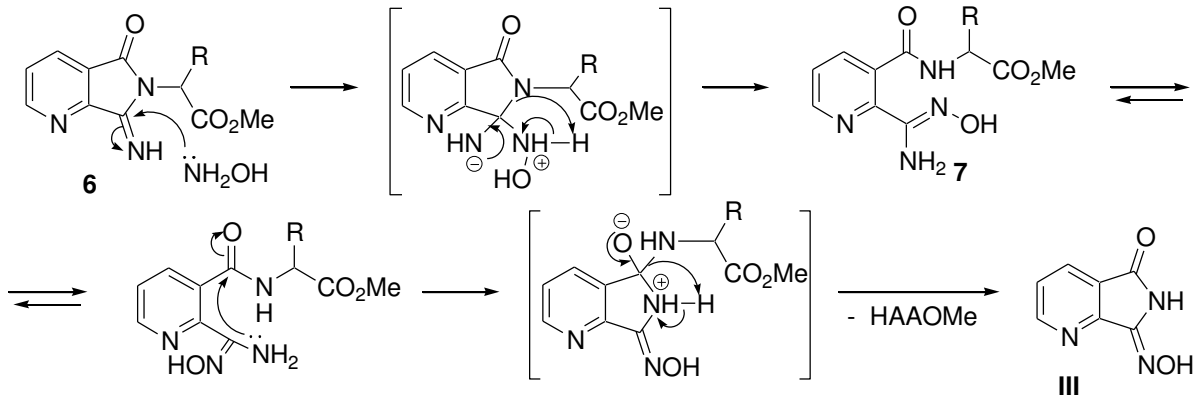

Scheme 2.8 Plausible mechanism of amidoxime **7** and oxime **III** formation *via* pyrrolidine ring opening by hydroxylamine

A precipitation of compound **III** was also observed after long storage or heating the corresponding amidoxime. The LC/MS analytical data detected the ion of oxime **III** as impurity in some cases (**7e,f**) or as a metabolite of the main ion that are assumed to be a result of substance degradation under the LC/MS analysis conditions (gradient elution of H_2O + 0.1% formic acid and MeCN + 0.1% formic acid).

4.3 Synthesis of pyrazine based amidoximes

Recently, amino acid derived pyrazine carboxamides have been synthesized from pyrazine-2,3-dicarboxylic anhydride and amino acids in refluxing toluene, and the conversion was accompanied by decarboxylation along with pyrazine-2,3-dicarboximide formation in some cases.[60] Our studies began with the synthesis of amino acid derived pyrazine-2-carboxamides with amidoxime groups at position 3. The synthesis was carried out in two steps utilizing the strategy elaborated before for the pyridine series[61]: coupling of 3-cyanopyrazine-2-carboxylic acid (**3**) with several methyl esters of L-α-amino acids was followed by further reaction of the obtained nitriles with hydroxylamine hydrochloride.

Esters of (2*S*)-*N*-(3-cyanopyrazin-2-yl)carbonyl substituted amino acids **5'** were prepared by coupling of 3-cyanopyrazine-2-carboxylic acid (**4'**) with commercially available methyl esters of the L-alanine, L-phenylalanine and L-proline amino acids according to a previously developed protocol[61] (Table 2.4). As an activating agent *N*-ethyl-*N'*-(3-dimethylaminopropyl)carbodiimide hydrochloride (EDCI) in the presence of 1-hydroxybenzotriazole (HOBt) was used. As a solvent, tetrahydrofuran instead of dichloromethane was taken due to the low solubility of the starting material in dichloromethane.

Table 2.4 Synthesis of Ala-, Phe-, Pro-containing pseudodipeptides **5'-7'**

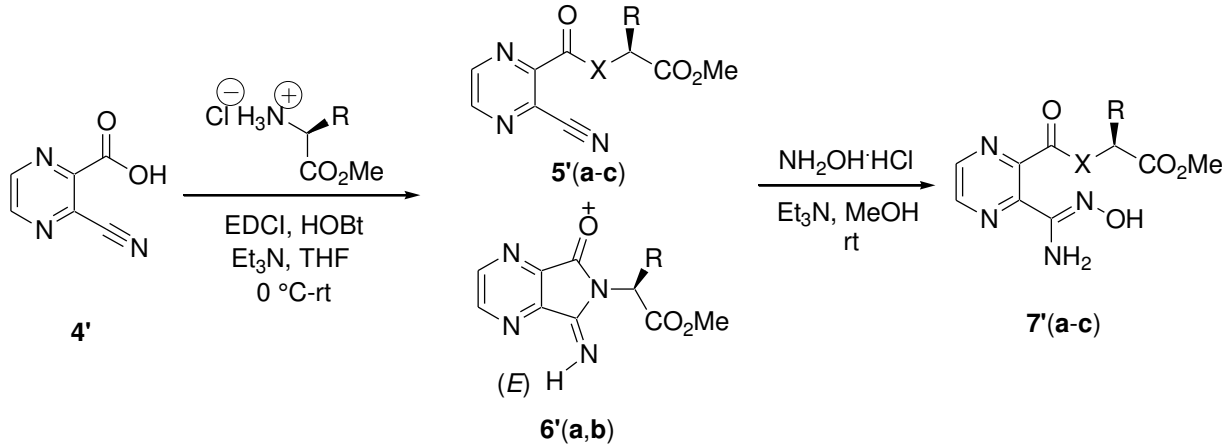

Entry	X	R	**5'** (yield %)[a]	**6'** (yield %)[a]	**7'** (yield %)[a]
1	NH	Me (**a**)	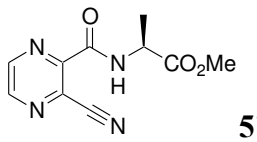 **5'a**	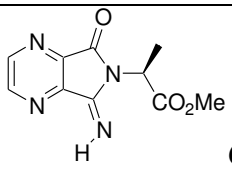 **6'a**	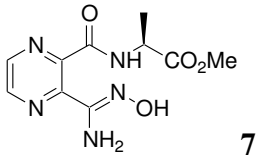 **7'a**
			23%	28%	84%
2	NH	Bn (**b**)	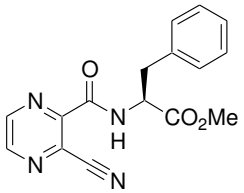 **5'b** 3%	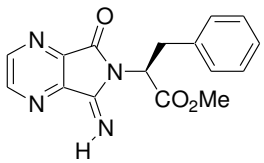 **6'b** 65%	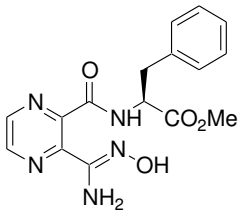 **7'b** 63%
3	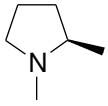 (**c**)		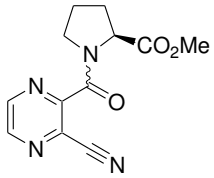 **5c** 49%	-	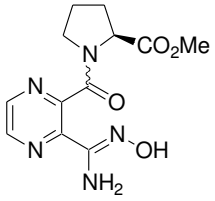

7'c 93%

[a]Isolated yields.

Along with the desired methyl esters of amino acid **5'a**,**b**, a tautomeric pyrrolopyrazine products **6'a**,**b** were produced. Separation and purification of derivatives **5'** and **6'** was achieved by column chromatography and allowed us to isolate the open **5'a**,**b** and cyclic **6'a**,**b** products in different ratios (Table 2.4). When alanine was used, the content of both products **5'a** and **6'a** was approximately the same while in the case of phenylalanine the cyclic form **6'b** largly predominated. The coupling with proline methyl ester necessarily afforded only the open-chain pyrazine derivative **5'c** in 49% yield.

The IR spectra of **5'a**-**c** showed a characteristic cyano group absorption band at 2240, 2237 and 2239 cm^{-1}, respectively. By analogy to the pyridine counterparts, the ^1H NMR spectra of the coupling products **5'**, **6'** revealed NH proton resonances at δ = 8.26 and 8.20 ppm for the open-chain compounds **5'a**,**b**, and a downfield shift of δ = 9.51 and 9.46 ppm for the tautomeric cyclic derivatives **6'a**,**b**. The values are very close to the values of those for the pyridine series 9.34 (Ala derivative **6a**) and 9.29 (Phe derivative **6b**) ppm (see Table 1).[61] Therefore, one could conclude by analogy with [61] that pyrrolopyrazines **6'a**,**b** adopt the *E* configuration at the C=N exocyclic bond and *syn* orientation of the NH proton to the heterocyclic ring.

Amidoximes **7'** could be prepared efficiently from single compounds **5'** or **6'** as well as from the mixture of **5'** and **6'** in a reaction with hydroxylamine hydrochloride (Table 2.4). Thus, as in the case of the pyridine analogs, the products **7'** were formed as a result of addition to nitriles **5'** as well as pyrrolidine ring opening of pyrrolopyrazines **6'**.

The ^1H NMR spectra of the amidoximes **7'** revealed a chemical shift of δ = 5.45 ppm for the NH_2 protons of the alanine derivative and δ = 5.82 ppm for the phenylalanine one.

X-Ray diffraction analysis of the amidoxime **7'b** (Figure 2.5) revealed *Z* configuration at C=N bond of the amidoxime group similarly to the pyridine analog **7b**. However, unlike for the pyridine derivative **7b**, the NH group of the pyrazine compound **7'b** is projected more inward (NH…N distance is 3.14 Å, NH…N angle 78°).

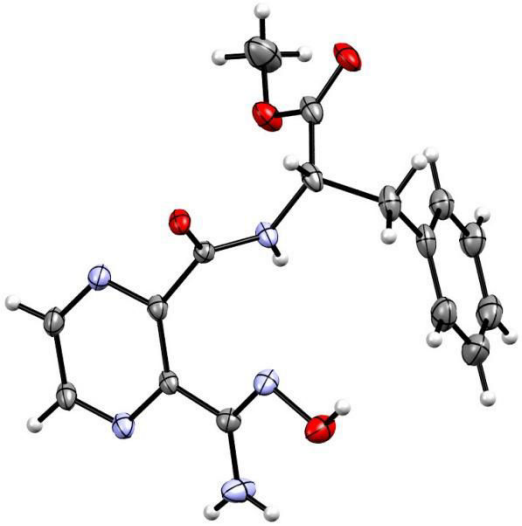

Figure 2.5 Molecular structure of methyl (2*S*)-2-({[3-(*N*′-hydroxycarbamimidoyl)pyrazin-2-yl]carbonyl}amino)-3-phenylpropanoate **7'b** according to results of the X-ray diffraction study; thermal ellipsoids are shown at 50% probability level

The formation of (7*Z*)-7-(hydroxyimino)-6,7-dihydro-5*H*-pyrrolo[3,4-*b*]pyrazin-5-one as a side product was observed only after long storage of the pyrazine amidoximes **7'**. Moreover, in our attempts to grow a crystal of **7'a** we were able to obtain the crystal of the corresponding pyrrolo[3,4-*b*]pyrazin-5-one oxime **IV** as a by-product (Figure 2.6).

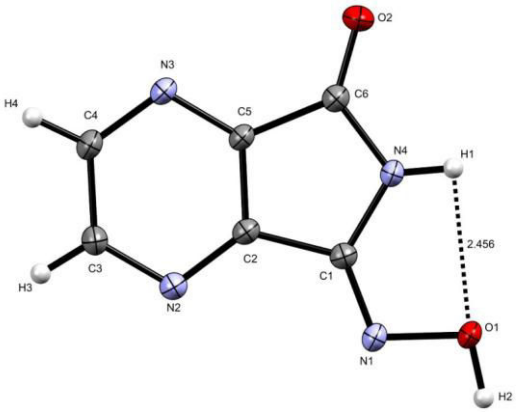

Figure 2.6 Molecular structure of (7*Z*)-7-(hydroxyimino)-6,7-dihydro-5*H*-pyrrolo[3,4-*b*]pyrazin-5-one **IV** according to results of the X-ray diffraction study, with the atom numbering used in the crystallographic analysis; thermal ellipsoids are shown at 50% probability level

As follows from the X-Ray crystallography data, compound **IV** adopts the *Z* configuration at the C=N bond. The molecule has a shot contact between H1-O1 2.43 Å (this

is shorter than the sum of the van der Waals radii of hydrogen and oxygen atoms which is 2.72 Å).

In addition, all compounds **5'**, **6'** and **7'** and reaction conditions were compared with similar ones from the pyridine series that were described previously (**5**-**7**, Table 2.5).[61] The coupling reaction proceeded easily for pyridine analogs in contrast to pyrazine ones because of a low solubility of the latter that led to decreased yields (Table 2.5). The EDCI/HOBt protocol was applied in both cases with the difference in solvents, DCM was used for the coupling with 2-cyanonicotinic acid (**4**) and THF was found to be the best solvent for 3-cyanopyrazine-2-carboxylic acid (**4'**). The ratio of isolated isomeric Ala-containing open form **5'a** and cyclic pyrrolopyrazines **6'a** vary as in the case of cyanonicotinic acid **4**. But when Phe was coupled, we succeed in isolation of a small portion of open form **5'b** along with a majoring pyrrolopyrazine **6'b** unlike for 2-cyanonicotinic acid (**4**) where only the cyclic pyrrolopyridine analog **6b** was obtained.

The comparison of NH proton signals in the ^{1}H NMR spectra of the pyridine and pyrazine derivatives **5**, **5'** revealed a low field shift above 1 ppm for the pyrazine compounds probably due to possible NH…N hydrogen bonding or an NH...π interaction[62,63] that was absent in the case of pyridine core.

Table 2.5 Comparison of compounds **5**, **5'** (**a**,**b**) and **6**, **6'** (**a**,**b**)

Pyrazine derivative	**ν_{max} CN (cm^{-1})**	**δ NH (ppm)**	**yield[a], % (THF)**	**Pyridine derivative**	**ν_{max} CN (cm^{-1})**	**δ NH (ppm)**	**yield[a], % (DCM)**
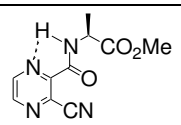 **5'a**	2240	8,26[b]	23	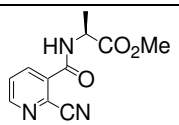 **5a**	2240	7,15[d]	15
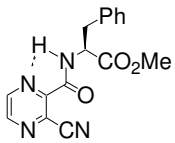 **5'b**	2237	8,20[c]	3	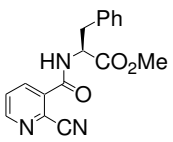 **5b**	-[e]	-[e]	-[e]
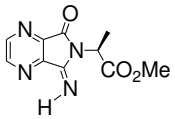 **6'a**	-	9,51	28	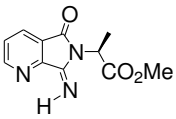 **6a**	-	9,34	58

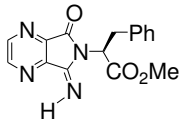 **6'b**	-	9,46	68	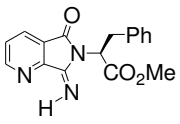 **6b**	-	9,29	76

[a] Isolated yield. [b] d, *J* = 7.4 Hz. [c] d, *J* = 7.9 Hz. [d] d, *J* = 5.7 Hz. [e] Not isolated.

The general tendency for pyrrolidine ring opening of **6'** by hydroxylamine to afford the open-chain amidoximes **7'** was observed; the same structures were obtained from the corresponding cyano esters **5'** similar to the formation of pyridine based amidoximes **7**.

Additionally, we decided to extend this protocol in order to synthesize novel pseudotripeptide with the *N*-terminal pyrazine amidoxime motif in the backbone. Proline-phenylalanine dipeptide was chosen to discover the steric effects of the *C*-terminal substitution in proline on the amide isomer equilibrium of the model prolyl surrogate. Likewise, *o*-substitution in non-peptidic fragment with dipeptide can provide additional conformational rigidity.

The target molecule was prepared utilizing the same strategy elaborated for nicotinic and pyrazinic acids based pseudodipeptides bearing an amidoxime residue.[61,64] A synthetic route to desired pseudotripeptide is shown in Scheme 11. The H-Pro-Phe-OMe dipeptide was synthesized by coupling reaction of Boc-protected L-proline and hydrochloride of H-Phe-OMe amino acid using EDCI in the presence of HOBt with further Boc-deprotection (Scheme 2.9, a). Subsequent coupling of acid **4'** with H-Pro-Phe-OMe, employing HATU/HOBt strategy to form the peptide bond, afforded the corresponding nitrile **5'd** in 68% yield. Treatment of the nitrile **5'd** with hydroxylamine hydrochloride in the presence of triethylamine allowed us to obtain amidoxime **7'd** in good yield (Scheme 2.9, b).

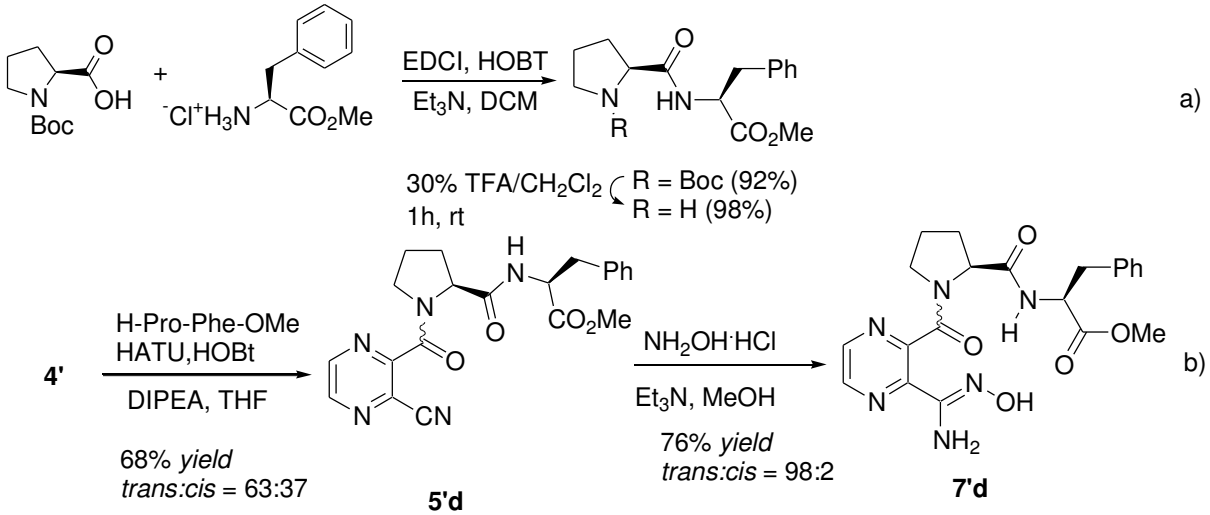

Scheme 2.9 Synthesis of pseudotripeptide **7'd**

Structural properties of the pseudotripeptide **7'd** have been investigated in order to determine its use in future applications (see Chapter 3).

5. Studies towards the synthesis of 1,2,4-oxadiazoles *via* amidoxime ester units

The 1,2,4-oxadiazole motif is an attractive heterocycle contained in many pharmaceuticals with widespread biological applications.[65,66] 1,2,4-Oxadiazole ring have long been known as isosteric replacement of the amide and/or ester group due to its high resistance to metabolic degradation.[67,68] A number of nonproteinogenic α-amino acid-derived 1,2,4-oxadiazoles have been utilized in the design of mimetics, as peptidomimetic building blocks,[69-73] dipeptidyl peptidase IV (DPP-4) inhibitors (**A**),[74] inhibitors of the Src SH2 domain (**B**),[75,76] sphingosine kinase inhibitors (**C**)[77,78] and immunomodulators (**D**)[79] (Figure 2.7).

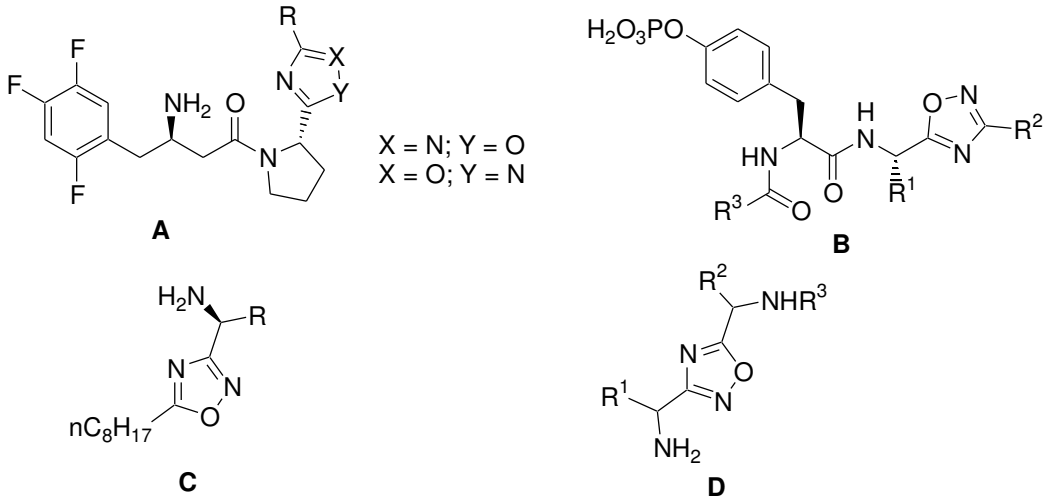

Figure 2.7 Representative bioactive compounds containing α-amino acid-derived 1,2,4-oxadiazoles

Therefore, we were interested in introducing the 1,2,4-oxadiazole ring into pyridine(pyrazine)-based peptidomimetics by transformation of the present amidoxime function (Scheme 2.10).

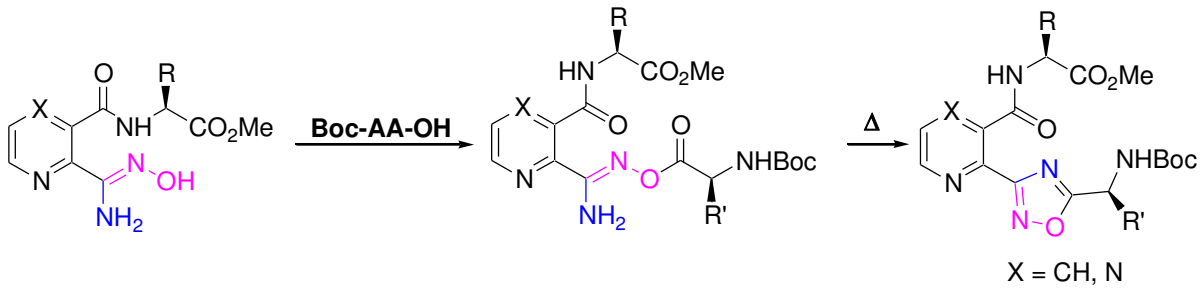

Scheme 2.10 Proposed route to amino acid derived 1,2,4-oxadiazoles

On the other hand, esterification and/or condensation of amidoximes presents a route towards the novel double prodrugs of amidines.[29,80,81] Hence, the synthesis and characterization of novel esterified amidoximes and 1,2,4-oxadiazoles are topics of our great interest. Additionally, we briefly describe an overview of synthetic approaches to 3,5-disubstituted 1,2,4-oxadiazoles.

5.1 Overview of synthetic approaches to 3,5-disubstituted 1,2,4-oxadiazoles *via* amidoxime esters

1,2,4-Oxadiazoles can generally be formed by the reaction of an amidoxime with a carboxylic acid or acid chloride followed by an intramolecular cyclodehydration (Scheme 2.11).[65,82,83]

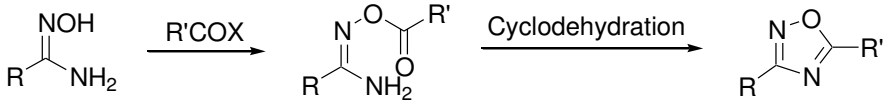

Scheme 2.11 Classical route to 1,2,4-oxadiazoles

The synthesis can be performed with the isolation of acylated intermediate in two steps or as a one-pot reaction without isolating the ester.

The two steps general route was followed for the preparation of 1,2,4-oxadiazole intermediates to inhibitor **B** (Figure 2.7).[75] Amidoximes were coupled to the appropriate amino acid derivatives, giving the intermediate *O*-acylamidoxime which underwent cyclization in refluxing pyridine followed by Boc deprotection (Scheme 2.12).

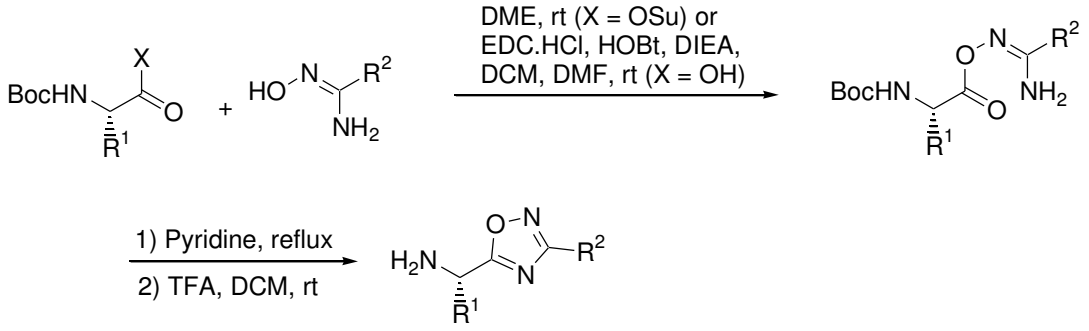

Scheme 2.12 1,2,4-Oxadiazoles synthesis reported by Buchanan *et al.* [75]

A library of twenty 1,2,4-oxadiazoles in a range of electron-rich and electron-poor benzamidoximes and both aromatic and aliphatic carboxylic acids was synthesized in a one-

pot procedure (Scheme 2.13).[84] The authors used 1,1'-carbonyldiimidazole (CDI) as a reagent for both formation and cyclodehydration of *O*-acyl benzamidoximes.

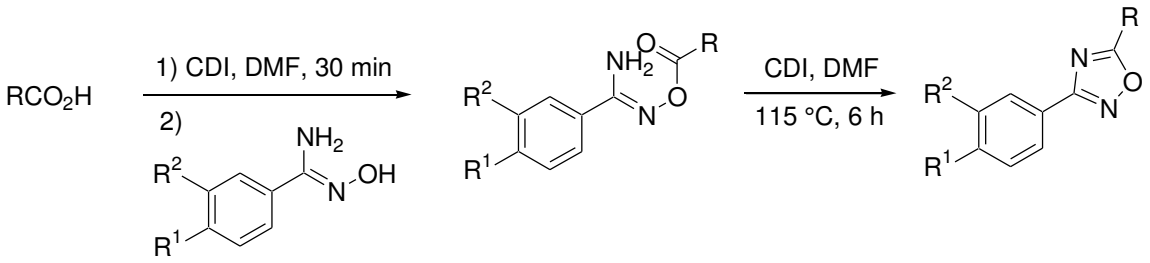

Scheme 2.13 1,2,4-Oxadiazoles synthesis reported by Deegan *et al.* [84]

Hamzé *et al.* succeeded in the synthesis of 1,2,4-oxadiazole-containing β^3-amino acids (Scheme 2.14).[85] Several coupling and cyclization conditions have been exemined. The use of DIC/HOBt for coupling step and sodium acetate in refluxing EtOH/H_2O for cyclic dehydration of acyl amidoxime was found to be the most suitable methods genereting oxadiazole compounds in good yields (50-84%).

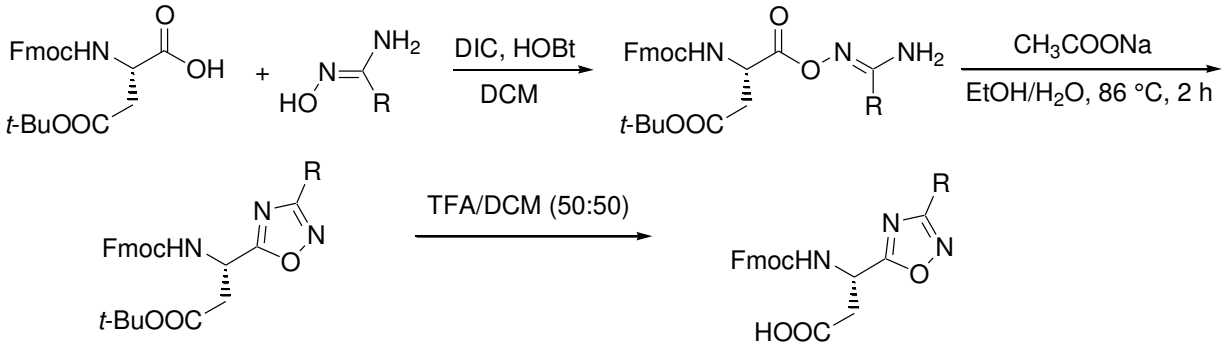

Scheme 2.14 1,2,4-Oxadiazoles synthesis reported by Hamzé *et al.* [85]

Similar methods were applied by authors for the synthesis of 1,2,4-oxadiazoles bearing α-amino acids.

Hébert and co-workers employed solid phase synthesis to prepare a library of 1,2,4-oxadiazoles (Scheme 2.15).[51] Amidoximes bound to the HMPA resin were first acylated with Boc or Fmoc protected amino acid anhydrides generated *in situ* from the amino acids and DIC in 2-methoxyethyl ether to give *O*-acylamidoximes. The cyclization of latter at 85 °C afforded resin bound oxadiazole compounds.

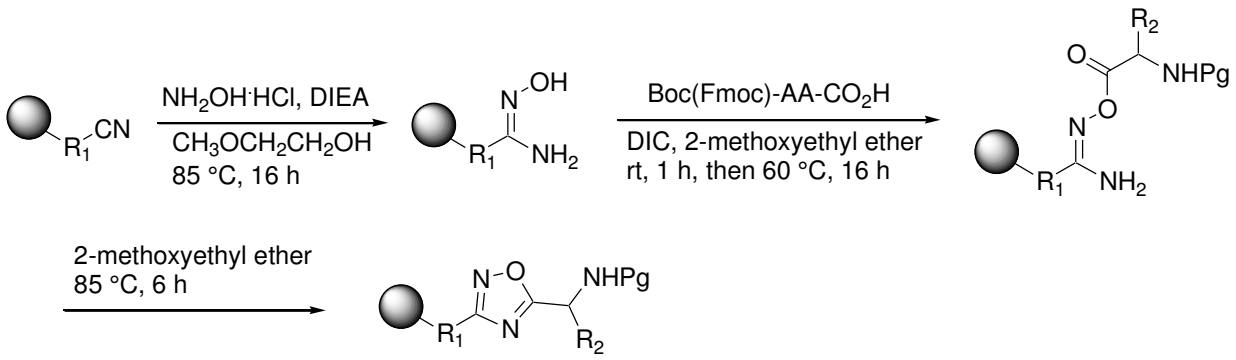

Scheme 2.15 1,2,4-Oxadiazoles synthesis reported by Hébert *et al.* [51]

Braga *et al.* described a convenient one-pot synthesis of chiral *N*-protected *α*-amino acid-derived 1,2,4-oxadiazoles, in which activation of the carboxylic acid moiety occurs in the presence of DCC with further acylation of the amidoxime in dioxane as solvent (Scheme 2.16).[86] The formed *O*-acylamidoximes immediately underwent a cyclodehydration reaction when heating to 100 °C for 8 h, delivering the 1,2,4-oxadiazole derivatives in good yields.

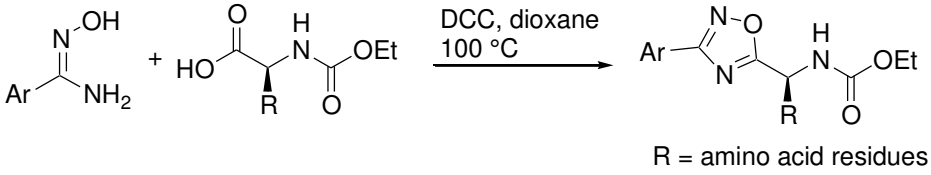

Scheme 2.16 1,2,4-Oxadiazoles synthesis reported by Braga *et al.* [86]

Another coupling method was used by Katritzky and co-workers using *N*-protected (*α*-aminoacyl)benzotriazoles to achieve the synthesis of chiral 1,2,4-oxadiazoles (Scheme 2.17).[87] The *O*-acylation of amidoximes with benzotriazole derivatives occurred immediately after treatment with Et_3N (1 eq.) in EtOH at room temperature. Subsequent refluxing of intermediates in EtOH in the presence of Et_3N proceeded quickly with the cyclization into 1,2,4-oxadiazoles in 70-94% yield with good (>97%) retention of chirality.

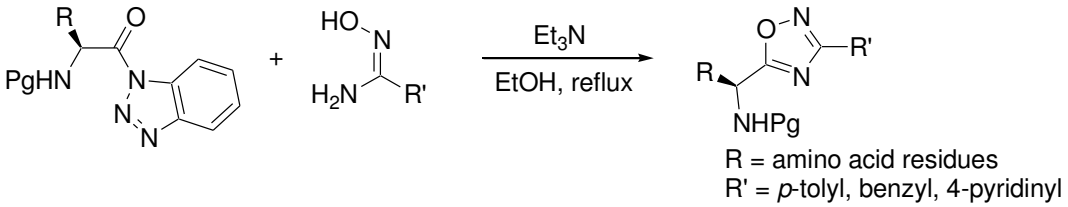

Scheme 2.17 1,2,4-Oxadiazoles synthesis reported by Katritzky *et al.* [87]

The 1,2,4-oxadiazole precursors of DPP-4 inhibitors **A** were synthesized from a suitable amidoximes and carboxylic acids by condensation using DIC for activation with subsequent cyclization employing intensive reflux conditions in pyridine (Scheme 2.18).[74]

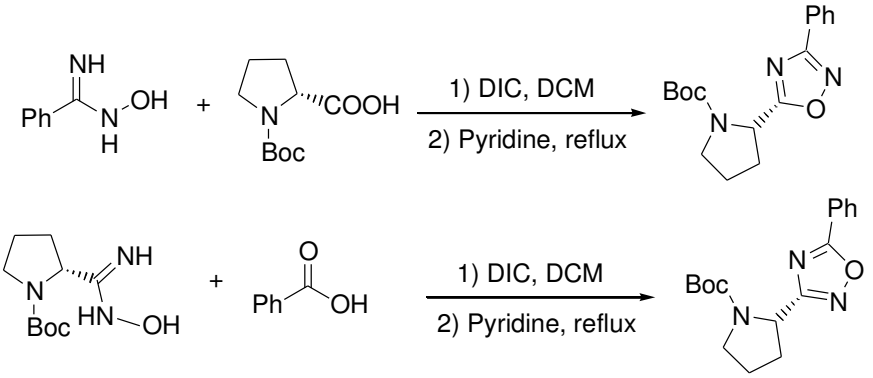

Scheme 2.18 1,2,4-Oxadiazoles synthesis reported by Nordhoff *et al.* [74]

Sureshbabu *et al.* performed the one-pot synthesis of 1,2,4-oxadiazole-linked orthogonally urethane-protected dipeptide mimetics (Scheme 2.19).[70] N-Protected amino acyl fluorides were first coupled to amino acid-derived amidoximes in presence of NMM in ethanol. After 15 min, an equimolar quantity of NaOAc was added and the reaction mixture was refluxed for 3 h. The resulting 1,2,4-oxadiazolyl dipeptides were isolated after workup followed by purification in a yield exceeding 60%.

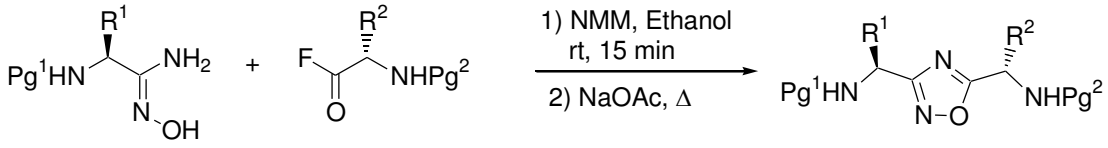

Pg^1 = Boc, Z
Pg^2 = Fmoc, Boc, Z
R^1, R^2 = amino acid residues

Scheme 2.19 1,2,4-Oxadiazoles synthesis reported by Sureshbabu *et al.* [70]

Jakopin prepared novel 1,2,4-oxadiazole-containing derivatives of L-Ala-D-Glu and L-Ala-D-iGln dipeptides by acetylation of the mono and diamidoxime compounds (Scheme 2.20).[73] The *O*-acetyl intermediates were then subjected to a fluoride-catalyzed cyclodehydration, affording the 1,2,4-oxadiazole-based peptidomimetic building blocks.

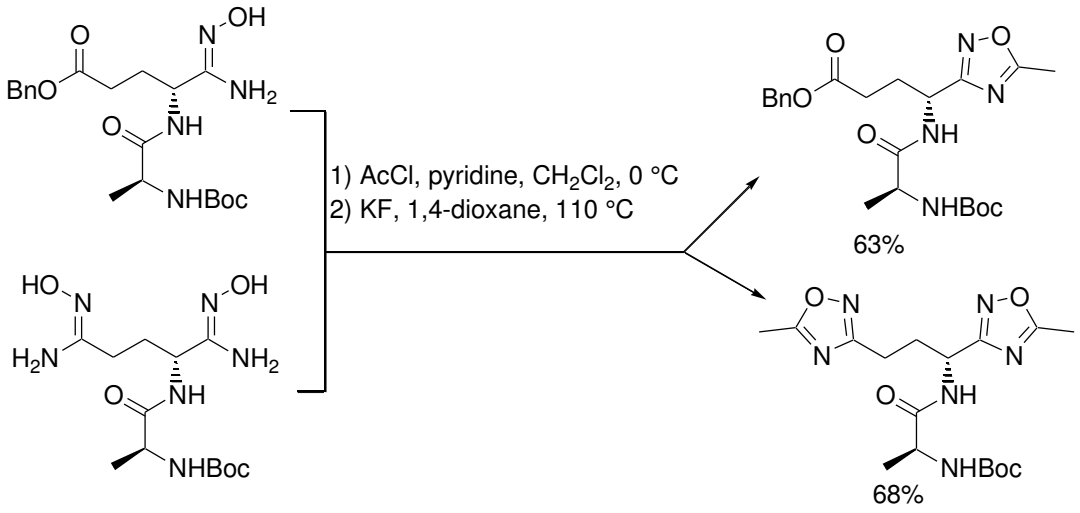

Scheme 2.20 1,2,4-Oxadiazoles synthesis reported by Jakopin [73]

The one-pot procedure was also used by the same laboratory for the synthesis of other peptidomimetics.[69]

In some cases prolonged heating at high temperatures is the reason for the low yield of the desired products or their total absence. Consequently, approaches have been proposed for improvement of the cyclodehydration: the use of basic reagents, microwave irradiation or ultrasound.

Gangloff *et al.* found that in the presence of tetrabutylammonium fluoride (TBAF) at room temperature alkanoyl- and aroyloxyamidines were converted to the corresponding 3,5-disubstituted-1,2,4-oxadiazoles (Scheme 2.21).[88]

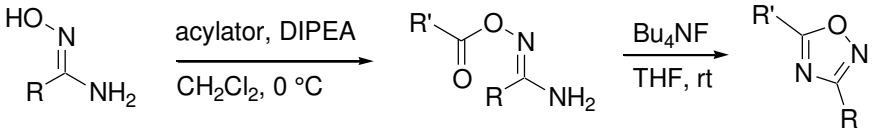

Scheme 2.21 1,2,4-Oxadiazoles synthesis reported by Gangloff *et al.* [88]

The numerous acyl amidoximes were examined in different concentration of TBAF in THF (from 0.1 to 1.0 equivalent) affording the 1,2,4-oxadiazole derivatives in high yields.

Synthesis of a new generation of chroman/catechol hybrids bearing 1,2,4-oxadiazole with using tetrabutylammonium fluoride as a mild and efficient catalyst was reported by Koufaki and co-workers (Scheme 2.22).[89] Specifically, *N*-hydroxysuccinimidyl-trolox ester reacted with the appropriate amidoxime to give the acyl amidoximes. Subsequent

intramolecular cyclization in the presence of TBAF produced the 3,5-disubstituted 1,2,4-oxadiazole derivatives.

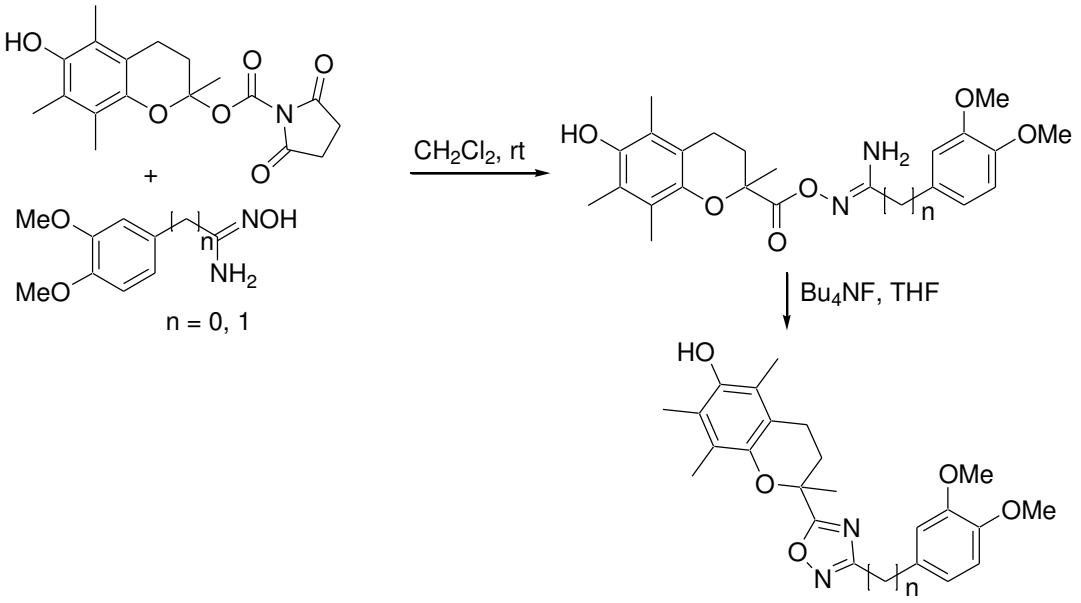

Scheme 2.22 1,2,4-Oxadiazoles synthesis reported by Koufaki *et al.* [89]

Oxadiazole-containing precursors of sphingosine kinase 2 inhibitors were synthesized in one pot by Congdon *et al.* (Scheme 2.23).[90] The treatment of HCTU-activated Boc-L-proline with the appropriate amidoxime and subsequent TBAF-mediated cyclization resulted in the formation of 1,2,4-oxadiazoles.

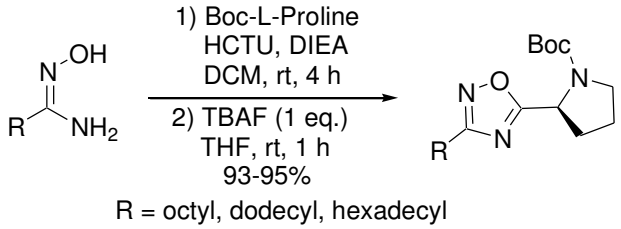

Scheme 2.23 1,2,4-Oxadiazoles synthesis reported by Congdon *et al.* [90]

The use of TBAF as a mild and efficient reagent for the cyclodehydration of acylated amidoximes on the solid support has been performed by Rice and Nuss (Scheme 2.24).[50]

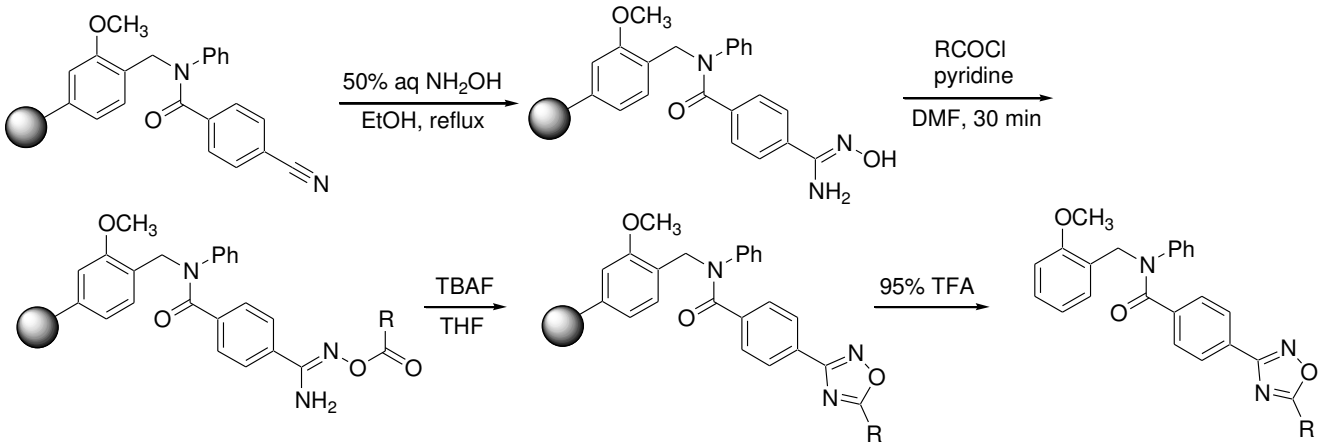

Scheme 2.24 1,2,4-Oxadiazoles synthesis reported by Rice and Nuss [50]

Amidoximes bound to Agropore MB-CHO resin were converted to *O*-acylamidoximes using a range of acid chlorides. Subsequent treatment with TBAF (2.2 eq.) in THF over 12 h under ambient conditions gave a library of 1,2,4-oxadiazoles. Cleavage of the desired products from resin was carried out using 95% TFA yielding 1,2,4-oxadiazoles in 70% or greater purity.

The alternative basic reagent has been suggested recently by Otaka (Scheme 2.25).[91] 3,5-Disubstituted 1,2,4-oxadiazoles with a wider range of functionality have been obtained in good yields utilizing tetrabutylammonium hydroxide (TBAH). Reaction times were reduced compared with those of TBAF and this catalyst does not lead to corrosion of reaction vessels.

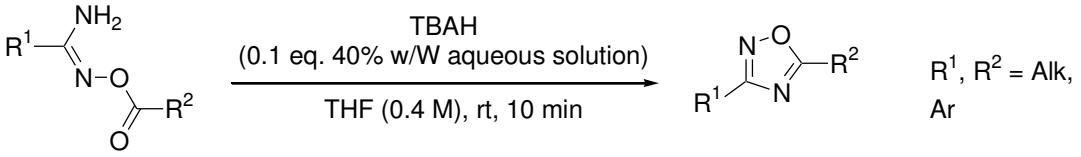

Scheme 2.25 1,2,4-Oxadiazoles synthesis reported by Otaka *et al.* [91]

An efficient method for DBU-catalyzed cyclization of acylamidoximes was developed by Lukin and Kishore to promote the formation of 1,2,4-oxadiazoles in 85-97% yield (Scheme 2.26).[92] The one-pot transformation was effected by CDI to form imidazolides of carboxylic acids followed by cyclodehydration in the presence of DBU at 60 °C for 1.5-2 hours.

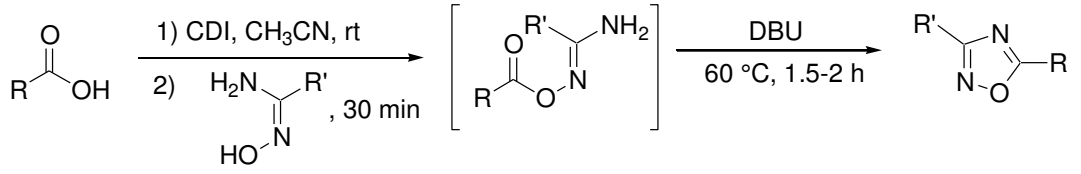

Scheme 2.26 1,2,4-Oxadiazoles synthesis reported by Lukin and Kishore [92]

Another base, caesium carbonate, was used by Lloyd and co-workers to promote the formation of 1,2,4-oxadiazole-based precursor to pyrazolodihydropyrimidines as potent and selective KV1.5 blockers (Scheme 2.27).[93]

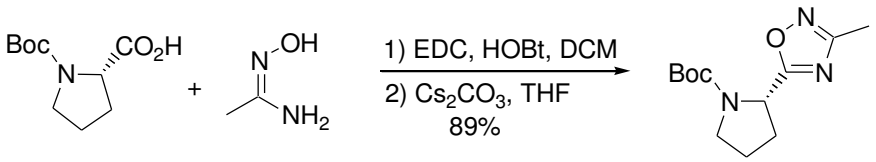

Scheme 2.27 1,2,4-Oxadiazoles synthesis reported by Lloyd *et al.* [93]

Mono- and bis-1,2,4-oxadiazoles were prepared in one-pot by the method reported by Amarasinghe *et al*. (Scheme 2.28).[94] The condensation of carboxylic acid esters and amidoximes in refluxing toluene in the presence of potassium carbonate was employed to synthesize a variety of oxadiazoles in moderate to excellent yields.

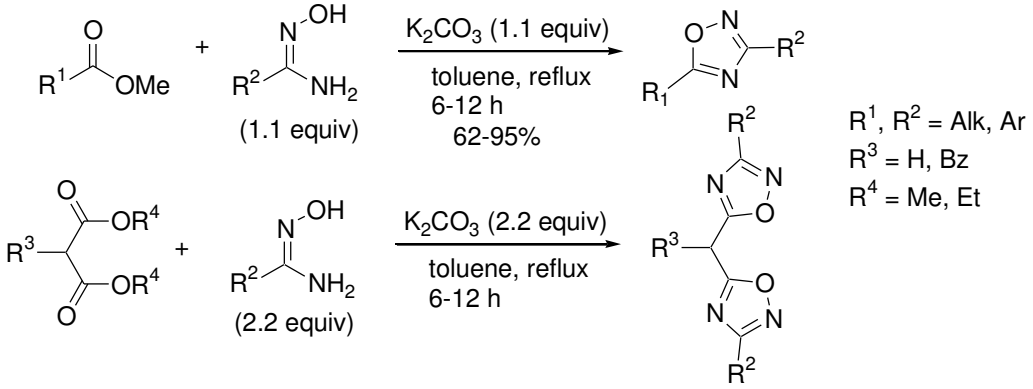

Scheme 2.28 1,2,4-Oxadiazoles synthesis reported by Amarasinghe *et al.* [94]

The different bases were also discovered by Baykov *et al.* who found that the superbase system MOH/DMSO (M = Li, Na, K) is an efficient route to the cyclodehydration of *O*-acylamidoximes to afford 3,5-disubstituted 1,2,4-oxadiazoles in good yields (Scheme 2.29).[95]

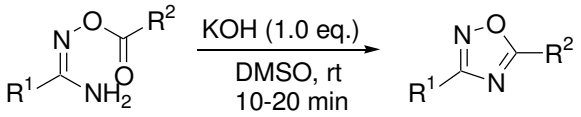

Scheme 2.29 1,2,4-Oxadiazoles synthesis reported by Baykov *et al.* [95]

The application of microwave energy can be employed to shorten reaction times and/or increase product purities and yields and to decrease formation of side products.[82,96]

The one-pot microwave-assisted synthesis of variously disubstituted 1,2,4-oxadiazoles including amino acid-derived 1,2,4-oxadiazoles with 100% enantiomeric purity was discovered by Porcheddu *et al.* (Scheme 2.30).[97]

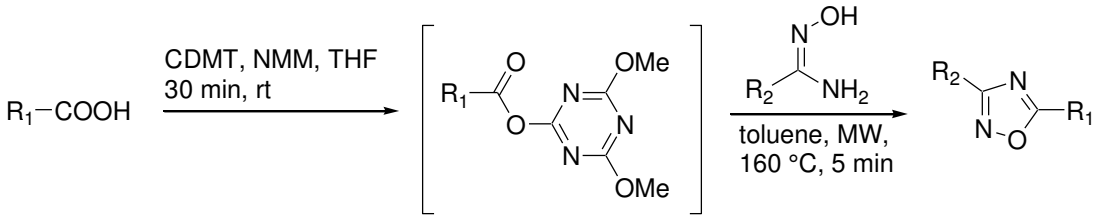

Scheme 2.30 Microwave-assisted synthesis of 1,2,4-oxadiazoles reported by Porcheddu *et al.* [97]

The starting acid was first treated with 2-chloro-4,6-dimethoxy-1,3,5-triazine (CDMT) and NMM in THF for 30 min at room temperature. The corresponding amidoxime and toluene were then added to the activated ester and the reaction mixture was irradiated for 5 min to afford 1,2,4-oxadiazoles in 62-95% yield.

A microwave-assisted synthesis of 2-trifluoroacetylthiophene oxadiazoles as potent and selective class II human histone deacetylase (HDAC) inhibitors was achived by Muraglia *et al.* using 5-(trifluoroacetyl)thiophene-2-carboxylic acid activated with CDI and different amidoximes (Scheme 2.31).[98] A further equivalent of CDI and microwave irradiation at 140 °C for 2 min gave the oxadiazole inhibitors.

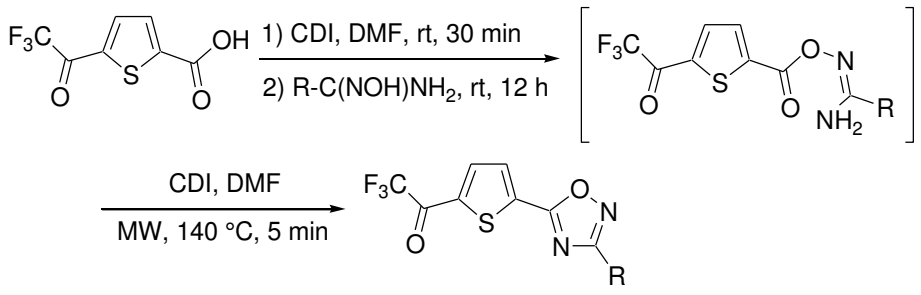

Scheme 2.31 Microwave-assisted synthesis of 1,2,4-oxadiazoles reported by Muraglia *et al.* [98]

Wang *et al.* combined the use of commercially available polymer-supported reagents with microwave heating to prepare libraries of 1,2,4-oxadiazoles (Scheme 2.32).[99]

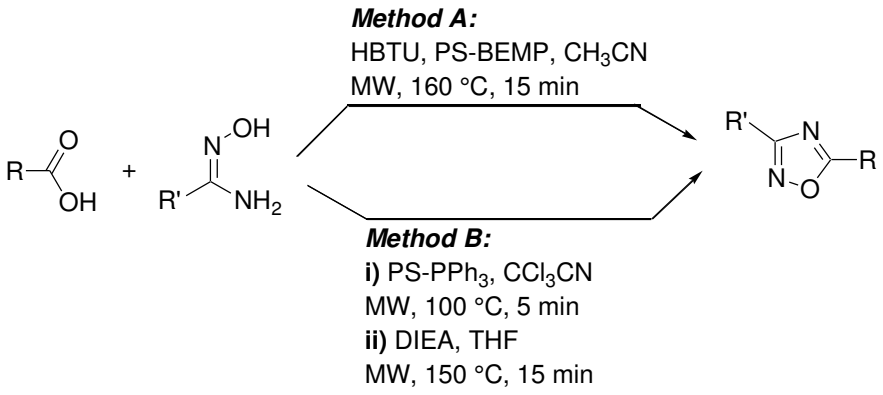

Scheme 2.32 Microwave-assisted synthesis of 1,2,4-oxadiazoles reported by Wang *et al.* [99]

An ultrasound-promoted synthesis of 3-trichloromethyl-5-alkyl(aryl)-1,2,4-oxadiazoles was achieved by Bretanha and co-workers using trichloroacetoamidoxime and acyl chlorides (Scheme 2.33).[100] The compounds were prepared in better yields and shorter reaction times compared to the conventional method.

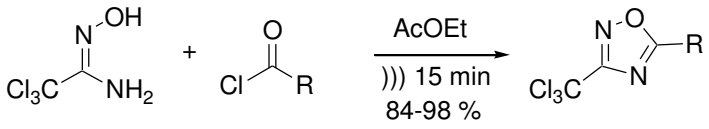

Scheme 2.33 Ultrasound-promoted synthesis of 1,2,4-oxadiazoles reported by Bretanha *et al.* [100]

A novel ionic liquid-phase strategy toward 3,5-disubstituted 1,2,4-oxadiazoles was developed by Duchet *et al.* for application in solution-phase combinatorial synthesis (Scheme 2.34).[52] The arylnitrile bound to the ionic liquid moiety (1-(2-hydroxyethyl)-3-methyl imidazolium hexafluorophosphate ([HOC_2mim][PF_6])) was chosen as task-specific ionic liquid (TSIL). The starting ionic liquid-phase (ILP) was produced from 1-methylimidazole and 2-chloroethanol. The esterification of 4-cyanobenzoic acid activated with DCC was followed by the reaction with hydroxylamine to obtain the arylamidoxime functionalized ILP. Acylation of amidoximes with a series of aliphatic, aromatic and heteroaromatic carboxylic acids in the presence of DCC and DMAP provided the target ILP bound O-acyl amidoximes. The cyclization of the latter to 1,2,4-oxadiazoles grafted on the ionic liquid phase, was carried out in deionized water for 24 h under reflux. Complete cleavage of the compounds was achieved by treatment with MeONa in refluxed methanol.

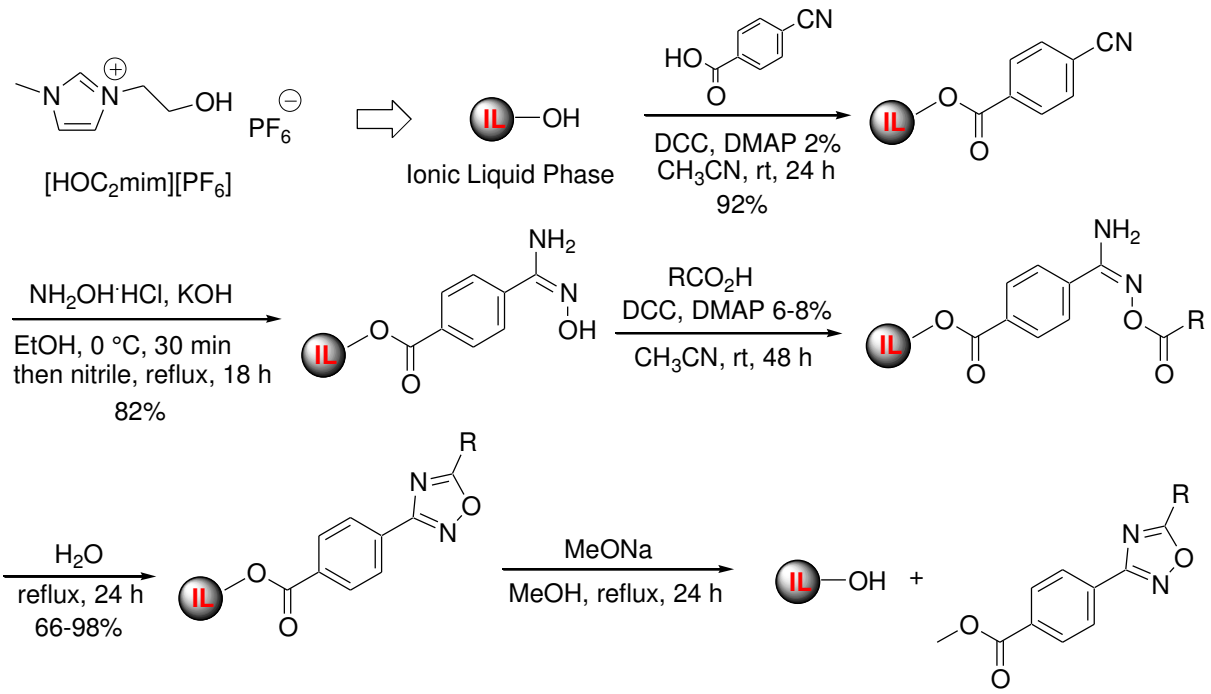

Scheme 2.34 Ionic liquid-phase strategy toward1,2,4-oxadiazoles reported by Duchet *et al.* [52]

5.2 Acylation of amidoximes with further conversion into amino acid derived 1,2,4-oxadiazoles

We describe herein an easy microwave assisted synthetic route for the preparation of a new variety of chiral α-amino acid derived 1,2,4-oxadiazoles. The following two-step reaction led to the desired 1,2,4-oxadiazoles **9**, **9'** which were submitted to the ring formation under microwave irradiation of the intermediate acylated amidoximes **8**, **8'** (Table 2.6). Firstly, Boc-protected L-valine was esterified with the corresponding amidoximes **7**, **7'** (**a**,**b**) using DCC/DMAP in anhydrous acetonitrile to obtain *O*-acyl amidoximes **8**, **8'** (**a**,**b**) in good yields. Recently, it has been shown that conjugation of amidoximes with L-valine amino acid can enhance water solubility and bioavailability of the molecules, thus the latter was employed as one of the carboxylic residues.[80]

Table 2.6 Synthesis of 1,2,4-oxadiazoles pseudopeptides **9**, **9'** (**a**,**b**)

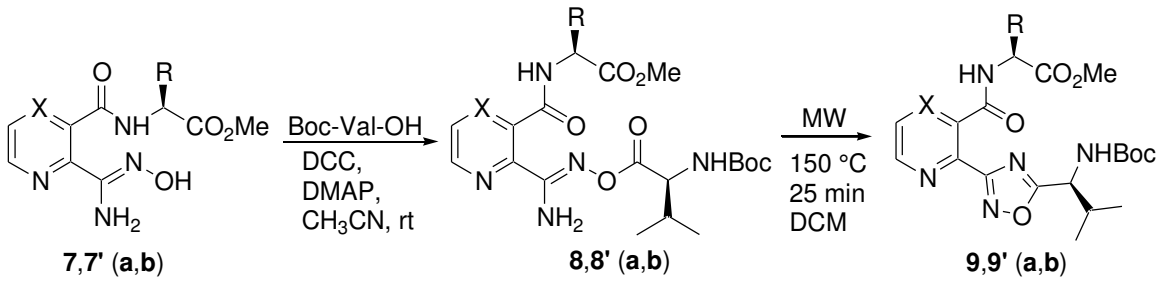

7,**7'** (**a**,**b**) **8**,**8'** (**a**,**b**) **9**,**9'** (**a**,**b**)

Entry	X	R		8, 8' (yield, %)[a]	9, 9' (yield, %)[a] (conversion, %)[b]
1	CH	Me (Ala)	**a**	64	63 (66)
2	CH	Bn (Phe)	**b**	91	81 (83)
3	N	Me (Ala)	**a**	84	75 (77)
4	N	Bn (Phe)	**b**	67	94 (96)

[a]Isolated yield.
[b]Conversion is determined by crude LC/MS.

Heating esters **8**, **8'** (**a**,**b**) under microwave irradiation afforded the 1,2,4-oxadiazoles **9**, **9'** (**a**,**b**) in high yields (Table 2.6). Different solvents, temperatures and prolonged heating were explored in order to provide the best conversion. Phenylalanine derivative **8'b** was selected as a model compound. The results are summarized in Table 2.7. The reaction in dichloromethane at 150 °C for 25 min under microwave heating afforded the highest conversion in the shortest time as judged by LC/MS analysis (entry 3).

Table 2.7 Optimization of microwave assisted condensation conditions for **8'b** as a model compound

Entry	Solvent	T, °C	Time, min	Conversion of 8'b, %[a]
1	CH_3CN	160	50	85
2	THF	150	50	77
3	DCM	150	25	96
4	DMF	150	60	49

[a]Conversion is determined by crude LC/MS.

To the best of our knowledge, the synthesis of 1,2,4-oxadiazolylpyridines(pyrazines) with amino acid substituted heteroaromatic and a chirally substituted 1,2,4-oxadiazole ring is unprecedented. The only examples of pyridines and pyrazines bearing 1,2,4-oxadiazole with proline [74,101-103] and phenylalanine [104] unit have been described recently.

L-phenylalanine amino acid was introduced into proline derivatives **7c** and **7'c** in order to investigate a propensity for *cis* amide bonds which is high when Pro is preceeded by an aromatic residue.[105] This is considered as a stabilizing Ar-Pro interaction in the *cis* conformation. Hence, the amidoximes **7c**, **7'c** were reacted with Boc-protected phenylalanine

to produce Phe-amidoxime esters **8c** and **8'c** in quantitative yields (Table 2.8). Further condensation under MW heating of the solution of **8c**, **8'c** in DCM (closed vessel, 300W, 150 °C, 25 min) delivered the 1,2,4-oxadiazole derivatives **9c** and **9'c** in 58% and 76% yields respectively.

Table 2.8 Synthesis of 1,2,4-oxadiazoles pseudopeptides with proline residue

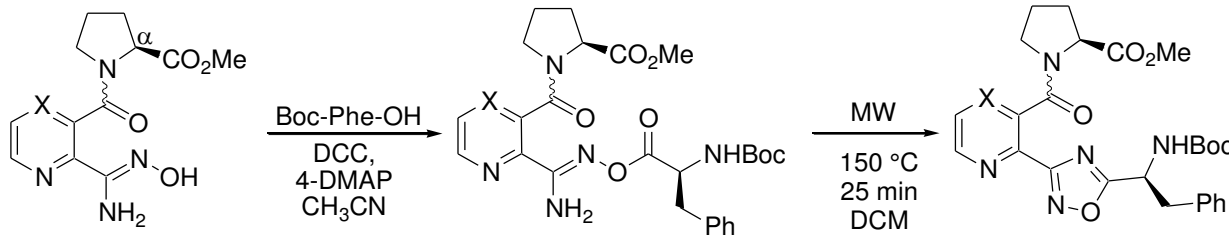

7,7' c **8,8' c** **9,9' c**

Entry	X		Yield, %	Conversion, %
1	CH	**8c**	quantitative	-
2	CH	**9c**	58	65
3	N	**8'c**	quantitative	-
4	N	**9'c**	76	80

Indeed, the population of the molecules **8c**, **8'c** in the *cis* conformation was slightly increased relative to that in **7c**, **7'c** (see Chapter 3).

6. Studies towards the synthesis of 1,2,4-triazoles *via N*-acylamidrazones

The 1,2,4-triazole scaffold displays a wide range of biological activities and can be used as amide bond replacement (isoster) in order to enhance stability towards proteolysis and introduction of rigidity that has been widely used in peptide mimicry.[106-108] This ring system can act as both hydrogen bond acceptor and donor which makes it useful in establishing intermolecular features in interactions between peptide ligands and receptors. Thus, various 1,2,4-triazoles containing chiral *α*-amino acids have been designed and synthesized. L-Tryptophane bearing 1,2,4-triazoles **A** have been reported as ghrelin receptor (GHS-R1a) ligands[109], lysine derivatives **B** exhibit histone deacetylase (HDAC) inhibitor activity[110] with high metabolic stability and dipeptido-1,2,4-triazole derivatives **C** posess a high level of central nervous system (CNS) activity[111] (Figure 2.8).

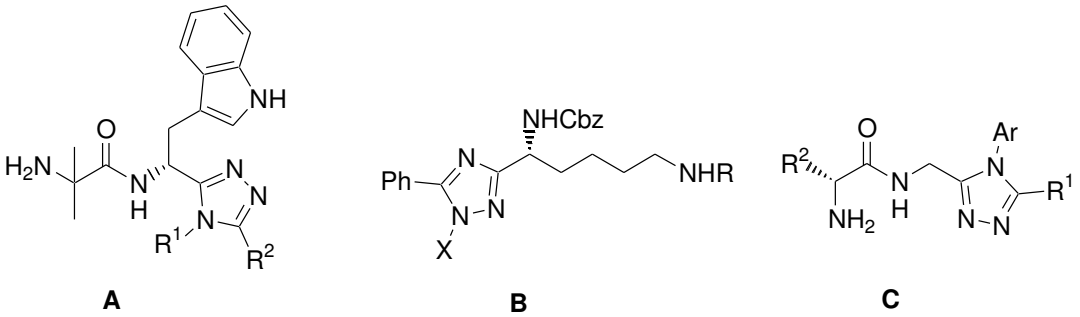

Figure 2.8 Selected biologically active 1,2,4-triazoles containing chiral α-amino acids

N-acylamidrazones substrates could be used as common intermediates to synthesize 1,2,4-triazoles.[112] We proposed the approach including the pyrrolidine ring opening of cyclic precursors **6**, **6'**, the same as for the amidoxime synthesis, with Boc-L-amino acid hydrazides in order to obtain *N*-acylamidrazones. This step would be followed by an intramolecular condensation of the latter and formation of 3,5-disubstituted-1,2,4-triazoles (Scheme 2.35).

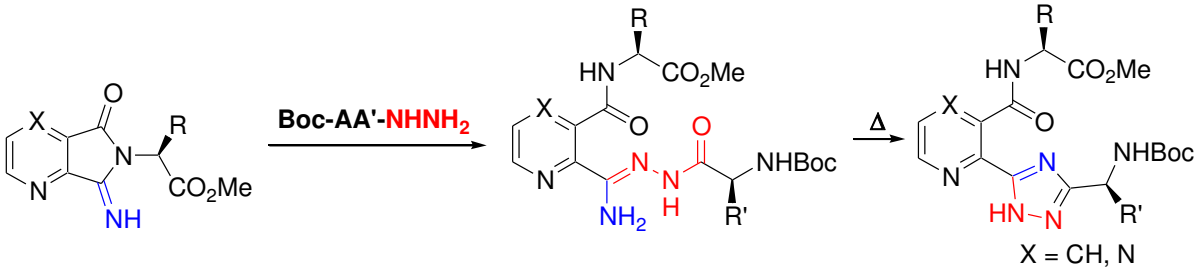

Scheme 2.35 Proposed route to amino acid derived 1,2,4-triazoles

Herein, we describe our attempts at the synthesis of 1,2,4-triazole-derived pseudopeptides, including an overview of synthetic approaches to 3,5-disubstituted-1,2,4-triazoles *via N*-acylamidrazones.

6.1 Overview of synthetic approaches *via N*-acylamidrazones

Among the numerous methods leading to *N*-acylamidrazones, the condensation of amidrazones and carboxylic acids (or carbonyl chlorides) is one of the most exemplified in the literature. As has been reported, amidrazones are readily available precursors, and reaction of nitriles with hydrazine in refluxing ethanol was used for their preparation (Scheme 2.36).[113,114] This is then reacted with adamantancarbonyl chloride and tolylcarbonyl chloride to yield the corresponding *N*-acylamidrazones. Condensation of these intermediates was performed to yield the 3,5-disubstituted-1,2,4-triazole derivatives as ligands in luminescent Pt(II) complexes. 2,4-Difluorophenyl and 2-naphthalenyl-substituted pyridine-1,2,4-triazoles have been studied as phosphorescent emitters, Ir(III) complexes.[115]

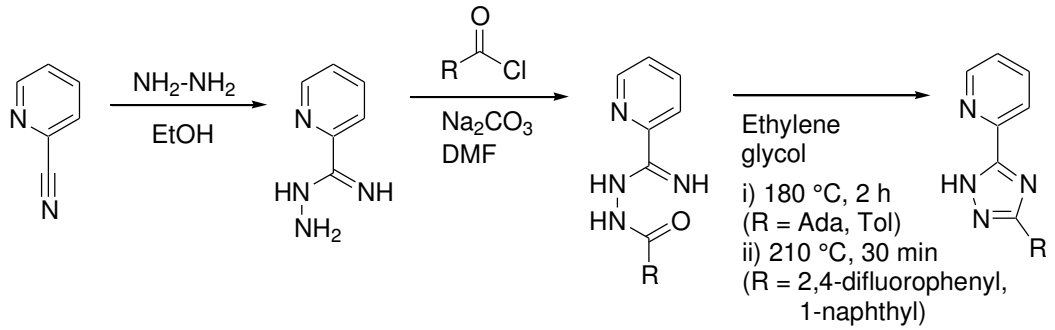

Scheme 2.36 1,2,4-Triazoles synthesis from amidrazones reported by Dumur *et al.* [115]

2,6-Pyridinediacylamidrazones have been synthesized from the corresponding 2,6-pyridinedicarbonitrile in the same way by the different research teams (Scheme 2.37).[116,117] They were used as precursors to 1,2,4-triazole-based tridentate ligands for Pt(II) complexes.

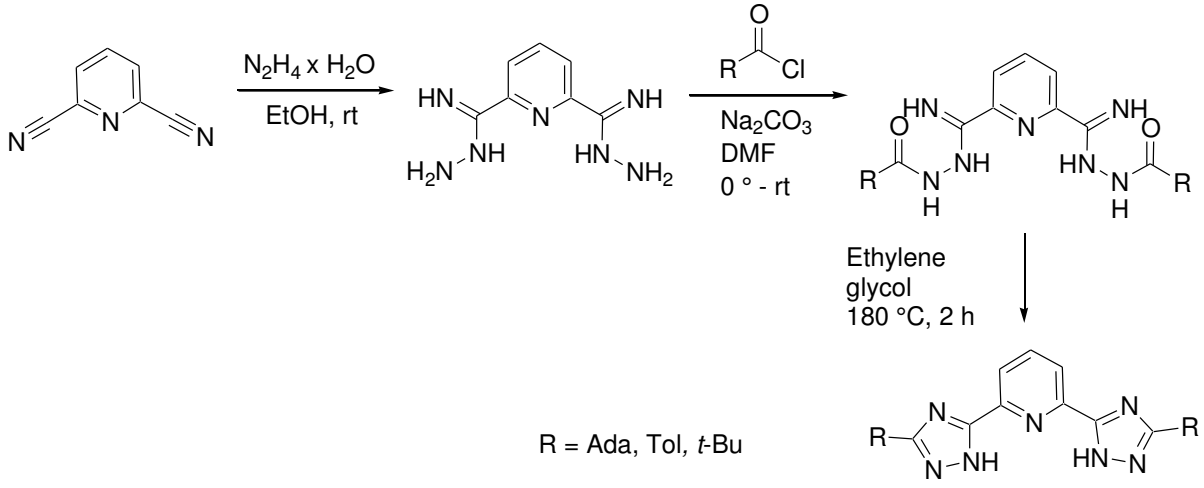

Scheme 2.37 1,2,4-Triazoles synthesis from amidrazones reported by Mydlak *et al.* and Sanning *et al.* [116, 117]

With the purpose of building triazole heterocycles for catalytic application (Pd(II) complexes), the amidrazones were prepared by reacting the nitriles of the isoxazole and isothiazole series with hydrazine hydrate (Scheme 2.38).[118] The reactions proceeded in methanol or ethanol solution at 50 °C for 2h. The target amidrazones were obtained in 80-95% yields. The latter were further acylated with acetyl chloride followed by thermal cyclization to the desired triazolylisoxazoles(isothiazoles) in glacial acetic acid in 85-98% yields.

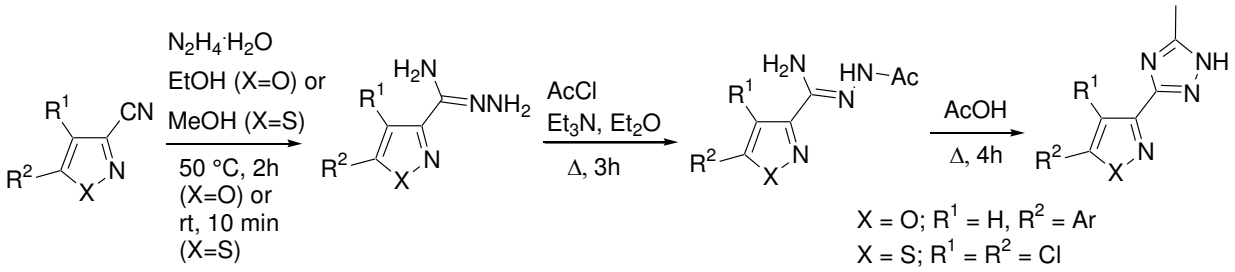

Scheme 2.38 1,2,4-Triazoles synthesis from amidrazones reported by Bumagin *et al.* [118]

Ghazvini Zadeh *et al.* used acylamidrazone intermediates to access 1,2,4-triazole-derived *α*-amino acids (Scheme 2.39).[119] The synthesis *N*-(Pg)-*α*-amino acyl conjugates of 1,2,4-triazole was envisaged to involve coupling 2-pyridylamidrazones with *N*-(Pg)-*α*-amino acylbenzotriazoles, followed by cyclization into 3,5-disubstituted 1,2,4-triazoles in yields of 54-72% over two steps.

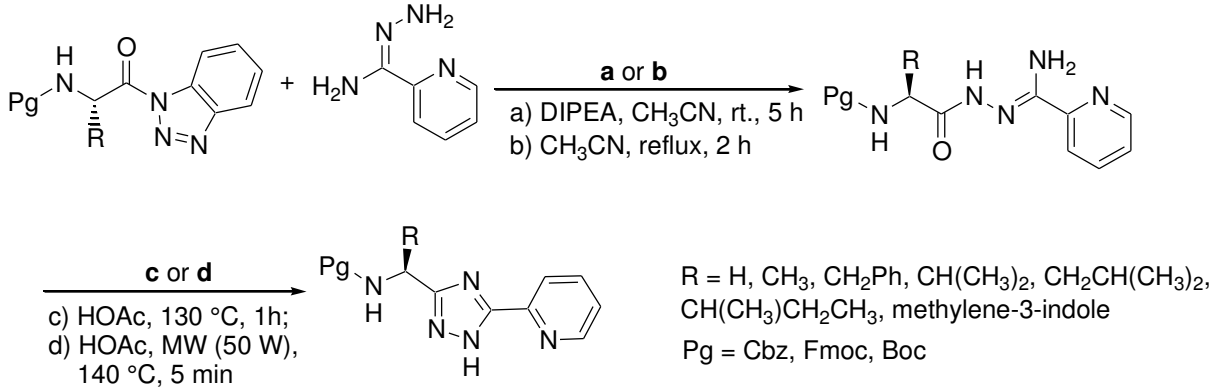

Scheme 2.39 1,2,4-Triazoles synthesis from amidrazones reported by Ghazvini Zadeh *et al.* [119]

An alternative standard method is the use of imidate and hydrazine precursors. Bocor and co-workers applied this reaction in the synthesis of *C*-glucopyranosyl-1,2,4-triazoles as new potent inhibitors of glycogen phosphorylase where 1,2,4-triazole served for bioisosteric

replacement of amide bond (Scheme 2.40).[120,121] To start the synthesis, *O*-perbenzoylated *β*-D-glucopyranosyl formimidate was reacted with tosylhydrazide to give the necessary tosylamidrazone in good yield. The reaction with acetyl chloride and further removal of the *O*-benzyl protecting groups yielded 1,2,4-triazole compounds in good to excellent yields.

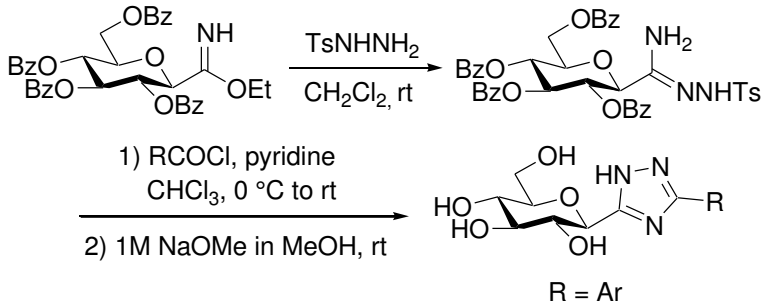

Scheme 2.40 1,2,4-Triazoles synthesis from imidates reported by Bocor *et al.* [120, 121]

Additionally, the authors examined the transformation of glucosyl formyl chloride with arenecarboxamidrazones and glucosyl in toluene yielded acylamidrazone intermediates from which the desired 1,2,4-triazoles were obtained in the ring closing step (Scheme 2.41).[121]

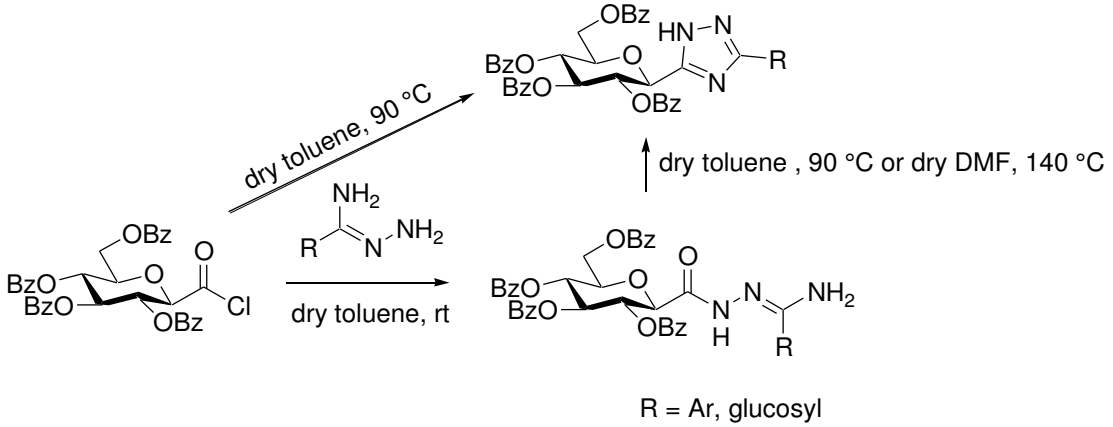

Scheme 2.41 1,2,4-Triazoles synthesis from amidrazones reported by Bocor *et al.* [121]

6-Imidatopurines were used in reaction with alkyl, aryl, heteroaryl hydrazides by Rocha *et al.* (Scheme 2.42) leading to purine-based *N*-acylamidrazone derivatives.[122]

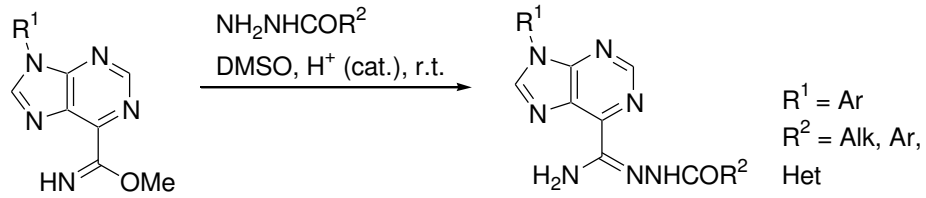

Scheme 2.42 *N*-acylamidrazones synthesis from imidates reported by Rocha *et al.* [122]

Treatment of different alkyl and aryl imidates with phenylacetic hydrazide in the presents of NaOEt gives the acylamidrazone derivatives (Scheme 2.43).[123]

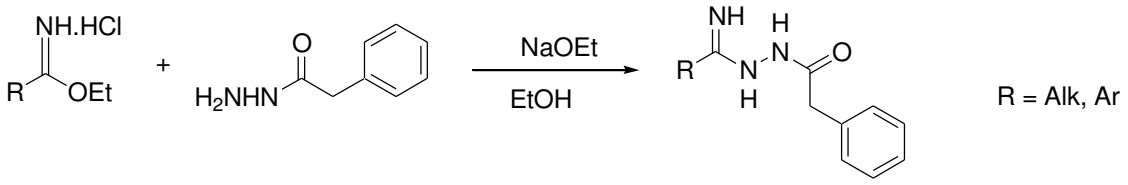

Scheme 2.43 *N*-acylamidrazones synthesis from imidates reported by Mentese *et al.* [123]

Liu *et al.*[124] reported a reaction of *in situ* generated 3-pyridine imidate and 3-pyridylcarbonyl hydrazide to yield N^3-(3-pyridoyl)-3-pyridinecarboxamidrazone (Scheme 2.44).

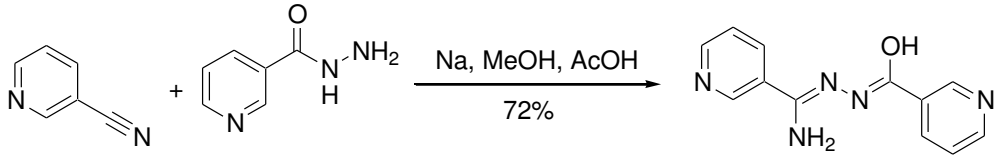

Scheme 2.44 *N*-acylamidrazones synthesis from *in situ* generated imidates reported by Liu *et al.* [124]

This method was also applied to 2-cyanopyrazine which reacted with metallic sodium for 2h to generate iminoester which was then brought to neutral pH with glacial acetic acid (Scheme 2.45). 2-(Hydroxyimino)-propanehydrazone was added to the solution and the corresponding acylamidrazone was obtained.[125]

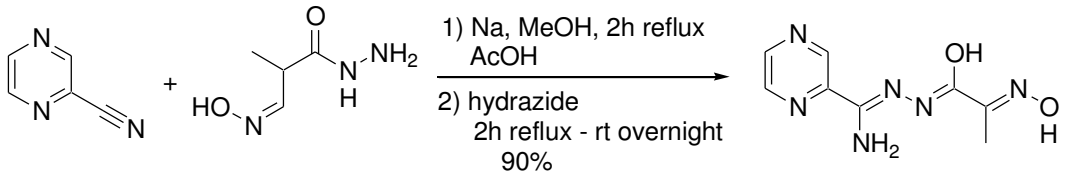

Scheme 2.45 *N*-acylamidrazones synthesis from *in situ* generated imidates reported by Drover *et al.* [125]

Epoxy imidates (*trans-cis* mixture, ratio 9:1) have been shown as highly reactive precursors of epoxy acylamidrazones reacting smoothly at room temperature with hydrazide nucleophiles with concomitant releasing of methanol (Scheme 2.46).[126] The *cis* isomer was recovered unreacted, presumably for steric reasons.

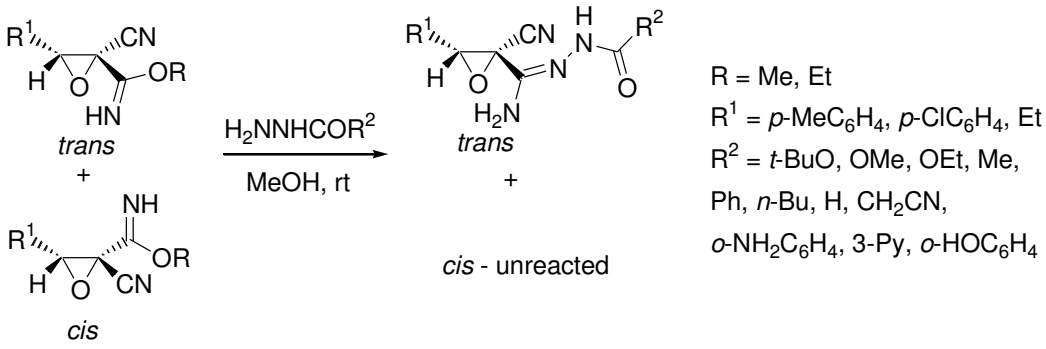

Scheme 2.46 *N*-acylamidrazones synthesis from imidates reported by Hurtaud *et al.* [126]

Another way to *N*-acylamidrazones is the condensation of thioamides with hydrazides. Bhuniya *et al.* described the synthetic route to amide bio-isosteric 1,2,4-triazoles from the corresponding amide *via* $Hg(OAc)_2$ induced condensation of thioamide with appropriate acylhydrazine followed by deprotection of 2,4-dimethoxy benzyl group (Scheme 2.47).[127]

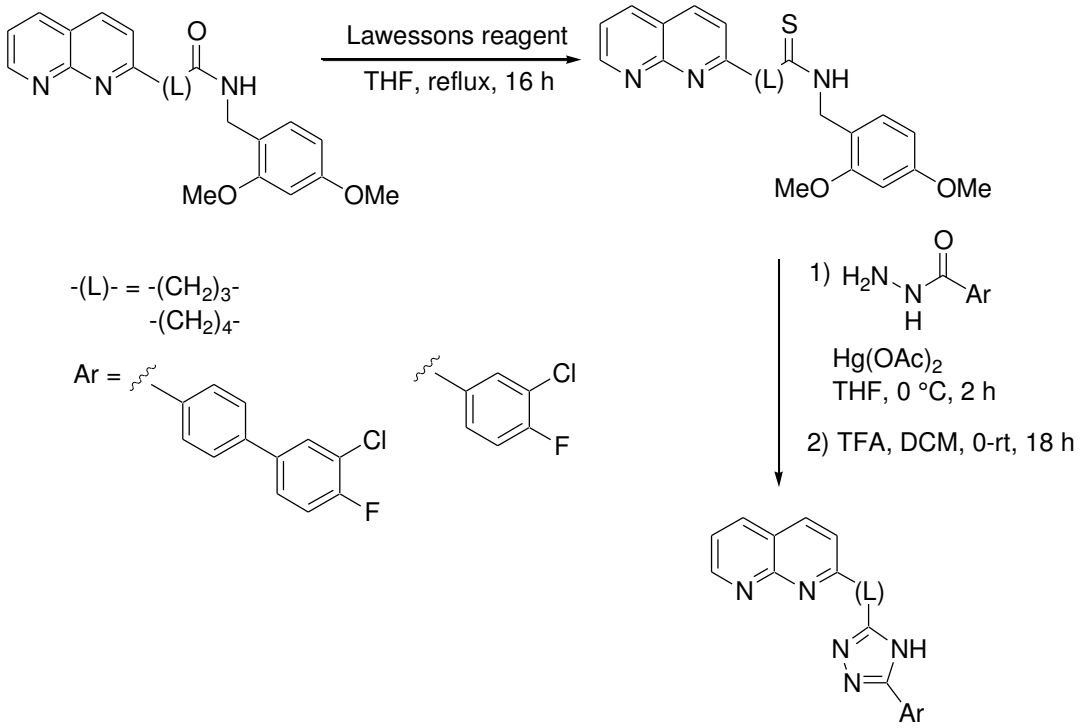

Scheme 2.47 1,2,4-Triazoles synthesis from thioamides reported by Bhuniya *et al.* [127]

Demange and co-workers also used condensation of thioamide precursor in the presence of $Hg(OAc)_2$ for the synthesis of a series of ghrelin receptor (GHS-R1a) ligands (Scheme 2.48).[109]

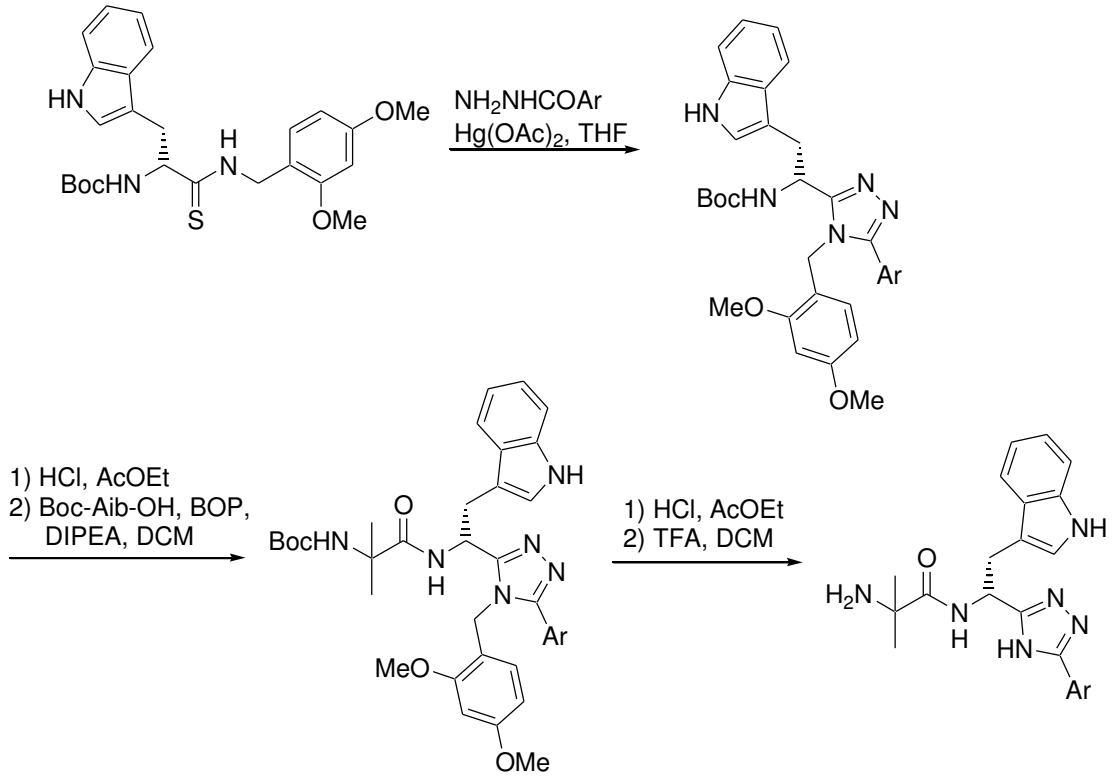

Scheme 2.48 1,2,4-Triazoles synthesis from thioamides reported by Demange *et al.* [109]

Amidines are described as alternative precursors of *N*-acylamidrazones. Balo *et al.* reported the preparation of 1,2,4-triazoles from amidine hydrochlorides reacting with amino hydrazides in an ethanolic CH_3ONa solution (Scheme 2.49).[128] Compounds were used as precursors for the synthesis of 1,2,4-triazolo[1,5-*c*]quinazolines showing adenosine antagonist activity.

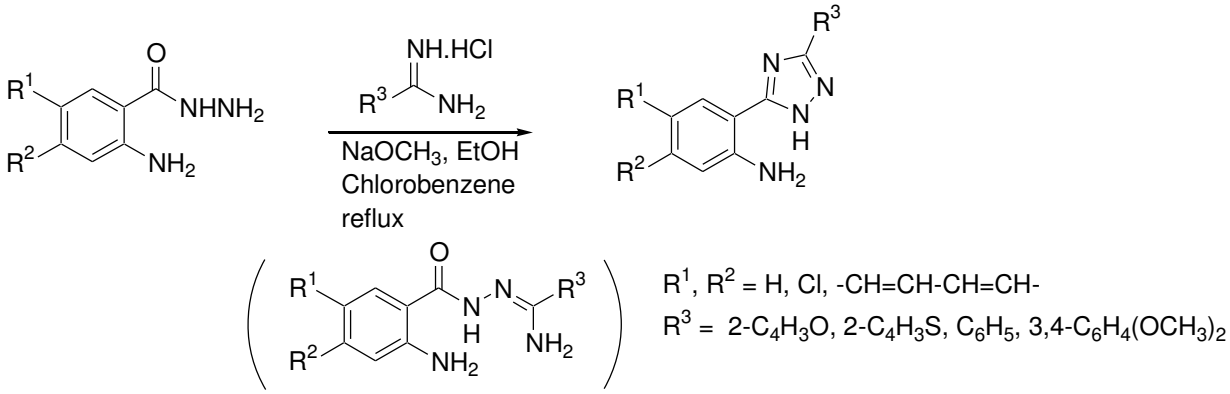

Scheme 2.49 1,2,4-Triazoles synthesis from amidines reported by Balo *et al.* [128]

The condensation of acyl and phenyl hydrazides with amidines to afford *N*-acylamidrazones, followed by thermal cyclization, was discovered by Francis *et al.* for preparing 3,5-disubstituted-1,2,4-triazoles in high yields (Scheme 2.50).[129]

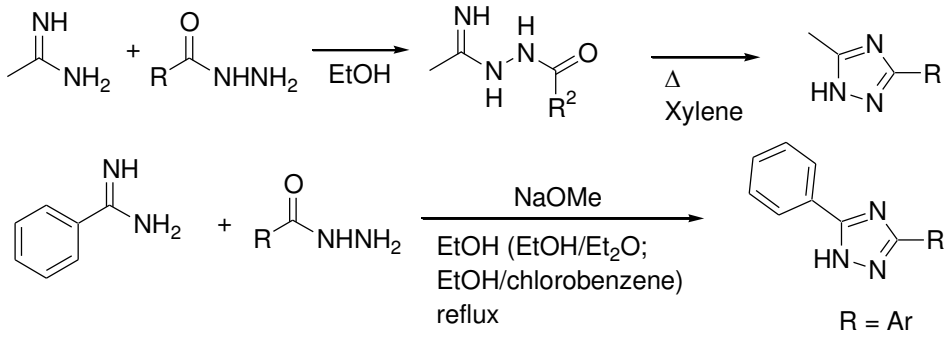

Scheme 2.50 1,2,4-Triazoles synthesis from amidines reported by Francis *et al.* [129]

This approach was also applied by Sanning and co-workers for the synthesis of 1,2,4-triazole-based ligands for Pt(II) complexes.[117] Treatment of trifluoroacetic acid ethyl ester with hydrazine hydrate generated *in situ* 2,2,2- trifluoroacetic hydrazide which was refluxed with the corresponding diamidine hydrochlorides and NaOH to give the 1,2,4-triazole derivatives (Scheme 2.51). With the same purpose, a suspension of dihydrazide in *n*-BuOH reacted with *t*-butyl and benzamidine hydrochloride after treatment with NaOMe in MeOH.

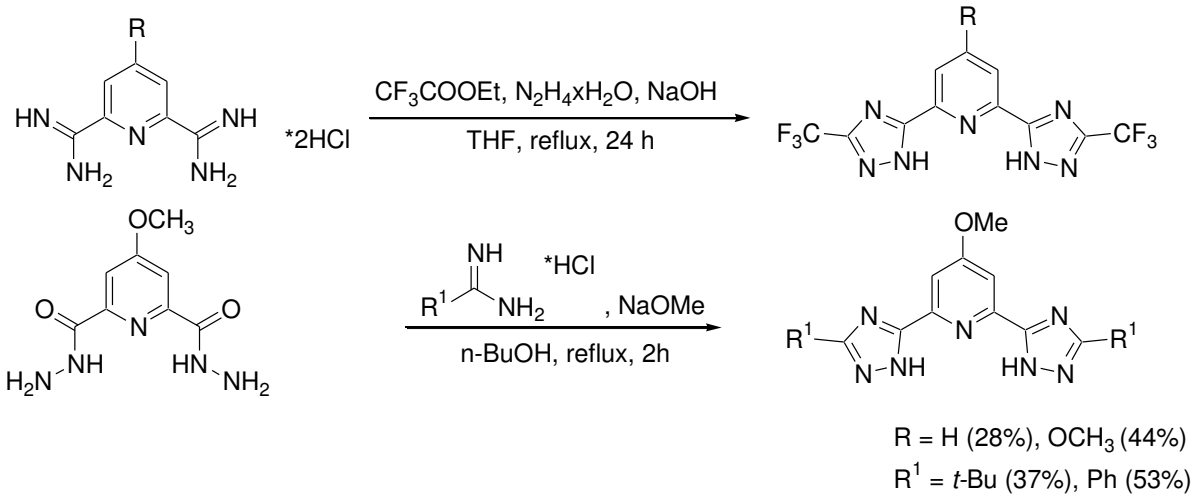

Scheme 2.51 1,2,4-Triazoles synthesis from amidines reported by Sanning *et al.* [117]

6.2 Synthesis of pyridine(pyrazine)-based *N*-acylamidrazones with further conversion into amino acid derived 1,2,4-triazoles

The application of pyrrolopyridines(pyrazines) **6**, **6'** (**a**,**b**) as precursors was chosen for the synthesis of *N*-acylamidrazones and further construction of amino acid derived 1,2,4-triazoles. First, the hydrazide of Boc-protected phenylalanine was synthesized from phenylalanine methyl ester starting with NH_2 protection using di-*tert*-butyl dicarbonate

followed by treatment with hydrazine monohydrate giving the corresponding precursor in quantitative yield (Table 2.9). Second, the preparation of *N*-acylamidrazones was performed by the reaction of **6**, **6'** (**a**,**b**) with BocPheNHNH$_2$ in MeOH at room temperature (Table 2.9). No cyclic pyrrolopyridines(pyrazines) derivatives **10''**, the formation of which could be expected according to a previously reported condensation of the 1-imino-1*H*-isoindol-3-amine and its pyrazine analogue with amino acid hydrazides that afforded 1*H*-isoindole- and 5*H*-pyrrolo[3,4-*b*]pyrazine-based peptidomimetics, were found.[130,131]

Table 2.9 Synthesis of the *N*-acylamidrazone derivatives **10**, **10'** (**a**,**b**)

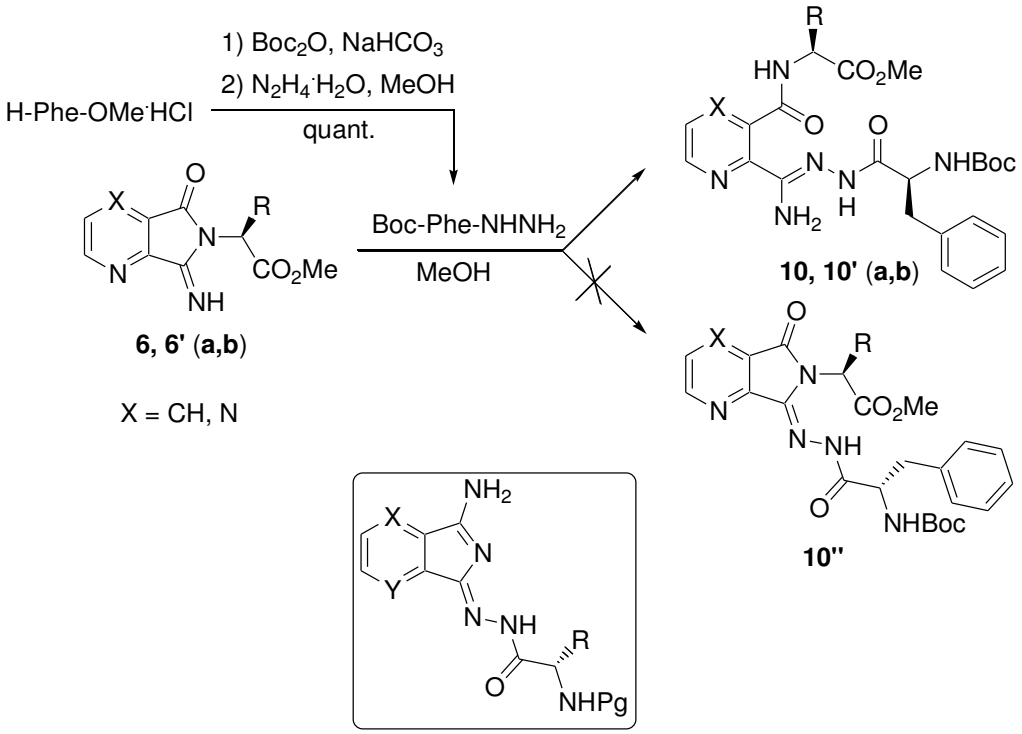

X	R		Isolated yield, %
CH	Me	**10a**	82
CH	Bn	**10b**	97
N	Me	**10'a**	50
N	Bn	**10'b**	82

The formation of acylamidrazones **10**, **10'**, similarly to the reaction with hydroxylamine, proceeded *via* pyrrolidine ring opening by hydrazide of amino acid and gave products **10a**,**b** and **10'b** in very good yields as analytically pure powders. However, we did not succeed to increase the yield of acylamidrazone **10'a** above 50%. Comparison of the reactivity of our starting material and known previously described acylamidrazone precursors towards the corresponding hydrazide nucleophiles allowed us to compare them with highly

reactive epoxy imidates, the precursors of epoxy acylamidrazones.[126] Therefore, we have found a new approach towards a straightforward and mild synthesis of *N*-acylamidrazones.

The presence of two sets of chemical shifts in the ^{1}H and ^{13}C NMR spectra of the products in DMSO-d_6 and duplication of signals in IR spectra demonstrated the existence of (*Z*)/(*E*) amide isomerism (see Chapter 3).

Following literature analogies, the cyclization of *N*-acylamidrazones **10, 10'** (**a**,**b**) into the corresponding 1,2,4-triazoles was attempted in different solvents (toluene, CH_3CN, THF, 1,4-dioxane, MeOH) at elevated temperatures (60 – 150 °C). However, we were able to convert only the pyrazine-based acylamidrazones **10'a**,**b** while in case of the pyridine counterparts the reaction lead to the pyrrolopyridines **6a**,**b** and conversion into the target 1,2,4-triazoles did not exceed 10% under any of the tested conditions (Table 2.10). The conventional cyclization of acylamidrazones **10'a,b** in toluene at 110 °C for 18 h furnished triazoles **11'a,b** in 45 and 64% yield respectively. Alternatively, microwave assisted reaction of **10'a,b** and cat. HOAc in CH_3CN offered several advantages: reduced reaction time up to 20 min and increased yields up to 87%.

Table 2.10 Synthesis of the target amino acid-derived 1,2,4-triazoles

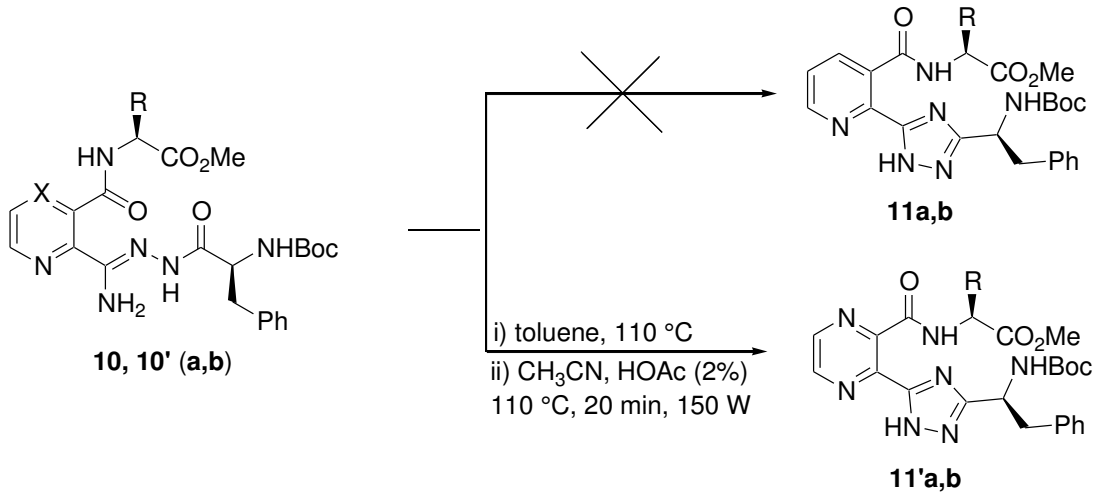

X	R		Isolated yield(i), %	Isolated yield(ii), %
CH	**Me**	**11a**	-	-
CH	**Bn**	**11b**	-	-
N	**Me**	**11'a**	45	85
N	**Bn**	**11'b**	64	87

The formation of pyrrolopyridines **6a**,**b** was suggested to be a result of termal decomposition followed by further intramolecular cyclization giving a pyrrolidine ring.

7. Synthesis of hydrazide modified turn mimics

On further developing constrained peptidomimetics, we are interested in the synthesis and conformational study of hydrazide modified turn mimics derived from amidoximes **7**,**7'**. The synthesized peptidomimetics might be considered as the hybride structures of azapeptides[132] with substitution of a nitrogen for the α-carbon center and aminoxy peptides[133,134] which are backbone-modified peptidomimetics with oxygen atom between the nitrogen atom and one of the backbone carbon atom (Figure 2.9).

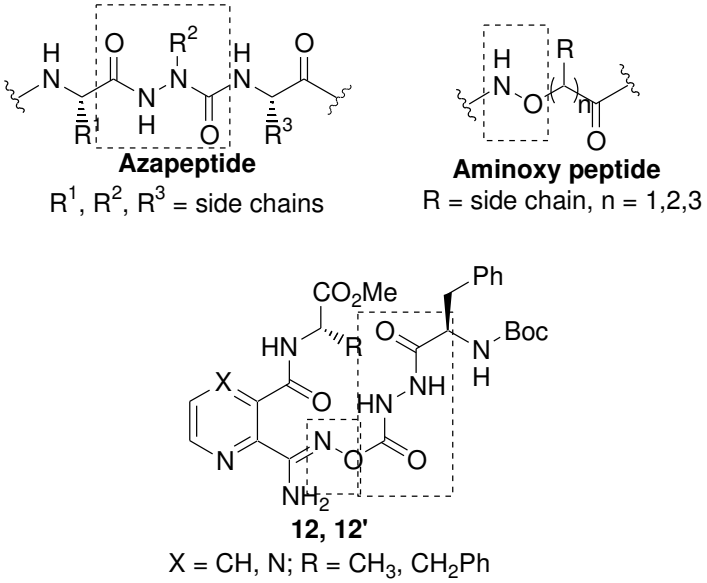

Figure 2.9 Comparison of **12**, **12'** with a azapeptide and a aminoxy peptide

The hydrazide of phenylalanine amino acid was introduced *via* condensation with pyridine and pyrazine-based amidoximes **7**, **7'** through carbonyl linkage. Thus, compounds **12**, **12'** were obtained by the reaction of **7**, **7'** (**a**,**b**) with triphosgene followed by the coupling with phenylalanine hydrazide in the presence of diisopropylethylamine in dichloromethane (Table 2.11). The phenylalanine products **12b** and **12'b** were obtained in 60 and 69% yields after purification by HPLC preparative. In the case of alanine derivatives **12a** and **12'a**, the reaction yields did not exceed 44% due to lower reactivity of the corresponding amidoxime with triphosgene which led to an increased amount of side product derived from the condensation of phenylalanine hydrazide with triphosgene. Attempts to improve the yield by changing times and temperatures were unsuccessful and need further improvement.

Table 2.11 Synthesis of hydrazide modified peptidomimetics

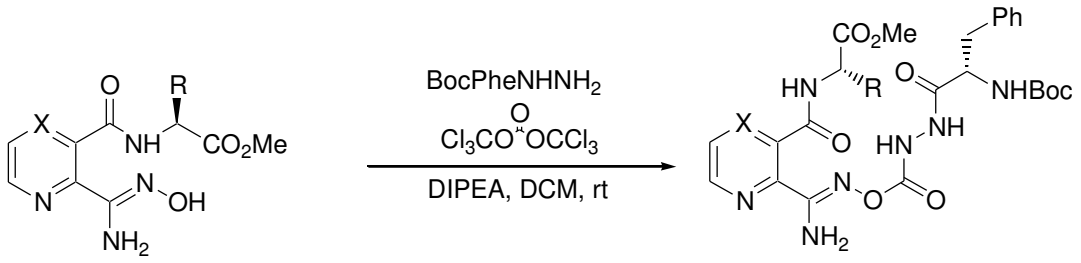

7, 7' (a,b) **12, 12' (a,b)**

Entry	X	R		Isolated yield, %
1	CH	Me (Ala)	**12a**	40
2	CH	Bn (Phe)	**12b**	60
3	N	Me (Ala)	**12'a**	44
4	N	Bn (Phe)	**12'b**	69

The conformations of peptidomimetics **12** and **12**' in solution were studied (see Chapter 3).

8. Conclusions

The synthesis of various novel 2,3-substituted pyridine(pyrazine) non-peptidic turn structures possessing amidoxime, esterified with amino acid and hydrazide modified amidoxime, amino acid derived *N*-acylamidrazone, chiral 1,2,4-oxadiazole and and 1,2,4-triazole residues has been developed (Scheme 2.52).

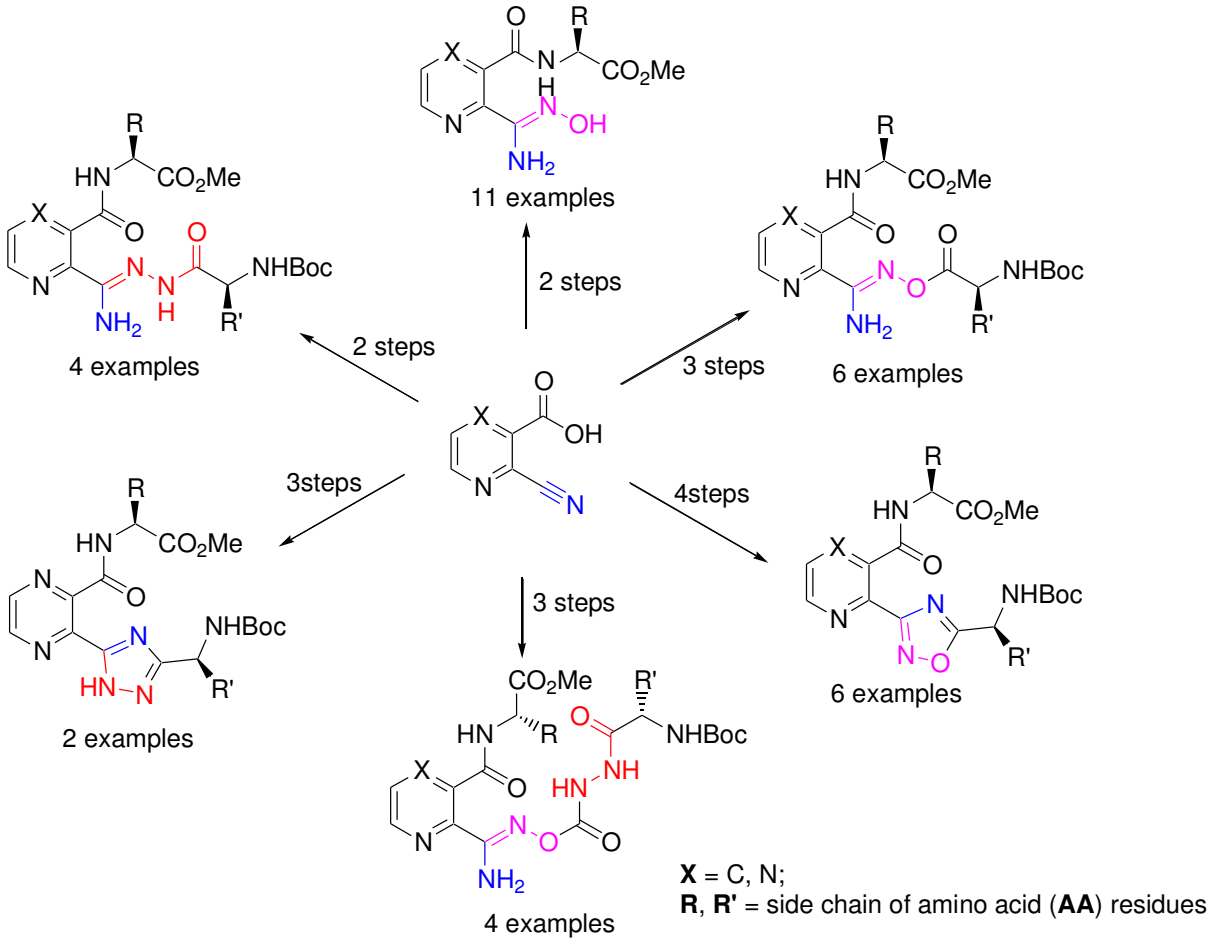

Scheme 2.52 Summary of all target compounds obtained

We have found that 2-cyanonicotinic and 3-cyanopyrazine-2-carboxylic acids react with methyl esters of different L-α-amino acids to afford methyl esters of (2*S*)-2-(cyanopyridin(pyrazin)-yl)carbonyl-substituted amino acids with an open structure. These esters undergo further intramolecular pyrrolidine ring closure leading to the tautomeric methyl esters of (2*S*)-2-(imino-oxo-dihydro-6*H*-pyrrolo[3,4-*b*]pyridine(pyrazin)-6-yl)alkanoic acids. Reaction of latter with hydroxylamine hydrochloride resulted in pyrrolidine ring opening to

afford open-chain amidoximes (63-94%) bearing the same structure as amidoximes obtained by direct hydroxyamination of the corresponding cyano esters.

This readily available variety of nicotinic and pyrazine acid based pseudopeptides with an amidoxime function on the heteroaromatic ring might be considered as potential amidine prodrugs, an arginine peptidomimetics and/or as nitric oxide donors for treatment of cardiovascular diseases.

Furthermore, the synthesis of new 3,5-disubstituted 1,2,4-oxadiazoles has been presented. It was shown that the use of optimized microwave-assisted conditions with a reduced reaction time afforded products in good to high yields (58-94%).

A new straightforward and mild synthesis of amino acid derived *N*-acylamidrazones *via* pyrrolidine ring opening by the hydrazide of amino acid has been reported. The pyrazine-based *N*-acylamidrazones appeared the effective precursors for cyclodehydration into the corresponding chiral α-amino acid-derived 1,2,4-triazoles. Moreover, the use of catalytic amount of HOAc along with microwave irradiation reduced reaction time and increased product yields up to 87%. Unfortunately, we were not able to obtain pyridine-linked 1,2,4-triazoles due to high thermo and solvent sensibility. This represented the major limitation of the developed protocol.

Finally, the first condensation of the amidoximes with Boc-protected hydrazide of amino acid in order to obtain hybride turn mimics with amidoxime-carbonyl-hydrazide linkage was performed. Products were obtained in moderate to good yields (40-69% yield).

Chapter 3: Structural Analysis

1. Introduction

The second chapter describes structural analysis of the compounds including hydrogen bond investigation, *cis-trans* conformational preferences and thermodynamic studies of the proline derivatives and *Z/E* isomerism study of the acylamidrazone compounds.

2. Methods and techniques of conformational study

Physico-chemical tools that were used to collect structural informations and identify interactions responsible of the structuration are presented below. The implemented strategy has combined spectroscopic methods, such as Nuclear Magnetic Resonance (NMR) and Infrared spectroscopy (IR), and molecular dynamics.

2.1 Infrared absorption spectroscopy (IR)

This analytical method was used to determine the involvement of NH and CO functions in hydrogen bond formation.

In the IR spectra of peptides the most interesting bands are found in the C=O bond stretching vibrations region (amide I bands in the region 1750-1580 cm^{-1}) and the N-H stretching vibrations region (3520-3200 cm^{-1}). Hydrogen bond of type C=O…H-N shifts the absorpsion bands to lower wavelengths and an absolute value of the shift reflect the relative strength of the interactions. It is commonly accepted in the literature that amidic NH which is bonded has IR absorpsion band below 3400 cm^{-1}.[133,135-137]

Unfortunately, the application field of this spectroscopic method is often limited by the transparency of solvents in the explored frequency range, by the solubility of molecules, by self-assembling in these environments and by the multiplicity and the overlapping of NH or CO bands that make difficult the assignment. To overcome this problem in some cases the deconvolution of bands is necessary. This has been realized in the spectroscopic software OPUS (Bruker) using the Levenberg-Maquardt mathematic algorithms.

2.2 Nuclear magnetic resonance spectroscopy (NMR)

Nuclear magnetic resonance is a crucial experimental technique in investigating the molecular properties in solution.

2.2.1 One dimensional NMR (1D)

As a labile proton, NH proton is really sensitive to modifications of its environment, as for example, the formation or break of a hydrogen bond. Therefore, four experiments can be used:

- NH chemical shift study: if the NH proton is involved in hydrogen bond, the nucleus will be deshielded that will led to the deplacement of chemical shift to low field.
- The effect of solvents: it consists of following the evolution of NH chemical shift while adding a polar solvent (DMSO) in a nonpolar solvent ($CDCl_3$). The NH proton which is not involved in an intramolecular hydrogen bond will be rapidly shifted to low field region (high $\Delta\delta$). In contrary, if it is involved in the intramolecular bonding, the chemical shift will be little affected by adding the polar solvent. The $\Delta\delta$ of these chemical shifts will be very low in case of strong intramolecular interaction.
- The temperature dependence: in the solvent – hydrogen bond acceptor, the temperature rise leads to the breaking of intermolecular hydrogen bonds and the evolution of the chemical shift; *vice versa*, the chemical shift of NH proton is independent on the temperature if it is involved in intramolecular hydrogen bond, as its not sufficient for breaking this type of interaction. This technique allows also to study *cis/trans* conformational equilibrium for proline-containing componds and to calculate thermodynamic parameters.

1D NMR study allows also measuring the population of the amide AA-Pro isomers in equilibrium mixture of *cis/trans* rotamers in solution. This method was efficiently used by teams of Dorman[138,139] and Beausoleil[140] in order to make the assignment of the isomer geometry of proline or pseudoproline derivatives based on the chemical shift values for the signals of the α- and δ-carbons. In the ^{13}C NMR spectra, the α-carbon signal of the *trans*-isomer appears upfield to that of the *cis*-isomer. The δ-carbon signal of the *trans*-isomer appears downfield from that of the *cis*-isomer. Furthermore, the γ-carbon of the *cis*-isomer appears upfield to that of the *trans*-isomer and the β-carbon of the *cis*-isomer appears downfield from that of the *trans*-isomer.

2.2.2 Two dimensional NMR (2D)

Unambiguous assignment of signals in pseudopeptides is obtained by using different two dimensional NMR experiments:

- Homonuclear through-bond correlations: COSY (Correlated SpectroscopY), TOCSY (Totally Correlated SpectroscopY) that show the correlations between coupled spins or all spins in a spin system.
- Through-space correlations: ROESY (Rotating frame Overhauser Effect SpectroscopY) and NOESY (Nuclear Overhauser Effect SpectroscopY) establishing correlations between nuclei which are physically close to each other (within about 5 Å) regardless of whether there is a bond between them.

- Heteronuclear through-bond correlations: Heteronuclear single-quantum correlation spectroscopy (HSQC) and Heteronuclear multiple-bond correlation spectroscopy (HMBC) that detect correlations between nuclei of two different types which are separated by one bond (HSQC) or of about 2–4 bonds (HMBC).

2.3 Molecular modelling

Molecular modelling calculations allow to visualize 3D structures of molecules for predicting, analyzing the properties and the behavior of the molecules with the equations of quantum (*ab initio* methods) and classical (molecular mechanic and molecular dynamic) physics.

3. Structural and thermodynamic studies of proline-containing peptidomimetics

3.1 Conformational preferences of proline derivatives

The singular behavior of proline in peptides and protein folding represents another way to introduce different turn motives into the amino acid backbone due to its *N*-terminal extremity that is involved in a cycle. However, unlike the majority of natural amino acids that adopt the *trans* configuration of peptidic bond, increased *cis* content along the Xaa-Pro bond is significant since both the *cis* and *trans* isomers are energetically similar.[141]

In this context, we studied the effect of substitution with proline on the conformational behavior of the products. Information concerning the conformation adopted by compounds **5c**, **5'c**, **7c-9c** and **7'c-9'c** in solution was obtained by 1D-, 2D-NMR and FT-IR absorption spectroscopies. The NMR spectra of proline-based compounds revealed two sets of resonances in $CDCl_3$ at room temperature corresponding to the *cis* and *trans* amide bond rotamers. From the ^1H NMR, ^{13}C NMR and NOESY spectra of derivatives **5c**, **5'c**, **7c-9c**, **7'c-9'c**, it was possible to assign and to estimate the approximate ratio of the rotamers. Cross-peaks in the NOESY spectra of **5c**, **7c-9c**, corresponding to the spatial interaction between the proton at the C4 position of the pyridine ring and the protons at the C5 position of the pyrrolidine residue indicated that the major product was the *trans*-isomer; accordingly, the minor product was *cis*-isomer (Figure 3.1 and Figures 1 - 3 in Appendix).

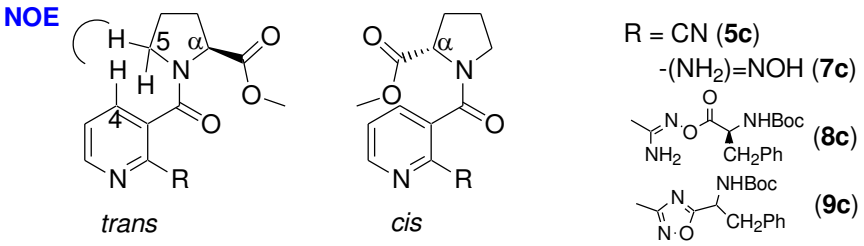

Figure 3.1 Correlation in pyridine derivatives **5c**, **7c-9c**

The assignments of pyrazine proline derivatives **5'c**, **7'c-9'c** were made based on the ^{13}C chemical shifts of the α- and δ-carbons in $CDCl_3$.[138-140] In the Pro derivatives, the α-carbon signal of the *trans* rotamer is shielded relatively to the *cis* rotamer due to the *syn* position to the carbonyl oxygen of the amides. The signal of the δ-carbon, however, should be more shielded in the *cis* isomer. Indeed, in the *trans* conformers of **5'c**, **7'c-9'c**, the chemical shifts of the α-carbon range from 59.3 to 60.2 ppm, while in the *cis* form range from 61.1 to 61.4 ppm (Table 3.1).

Table 3.1 Selected carbon chemical shifts in pyrrolidine ring of proline derivatives **5'c**, **7'c-9'c** in $CDCl_3$

Entry	Product	C^{α}		C^{β}		C^{γ}		C^{δ}	
		cis	***trans***	***cis***	***trans***	***cis***	***trans***	***cis***	***trans***
1	**5'c**	61.2	60.2	31.8	29.4	22.6	25.6	48.4	49.5
2	**7'c**	61.1	59.3	31.5	30.2	23.5	25.2	47.3	48.3
3	**8'c**	61.4	59.4	31.5	30.2	23.5	25.4	47.2	48.7
4	**9'c**	61.2	59.5	31.7	30.1	23.3	25.5	47.4	48.8

The δ resonances of the *trans* conformers vary from 48.3 to 49.5 ppm and lie within the range 47.2 - 48.4 ppm for the *cis*, respectively. Furthermore, the β-carbon signal of the *trans* isomer appears upfield from the *cis* isomer and the γ-carbon of the *trans* rotamer is downshifted relative to that of *cis* rotamer.

Additionally, the comparison of the α proton chemical shifts revealed unclear at first sight, downfield shift of the H_{α} signal in *cis* **5'c** (δ = 4.80 ppm) compare to *trans* isomer H_{α} (δ = 4.64 ppm) that is probably a result of a deshielding effect by the ring current of neighboring pyrazine cycle (Table 3.2). The upfield shift for **5c, 7c-9c**, **7'c-9'c** can be a result of shielded H_{α} due to the *syn* position to the carbonyl oxygen of the ester group or due to the shielding effect by the pyrazine ring (Figure 3.2, structure I).

Table 3.2 Chemical shifts of the α proton derived from ^1H NMR ($CDCl_3$, 300K)

	5c	**5'c**	**7c, 7'c**	**8c**	**8'c**	**9c**	**9'c**
δH_{α} (*trans*)	4.71	4.64	4.74	4.80	4.77	4.66	4.60
δH_{α} (*cis*)	4.28	4.80	4.11	4.29	4.28	4.01	4.26
$\Delta\delta_{\alpha}$	-0.43	+0.16	-0.63	-0.51	-0.49	-0.65	-0.34

The population of the amide isomers were measured in the ^1H NMR spectra by integration of all well-resolved proton signals. The major contributions into *cis-trans* equilibrium mixture have been clearly determined by NMR spectroscopy to be the *trans* conformers (Table 3.3).

Table 3.3 The population of amide isomers **5c**, **5'c**, **7c-9c**, **7'c-9'c** measured from the ^1H NMR spectra in $CDCl_3$

Pyridine derivative	*cis*-rotamer, %	*trans*-rotamer, %	Pyrazine derivative	*cis*-rotamer, %	*trans*-rotamer, %
5c	23	77	**5'c**	46	54
7c	32	68	**7'c**	26	74
8c	37	63	**8'c**	29	71
9c	27	73	**9'c**	24	76

Interestingly, in most cases the content of the *trans* isomer was about 63-77% while *cis* isomer was 23-37%. However, when **5'c** was studied, a decreased *trans/cis* ratio to 54/46 was observed. We assumed the presence of a noncovalent intramolecular n → π* interaction between the N lone pair of the pyrazine ring and the antibonding orbital of the C=O of the pyrrolidine ring for all Pro-based derivatives (Figure 3.2, structure I). However, there is an increased amount of the *cis* conformation for cyano compound **5'c**, as the *trans* product is stabilized by a relatevely weaker interaction between the more electronegative oxygen and the carbonyl (Figure 3.2, structure II). Evidence for this nonbonding interaction can be downfield shift for H_α of the Pro residue in the *cis*-**5'c** only (Table 3.2).

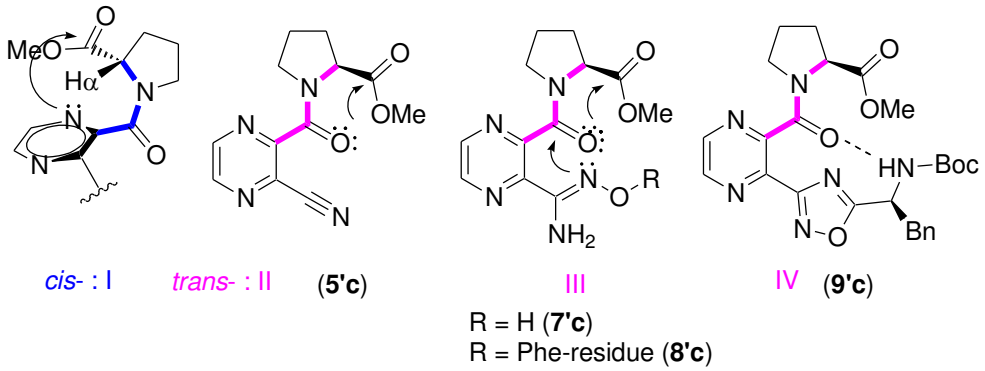

Figure 3.2 *Trans*/*cis* conformational states of proline-containing derivatives **5'c**, **7'c**, **8'c** and **9'c**

In the cases of **7'c** and **8'c**, we observed a general tendency to adopt the stabilized *trans* conformation probably due to the presence of the two different n → π* interactions. The first one between the oxygen lone pair of the amide C=O and the antibonding orbital of the ester C=O bond belonging to the Pro-residue and second between the nitrogen lone pair of the amidoxime and the antibonding orbital of the amide C=O (Figure 3.2, structure III).[105,142-144] This assumption has been verified using the corresponding distances from molecular dynamics simulation of the proline derivatives **7'c** and **8'c** (Table 3.4).

Table 3.4 Dimensions with standard deviations of the possible n → π* interactions in the proline derivatives **7'c** and **8'c**

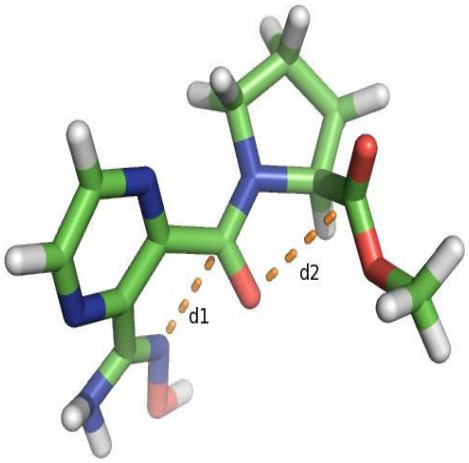

7'c

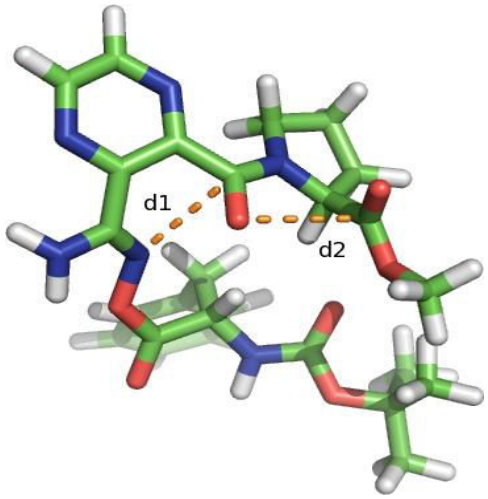

8'c

Mean distance d_1 (N…C)	**Mean distance d_2 (O…C)**	**Mean distance d_1 (N…C)**	**Mean distance d_2 (O…C)**
2.99±0.087 Å	3.07±0.175 Å	3.10±0.17 Å	2.95±0.084 Å
Mean angle θ_1 (N…C=O)	**Mean angle θ_2 (O…C=O)**	**Mean angle θ_1 (N…C=O)**	**Mean angle θ_2 (O…C=O)**
58.6±2.6°	95.2±14.5°	70±4.6°	110.9±15.9°

Indeed, all mean distances found (d_1 and d_2) are ≤ 3.2 Å, where the Van der Waals surfaces of the carbonyl oxygen and ester carbon (d_2) and the nitrogen lone pair and amide carbon (d_1) interpenetrate. Interestingly, the n → π* interaction of the two carbonyl groups in **8'c** seems to be stronger, according to the measured distance d_2 of 2.95 Å, which is less than for **7'c**, where d_2 is equal to 3.07 Å (Table 3.4). The allowed angles are reminiscent of the Bürgi-Dunitz trajectory for nucleophilic attack on a carbonyl carbon (~107°). The mean θ_1 angles (N…C=O) are less of this value that decreases the probability of the n → π* interraction between the nitrogen lone pair and the amide carbonyl, whereas the mean θ_2 angles (O…C=O) allow the attack.

The *trans* conformation of **9'c** is stabilized by the plausible H-bonding of Phe NHBoc and proline carbonyl, although an n → π* interaction may also contribute to its stabilization.

Furthermore we investigated the impact of temperature (in the range 25 – 90° C) on the *trans/cis* equilibrium constant ($K_{t/c}$). The $K_{t/c}$ values were measured by determining the relative concentrations of each isomer by integrating of all well-resolved proton signals in ^{1}H

NMR spectrum in DMSO-d_6 at each temperature. The results are illustrated in Van't Hoff analysis (Figure 3.3, Table 3.5).

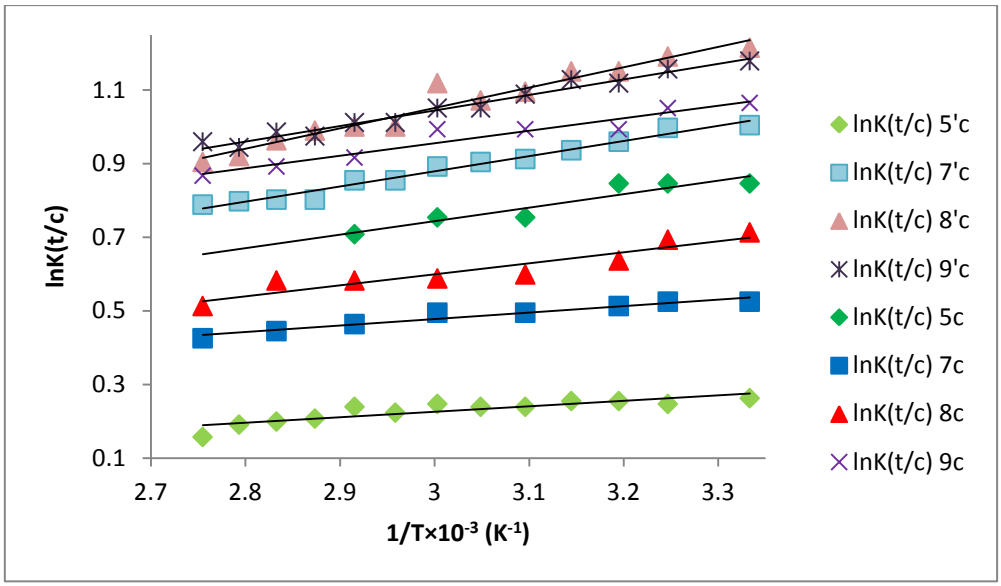

Figure 3.3 Van't Hoff plots for **5c**, **5'c, 7c-9c, 7'c-9'c** in DMSO-d_6

Values of ΔH° and ΔS° were calculated from linear least-squares fits of the data in the plots to eq. 1.

$$\ln K_{t/c} = (-\Delta H°/R)(1/T) + \Delta S°/R \qquad (1)$$

All derivatives have a slight positive slope demonstrating a temperature-dependence. For the Pro derivative **5'c** and **7c**, a reduction in the magnitude of $K_{t/c}$ was observed, demonstrating a smaller enthalpic preference to the *trans* conformation.

Although differences in entropy favor the *cis* isomer, the *trans* isomer in all cases is favored by enthalpy. The equivalent constants decrease with increasing temperature in the order **8'c>9'c>9c>7'c>5c>8c>7c>5'c** (Table 3.5).

Table 3.5 Thermodynamic parameters for compounds **5c**, **7c-9c, 5'c, 7'c-9'c**. Additionaly the *trans/cis* equilibrium constant at 300K is given

Proline derivative	**$K_{t/c}$ DMSO-*d6* ($CDCl_3$)**	**ΔH^0 (kJ mol^{-1})**	**ΔS^0 (J mol^{-1} K^{-1})**	**ΔG^0_{300K} (kJ mol^{-1})**
5c	2.33	-3.05	-2.96	-2.16

7c	1.69	-1.43	-0.43	-1.30
8c	2.04	-2.48	-2.45	-1.74
9c	2.90	-2.82	-0.52	-2.66
5'c	1.30 (1.17)	-1.24	-1.84	-0.69
7'c	2.73 (2.73)	-3.43	-2.97	-2.53
8'c	3.37 (2.63)	-4.60	-5.06	-3.08
9'c	3.25 (3.54)	-3.51	-1.84	-2.96

The energy barrier ($\Delta G^{\ddagger}$) for amide isomerization in **5c** was determined by NMR spectroscopy. The equilibrium between *cis* and *trans* rotamers of **5c** shown in Figure 3.1, is related to rate constant *k*, which can be calculated using the Eyring equation (2).

$$k = (k_B * T/h) * e^{(-\Delta G^{\ddagger}/RT)} \qquad (2)$$

In this equation, k_B is Boltzmann's constant, h is Planck's constant, R is the gas constant and $\Delta G^{\ddagger}$ is the Gibbs free energy of activation. Hence, when the exchange rate between *cis* and *trans* of **5c** is slow, two sets of signals are observed in the NMR spectrum, one for each rotamer. In contrast, with a fast rate of interconversion, only the average signal is present. Between these two limits a broad and flat peak should appear. The temperature when this happens is called the coalescence temperature, T_c. At T_c, the rate constant is given by equation (3).

$$k = (\pi * \Delta\nu)/\sqrt{2} = 2.22 * \Delta\nu \qquad (3)$$

where $\Delta\nu$ is the difference in Hertz of the same proton frequencies of two isomers at a slow rate of interconversion. At this point, $\Delta G^{\ddagger}$ can be calculated using equation (4).

$$\Delta G^{\ddagger} = RT_c[22{,}96 + \ln(T_c/\Delta\nu)] \qquad (4)$$

Knowing $\Delta G^{\ddagger}$, it is possible to calculate the rate constant *k* at different temperatures using the Eyring equation 2, assuming that there is no changing in entropy on changing the temperature. Finally, the half-life for rotation is given by equation (5).

$$t_{1/2} = \ln 2/k \qquad (5)$$

Thus, a series of ^{1}H NMR spectra were recorded in DMSO-d_6 at increasing temperatures until the resonances for the two isomer populations were observed to coalesce at 90 °C (Figure 3.4).

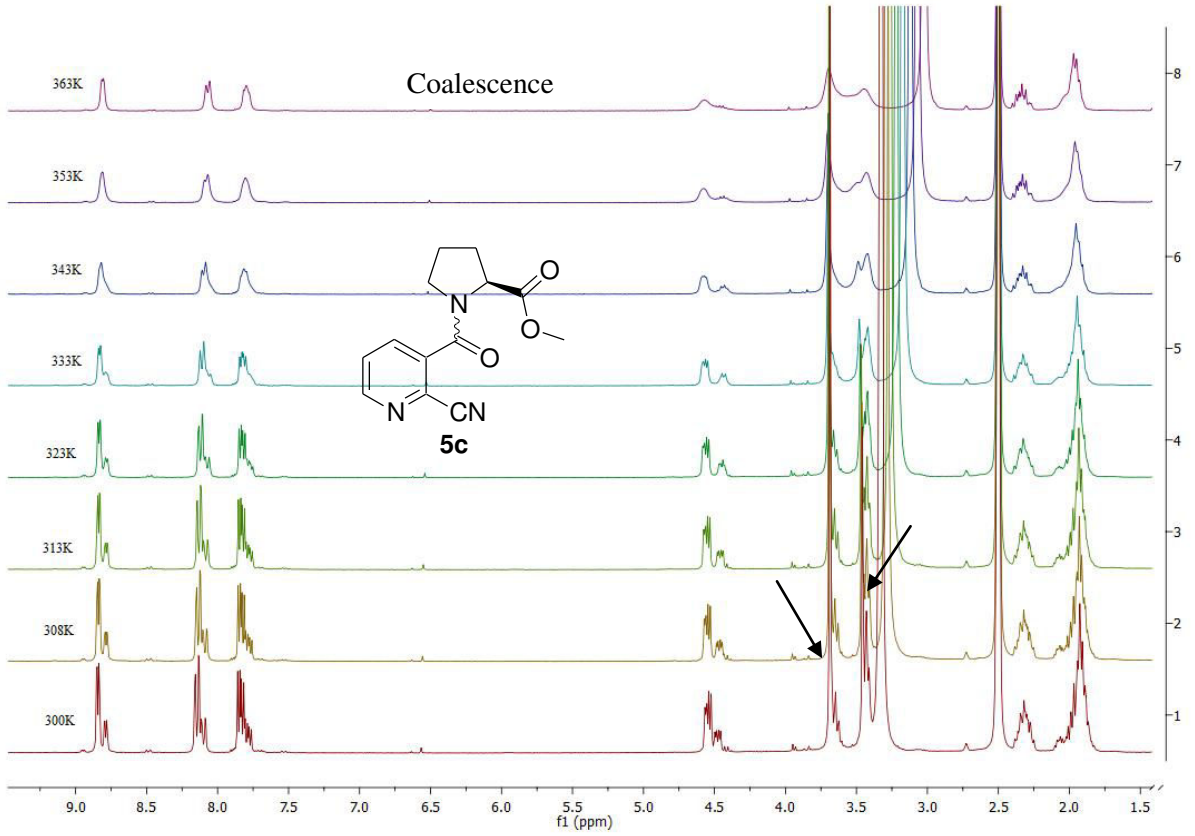

Figure 3.4 Temperature dependence of ^{1}H NMR chemical shifts of **5c** in DMSO-d_6

The signals of the OMe group were separated, at δ equal to 3.69 and 3.46 ppm (in DMSO-d_6) and at 300K $\Delta\nu$ = 68 Hz. This value gives a rate of interconversion, k = 151 s^{-1} and a half-life for rotation, $t_{1/2} = 4.6\times10^{-3}$ s at T_c. The energy barrier for amide isomerization, $\Delta G^{\ddagger}$, was calculated to be 74.35 kJ/mol. Insufficient exchange broadening below 100 °C in DMSO-d_6 prevented us from obtaining the coalescence temperatures for **5'c, 7c-9c, 7'c-9'c**.

3.2 Stuctural and thermodynamic analysis of pseudotripeptide methyl (2*S*)-2-({[(2*S*)-1-({3-[(*Z*)-(hydroxyamino)(imino)methyl]pyrazin-2-yl}carbonyl)pyrrolidin-2-yl]carbonyl}amino)-3-phenylpropanoate 7'd

Structural properties of the pyrazine amidoxime motif incorporated at N-terminus of the pseudotripeptide chain were investigated in order to determine its use in future applications. Information concerning the conformation adopted in solution by pseudotripeptide **7'd** was obtained by combining ^{1}H NMR and FT-IR absorption

spectroscopy analyses. Unfortunately, it has been difficult to perform NOESY or ROESY experiments with enough structural informations to calculate 3D structures of our molecules, neither good quality mono crystals could be obtained. The mobility of the peptidic part is probably a reason for these factual situations in both cases. Especially several conformations have been observed in NMR spectra. The strategy, repeatedly used successfully by our group and others, is to highlight the presence of hydrogen bonds.[63,64,136,137] For that purpose two spectroscopic methods were used combined to molecular dynamic calculations.

3.2.1 FT-IR and NMR investigations

First, FT-IR spectroscopy in solution was applied in order to observe the NH and CO stretching vibrations at around 3500-3200 cm^{-1} and 1600-1800 cm^{-1} region, respectively. Second, 1D 1H-NMR spectra in $CDCl_3$/DMSO-d_6 varying ratio highlights the labile protons not influenced by the environment changes because they are involved in hydrogen bonds.

FT-IR experiment of **7'd** at 25 °C shows a large peak at 3319 cm^{-1} which means that at least one NH and/or OH proton is involved in the hydrogen bond. In the carbonyl region of the spectrum, six bands are observed at 1743 cm^{-1}, 1722 cm^{-1}, 1679 cm^{-1}, 1670 cm^{-1}, 1656 cm^{-1} and 1653 cm^{-1} (Figure 3.5, Table 3.6).

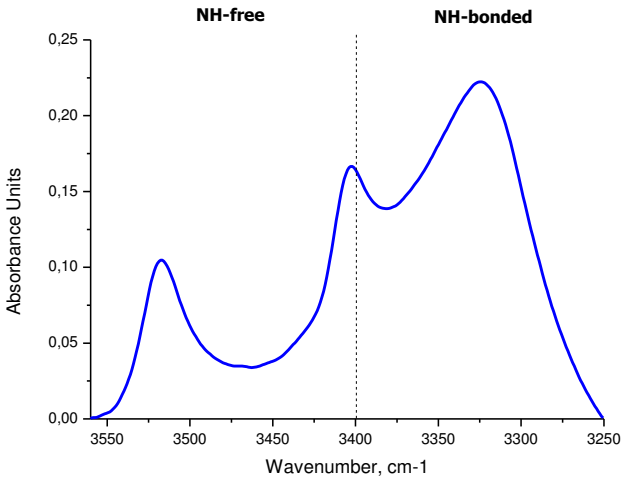

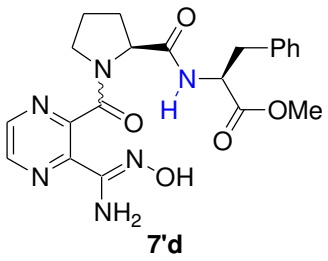

7'd

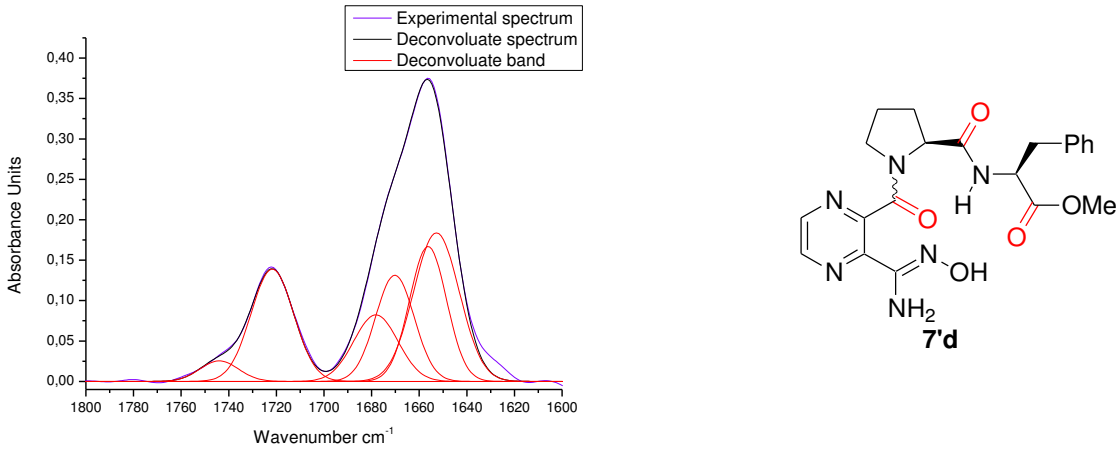

Figure 3.5 FT-IR spectra of pseudotripeptide **7'd** in $CHCl_3$ (10 mM)

The number of bands indicates that at least two of the three carbonyl groups of the molecule are involved in hydrogen bonds. According to their wavelengths, the two bands at 1743 cm^{-1} and 1722 cm^{-1} were assigned to the ester C=O free and involved in the hydrogen bond, respectively. The next four bands were assigned using the absorbance spectra of the shorter peptides with one amino acid and the pyrazine amidoxime motif **7'b** and **7'c** (Table 3.6, Figure 3.6).

Table 3.6 FT-IR adsorption in the C=O stretching regions for 10 mM concentration samples of AOPzPhe (**7'b**), AOPzPro (**7'c**) and AOPzProPhe (**7'd**) in chloroform at room temperature

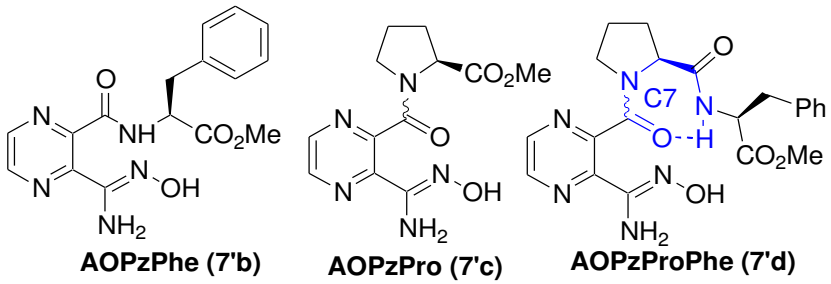

Product	*v*, cm^{-1} (C=O ester)	*v*, cm^{-1} (C=O amide)	*v*, cm^{-1} (C=N)
AOPzPhe	1743/1691	1680	1659
AOPzPro	1743	1655	1642
AOPzProPhe	1743/1722	1679 1670/1656	1653

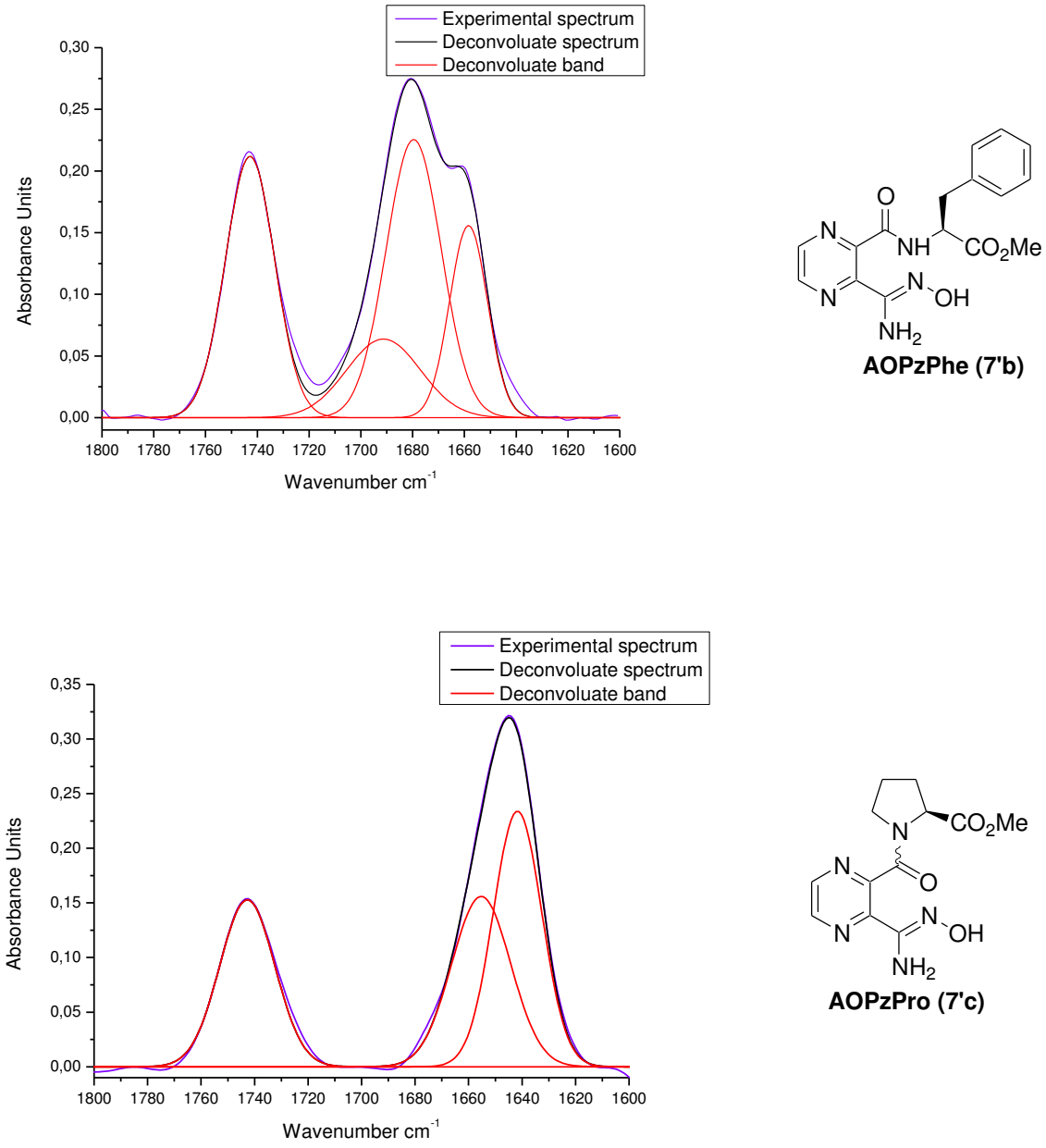

Figure 3.6 IR spectrum (C=O deconvoluted bands) of AOPzPhe (**7'b**) and AOPzPro (**7'c**) recorded in $CHCl_3$ (10 mM)

Therefore, the amide stretching vibration at 1679 cm^{-1} corresponds to C=O of the peptide bond between proline and phenylalanine as it is close to the value obtained for AOPzPhe (**7'b**). The bands at 1670 and 1656 cm^{-1} were attributed to the amide bond of the pyrazine ring and proline-phenylalanine dipeptide in both free and bonded forms, respectively. The C=N stretching vibration of the amidoxime group was then assigned to the band at 1653 cm^{-1}.

Results issued from IR spectroscopy experiments were complemented by ^{1}H NMR experiments in solvent mixtures, which showed that two sets of signals are present at every solvent mixture ratio (Figure 3.7).

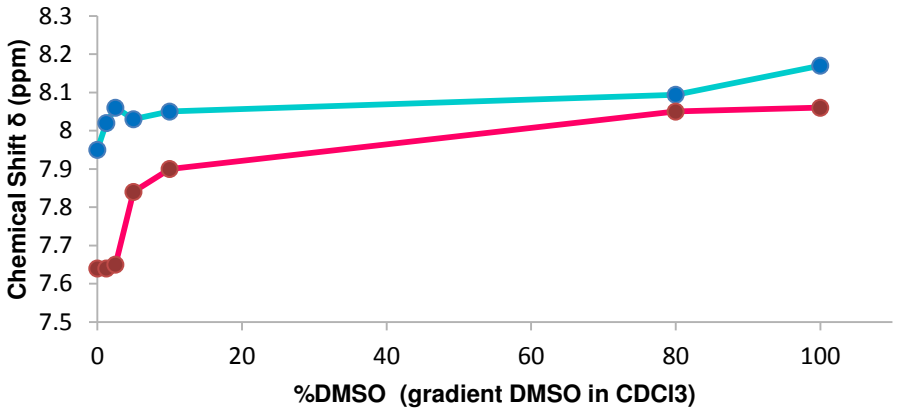

Figure 3.7 Effect of varying ratios of solvent in the mixture of $CDCl_3$ and DMSO-d_6 on the chemical shifts of the NH proton of **7'd** (3 mM)

This observation means that in solution, the structure of **7'd** is in equilibrium between at least two conformations. These results are consistent with the presence of the *cis/trans* isomers about the X-Pro peptide bond. Moreover, in both sets the amide proton of phenylalanine reveals no significant shift ($\Delta\delta$ = +0.22 and +0.42 ppm), which means that for both conformations the NH proton is involved in an intramolecular hydrogen bond. This result is consistent with the large band below 3400 cm^{-1} in the IR spectrum, which probably is the envelope of several bands.

Hence, the NH amide group of phenylalanine is involved in the hydrogen bond with the carbonyl group of pyrazine close to it (band at 1656 cm^{-1}) and adopt a seven-membered γ-turn conformation (Table 17).

Therefore, to confirm our observations, molecular modeling calculations in explicit solvent and without restraints have been undertaken.

3.2.2 Molecular modeling

Molecular dynamics calculations on the molecule **7'd** and on the simplified pseudodipeptide analogues AOPzPro (**7'c**) and AOPzPhe (**7'b**) were run in $CHCl_3$ and DMSO.

The superimposition of the three structures issued from simulation in $CHCl_3$ shows that the amidoxime-pyrazine moiety introduces rigidity of the molecules. (Figure 3.8). The superimpositions of the structures two by two show the good conservation of the structure of the motif since the rmsd on the position of amidoxime-pyrazine atoms are below 0.5 Å (Figures 4 - 6 in Appendix).

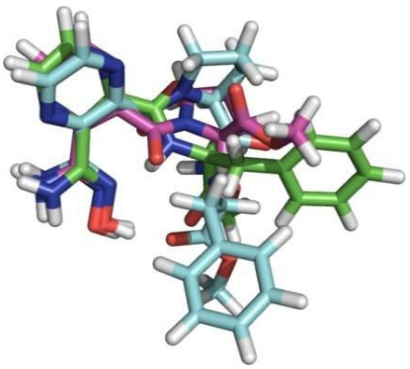

Figure 3.8 Superposition of **7'd** (blue) and its pseudodipeptide analogues AOPzPhe (**7'b**, green) and AOPzPro (**7'c**, pink); graphic representations were done in the PyMOL Molecular Graphics System, Version 1.8 Schrödinger, LLC

φ, ψ and ω dihedrals were measured over the trajectory of molecular dynamics simulations for all three molecules AOPzPhe **7'b**, AOPzPro **7'c** and AOPzProPhe **7'd**. The results show that all ω dihedral angle values are in favor of the *trans* peptide bonds in our simulations (Table 3.7).

Table 3.7 Mean dihedral angles of **7'b**, **7'c** and **7'd** calculated from 25000 structures issued of the molecular dynamics simulations

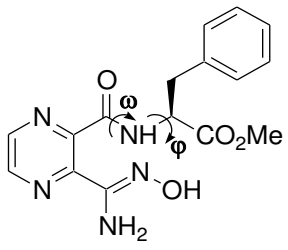

AOPzPhe (7'b)

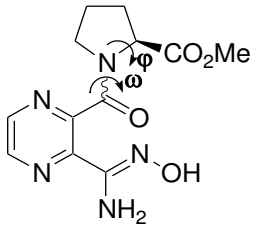

AOPzPro (7'c)

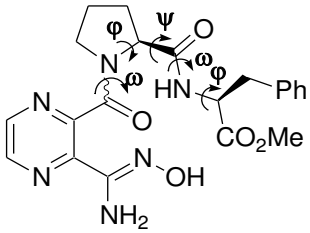

AOPzProPhe (7'd)

	φPro	φPhe	ψ	ωPro	ωPhe
AOPzProPhe (**7'd**)	-71±9	-139±18	|19±14|	|171±6|	|169±7|
AOPzPro (**7'c**)	|169±7|	-	-	|168±7|	-
AOPzPhe (**7'b**)	-	|94±57|	-	-	|156±21|

The mean φ and ψ angles for the proline residue for AOPzProPhe pseudopeptide **7'd** are depicted on the left-hand side of the Ramachandran plot in the favored region (Figure 3.9), which is close to the distribution of these average value of angles for proline residues measured in natural peptides for the α-region in Ramachandran plot (φ, ψ = -61°, -35°).[145]

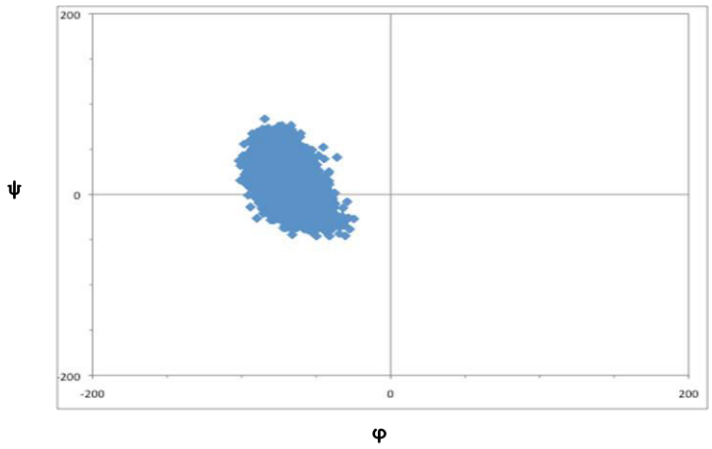

Figure 3.9 Ramachandran plot of proline in pseudotripeptide **7'd**

This correlation suggested that pyrazine-proline motif induced torsion when placed before proline residue and it could be particularly suited for peptidomimetic construction. The dihedral angle φ in crystalline AOPzPhe **7'b** is -108.2(2)° according to results of the X-Ray diffraction study.

However, we noted a major point of difference in the structures: the carbonyl group near the pyrazine ring is oriented differently in pseudopeptide **7'b** compared to **7'c** and **7'd**. In AOPzProPhe **7'd** and AOPzPro **7'c** the proline amino acid imposes an additional constraint associated with the steric hindrance due to the cyclic residue. This forces the proline carbonyl in **7'd** been angled outwards and promotes the hydrogen bonding between phenylalanine amide proton and the carbonyl next to the pyrazine ring (Figures 3.8, 3.10).

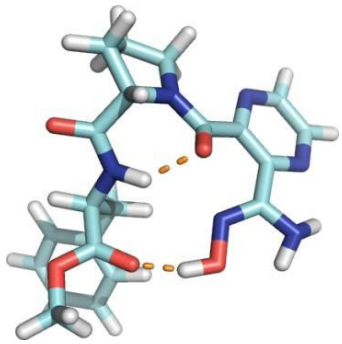

Figure 3.10 Solution conformations of pseudotripeptide **7'd**; hydrogen bonds (orange dots) in in solution ($CHCl_3$) as obtained from molecular dynamics simulation

Hence, two potential hydrogen bonds were observed for molecule **7'd**: first between carbonyl oxygen atom of the C-terminal ester group and the hydrogen atom of the amidoxime OH, and second between the oxygen atom of the amide carbonyl next to the pyrazine ring and the hydrogen of the amide group of phenylalanine with occurrence ratios of 98% and 42% respectively (Figure 3.10). Moreover, the strong hydrogen bond observed in molecular modeling of **7'd** is corroborated by the infrared experiments in solution. In the shorter molecule AOPzPhe **7'b** only one hydrogen bond was observed in $CHCl_3$ with an occurrence ratio of 31%, between ester C=O and OH of the amidoxime group (Figure 3.11a). The turns observed might be related to the β N-O turn defined by Chang and co-workers,[133] even if in our case a OH group is involded instead an amide group. However, as it follows from crystallography data, this hydrogen bond has not been observed in the crystal structure (Figure 3.11b).

a) 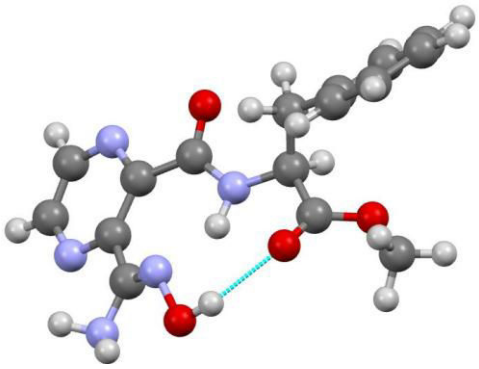 b) 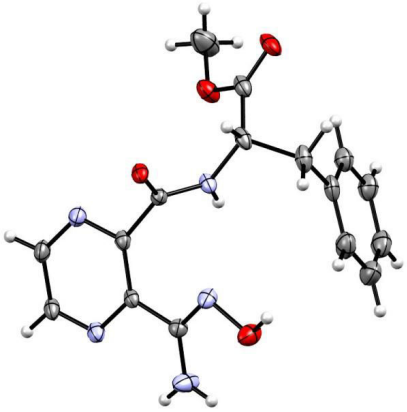

Figure 3.11 Structure of **7'b**: a) obtained from molecular dynamics simulation; b) according to results of the X-ray diffraction study

No hydrogen bond has been demonstrated in **7c'** molecule in solution (Figure 7 in Appendix) and no crystal was obtained. Simulations in DMSO, as expected, show that DMSO does not promote the establishment of hydrogen bonds except for AOPzProPhe **7'd** where the bond between the N-term OH and the C-term carbonyl group exist with an occurrence ratio of 96%.

With regards to the proline residue, two conformers were observed in NMR spectra of the proline derivatives and we decided to investigate further forward the *cis/trans* isomerization of **7'd**. In particular, we decided to consider the thermodynamics for *trans* and *cis* isomers of the prolyl peptide bond.

3.2.3 *cis-trans* isomerization study

Hydrogen bonds in $CHCl_3$ solution of **7'd** augment extremely the *trans* rotamer population up to 98%. Therefore, variable temperature ^1H NMR studies of the *cis/trans* conformational equilibrium were performed on the synthesized tripeptide **7'd**. The effects of temperature (in the range 25 – 90 °C) on the values of $K_{t/c}$ are illustrated by Van't Hoff plots in Figure 3.12. The corresponding results were compared to those obtained for the simple Pro-containing amidoxime **7'c**.

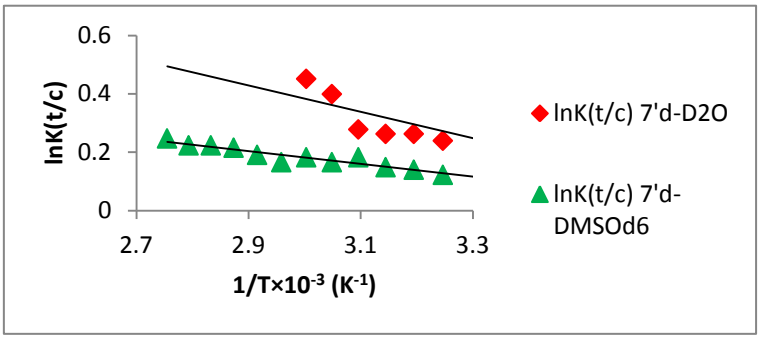

Figure 3.12 Van't Hoff plots for **7'd** in D_2O and DMSO-d_6

Interestingly, an increased amount of the *cis* conformation of **7'd** in polar solvents was observed. The *trans/cis* ratio of about 52/48, according to the relative intensities of their well-resolved peaks in the ^1H NMR spectra, does show important difference to the 73/27 ratio for **7'c** in DMSO solution. The increase of the *cis* isomer of **7'd** and the difference in $K_{t/c}$ between AOPzPro (**7'c**) and AOPzProPhe (**7'd**) may be due in part to interaction of the NH group with either the imide nitrogen lone pair or the imide carbonyl oxygen[140,146] or due to the stabilizing effect of the n $\rightarrow$ π^* interaction between the pyrazine nitrogen and C_{co} of the pyrrolidine ring.

The thermodynamic parameters of the *cis/trans* isomerization for prolyl amide bond of **7'd** were calculated from linear least-squares fits of the data in these plots to eq. 1 (Table 3.8).

Although all proline-containing molecules demonstrate a temperature-dependence with a slight positive slope (Figure 3.3), the tripeptide **7'd** shows negative slope in both D_2O and DMSO-d_6 (Figure 3.12).

Table 3.8 Thermodynamic parameters for compound AOPzProPhe (**7'd**). Additionally the *trans/cis* equilibrium constant at 300K is given

	$K_{t/c}$ at 300K	ΔH^0 (kJ mol^{-1})	ΔS^0 (J mol^{-1} K^{-1})	ΔG^0_{300K} (kJ mol^{-1})	$\Delta G^{\ddagger}$ (kJ mol^{-1})
7'd – DMSO-d_6	1.12	1.82	6.96	-0.27	-
7'd – D_2O	1.37	3.75	14.43	-0.58	75.3

As we can see the $K_{t/c}$ values of **7'd** are dependent on temperature such that the *trans* isomer becomes favored as the temperature increase, in other words, it is favored by enthropy. The *cis* rotamer is favored by enthalpy showing opposite behavior to the other proline derivatives (Tables 3.5, 3.8, Figures 3.3, 3.12). Hence, C-terminal proline substitution with the phenylalanine amino acid has significant influence on the *cis/trans* equilibrium and thermodynamics of **7'd**.

The free energy of activation ($\Delta G^{\ddagger}$) was determined to be 75.3 kJ/mol at the coalescence temperature 70°C in D_2O (Table 3.8, Figure 3.13). The rate of interconversion at T_c = 70 °C was found to be 24.4 s^{-1} (the separation of the OMe group signals, at δ 3.78 (ν = 1135 Hz) and 3.74 ppm (ν = 1124 Hz), $\Delta\nu$ = 11 Hz) and the half-life, $t_{1/2} = 63\times10^{-3}$ s.

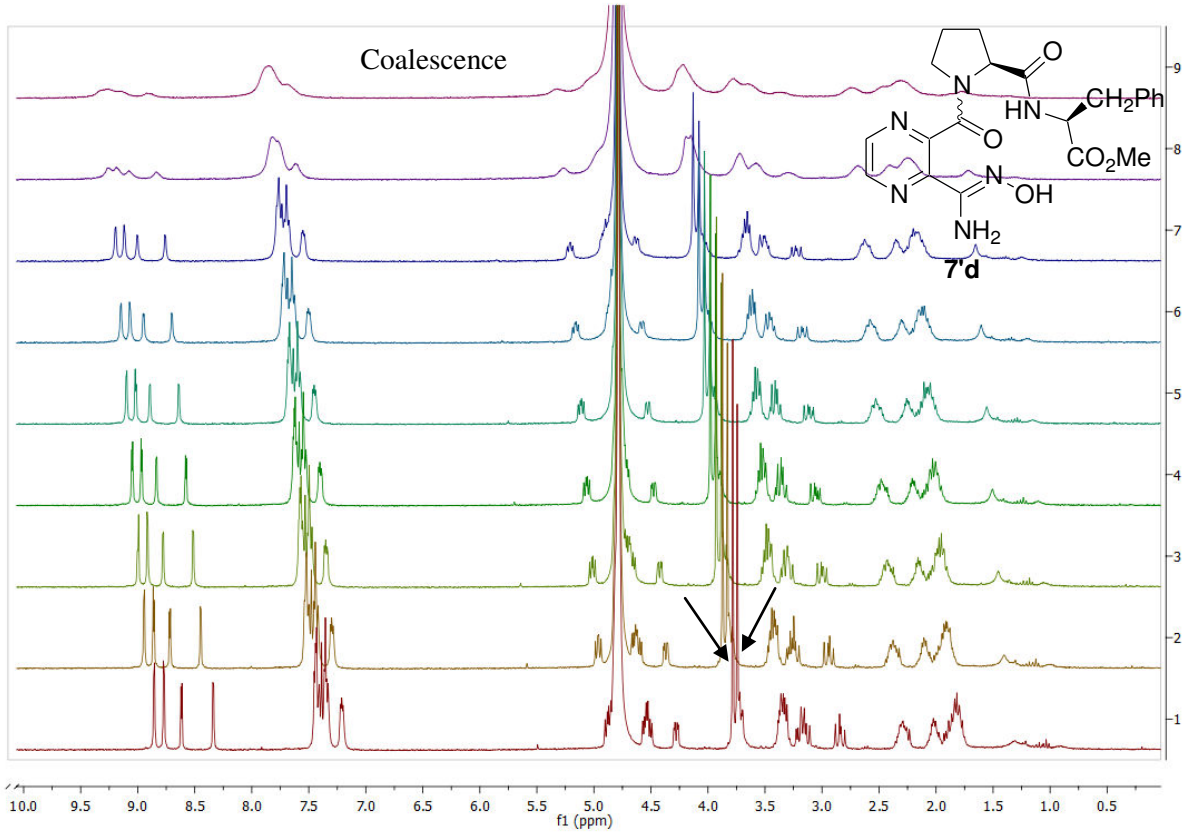

Figure 3.12 Temperature dependence of ^{1}H NMR chemical shifts of **7'd** in D_2O

3.2.4 A tentative correlation between toxicity and structure

The cellular toxicity of compounds was tested in order to verify a possibility of their use as therapeutics (Figure 3.14).

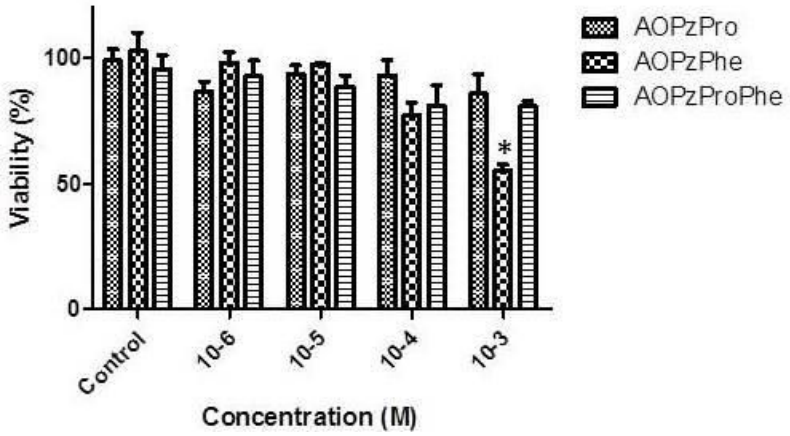

Figure 3.14 *In vitro* cytocompatibility of the three different pyrazine amidoxime derivatives (AOPzPhe (**7'b**), AOPzPro (**7'c**) and AOPzProPhe (**7'd**)) on smooth muscle cell line (A-10) compared to control cells (culture medium). A-10 cells were treated with the indicated concentrations of pyrazine amidoxime derivatives for 24 h at 37 °C. Viability was estimated

by the MTT assay. Data are expressed as mean ± sem (n = 3). *p<0.05 *versus* control Two way ANOVA, Bonferroni posttest

Cells bearing a mitochondrial activity between 100 to 80% are considered as viable. AOPzPro (**7'c**) and AOPzProPhe (**7'd**) were non-toxic whatever the concentration was. AOPzPhe (**7'b**) was toxic at 10^{-3} M, which promotes the use of proline containing pyrazine-amidoxime scaffold in therapeutics. However, this is a high concentration that will probably never be used in treatment.

4. Stuctural analysis of esterified amidoximes 8, 8' and oxadiazoles 9, 9'

4.1 Conformational analysis of alanine and phenylalanine derivatives 8, 8' (a,b) and 9, 9' (a,b)

Considering that *o*-substitution in the structures **8**, **8'** and **9**, **9'** could introduce an intramolecular hydrogen-bonding site forming turn-like structures, the conformational tendencies were investigated by FT-IR absorption and ^{1}H NMR experiments. Firstly, FT-IR spectra in $CHCl_3$ of **8**, **8'** (**a**,**b**) (Figure 3.15) were studied, and the presence of non-hydrogen-bonded amide N-H bands above 3400 cm^{-1} demonstrate that the Boc and ester carbonyl groups are not H-bonded.

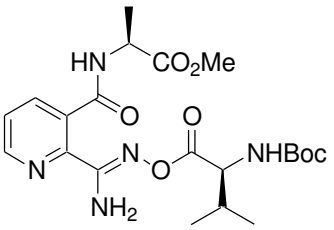

8a

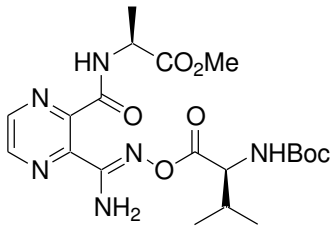

8'a

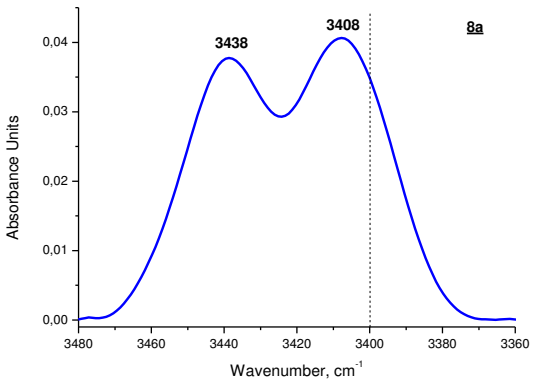

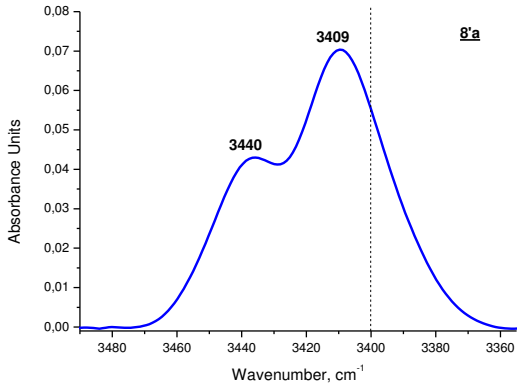

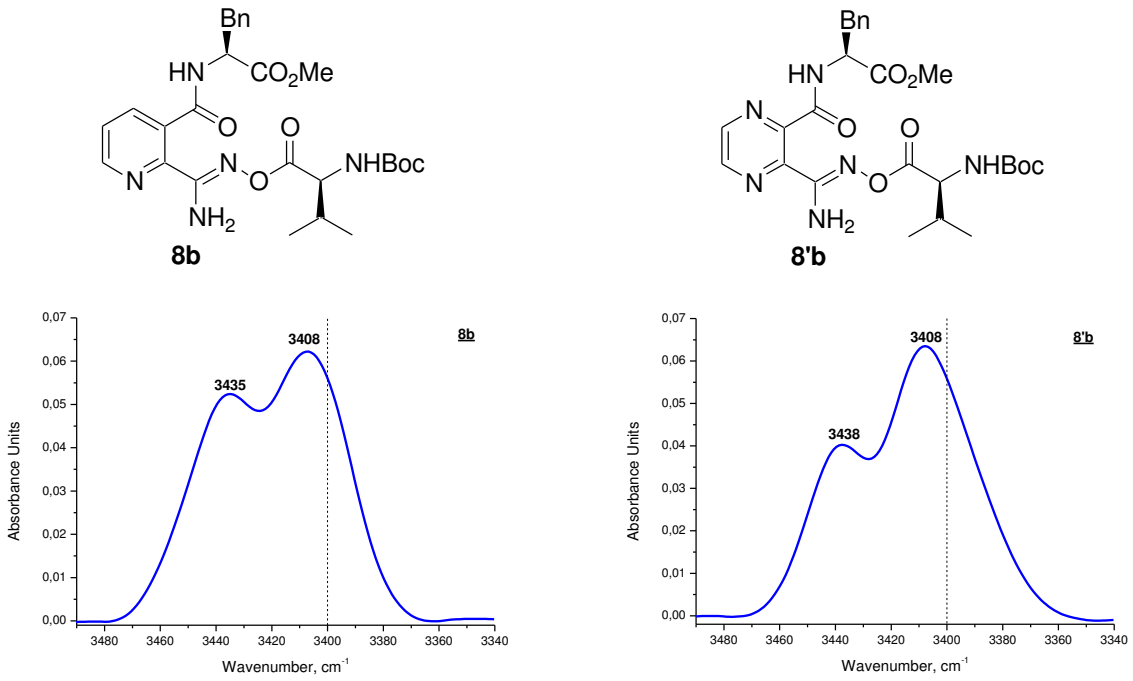

Figure 3.15 NH stretching vibrations of amidoxime esters **8**, **8'** (**a,b**) in $CHCl_3$ (10 mM)

The vibrations in the C=O region also did not show extra bands that could correspond to hydrogen bonded carbonyls (Table 3.9).

Table 3.9 Stretching vibrations in the C=O region of compounds **8**, **8'** (**a,b**) in $CHCl_3$ (10 mM)

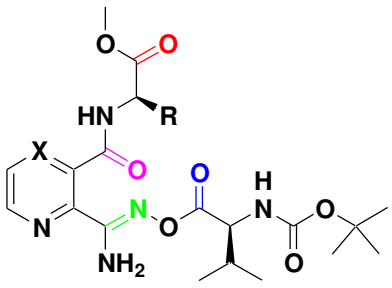

X, R		*ν*, cm^{-1}				
		C=O	C=O	C=O	C=O	C=N
CH, Me	**8a**	1767	1741	1712	1670	1651
CH, Bn	**8b**	1766	1743	1711	1670	1648
N, Me	**8'a**	1764	1743	1711	1688	1645
N, Bn	**8'b**	1766	1745	1712	1686	1645

IR-spectra of oxadiazole derivatives **9'a**,**b** exibit NH stretching vibrations at 3398 cm^{-1} and 3395 cm^{-1}, respectively (Figure 3.16). The corresponding pyridine counterparts **9a,b** display two NH stretching absorptions at higher frequency above 3400 cm^{-1}.

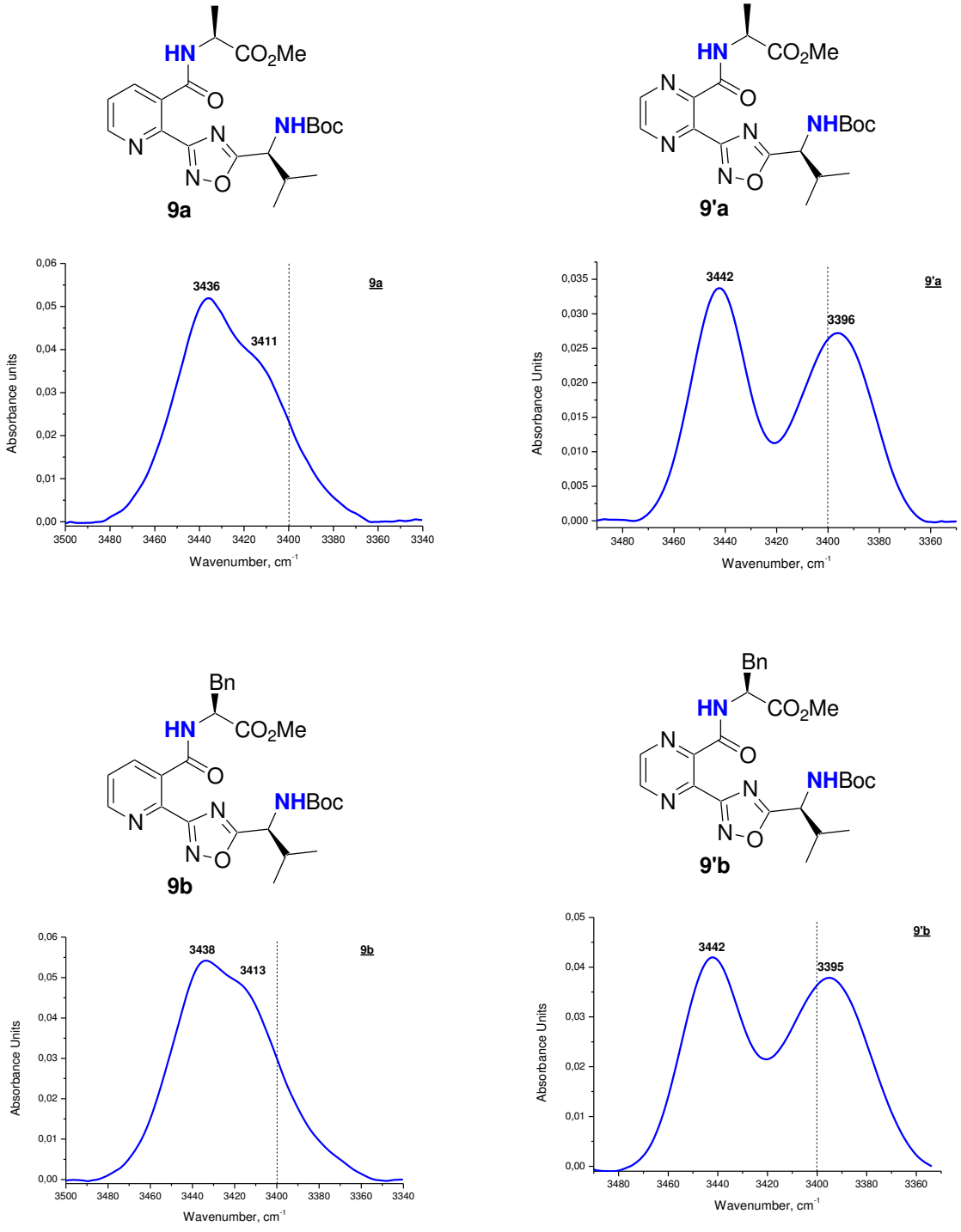

Figure 3.16 NH stretching vibrations of oxadiazole derivatives **9, 9'** (**a,b**) in $CHCl_3$ (10 mM)

It may be due to involvement of the NH amide protons and the pyrazine moiety in an NH…π interaction (Figure 3.17).[62,63]

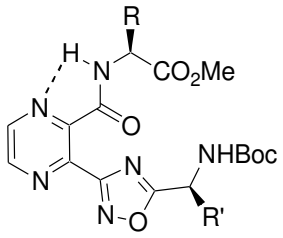

9'a,b

Figure 3.17 Intramolecular interactions in oxadiazole derivatives **9'a,b**

This is in agreement with the ^{1}H NMR data showing the downfield shifting $\Delta\delta$ NHamide = +0.23 ppm ongoing from **8'a,b** to **9'a,b** (Table 3.10).

Table 3.10 Chemical shifts and solvent sensitivity of the NH protons in **8'a,b** and **9'a,b**

	δNH (ppm)		**$\Delta\delta$ (ppm)**	**δNH (ppm)**		**$\Delta\delta$ (ppm)**	**$\Delta\delta$ (ppm) = δ (DMSO-d_6) – δ ($CDCl_3$)**	
	8'a	**9'a**		**8'b**	**9'b**		**9'a**	**9'b**
NH-amide	7.82	8.05	+0.23	7.72	7.95	+0.23	1.17	1.28
NHBoc	5.17	5.20	+0.03	5.15	5.19	+0.04	2.59	2.58

It is also notable that this interaction is little affected by solvation (up to 20% of DMSO-d_6) ($\Delta\delta$ NHamidic = +0.43 and +0.39 ppm; Figure 3.18).

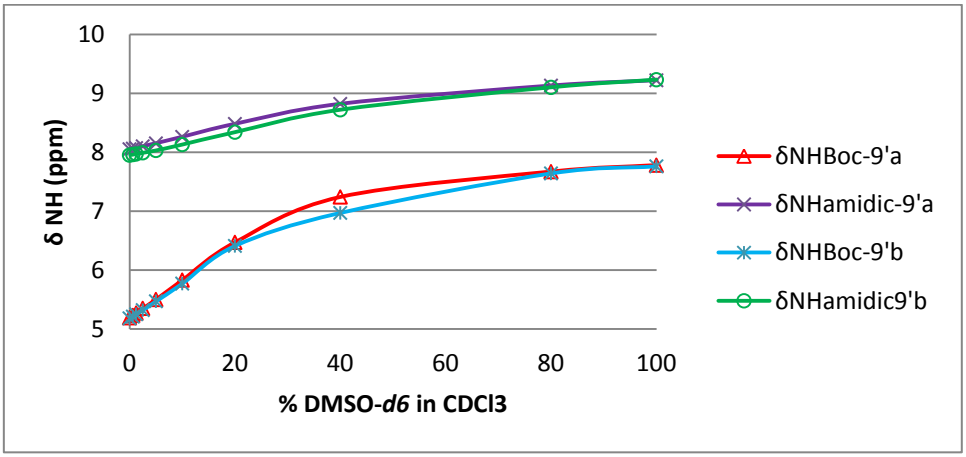

Figure 3.18 Effects of varying ratios of solvent in the mixture of $CDCl_3$/DMSO-d_6 on the chemical shifts of the NH protons of **9'a,b** (3 mM)

On the other hand, the signals NH amide of **9a,b** are shielded by the ring current of the pyridine cycle comparing to the same protons in **8a,b** and an upfield shift is observed (Table 3.11).

Table 3.11 Chemical shifts of the NH protons of **8a,b** and **9a,b**

	δNH (ppm)		Δδ	δNH (ppm)		Δδ
	8a	**9a**	**(ppm)**	**8b**	**9b**	**(ppm)**
NH-amide	7.58	6.78	-0.8	7.34	6.81	-0.53
NHBoc	5.08	5.39	+0.31	5.12	5.44	+0.32

4.2 Conformational analysis of the proline derivatives 8c, 8'c and 9c, 9'c

FT-IR spectra in $CHCl_3$ of **8c**, **8'c** (Figure 3.19) were studied demonstrating only the presence of non hydrogen-bonded amide N-H bands. Oxadiazole derivative **9'c** in its FT-IR spectrum exibits bands due to both free NH (3438 cm^{-1}) and hydrogen-bonded NH (3363 cm^{-1}) stretching vibrations over the concentration of 10 mM; and further dilution confirms the absence of solute-solute interactions (Figure 3.19).

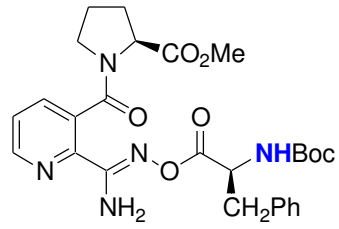

8c

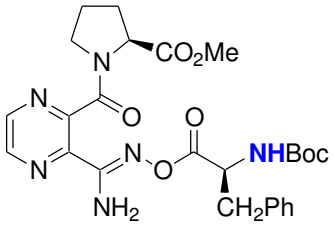

8'c

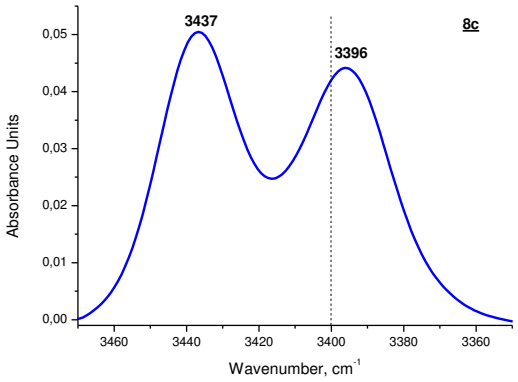

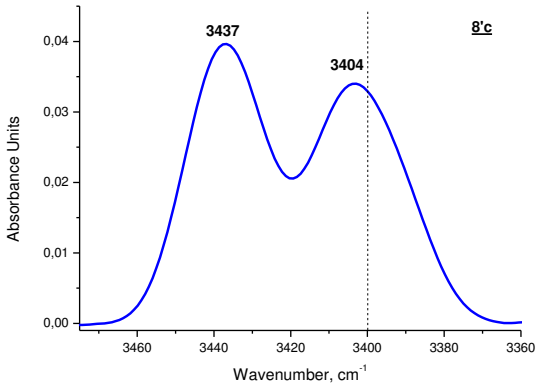

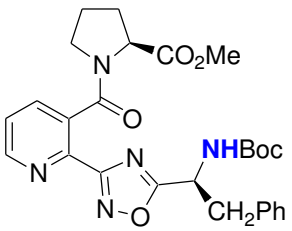

9c

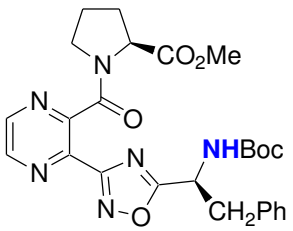

9'c

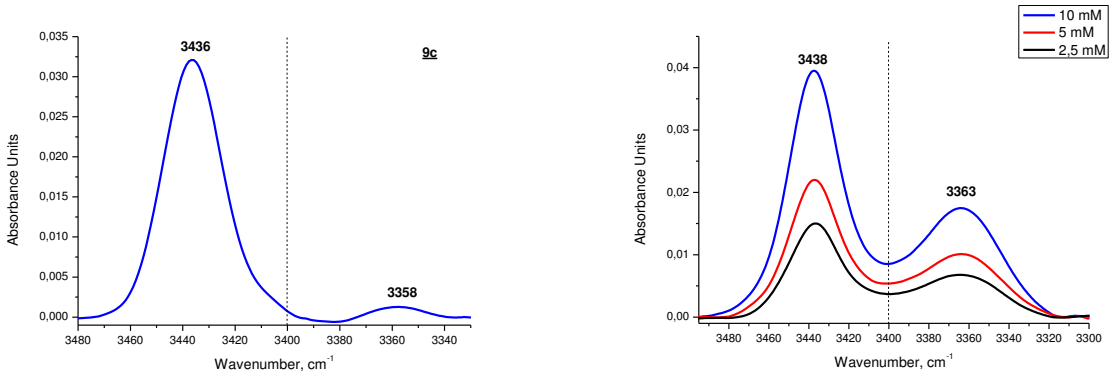

Figure 3.19 NH stretching vibrations of proline derivatives **8c**, **8'c** and **9c**, **9'c** in $CHCl_3$ (10 mM)

The investigation of the CO-stretching bands in $CHCl_3$ did not give us to separate the H-bonded CO band presumably due to the low intensity and/or overlapping of some bands (Figure 3.20). However, we supposed a weak interaction of the NH with amide carbonyl as CO ester should be oriented outward to form C=O…C=O an n → π* interaction similarly to **7'c** and **8'c** (Table 3.4).

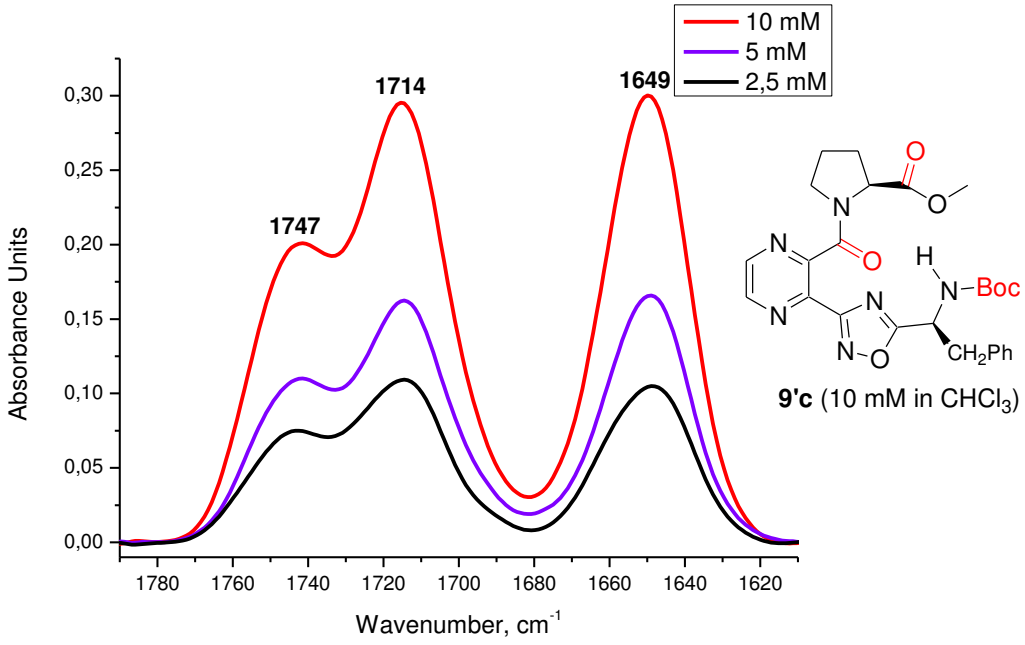

Figure 3.20 IR spectrum (C=O deconvoluted bands) of **9'c**

This result provides support that NHBoc of the phenylalanine of **9'c** is H-bonded with the amide carbonyl group of pyrazinyl-Pro amide bond.

The NMR spectra of **8c**, **8'c** and **9c**, **9'c** revealed two sets of resonances in $CDCl_3$ at room temperature corresponding to the *cis* and *trans* amide bond rotamers. The NH signal shifting in the *trans* isomer of **9'c** compared to the free NH of **8'c** ($\Delta\delta$ NHBoc = +0.48 ppm) supported the presence of the interaction in **9'c**. This hydrogen bond seems possible also looking at NOESY experiment for **9'c** in solution in $CDCl_3$ where a NOE correlation is observed for the NHBoc proton when the Pro-OMe resonance was saturated (Table 3.12, Figure 3.21).

Table 3.12 Chemical shifts and solvent sensitivity of the NH protons of **8c**, **8'c** and **9c**, **9'c**

	δNH (ppm)		**$\Delta\delta$ (ppm)**	**δNH (ppm)**		**$\Delta\delta$ (ppm)**	**$\Delta\delta$ (ppm) = δ (DMSO-d_6) - δ ($CDCl_3$)**	
	8c	**9c**		**8'c**	**9'c**		**9c**	**9'c**
NHBoc-*trans*	5.11	5.53	+0.42	5.15	5.63	**+0.48**	3.62	2.22
NHBoc-*cis*	5.09	5.27	+0.18	5.05	5.17	+0.12	-	2.67

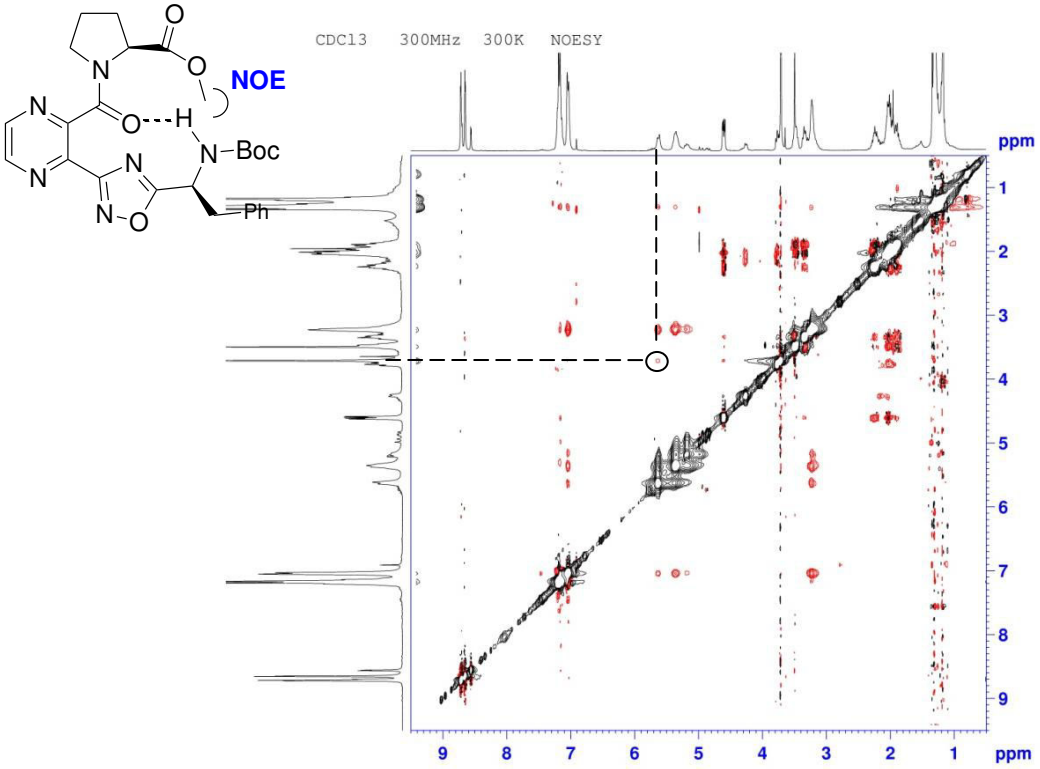

Figure 3.21 NOESY NMR spectrum of pseudopeptide **9'c**

The titration of the NH proton shift of peptidomimetics **9c**, **9'c** revealed that DMSO-d_6, a strong hydrogen-bonding solvent, produces a significant downfield shifting (Table 3.12). However, in case of the pyrazine-based oxadiazole **9'c**, the initial steps of titration reveal low downfield shifts $\Delta\delta$ = 0.44/0.53 ppm (*trans/cis* at 5% DMSO-d_6) and $\Delta\delta$ = 0.8/1 ppm (*trans/cis* at 10% DMSO-d_6, Figure 3.22). This could be evidence of a weakly H-bonded Phe NHBoc proton at low concentrations of DMSO-d_6, that become solvent-exposed as a result of conformational change at polar solvent higher concentration.[147]

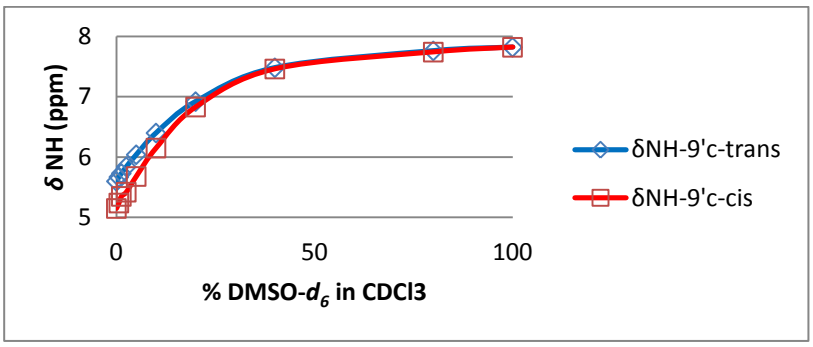

Figure 3.22 Effects of varying ratios of solvent in the mixture of $CDCl_3$/DMSO-d_6 on the chemical shifts of the NH protons of **9'c** (3 mM)

5. Structural and thermodynamic studies of acylamidrazones 10, 10'

In the ^1H and ^{13}C NMR spectra of acylamidrazone derivatives **10**, **10'**, two sets of signals are observed in DMSO-d_6 for most of the protons and carbons. This indicates that compounds exist as a mixture of *Z* and *E* isomers. Our literature survey has revealed that acylamidrazones can display amide hydrazone (**A**) - hydrazide imide (**B**) tautomerism because of C=N bond or they can exist as *Z* and *E* isomers due to C=N or amide bond isomerism (Scheme 3.1).[121,123,148] From these observations the problem of resonance assignment has become apparent.

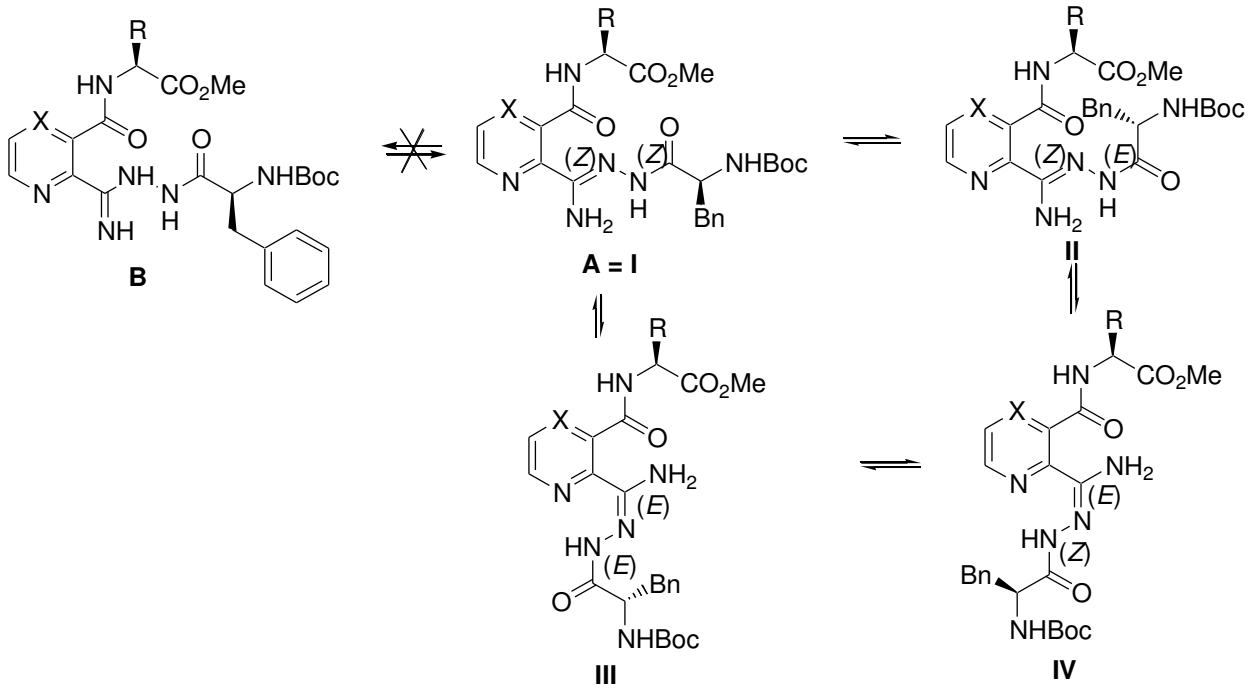

Scheme 3.1 Possible isomerism in *N*-acylamidrazones **10** (X = CH) and **10'** (X = N)

Two sets of signals were observed in the ^{1}H NMR spectra for most of the protons of compounds **10**, **10'** indicating the presence of only two forms. We abandoned plausible tautomeric forms **A** and **B**, as two singlets due to NH_2 signals were observed in the ^{1}H NMR spectra corresponding to each isomer. A COSY and NOESY experiments were performed for assignment of two populations. A NOE peak between the =N-N<u>H</u>- and the NH_2 protons of compound **10b** was observed for each conformation which indicated the presence of only *Z* isomers around C=N double bond and supported the occurrence of *Z* and *E* rotamers due to amide-type isomerism (Figure 3.23).

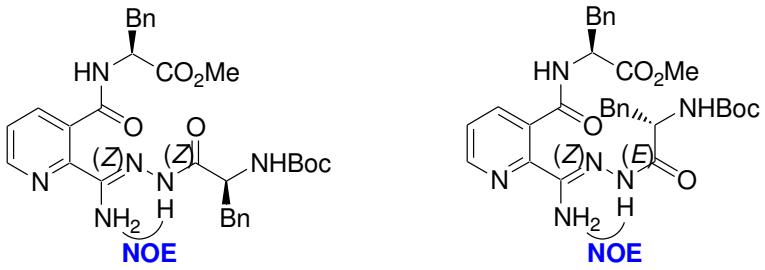

Figure 3.23 NOE effects in a mixture of *Z* and *E* amide isomers of **10b**

However, the =N-N<u>H</u>- protons in the rest of the series (**10a**, **10'a**, **10'b**) appeared with the same chemical shifts, thus we were unable to prove amide isomerism for these compound. Moreover, no correlations were found in NOESY spectra that could help to assign proton

signals to either *Z* or *E* isomers. In order to find the most stable structures, calculations were performed on compound **10a** (X = CH, R = CH_3) and the results are listed in Figure 3.24.

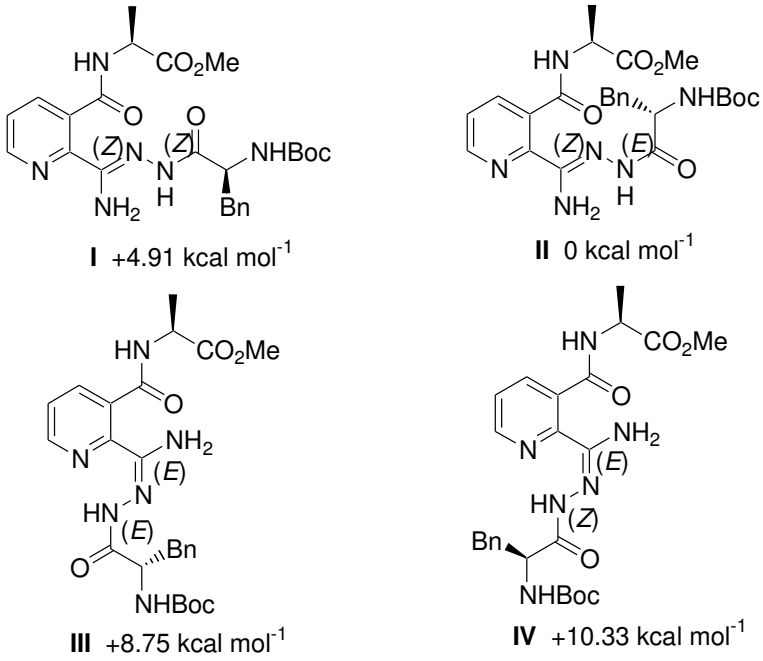

Figure 3.24 Comparison of the energies of the isomeric forms of compound **10a**; all structures were optimized using B3LYP/6-31G(d,p) density functional level of theory and energies are listed relatively to the lowest energy form

From Figure 3.34 it can be seen that isomeric forms **I** and **II** corresponding to *Z/E* amide isomers, have the lowest energies therefore are the most stable in *vacuo* according to the calculations which is in agreement with experimental data for compound **10b**. Isomers **III** and **IV** exhibit the *E* form around C=N bond and have higher energies hence are unfavorable. Calculations were then performed on all conformers of *N*-acylamidrazones **10b**, **10'a** and **10'b** (Table 3.13). Pyridine derivative **10b** revealed the same *Z/E* amide isomerism according to the calculations. However, pyrazine counterparts **10'a** and **10'b** showed *Z/E* isomerism around C=N bond, as it follows from the lowest energies values for conformers **II** and **III** (Table 3.13). In accord with previous calculations, the *E* amide isomer has the lowest energy in all series. The obtained energy differences (ΔE) between **I** and **II** for **10a,b** and between **II** and **III** for **10'a,b** were in the range 2.49-4.91 kcal/mol and depended mainly on the heterocycle (higher for pyridine derivatives **10a,b** and lower for pyrazine derivatives **10'a,b**).

Table 3.13 Absolute and relative energies (in atomic units and kcal/mol, respectively) for isomers of *N*-acylamidrazones calculated at B3LYP level of theory using 6-31G(d,p) basis set

X, R	E_I [a.u.]	E_{II} [a.u.]	E_{III} [a.u.]	E_{IV} [a.u.]	ΔE [kcal/mol]
CH, Me (**10a**)	-1751.286540	-1751.294366	-1751.280429	-1751.277908	4.91
CH, Bn (**10b**)	-1982.258785	-1982.265883	-1982.256207	-1982.252817	4.45
N, Me (**10'a**)	-1767.328071	-1767.335808	-1767.331841	-1767.326273	2.49
N, Bn (**10'b**)	-1998.299683	-1998.306963	-1998.300874	-1998.298101	3.82

Note: Energies include both electronic and thermal energies. Geometries were obtained by energy minimization at the stated level of theory. ΔE was calculated as a difference between energies of the most stable configurations (underligned values).

The energy barriers ($\Delta G^{\ddagger}$) and other parameters for amide isomerization in **10a**,**b** and *Z/E* isomerization around C=N bond in **10'a**,**b** were determined by NMR spectroscopy using equations 3-5 (Table 3.14). ^{1}H NMR spectra were recorded at increasing temperatures in DMSO-d_6 until the coalescence of the two isomer populations was observed. The barrier for isomerization in **10a** was calculated to be 74.73 kJ/mol at 65 °C while in the case of **10b** – 75.69 kJ/mol at 80 °C. This difference is probably due to the influence of the more bulky phenylalanine residue on the amide isomerization. The barriers in pyrazine derivatives **10'a** and **10'b** were calculated to be 75.55 kJ/mol at 80 °C. For the *Z/E* isomerization around C=N bond in **10'a**,**b** the difference in C-terminal amino acid residue does not influence on the rotational barrier values.

Table 3.14 Rotational barriers for the *Z/E* isomerization

Compound	T_c, K	$\Delta\nu$, Hz	k, s^{-1}	$t_{1/2}$, s	$\Delta G^{\ddagger}$ at T_c, kJ/mol
10a	338	9	20.0	0.03	74.73
10b	353	21	46.6	0.01	75.69
10'a	353	22	48.8	0.01	75.55
10'b	353	22	48.8	0.01	75.55

Note: $\Delta\nu$ – the separation of the OMe groups signals in DMSO-d_6

A resonance assignment of the NH chemical shifts was performed for **10**, **10'** which exhibited two sets of signals, the downfield NH resonances being associated with the major *E* amide isomers of **10a**,**b** and with the *Z* isomers around C=N bond for **10'a**,**b** (Table 3.15). However, it was not possible to distinguish the NH-amide protons for **10'** due to overlapping of signals with the CH protons of the pyrazine ring.

Table 3.15 Comparison of the chemical shifts of the NH protons for two ismers in DMSO-d_6

	δNH-N=		**Δδ**	**δNH-amide**		**Δδ**	**δNHBoc**		**Δδ**
	E	***Z***		***E***	***Z***		***E***	***Z***	
10a	9.86	9.86	0	8.77	8.54	0.23	7.01	6.21	0.80
10b	9.91	9.87	0.04	9.03	8.64	0.39	7.00	6.11	0.89
	Z	***E***	**Δδ**	***Z***	***E***	**Δδ**	***Z***	***E***	**Δδ**
10'a	9.91	9.91	0	-	-	-	7.03	6.38	0.65
10'b	9.93	9.92	0.01	-	-	-	7.02	6.32	0.70

We have also determined isomeric ratio of compounds in DMSO-d_6 (Table 3.16). The population of the *Z* conformer slightly decreases with increasing size of the R group in amino acid residue which is presumably due to some steric hindrance. We next wanted to test the effect of solvent polarity on the isomeric ratio. Surprisingly, a partial decomposition of the pyridine derivatives **10a,b** occurred after adding $CDCl_3$ (Table 3.16, Scheme 3.2). The proton signals of the pyrrolopyridines **6a,b** appear in a mixture DMSO-d_6/$CDCl_3$ and become predominant with increasing the ratio up to 1:3. The instant formation of **6a,b** was also detected by LCMS analysis.

Table 3.16 Influence of solvent polarity on the *E/Z* isomeric ratio of compounds **10**, **10'**

	E/Z ratio		
DMSO-d_6/$CDCl_3$	**1:0**	**1:1**	**1:3**
10a	1/0.63	-[a]	-[b]
10b	1/0.56	-[c]	-[d]
	Z/E ratio		
10'a	1/0.70	1/0.66	1/0.50
10'b	1/0.67	1/0.69	1/0.55

[a]Mixture containing **10a** and **6a** (~45% of **6a**);
[b]Mixture containing **10a** and **6a** (~65% of **6a**);
[c]Mixture containing **10b** and **6b** (~35% of **6a**);
[d]Mixture containing **10b** and **6b** (~55% of **6a**).

We have suggested the mechanism different to the route proposed for the amidoxime decomposition which involves nucleophilic attack of the NH_2 on the carbon of amide carbonyl, as in this case the formation of **6** does not occur (Scheme 2.8). A proposed mechanism includes nucleophilic attack of the NH on the carbon of C=N acylamidrazone followed by cyclyzation depicted in Scheme 3.2.

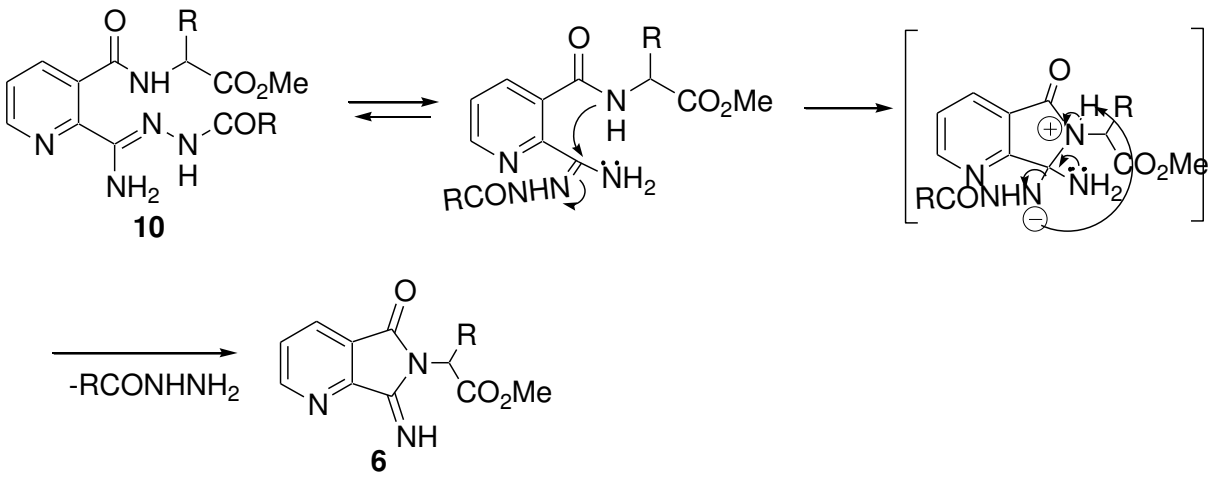

Scheme 3.2 Suggested mechanism of intramolecular cyclization in non hydrogen bonding solvents for pyridine-based compounds **10a,b**

Such intramolecular cyclization in $CDCl_3$ is negligible (<5%) in case of the pyrazine analogues **10'** and the proportion of the *Z* conformer decreasing with increasing solvent polarity. From these results, it is clear that in polar solvent like DMSO all compounds are stabilized by hydrogen bonding with solvent molecules. We suggest a hydrogen bond between NH-amide and nitrogen of the pyrazine ring that can stabilize the pyrazine derivatives and exists even in non hydrogen bonding solvents, precluding intramolecular cyclization into the precursors **6'**. According to density functional quantum chemical calculations the lowest energy structures of acylamidrazones **10'** indeed possess hydrogen bonds which is confirmed by the NH…N distances 2.41 and 2.39 Å and the NH…N angles values 99° and 100° for **10'a** and **10'b** respectivly (Figure 3.25)

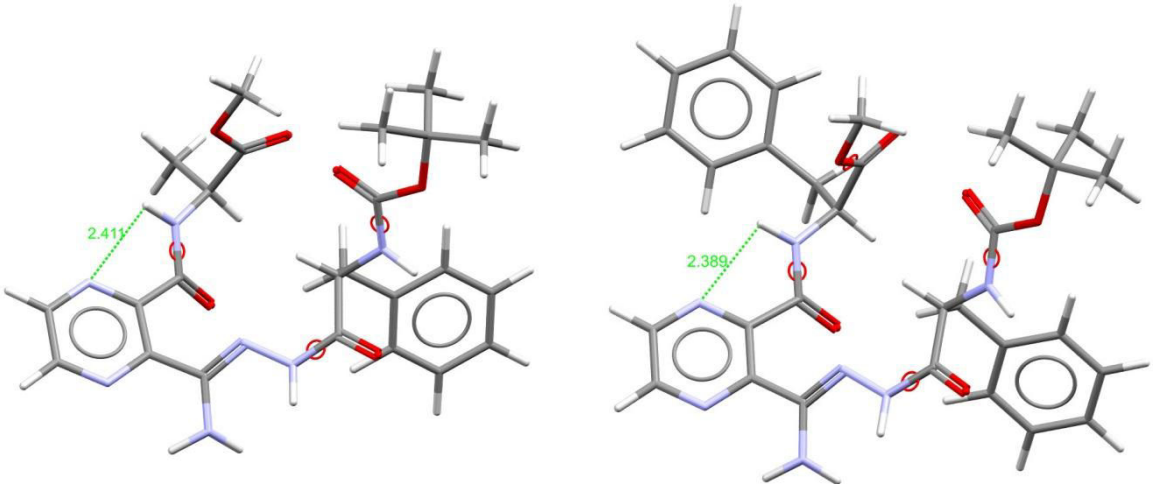

Figure 3.25 Hydrogen bonding in the lowest energy acylamidrazones **10'a**,**b**

6. Stuctural analysis of hydrazide modified peptidomimetics 12, 12'

The assignment of all NH protons of the pyrazine-based hydrazide products was made by means of COSY and NOESY NMR spectra at first. As for the other pyridine and pyrazine derivatives, the comparison of the NH-amide protons revealed a downfield shift above 1 ppm ongoing from pyridine derivatives **12a,b** to pyrazine analoges **12'a,b** (Table 3.17).

Table 3.17 NH chemical shifts of peptidomimetics **12**, **12'** in $CDCl_3$ (3 mM)

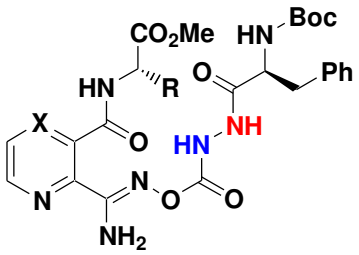

X, R	δ (ppm)			
	NHBoc	NH-amide	NH-hydrazide	NH-hydrazide
CH, Me (**12a**)	5.02	**6.37**	7.39	8.22
CH, Bn (**12b**)	5.03	**6.44**	7.74	8.36
N, Me (**12'a**)	5.01	**7.4**	7.86	8.3
N, Bn (**12'b**)	5.13	**7.27**	7.84	8.34

To highlight the presence of hydrogen bonds two spectroscopic methods were used. First, FT-IR spectroscopy in solution in order to observe the NH and CO stretching vibrations at around 3500-3200 cm^{-1} and 1600-1800 cm^{-1} regions, respectively. Second, ^{1}H-NMR spectra in $CDCl_3$/DMSO varying ratio hightlight the labile protons not influenced by the environment changes because they are involved in hydrogen bonds.

FT-IR experiment of pyridine derivatives **12a,b** at 25°C showed a broad peak below 3400 cm^{-1} which consists of at least two NH protons of the hydrazide fragment. Unfortunately, it was not possible to distinguish the different NH bands under this peak (Figure 3.26).

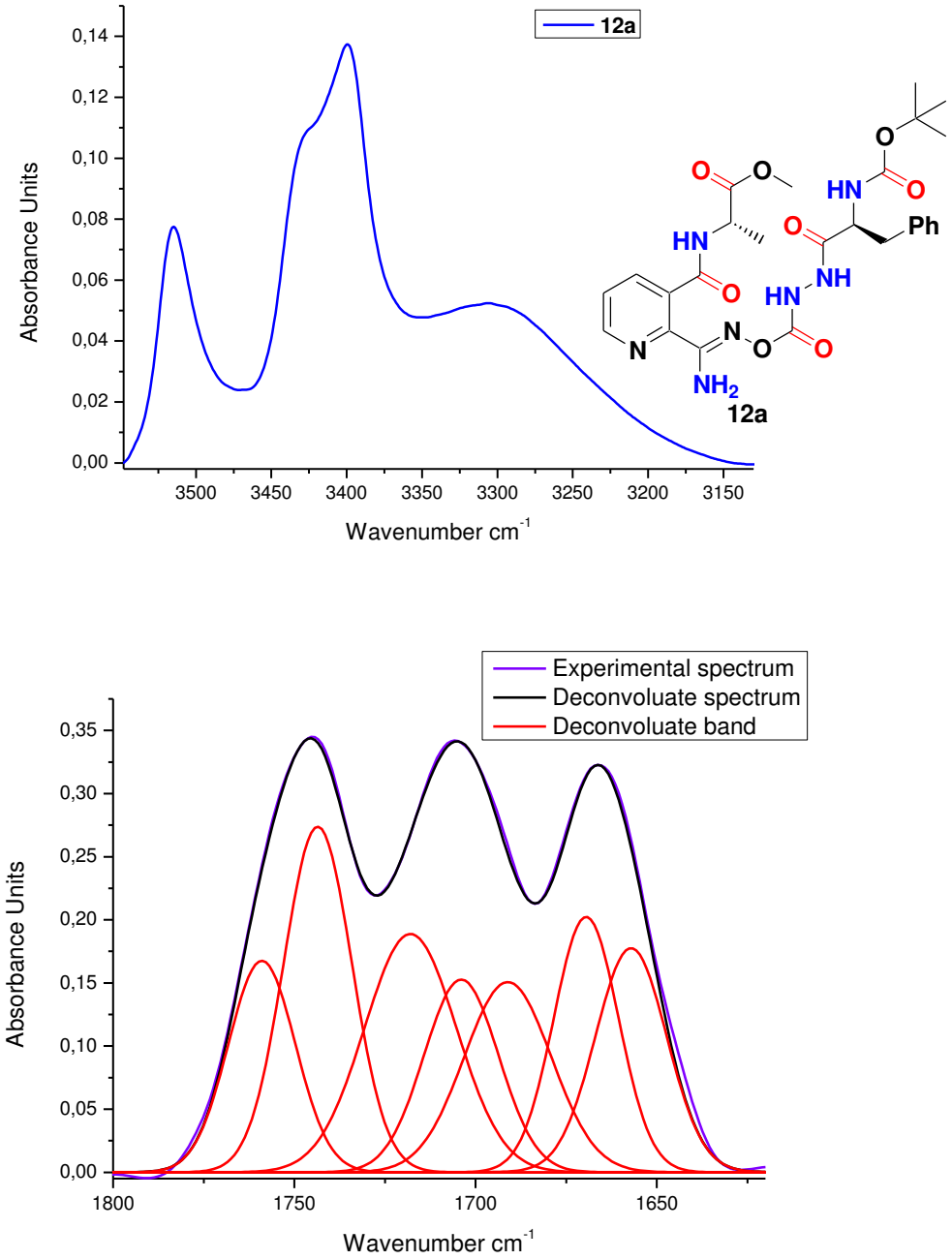

Figure 3.26 FT-IR spectra of **12a** in $CHCl_3$ (10 mM)

In the carbonyl region of the spectrum, seven bands were observed (Figure 3.26, Table 3.18). Number of bands indicates that one of the carbonyl in the molecule is involved in hydrogen bond. According to their wavelengths, two bands at 1693 cm^{-1} and 1668 cm^{-1} were assigned to the amide carbonyl free and involved in a hydrogen bond, respectively. In case of **12b**, similar tendencies were observed in the NH and C=O regions (Figure 3.27, Table 3.18).

Therefore, two bands at 1699 cm^{-1} and 1669 cm^{-1} were attributed to the free and bonded amidic carbonyl.

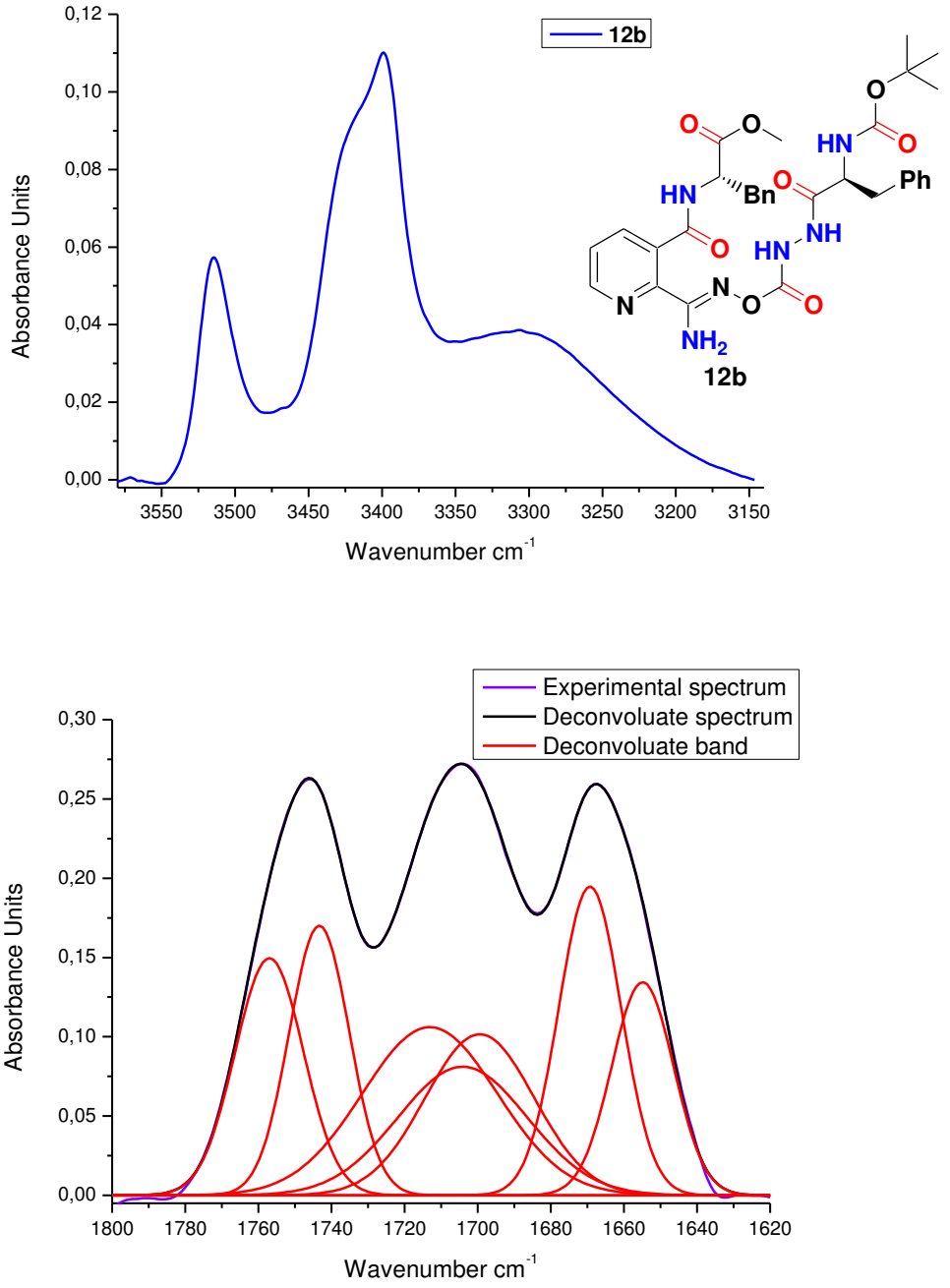

Figure 3.27 FT-IR spectra of **12b** in $CHCl_3$ (10 mM)

Table 3.18 Carbonyl stretching vibrations of pyridine-based peptidomimetics **12a**,**b**

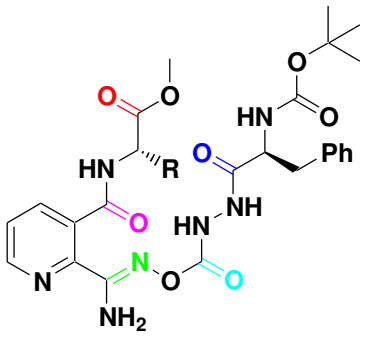

	ν, cm^{-1}						
	C=O	C=O	C=O	C=O	C=O free	C=O bonded	C=N
12a (R = Me)	1755	1742	1708	1703	1693	1668	1661
12b (R = Bn)	1754	1745	1713	1705	1699	1669	1657

The FT-IR spectra of pyrazine-based analogues in the NH region also revealed a broad shoulder below 3400 cm^{-1}, however we did not succeed to assign the stretching vibrations in the C=O region (Figure 3.28)

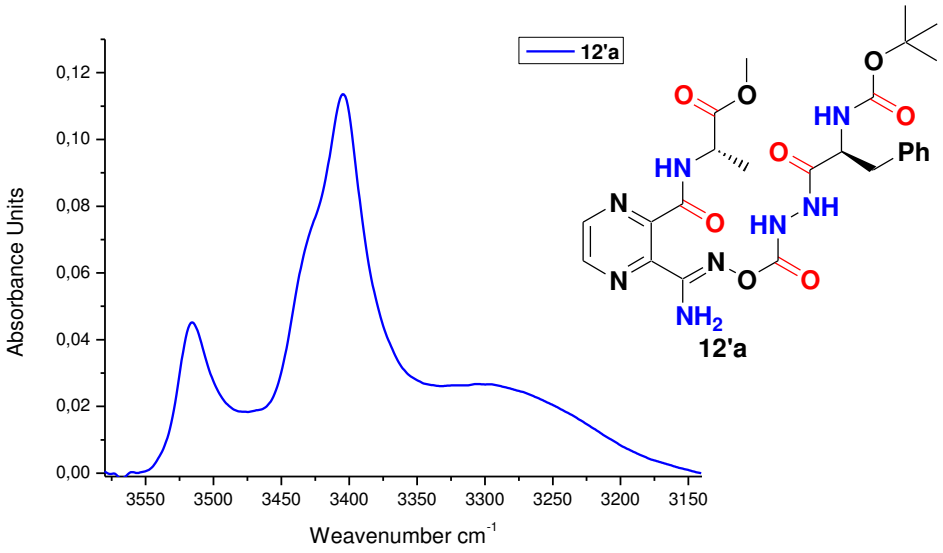

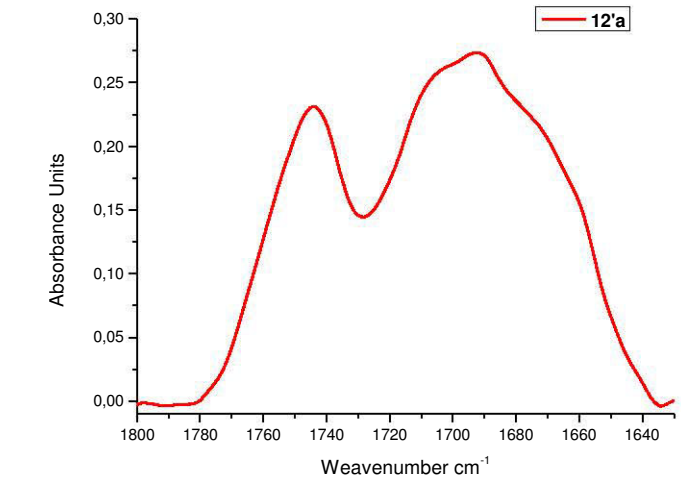

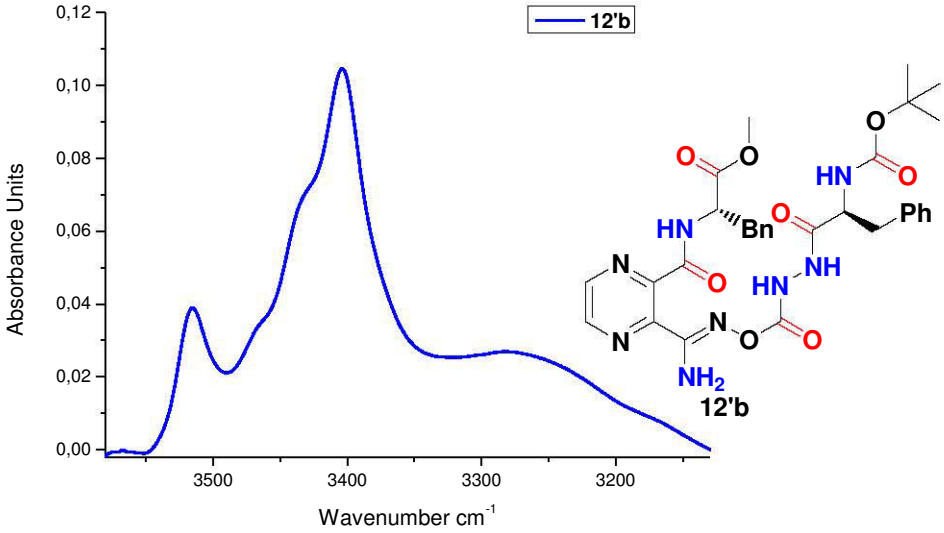

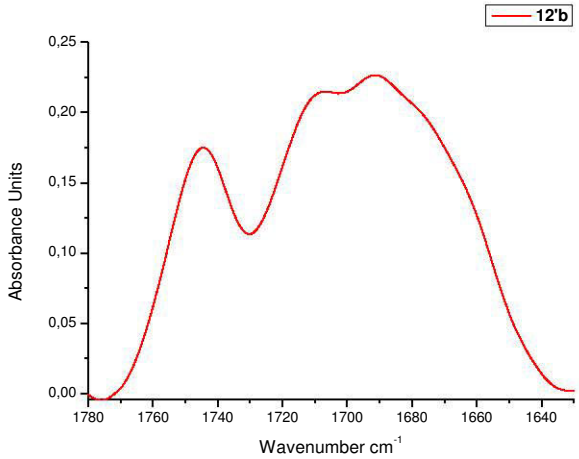

Figure 3.28 FT-IR spectra of **12'a**, **12'b** in $CHCl_3$ (10 mM)

Results issued from IR spectroscopy experiments were complemented by ^{1}H NMR experiments in the variable concentration mixtures of $CDCl_3$/DMSO-d_6. The titration of the NH protons shifts showed that only one NH-hydrazide[2] proton is involved in the strong intramolecular hydrogen bonding based on the $\Delta\delta$ which is in the range 0.18 - 0.48 ppm (Table 3.19, Figure 3.29). Moreover, the NHBoc proton showed moderate sensitivity to solvation and its chemical shift did not show significant change up to 10% of DMSO-d_6 ($\Delta\delta$ NHamidic = +0.64 and +0.44 ppm for **12a** and **12b**; $\Delta\delta$ NHamidic = +0.64 and +0.46 ppm for **12'a** and **12'b** Figure 3.29). This can be due to the weak intramolecular hydrogen-bonding of the NHBoc proton with oxygen of OMe group. The interaction is a bit stronger for phenylalanine derivatives **12b**,**12'b**. The amide NH protons of the pyrazine derivatives **12'a**,**b** revealed low downfield shifts at the initial steps of titration $\Delta\delta$ = +0.77 and +0.62 ppm respectively (10% DMSO-d_6, Figure 3.29) which could be the result of a weak bonding with the nitrogen of the pyrazine ring.

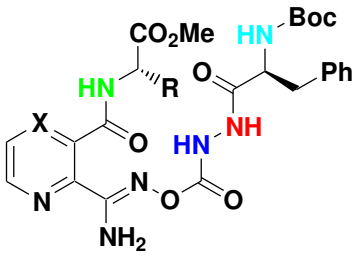

	X	R
12a	CH	Me (Ala)
12b	CH	Bn (Phe)
12'a	N	Me (Ala)
12'b	N	Bn (Phe)

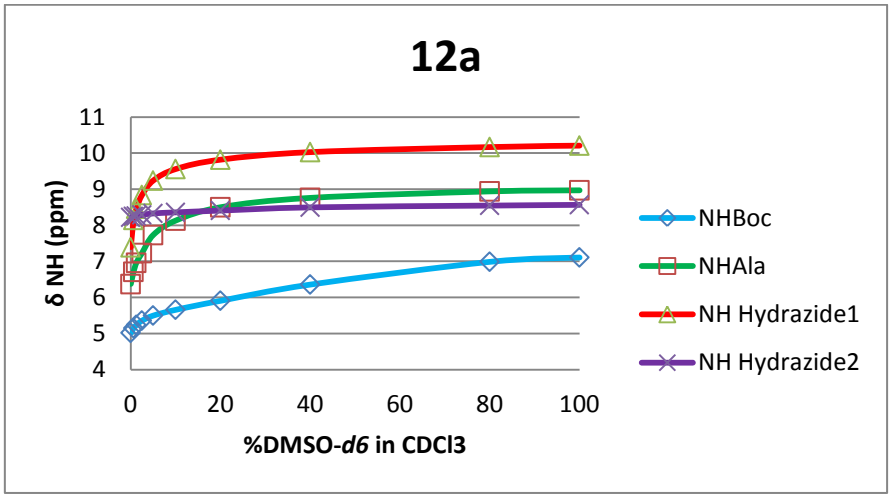

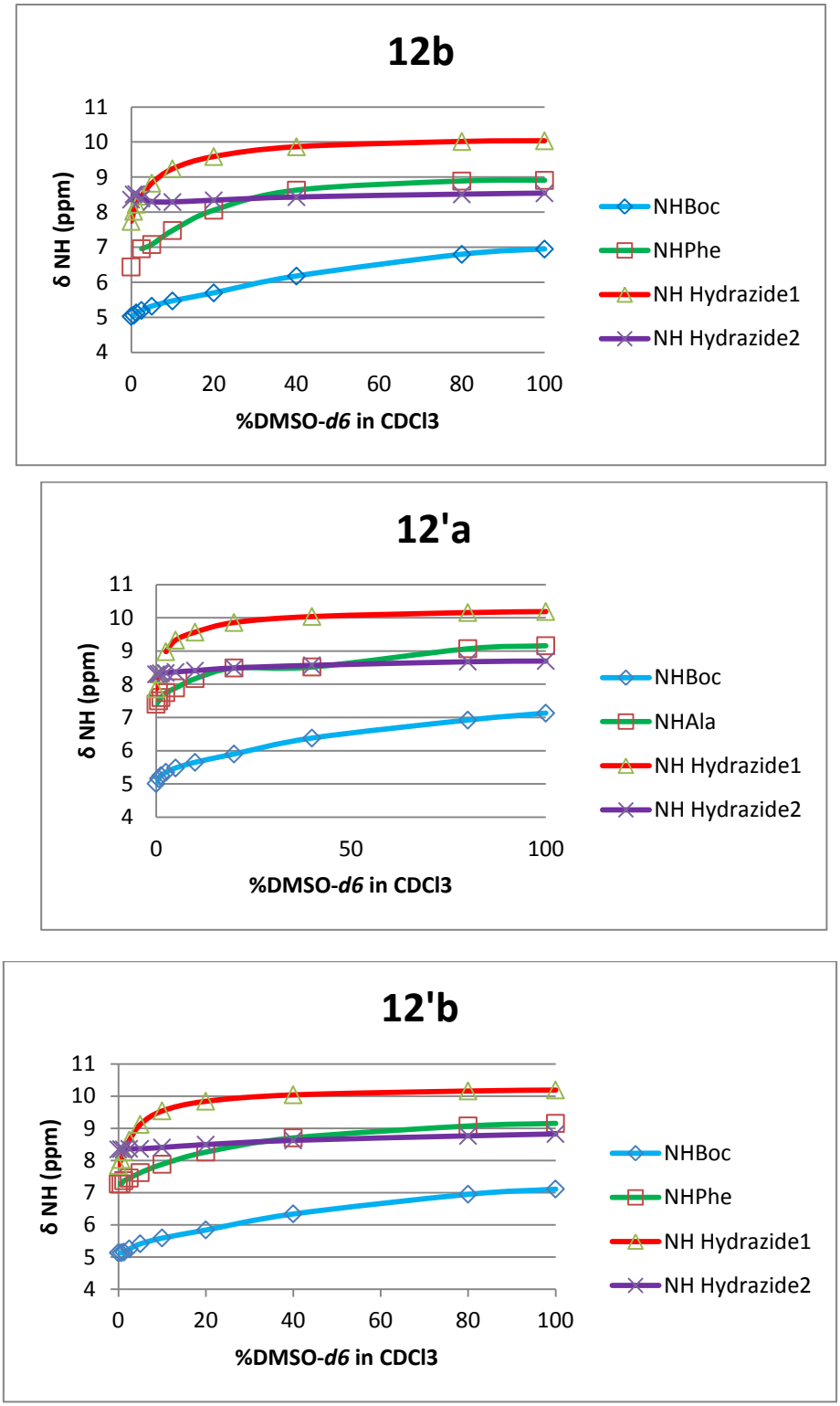

Figure 3.29 Effects of varying ratios of solvent in the mixture of $CDCl_3$/DMSO-d_6 on the chemical shifts of the NH protons of **12a,b** and **12'a,b** (3 mM)

Table 3.19 Solvent sensitivity of the NH protons in **12a,b** and **12'a,b**

Product	$\Delta\delta$ (ppm) = δ (DMSO-d_6) - δ ($CDCl_3$)			
	NHBoc	**NH-amidic**	**NH-hydrazide**	**NH-hydrazide**
12a	2.09	2.6	2.82	0.35
12b	1.92	2.47	2.3	0.18
12'a	2.12	1.76	2.33	0.4
12'b	1.98	1.88	2.35	0.48

More information on the conformation in solution was obtained from NOESY experiment recorded in $CDCl_3$. Two correlations of NH-hydrazide protons were found in NOESY spectrum of **12b** showing the spatial proximity of **NH**-hydrazide with CH of the *N*-terminal Phe moiety and **NH**-hydrazide with CH of the *C*-terminal Phe residue (Figure 3.30). This kind of NOE pattern of compound **12b** supported the view that it adopts a turn structure.

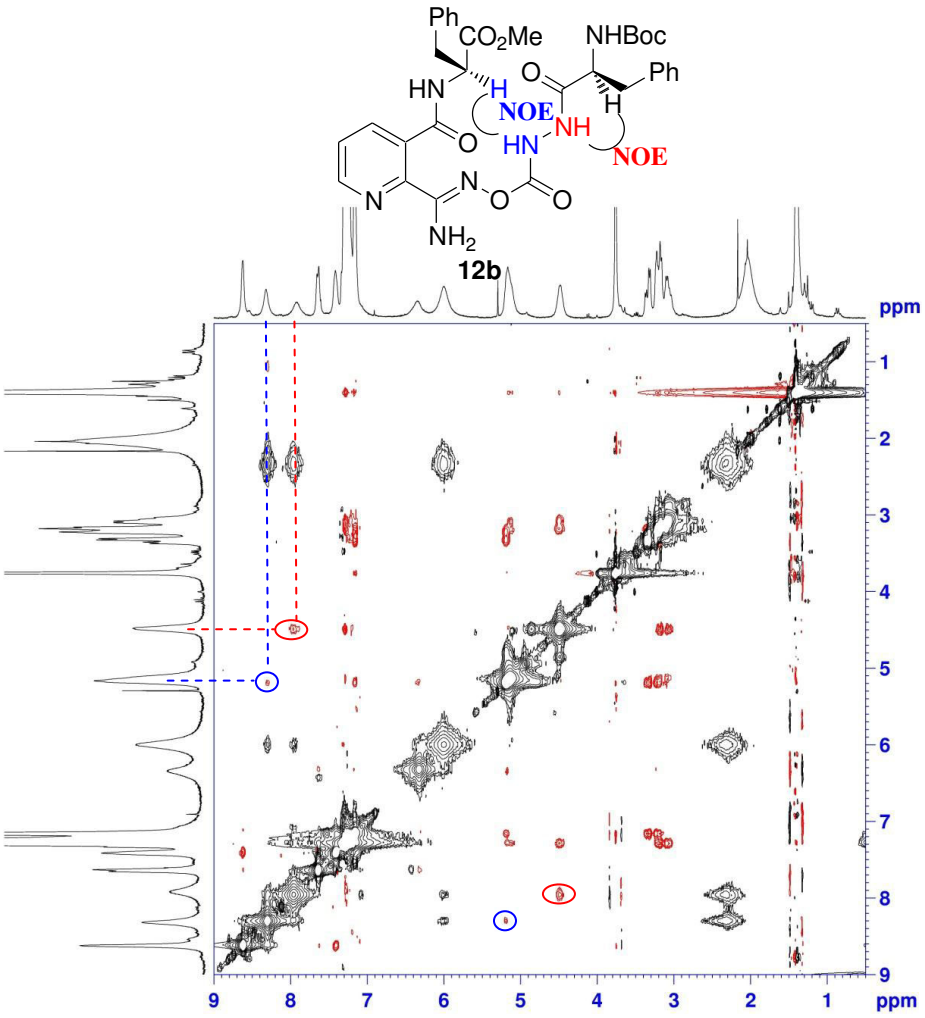

Figure 3.30 NOESY spectrum of **12b** in $CHCl_3$

Hence, peptidomimetics **12,12'** adopt a turn structure stabilized by the hydrogen bond between the C=O amidic and the NH-hydrazide forming C_{10}-pseudocycle (Figure 3.31) Moreover, the moderate solvent accessibility on titration by DMSO-d_6 (up to 10%) was depicted which could be an evidence of the interaction NH…N for the pyrazine compounds **12'a**,**b** (Figure 3.31).

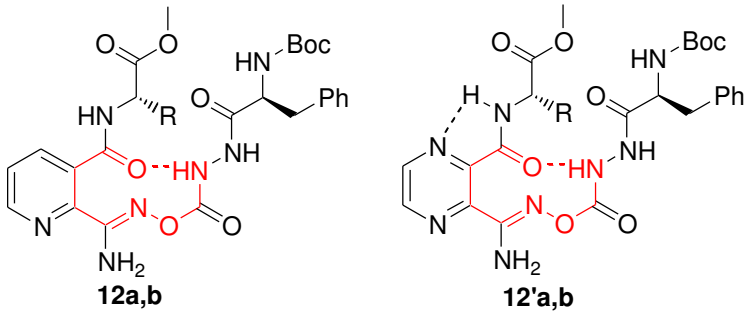

Figure 3.31 Structure of hydrazide modified peptidomimetics **12**, **12'**

7. Conclusions

Structural and thermodynamic studies of proline-containing peptidomimetics were accomplished. Conformational behavior and the steric effects of pyridine and pyrazine substitution at position 2 on the *cis*/*trans* equilibrium of proline-pyridine(pyrazine) peptidomimetics was estimated demonstrating a general tendency for *trans* isomer predomination. The increased fraction of the *cis* isomer up to 46% for Pro-containing 3-cyanopyrazinic acid **5'c** due to the stabilizing effect of the n $\rightarrow$ π^* interaction between the pyrazine nitrogen and C_{co} of the pyrrolidine ring on the *cis*/*trans* equilibrium was observed.

A new ProPhe pyrazine-based pseudotripeptide was investigated with respect to conformation and rigidity. Based on the experimental data and molecular dynamics calculations, we have elucidated the major solution structure of pseudotripeptide in comparison with the solution structure of two simplified pseudodipeptide analogues. It was shown that the amidoxime residue in **7'd** reduces the mobility and promotes the hydrogen bond formation between the proton of the OH and the carbonyl oxygen of the *C*-terminal phenylalanine.

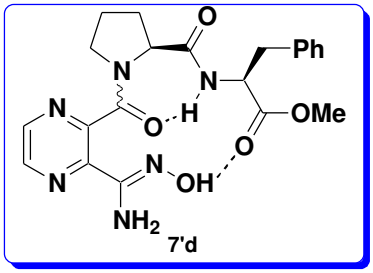

Simulation in DMSO showed that this hydrogen bond is present in DMSO as well. Likewise, the pyrazine amidoxime coupled with proline-phenylalanine dipeptide induces the hydrogen bond that adopts γ-turn conformation. Therefore, a dramatic increase of the *trans* rotamer up 98% was observed in weakly polar solvent, such as $CHCl_3$. Experimental data provide evidence for the retention of the NH into hydrogen bonding in DMSO, which is in agreement with the low sensitivity of the NH proton resonance to solvation. This interaction and/or the n $\rightarrow$ π^* interaction between the pyrazine nitrogen and C_{co} of the pyrrolidine ring significantly augments the *cis* isomer population in polar solvents. Thus, **7'd** appears to be interesting as a model pseudotripeptide for conformational study of the *cis/trans* isomerization for prolyl amide bond.

Conformational analysis of esterified amidoximes **8, 8'** and oxadiazoles **9, 9'** did not reveal hydrogen bonding exept for the oxadiazole **9'c** with the weak interraction between the NHBoc proton and the imide CO oxygen.

The *Z*/*E* isomerism in acylamidrazones was found to be dependent on the heterocycle and was studied by means of NMR spectroscopy and quantum chemical calculations. The latter showed amide-type isomerizm in pyridine derivatives **10a**,**b** and *Z/E* isomerization around C=N bond in pyrazine acylamidrazones **10'a**,**b**. Furthermore, testing the effect of solvent polarity on the *E/Z* isomeric ratio, a partial decomposition of the pyridine derivatives **10a,b** after adding $CDCl_3$ was observed. The instant formation of the pyrrolopyridines **6a,b** was detected by LCMS analysis and NMR spectroscopy. This was explained by stabilized effect of the hydrogen bond between the NH-amide proton and the nitrogen of the pyrazine ring in non hydrogen bonding solvents.

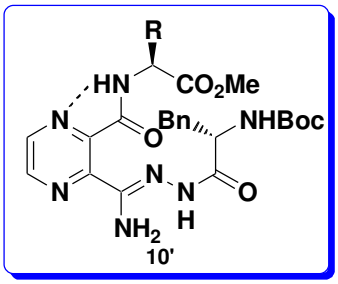

10'

Ultimately, it was found that the hydrazide-modified peptidomimetics **12,12'** adopt the turn structure stabilized by the hydrogen bond between the C=O amide and the NH-hydrazide forming C_{10}-pseudocycle.

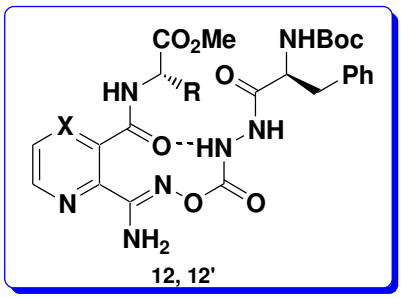

12, 12'

Chapter 4: Preliminary Biologycal Evaluation of Amidoximes as NO Donors

Griess method

One means to investigate nitric oxide formation is to measure nitrite (NO_2^-), which is one of two primary, stable and nonvolatile breakdown products of NO. This assay relies on a diazotization reaction that was originally described by Griess in 1879.[149] The Griess Reagent System is based on the chemical reaction shown in Scheme 4.1, which uses sulfanilamide and *N*-(1-napthyl)-ethylenediamine dihydrochloride (NED) under acidic conditions. This system detects NO_2^- formed by the spontaneous oxidation of NO under physiological conditions in a variety of biological and experimental liquid matrices such as plasma, serum, urine and tissue culture medium.

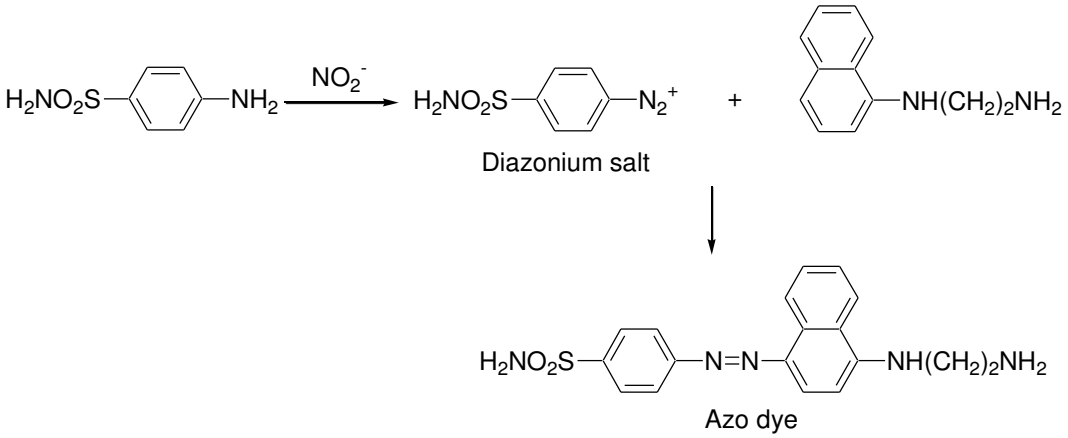

Scheme 4.1 Chemical reactions involved in the measurement of NO_2^- using the Griess Reagent System

Protocol:

A NED solution was prepared by dissolving 0.6 g of *N*-(1-naphthyl)-ethylenediamine·2HCl in 40 mL of 1 M hydrochloric acid solution and reaching a volume of 100 mL with water. A sulfanilamide solution was prepared by dissolving 0.6 g of the reagent in 40 mL of 1 M hydrochloric acid solution and reaching a volume of 100 mL with water.

A stock solution of nitrite (10^{-2} M) was prepared from $NaNO_2$. For calibration, a set of solutions of increasing NO_2^- concentration in the range of 0-10^{-5} M was prepared by successive dilutions of the stock solution in phosphate buffer. 200 µL of sulfanilamide solution was added to each solution and 3 minutes later 50 µL of NED solution was also added and keeping reacting for 5 minutes. The absorbance measures were taken 5 minutes after the solution was complete at 570 nm (Figure 4.1).

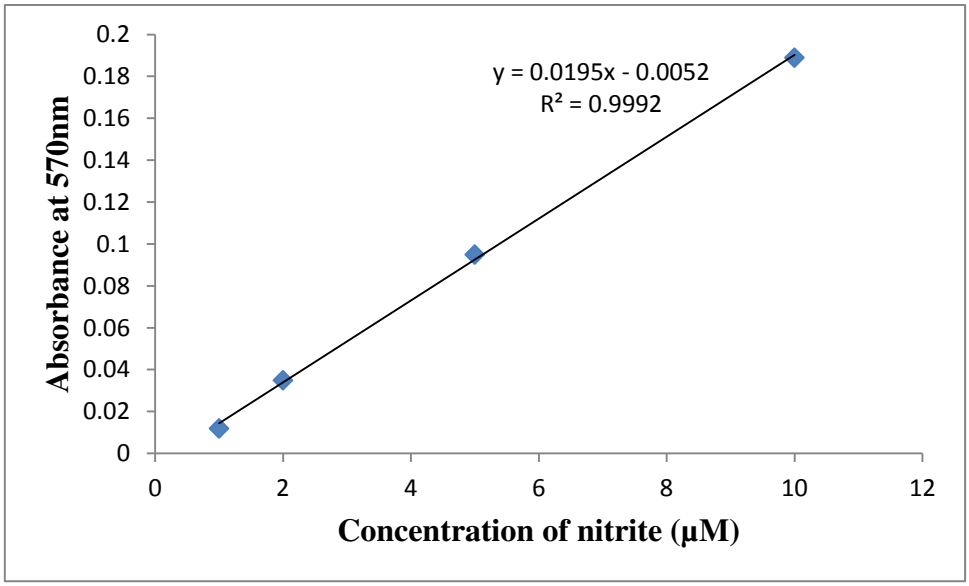

Figure 4.1 Nitrite Standard reference curve

Protocol for Determining Nitrite Concentration from amidoximes

Preparation of incubation medium

Reagents :

- Phosphate baffer 148mM pH7.4 (PBS 0.148)
- Solution of NADPH 10mM in sacrose
- Microsomes from liver (from rat male, not activated) 20mg/mL
- Amidoxime solution (25mM) in EtOH

In a microtube is added:

- 385.5µL of PBS
- 2µL of amidoxime solution (100µM)
- 12.5µL of microsome (0.5nmol P450 ≈ 0.3-0.5mg of proteines)
- V_T = 500µL

We pre-incubate microtube during 1 minute at 37°C. Then, 50µL of NADPH (1mM) in each tube is added. The reaction is initiated and the mixture incubates at 37°C for 10 minutes. 100µL of the working solution is taken from the medium and heated for 3min at 100°C. Microtube is centrifugated at 10000rpm during 15min at 4°C. We take this 100µL to achieve the determination of nitrite ions by Griess.

Two controls were prepared: control 1 without microsomes for each amidoxime and control 2 without amidoxime.

Concentration of nitrite was calculated from fits of the absorbance data to equation:

$A = a[NO_2^-] + b$

The preliminary results are shown in Table 4.1.

Table 4.1 Preliminary results of the NO release assay on amidoximes

Entry	Compound	$[NO_2^-]_1$ µM	$[NO_2^-]_2$ µM	$[NO_2^-]_3$ µM	Mean value (µM)	Standard deviation
1	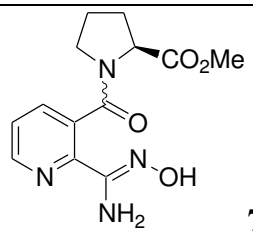 **7c**	1.34	2.62	1.22	**1.73**	0.776
2	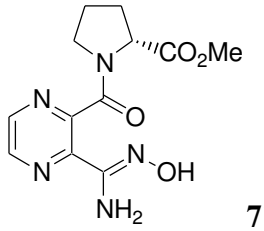 **7'c**	1.95	0.98	0.53	**1.15**	0.726
3	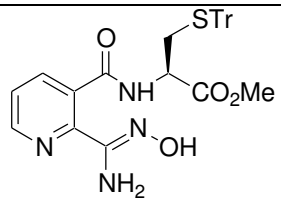 **7h**	3.81	0.99	1.15	**1.98**	1,584
4	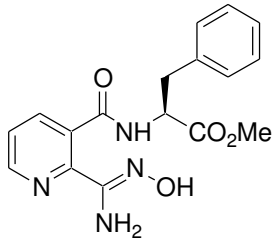 **7b**	1.50	2.62	-	**2.06**	0.792

5	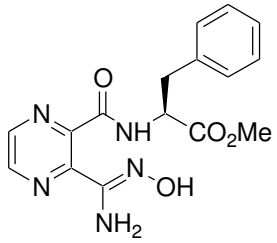 **7'b**	0.98	-	-	**0.98**	-
6	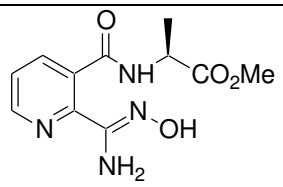 **7a**	0.83	-	-	**0.83**	-
7	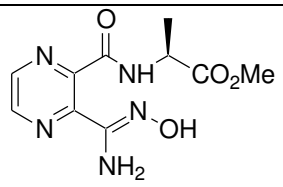 **7'a**	1.95	1.81	-	**1.88**	0.099
8	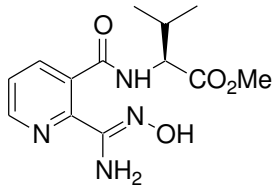 **7e**	1.60	2.42	-	**2.01**	0.580
9	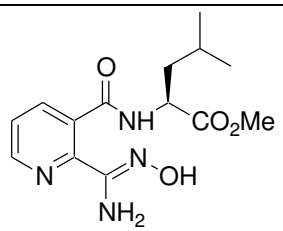 **7f**	1.45	1.40	-	**1.43**	0.035
10	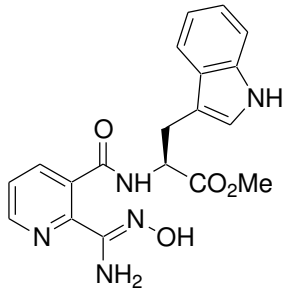 **7g**	1.10	-	-	**1.10**	-

11	4-chlorobenzamidoxime	2.40	3.39	1.26	**2.35**	1.066

Compounds with the highest NO release were tested tree times (**7c**, **7'c**, **7h**), with the moderate values – two times (**7b**, **7'a**, **7e**, **7f**) and products possessing the lowest NO release ability only once (**7'b**, **7a**, **7g**). The comparison was made with the known molecule 4-chlorobenzamidoxime which exhibits good NO release ability. A tentative correlation between the values for the pyridine and pyrazine analogs (**7**, **7'** (**a**) - **7**, **7'** (**c**)) showed better effect of the pyridine ring for phenylalanine and proline derivatives, however in the case of alanine-derived amidoximes, the pyrazine product appeared to be more efficiant than its pyridine counterpart. The correlation between the amino acid side chains and the nitrite concentration of the pyridine derivatives let us to put them in the order Phe>Val>Cys(Tr)>Pro>Leu>Trp>Ala. In the case of pyrazine compounds the opposite ability to NO release is observed: Ala>Pro>Phe.

In conclusion, amidoxime compounds were tested for nitric oxide release and all derivatives showed NO release in concentration sufficient for pharmacological effects (≥1 μM). A tentative correlation between the structures and the activity has been done.

General Conclusions and Perspectives

The aim of this project was the synthesis, structural study and preliminary biological evaluation of pyridine and pyrazine-based arginine mimics. This goal was accomplished with the synthesis of six-membered heterocyclic carboxylic acids with neighbor amidoxime moiety and their further modification. Target structures were functionalized to give novel esterified with amino acid and hydrazide modified amidoximes, amino acid derived *N*-acylamidrazones, chiral 1,2,4-oxadiazole and 1,2,4-triazole derivatives, bearing amidine motif incorporated into peptide chain. Hence, the synthesized molecules may be considered as arginine turn mimics possessing azine (pyridine or pyrazine) linkage.

A new convenient and mild synthesis of amidoximes and *N*-acylamidrazones *via* pyrrolidine ring opening by hydroxylamine and hydrazide of amino acid has been reported.

Structures of products were studied by NMR, IR spectroscopic studies and molecular modelling. Crystal structures of some compounds were analyzed by X-Ray diffraction study. Some compounds revealed intramolecular hydrogen bonding that promote turn-like structure.

It was shown that pyridine and the pyrazine moiety in some cases can be used as a structural motif to stabilize the *cis* conformation of Pro-peptidomimetics. The nitrogen of the pyrazine ring can also interect with the NH-amide proton which prevents nucleophilic attack of the NH nitrogen on the carbon of C=N, allowing the 1,2,4-triazole condensation and giving the higher yields of the 1,2,4-oxadiazole cyclization.

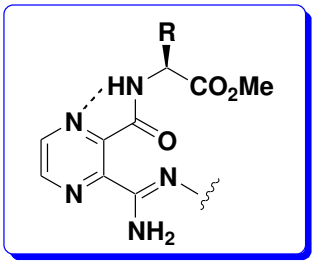

Amidoxime compounds were tested for nitric oxide release demonstrating NO release in concentrations 0.83 – 2.06 µM. Some tentative structure-activity relations have been presented. The most promising compounds will be subjected to further tests *in vivo*.

In perspective, amidoximes could be tested for there ability to be reduced *in vitro*/*in vivo* into pharmacologically active amidines, an arginine mimics.

Chapter 5: Experimental part

General Methods

The chemicals were purchased as the highest purity commercially available and were used without further purification. Dry THF was obtained by distillation over sodium and benzophenone. Methanol, acetonitrile and DMF were purchased in anhydrous form.

Microwave-assisted reactions were performed using CEM Focused Microwave^{TM} Synthesis System, Model Discover, in a septa capped 10 mL reaction vessels with stirring. The reaction temperature was monitored by Infrared Temperature Control System with infrared sensor to measure temperature. Power required to maintain the target temperature was controlled by the Discovery System. Reaction times under microwave conditions reflect actual reaction times at a given temperature.

Reactions were monitored by LC/MS or TLC using Kieselgel 60 with fluorescent indicator UV254 (purchased from Merck or Macherey-Nagel) with UV method of detection (254 nm). NMR spectra were measured with a Bruker Avance 300 (300 MHz for ^{1}H and 75 MHz for ^{13}C) with tetramethylsilane as standard.

IR spectra were recorded with a Bruker Alpha Platinum ATR Spectrometer. FT-IR spectra (64 scans) were obtained at 2 cm^{-1} resolution using a 50 µm CaF_2 solution cell and a dry air purged Bruker Tensor 27 equipped with liquid nitrogen cooled MCT-detector. All samples were dissolved at concentration of 10 mM in spectrophotometric grade chloroform (≥ 99.8 %, Sigma-Aldrich) or DMSO.

Electron spray ionization mass spectra (ESI-MS) were recorded on a Brucker MicroTof-Q HR spectrometer, Faculté des Sciences et Techniques, Vandoeuvre-lès-Nancy, France. Elemental analyses (C, H, N) were conducted using the Vario Micro Cube. Melting points were measured on a Buchi M–560 Melting Point apparatus. All melting points are uncorrected.

Preparative column chromatography was carried out with silica gel 60 (40–63 µm). All yields were calculated from pure isolated products.

Preparative NP-HPLC was perforemed on Waters equipment using Hibar pre-packed column RT 250-25 LiChrosorb Si 60 (7 µm), eluting with flow rate of 20 mL/min and on Varian 179125 pre-packed column ChromSpher Si (5 µm) (250 × 4.6 mm), eluting with flow rate of 10 mL/min. The elution was performed with UV monitoring at 254 nm.

LC/MS spectra were recorded using high-perfomance liquid chromatograph (UFLC Shimadzu) and LCMS-2020 Shimadzu mass-selective detector. Parameters for LC/MS

analyses: Nucléodur RP-C18 (10µm), 250 × 4.6 mm; gradient elution of solvent A = CH_3CN/H_2O:1/9 + 0.1% formic acid and solvent B = CH_3CN + 0.1% formic acid; eluent flow: 1mL/min; volume of injected sample: 1 µL; UV-detectors operating at 215 and 254 nm; ionization method: electro spray ionization (positive ions ionization mode)

Molecular dynamics

Molecular dynamics calculations on the molecule **7'd** and on the simplified pseudodipeptide analogues AOPzPro (**7'c**) and AOPzPhe (**7'b**) were run according to the following protocol: 2 µs with 2 fs steps molecular dynamics simulations were calculated in explicit solvent (chloroform or DMSO) with constant pressure periodic boundary conditions, pressure relaxation time of 2µs, and constant temperature at 300 K, using the package of molecular dynamics simulations programs AMBER 10.0.[150] The starting molecules were constructed using MarvinSketch (ChemAxon) Antechamber and Xleap programs. Molecular simulation was done with Sander program with general AMBER force field (GAFF) and included amino acids parameters (ff99SB). Ptraj was employed for the analysis of 25000 structures in order to assess the possibility of a hydrogen bond formation.

Cytocompatibility with vascular smooth muscle cell

The cytocompatibility of pyrazine amidoxime derivatives AOPzPro (**7'c**), AOPzPhe (**7'b**), AOPzProPhe (**7'd**) were evaluated on rat smooth muscle cells (SMC) line (A-10) ATCC® CRL-1476™. SMC were grown in complete medium made of Dulbecco's Modified Eagle's Medium DMEM supplemented with 10% (v/v) FBS, 2% (v/v) glutamine, 100 U/mL penicillin and 100 µg/mL streptomycin mixture, and 4 mM sodium pyruvate. Cells were cultivated at 37 °C under 10% (v/v) of CO_2 in a humidified incubator. SMC were seeded in 96-wells plates at 60,000 cells/well 48 h before exposure to pyrazine amidoxime derivatives for 24 h (complete medium was used as control). Pyrazine amidoxime derivatives were firstly resuspended in 100% methanol at a concentration of 10^{-1}, 10^{-2}, 10^{-3} and 10^{-4} M. Finally, pyrazine amidoxime derivatives were diluted in complete medium for final concentrations of 10^{-6}, 10^{-5}, 10^{-4}, 10^{-3} M. Cytocompatibility through metabolic activity was checked with MTT assay. Briefly, 0.5 mg/mL MTT was incubated with the cells for 4 h. Then, 250 µL DMSO was added under stirring for 10 min to extract the formazan crystals. The absorbance was read at 570 nm with a reference at 630 nm using EL 800 microplate reader (Bio-TEK Instrument, INC®, France). Metabolic activity in the presence of pyrazine amidoxime derivatives was compared to the control condition (culture medium alone).

Statistical analysis

Results are shown as mean ± standard error of the mean (sem) values. Statistical comparisons were performed using the two-way ANOVA woth Bonferroni posttest. $p < 0.05$ was considered significantly different. Statistical analyses were performed using the GraphPad Prism software (GraphPad Software version 5.0, San Diego, USA)

Experimental procedures

2-Carbamoylnicotinic acid (2)[46]

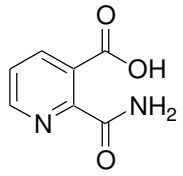

Acid **2** was prepared from quinolinic anhydride (**1**) and aqueous ammonia according to a literature procedure.[46] A suspension of anhydride **1** (7.45 g, 50 mmol) in 28% NH_4OH (37 mL) was stirred at 70 °C for 10 min, whereupon the reactant had dissolved. After the mixture was cooled to 0 °C, a precipitation was performed by adding 12M HCl (dropwise) while cooling. The precipitate was collected by filtration and dried.

White solid; yield: 4.65 g (56%); mp 176 ˚C (Lit.[48] 175 ˚C).

^{1}H NMR (300 MHz, DMSO-d_6, 25 °C): δ = 13.26 (s, 1H, COOH), 8.67 (dd, J = 4.8, 1.4 Hz, 1H, H_{Ar}), 8.04 (dd, J = 7.8, 1.3 Hz, 2H, 2×H_{Ar}), 7.72 – 7.44 (m, 2H, NH_2).

^{13}C NMR (75 MHz, $CDCl_3$, 25 °C): δ = 168.1, 167.1, 150.4, 149.6, 136.7, 129.2, 125.2.

Methyl 2-Cyanonicotinate (3)[47,48]

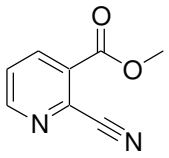

To a stirred suspension of 2-carbamoylnicotinic acid (**2**; 7.47 g, 45 mmol) in CH_2Cl_2 (50 mL) at 0 °C were added Et_3N (13.08 mL, 94 mmol) and methyl chloroformate (7.65 mL, 99 mmol). After the reaction mixture was stirred at r.t. for 8 h, it was diluted with $CHCl_3$ (50 mL) and washed with H_2O, dried over $MgSO_4$ and concentrated *in vacuo*. The product was washed with hexane and dried.

Pale yellow solid; yield: 5.76 g (79%); mp 80-83 ˚C (Lit.[48] 89 °C).

IR (KBr): 3090, 2959, 2241, 1726, 1578, 1287 cm^{-1}.

^{1}H NMR (300 MHz, DMSO-d_6, 25 °C): δ = 8.94 (d, J = 4.8 Hz, 1H, H_{Ar}), 8.48 (d, J = 8.1 Hz, 1H, H_{Ar}), 7.88 (dd, J = 8.1, 4.8 Hz, 1H, H_{Ar}), 3.95 (s, 3H, OMe).

^{13}C NMR (75 MHz, DMSO-d_6, 25 °C): δ = 163.0, 153.9, 138.8, 132.4, 129.4, 127.5, 116.2, 53.1.

2-Cyanonicotinic acid (4)[48]

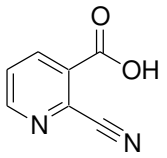

A mixture of ester **3** (3.16 g, 19.5 mmol), MeOH (60 mL) and 1M NaOH (22 mL) was stirred at r.t. for 8 h, and then concentrated *in vacuo*. The residue was diluted with water (20 mL) and CH_2Cl_2 (50 mL), and then the solution was acidified with 1M HCl under cooling. The resulting precipitate was collected, washed with H_2O and hexane, and dried *in vacuo*.

Pale-yellow solid; yield: 1.84 g (64%); mp 186 ˚C [Lit.[48] 214 ˚C, 185 ˚C (sublimation)].

^{1}H NMR (300 MHz, DMSO-d_6, 25 °C): δ = 14.25 (s, 1H, COOH), 8.92 (dd, J = 4.8, 1.5 Hz, 1H, H_{Ar}), 8.47 (dd, J = 8.1, 1.5 Hz, 1H, H_{Ar}), 7.86 (dd, J = 8.1, 4.8 Hz, 1H, H_{Ar}).

^{13}C NMR (100 MHz, DMSO-d_6 + CCl_4, 1:1, 25 °C): δ = 164.2, 153.5, 139.1, 133.1, 130.9, 127.2, 116.4.

Anal. Calcd for $C_7H_4N_2O_2$: C, 56.76; H, 2.72; N, 18.91. Found: C, 56.74; H, 2.73; N 18.88.

Methyl 3-cyanopyrazine-2-carboxylate (3')[49]

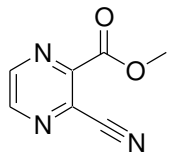

To a stirred suspension of pyrazine-2,3-dicarboxylic acid monoamide 2' (10.86 g, 65 mmol) in CH_2Cl_2 (100 mL) at 0 °C were added Et_3N (19.00 mL, 136.5 mmol) and methyl

chloroformate (11.05 mL, 143 mmol) and the mixture was allowed to reach r.t. and stirred for 2 h. Water and $NaHCO_3$(sat.) ~ 1:1 were added and the mixture was extracted with CH_2Cl_2. The organic phase was washed with H_2O, dried over $MgSO_4$, and concentrated to give the *title compound* 2.

Yellow solid; yield: 9.22 g (87%); mp 70-72 ˚C. ^{1}H NMR (300 MHz, DMSO-d_6, 25 °C): δ = 8.89 (s, 2H, 2×H_{Ar}), 4.09 (s, 3H, OMe). ^{13}C NMR (75 MHz, DMSO-d_6, 25 °C): δ = 162.8, 147.7, 146.8, 146.6, 131.4, 115.0, 54.5.

3-cyanopyrazine-2-carboxylic acid (4')

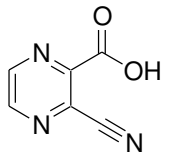

A mixture of 3' (0.978 g, 6.0 mmol), MeOH (50 mL) and 1M NaOH (12 mL) was stirred at r.t. for 3 h and then concentrated *in vacuo*. The residue was diluted with water and CH_2Cl_2, and then acidified with 1M HCl under cooling. The resulting precipitate was collected, washed with H_2O and hexane, and dried *in vacuo*.

Pale-yellow solid; yield: 0.742 g (82%); mp 157-158 ˚C. ^{1}H NMR (300 MHz, DMSO-d6, 25 °C): δ = 9.00 (d, J = 2.3 Hz, 1H, H_{Ar}), 8.96 (d, J = 2.3 Hz, 1H, H_{Ar}). ^{13}C NMR (75 MHz, DMSO-d6, 25 °C): δ = 164.5, 155.1, 146.6, 144.6, 128.1, 116.7.

Synthesis of Compounds 5, 6 (a-f); General Procedure

To a solution of 2-cyanonicotinic acid (**4**; 740 mg, 5 mmol) in CH_2Cl_2 (30 mL) were added Et_3N (1.39 mL, 10 mmol), the corresponding methyl ester of an amino acid hydrochloride (5 mmol) and HOBt (0.675 mg, 5 mmol). The mixture was stirred at 0 °C and EDCI (0.967 g, 5.05 mmol) was added. Then, the mixture was stirred at r.t. overnight. The mixture was diluted in CH_2Cl_2 (50mL); then, the solution was washed with 0,1M HCl (3×15 mL) and brine (20 mL), dried over $MgSO_4$ and concentrated *in vacuo*.

Methyl (2*S*)-2-{[(2-cyanopyridin-3-yl)carbonyl]amino}propanoate (5a)

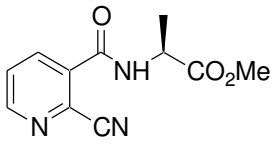

Purification by flash column chromatography (AcOEt/CH_2Cl_2, 1:1) gave **5a** as a white solid; yield: 0.177 g (15%); mp 135-137 °C.

IR (KBr): 3273, 3080, 2997, 2941, 2237 (CN), 1739, 1648, 1581, 1548, 1226 cm^{-1}.

^1H NMR (300 MHz, $CDCl_3$, 25 °C): δ = 8.79 (d, J = 4.8 Hz, 1H, H_{Ar}), 8.15 (d, J = 8.1 Hz, 1H, H_{Ar}), 7.61 (dd, J = 8.1, 4.8 Hz, 1H, H_{Ar}), 7.15 (d, J = 5.7 Hz, 1H, NH), 4.80 (m, 1H, CHNH), 3.78 (s, 3H, OMe), 1.56 (d, J = 7.2 Hz, 3H, CH_3).

^{13}C NMR (75 MHz, $CDCl_3$, 25 °C): δ = 173.4, 163.6, 153.0, 137.4, 135.53, 132.0, 127.3, 116.5, 53.4, 49.7, 18.7.

Anal. Calcd for $C_{11}H_{11}N_3O_3$: C, 56.65; H, 4.75; N, 18.02. Found: C, 56.48; H, 4.76; N, 17.95.

LCMS: MH^+, 234.

Methyl (2*S*)-2-[(7*E*)-7-imino-5-oxo-5,7-dihydro-6*H*-pyrrolo[3,4-*b*]pyridin-6-yl]propanoate (6a)

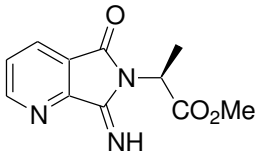

Purification by flash column chromatography (AcOEt/CH_2Cl_2, 1:1) gave **6a** as a white solid; yield: 0.671 g (58%); mp 90 °C.

IR (KBr): 3294, 3238, 1743, 1731, 1665, 1403, 1410, 1258 cm^{-1}.

^1H NMR (300 MHz, $CDCl_3$, 25 °C): δ = 9.34 (br s, 1H, NH), 8.86 (d, J = 4.8 Hz, 1H, H_{Ar}), 8.14 (d, J = 8.1 Hz, 1H, H_{Ar}), 7.57 (dd, J = 8.1, 4.8 Hz, 1H, H_{Ar}), 5.24 (q, J = 7.2 Hz, 1H, CH), 3.73 (s, 3H, OCH_3), 1.74 (d, J = 7.2 Hz, 3H, CH_3).

^{13}C NMR (75 MHz, $CDCl_3$, 25 °C): δ = 171.1, 165.9, 159.6, 154.8, 150.4, 132.1, 127.1, 125.5, 53.3, 48.6, 15.7.

Anal. Calcd for $C_{11}H_{11}N_3O_3$: C, 56.65; H, 4.75; N, 18.02. Found: C, 56.45; H, 4.77; N, 17.96.

LCMS: MH^+, 234.

Methyl (2*S*)-2-[(7*E*)-7-imino-5-oxo-5,7-dihydro-6*H*-pyrrolo[3,4-*b*]pyridin-6-yl]-3-phenylpropanoate (6b)

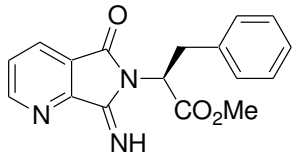

Purification by flash column chromatography (AcOEt/petroleum ether, 7:3) gave **6b** as a light-yellow solid; yield: 0.953 g (76%); mp 72-73 °C.

IR (KBr): 3275, 3252, 3201, 3062, 3030, 2955, 2923, 2853, 1741, 1731, 1666, 1408, 1256 cm^{-1}.

^{1}H NMR (300 MHz, $CDCl_3$, 25 °C): δ = 9.29 (s, 1H, NH), 8.81 (d, J = 4.8 Hz, 1H, H_{Ar}), 8.06 (d, J = 7.8 Hz, 1H, H_{Ar}), 7.51 (dd, J = 7.8, 4.8 Hz, 1H, H_{Ar}), 7.20 – 7.14 (m, 5H, 5×H_{Ar}), 5.47 (dd, J = 10.8, 5.4 Hz, 1H, CH), 3.78 (s, 3H, OCH_3), 3.72 – 3.59 (m, 2H, CH_2).

^{13}C NMR (75 MHz, $CDCl_3$, 25 °C): δ = 170.2, 166.0, 159.7, 154.7, 149.9, 137.6, 132.0, 129.5, 129.0, 127.3, 127.0, 125.1, 54.2, 53.4, 35.1.

Anal. Calcd for $C_{17}H_{15}N_3O_3$: C, 66.01; H, 4.89; N, 13.58. Found: C, 65.81; H, 4.91; N, 13.53.

LCMS: MH^+, 310.

Methyl (2*S*)-1-[(2-cyanopyridin-3-yl)carbonyl]pyrrolidine-2-carboxylate (5c)

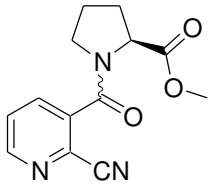

Purification by flash column chromatography (AcOEt/CH_2Cl_2, 1:1) gave **5c** as a pale-yellow oil; yield: 1.127 g (87%).

IR (KBr): 2952, 2237 (CN), 1736, 1634, 1428, 1407, 1175 cm^{-1}.

^1H NMR (300 MHz, $CDCl_3$, 25 °C): δ = 8.74 and 8.70 (2×d, J = 4.5 Hz, 1H, H_{Ar}), 7.90 and 7.79 (2×d, J = 7.8 Hz, 1H, H_{Ar}), 7.62 - 7.51 (m, 1H, H_{Ar}), 4.71 and 4.28 (2×m, 1H, CH), 3.77 and 3.55 (2×s, 3H, OCH_3), 3.51 –3.38 (m, 2H, CH_2N), 2.42 – 2.31 (m, 1H, CH_2), 2.21 – 1.77 (m, 3H, CH_2CH_2).

^{13}C NMR (75 MHz, $CDCl_3$, 25 °C): δ = 172.4, 165.2, 164.8, 152.1, 151.9, 138.2, 137.9, 136.4, 136.2, 131.3, 127.4, 127.2, 116.0, 61.4, 59.7, 53.3, 53.1, 49.6, 47.5, 31.8, 29.9, 25.5, 23.3.

Anal. Calcd for $C_{13}H_{13}N_3O_3$: C, 60.22; H, 5.05; N, 16.21. Found: C, 59.98; H, 5.07; N, 16.15.

LCMS: MH^+, 260.

Methyl [(7*E*)-7-imino-5-oxo-5,7-dihydro-6*H*-pyrrolo[3,4-*b*]pyridin-6-yl]acetate (6d)

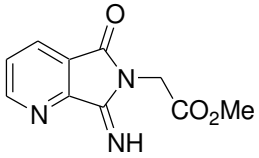

Acetate **6d** was obtained as a white solid of analytical purity without further purification; yield: 0.63 g (58%); mp 160 °C.

IR (KBr): 3198, 3057, 2937, 1736, 1669, 1593, 1440, 1281, 1267, 1248 $см^{-1}$.

^1H NMR (300 MHz, $CDCl_3$, 25 °C): δ = 9.33 (s, 1H, NH), 8.87 (dd, J = 4.8, 1.5 Hz, 1H, H_{Ar}), 8.17 (dd, J = 7.8, 1.5 Hz, 1H, H_{Ar}), 7.58 (dd, J = 7.8, 4.8 Hz, 1H, H_{Ar}), 4.66 (s, 2H, CH_2), 3.77 (s, 3H, OCH_3).

^{13}C NMR (75 MHz, $CDCl_3$, 25 °C): δ = 168.5, 166.0, 159.8, 154.8, 150.4, 132.1, 127.0, 125.6, 53.1, 40.0.

Anal. Calcd for $C_{10}H_9N_3O_3$: C, 54.79; H, 4.14; N, 19.17. Found: C, 54.57; H, 4.15; N, 19.10.

LCMS: MH^+, 220.

Methyl (2*S*)-2-{[(2-cyanopyridin-3-yl)carbonyl]amino}-3-methylbutanoate (5e)

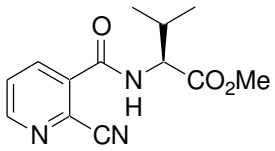

Purification by flash column chromatography (AcOEt/petroleum ether, 1:1) gave **5e** as a white solid; yield: 0.488 g (37%); mp 142-143 °C.

IR (KBr): 3270, 3081, 2972, 2238 (CN), 1730, 1645, 1549, 1205 cm^{-1}.

^{1}H NMR (300 MHz, $CDCl_3$, 25 °C): δ = 8.81 (d, J = 4.8 Hz, 1H, H_{Ar}), 8.18 (d, 9.0 Hz, 1H, H_{Ar}), 7.62 (dd, J = 9.0, 4.8 Hz, 1H, H_{Ar}), 6.97 (br m, 1H, NH), 4.79 (m, 1H, CHNH), 3.78 (s, 3H, OCH_3), 2.39 – 2.28 (m, 1H, $CH(CH_3)_2$), 1.07 (d, J = 6.0 Hz, 3H, CH_3), 1.03 (d, J = 6.0 Hz, 3H, CH_3).

^{13}C NMR (75 MHz, $CDCl_3$, 25 °C): δ = 172.5, 164.0, 153.1, 137.9, 135.8, 131.6, 127.4, 116.7, 58.9, 53.2, 32.2, 19.7, 18.5.

Anal. Calcd for $C_{13}H_{15}N_3O_3$: C, 59.76; H, 5.79; N, 16.08. Found: C, 59.55; H, 5.81; N, 16.12.

LCMS: MH^+, 262.

Methyl (2*S*)-2-[(7*E*)-7-imino-5-oxo-5,7-dihydro-6*H*-pyrrolo[3,4-*b*]pyridin-6-yl]-3-methylbutanoate (6e)

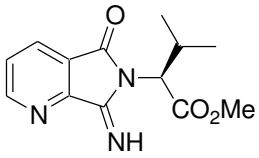

Purification by flash column chromatography (AcOEt/petroleum ether, 1:1) gave **6e** as a white solid; yield: 0.438 g (34%); mp 141 °C.

IR (KBr): 3271, 2968, 1734, 1668, 1406, 1212, 1096 cm^{-1}.

^1H NMR (300 MHz, $CDCl_3$, 25 °C): δ = 9.33 (br s, 1H, NH), 8.87 (d, J = 4.8 Hz, 1H, H_{Ar}), 8.15 (d, J = 9.0 Hz, 1H, H_{Ar}), 7.58 (dd, J = 9.0, 4.8 Hz, 1H, H_{Ar}), 4.80 (d, J = 9.0 Hz, 1H, CHNH), 3.68 (s, 3H, OMe), 2.92 – 2.80 (m, 1H, $CH(CH_3)_2$), 1.20 (d, J = 6.0 Hz, 3H, CH_3), 0.88 (d, J = 6.0 Hz, 3H, CH_3).

^{13}C NMR (75 MHz, $CDCl_3$, 25 °C): δ = 170.3, 166.2, 160.2, 154.9, 150.1, 132.2, 127.2, 125.3, 58.7, 52.9, 28.8, 21.8, 20.1.

Anal. Calcd for $C_{13}H_{15}N_3O_3$: C, 59.76; H, 5.79; N, 16.08. Found: C, 59.57; H, 5.80; N, 16.04.

LCMS: MH^+, 262.

Methyl (2*S*)-2-{[(2-cyanopyridin-3-yl)carbonyl]amino}-4-methylpentanoate (5f)

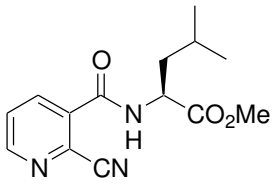

Purification by flash column chromatography (AcOEt/petroleum ether, 1:1) gave **5f** as a white solid; yield: 0.117 g (9%); mp 117-118 °C.

IR (KBr): 3280, 3080, 2956, 2871, 2237 (CN), 1740, 1666, 1645, 1584, 1545, 1407, 1205 cm^{-1}.

^1H NMR (300 MHz, $CDCl_3$, 25 °C): δ = 8.78 (d, J = 4.8 Hz, 1H, H_{Ar}), 8.15 (d, J = 8.1 Hz, 1H, H_{Ar}), 7.61 (dd, J = 8.1, 4.8 Hz, 1H, H_{Ar}), 7.06 (d, J = 6.9 Hz, 1H, NH), 4.87 – 4.79 (m,

1H, CHNH), 3.76 (s, 3H, OCH_3), 1.85 – 1.66 (m, 3H, CH+CH_2), 0.99 – 0.95 (2×d, 6H, $(CH_3)_2$).

^{13}C NMR (75 MHz, $CDCl_3$, 25 °C): δ = 173.5, 163.9, 153.0, 137.5, 135.49, 131.8, 127.3, 116.5, 53.2, 52.4, 42.0, 25.5, 23.4, 22.5.

Anal. Calcd for $C_{14}H_{17}N_3O_3$: C, 61.08; H, 6.22; N, 15.26. Found: C, 60.89; H, 6.23; N, 15.22.

LCMS: MH^+, 276.

Methyl (2*S*)-2-[(7*E*)-7-imino-5-oxo-5,7-dihydro-6*H*-pyrrolo[3,4-*b*]pyridin-6-yl]-4-methylpentanoate (6f)

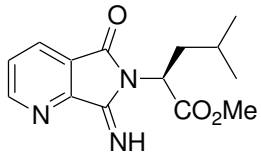

Purification by flash column chromatography (AcOEt/petroleum ether, 1:1) gave **6f** as a light-yellow oil; yield: 1.046 g (76%).

IR (KBr): 3276, 2956, 1734, 1665, 1593, 1405, 1257, 1209 cm^{-1}.

^{1}H NMR (300 MHz, $CDCl_3$, 25 °C): δ = 9.37 (br s, 1H, NH), 8.81 (s, 1H, H_{Ar}), 8.09 (d, J = 6.6 Hz, 1H, H_{Ar}), 7.54 (m, 1H, H_{Ar}), 5.23 – 5.16 (m, 1H, CHNH), 3.64 (s, 3H, OCH_3), 2.44 – 2.36 (m, 1H, CH_2), 1.95 – 1.90 (m, 1H, CH_2), 1.44 (m, 1H, $CH(CH_3)_2$), 0.90 and 0.85 (2×d, J = 5.7 Hz, 6H, $(CH_3)_2$).

^{13}C NMR (75 MHz, $CDCl_3$, 25 °C): δ = 171.0, 166.1, 159.8, 154.7, 150.06, 132.0, 127.0, 125.3, 53.0, 51.6, 37.7, 25.6, 23.7, 21.7.

Anal. Calcd for $C_{14}H_{17}N_3O_3$: C, 61.08; H, 6.22; N, 15.26. Found: C, 60.85; H, 6.24; N, 15.21.

Methyl (2*S*)-2-[(7*E*)-7-imino-5-oxo-5,7-dihydro-6*H*-pyrrolo[3,4-*b*]pyridin-6-yl]-3-(1*H*-indol-3-yl)propanoate (6g)

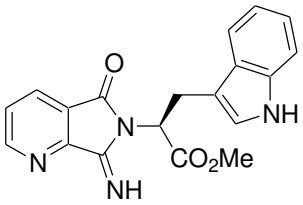

Purification by flash column chromatography (CH_2Cl_2/CH_3CN, 8:2) gave **6g** as a yellow solid; yield: 1.436 g (83%); mp 119-121 °C.

IR (KBr): 3396, 3266, 3067, 1732, 1664, 1429, 1407, 1260 cm^{-1}.

^1H NMR (300 MHz, $CDCl_3$, 25 °C): δ = 9.33 (s, 1H, NH), 8.69 (d, J = 4.8 Hz, 1H, H_{Ar}), 8.29 (s, 1H, NH_{Ar}), 7.91 (d, J = 7.8 Hz, 1H, H_{Ar}), 7.58 (d, J = 7.5 Hz, 1H, H_{Ar}), 7.36 (dd, J = 7.8, 4.8 Hz, 1H, H_{Ar}), 7.18 (d, J = 7.8 Hz, 1H, H_{Ar}), 7.09 – 6.98 (m, 3H, 3×H_{Ar}), 5.58 (dd, J = 10.2, 4.8 Hz, 1H, CH), 3.95 – 3.72 (m, 2H, CH_2), 3.77 (s, 3H, OCH_3).

^{13}C NMR (75 MHz, $CDCl_3$, 25 °C): δ = 170.6, 166.1, 159.8, 154.5, 149.8, 136.6, 131.8, 127.8, 126.9, 125.0, 123.3, 122.4, 119.8, 119.0, 111.7, 111.6, 53.6, 53.3, 25.1.

Anal. Calcd for $C_{19}H_{16}N_4O_3$: C, 65.51; H, 4.63; N, 16.08. Found: C, 65.29, H, 4.64; N, 16.02.

LCMS: MH^+, 349.

Methyl (2*S*)-2-{[(2-cyanopyridin-3-yl)carbonyl]amino}-3-(tritylsulfanyl)propanoate (5h)

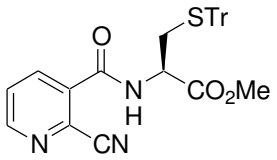

Purification by flash column chromatography (AcOEt/petroleum ether, 7:3) gave **5h** as a light-yellow solid; yield: 1.521 g (60%); mp 78-81 °C.

^1H NMR (300 MHz, $CDCl_3$): δ = 8.77 (d, J = 4.8, 1H, H_{Ar}), 8.04 (d, J = 7.8 Hz, 1H, H_{Ar}), 7.46 (dd, J = 7.8, 4.8 Hz, 1H), 7.36 - 7.02 (m, 16H, NH, 15×H_{Ph}), 4.76 (dd, J = 11.1, 4.5 Hz, 1H, CH), 3.52 (s, 3H, OCH_3), 3.46 – 3.34 (m, 1H, C<u>H</u>H), 3.00 (dd, J = 13.3, 4.5 Hz, 1H, CH<u>H</u>).

^{13}C NMR (75 MHz, $CDCl_3$): δ = 169.32, 165.85, 159.41, 154.88, 150.19, 145.06, 132.25, 130.32, 128.94, 127.41, 127.11, 125.34, 67.98, 53.39, 52.64, 31.38.

Synthesis of Compounds 7a-h; General Procedure

To a solution of the methyl ester of a (2*S*)-*N*-[2-cyanopyridine-3-yl]carbonyl substituted amino acid **5** and/or the methyl ester of a (2*S*)-2-(7-imino-5-oxo-5,6-dihydro-6*H*-pyrrolo[3,4-*b*]pyridine-6-yl)alkanoic acid **6** (2 mmol) in MeOH (15 mL) was added Et_3N (0.56 mL, 4 mmol) followed by hydroxylamine hydrochloride (0.278 mg, 4 mmol), and the reaction was stirred at r.t. overnight. The mixture was then concentrated to dryness. The residue was dissolved in EtOAc (100 mL) and the solution was washed with H_2O (20 mL). The organic layer was dried with $MgSO_4$ and the solvent was removed *in vacuo*. The residue was purified by column chromatography.

Methyl (2*S*)-2-({[2-(*N*'-hydroxycarbamimidoyl)pyridin-3-yl]carbonyl}amino)propanoate (7a)

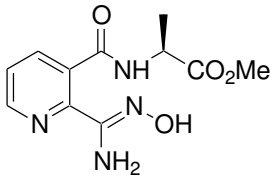

Purification by flash column chromatography (CH_2Cl_2/EtOH, 91:9) gave **7a** as a white solid; yield: 0.362 g (68%); mp 74-75 °C.

IR (KBr): 3470, 3322, 3067, 2918, 2849, 1739, 1731, 1641, 1582, 1565, 1547, 1538, 1454, 1216 cm^{-1}.

^{1}H NMR (300 MHz, $CDCl_3$, 25 °C): δ = 8.60 (d, J = 4.5 Hz, 1H, H_{Ar}), 7.92 (d, J = 7.8 Hz, 1H, H_{Ar}), 7.46 (d, J = 7.2 Hz, 1H, NH), 7.36 (dd, J = 7.8, 4.8 Hz, 1H, H_{Ar}), 5.47 (s, 2H, NH_2), 4.75 (m, 1H, CH), 3.75 (s, 3H, OCH_3), 1.48 (d, J = 7.2 Hz, 3H, CH_3).

^{13}C NMR (75 MHz, $CDCl_3$, 25 °C): δ = 174.1, 168.3, 151.2, 150.0, 147.3, 137.9, 131.7, 124.3, 53.0, 49.3, 18.2.

Anal. Calcd for $C_{11}H_{14}N_4O_4$: C, 49.62; H, 5.30; N, 21.04. Found: C, 49.48; H, 5.32; N, 20.96.

LCMS: MH^+, 267.

Methyl (2*S*)-2-({[2-(*N*'-hydroxycarbamimidoyl)pyridin-3-yl]carbonyl}amino)-3-phenylpropanoate (7b)

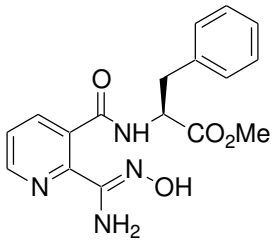

Ester **7b** was obtained as a white solid of analytical purity without further purification; yield: 0.527 g (77%); mp 172 °C.

IR (KBr): 3359, 3201, 3020, 2886, 1723, 1672, 1644, 1586, 1575, 1537, 1276, 934 cm^{-1}.

^1H NMR (300 MHz, $CDCl_3$, 25 °C): δ = 8.60 (d, J = 4.8 Hz, 1H, H_{Ar}), 7.88 (d, J = 7.8 Hz, 1H, H_{Ar}), 7.63 (d, J = 7.5 Hz, 1H, NH), 7.37 – 7.19 (m, 6H, 6×H_{Ar}), 5.49 (br s, 2H, NH_2), 5.11 (dd, J = 13.5, 6.0 Hz, 1H, CH), 3.72 (s, 3H, OCH_3), 3.24 – 3.21 (m, 2H, CH_2).

^{13}C NMR (100 MHz, DMSO-d_6+CCl_4, 1:1, 25 °C): δ = 171.9, 167.5, 149.9, 148.7, 147.4, 137.4, 136.8, 131.7, 129.5, 128.4, 126.6, 123.3, 54.2, 51.9, 37.5.

Anal. Calcd for $C_{17}H_{18}N_4O_4$: C, 59.64; H, 5.30; N, 16.37. Found: C, 59.51; H, 5.32; N, 16.31.

LCMS: MH^+, 343.

(2*S*)-1-{[2-(*N*'-hydroxycarbamimidoyl)pyridin-3-yl]carbonyl}pyrrolidine-2-carboxylate (7c)

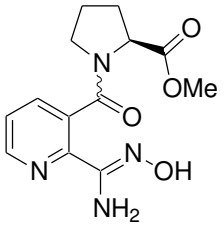

Purification by flash column chromatography (CH_2Cl_2/MeOH, 94:6) gave **7c** as a white solid; yield: 0.409 g (70%); mp 135-136 °C.

IR (KBr): 3521, 3159, 3117, 3080, 2886, 2867, 2835, 1732, 1651, 1608, 1537, 1471, 1433, 1368, 1199, 1177 cm^{-1}.

^1H NMR (300 MHz, $CDCl_3$, 25 °C): δ = 8.57 (m, 1H, H_{Ar}), 8.08 (br s, 1H, OH), 7.69 and 7.61 (2×dd, J = 7.8, 1.5 Hz, 1H, H_{Ar}), 7.39 – 7.26 (m, 1H, H_{Ar}), 5.50 (br s, 2H, NH_2), 4.74 and 4.11 (2×dd, J = 8.6, 4.3 Hz, J = 6.1 Hz 1H, CH), 3.79 and 3.48 (2×s, 3H, OCH_3), 3.75 (m) and 3.25 (t, J = 6.5 Hz, 2H, CH_2), 2.38 – 2.20 and 1.96 – 1.86 (2×m, 4H, CH_2-CH_2).

^{13}C NMR (75 MHz, $CDCl_3$, 25 °C): δ = 173.6, 173.3, 169.5, 169.2, 150.6, 150.3, 149.2, 145.7, 145.2, 137.2, 136.5, 131.5, 131.1, 124.4, 124.0, 61.2, 59.3, 52.9, 52.7, 48.9, 47.4, 31.5, 30.3, 25.2, 23.8.

Anal. Calcd for $C_{13}H_{16}N_4O_4$: C, 53.42; H, 5.52; N, 19.17. Found: C, 53.25; H, 5.54; N, 19.10.

LCMS: MH^+, 293.

Methyl (2*S*)-2-({[2-(*N*'-hydroxycarbamimidoyl)pyridin-3-yl]carbonyl}amino)-3-methylbutanoate (7e)

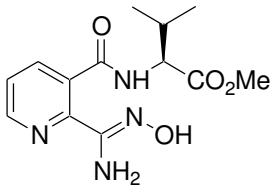

Purification by flash column chromatography (CH_2Cl_2/EtOH, 95:5) gave **7e** as a white solid; yield: 0.465 g (79%); mp 120-121 °C.

IR (KBr): 3297, 1739, 1646, 1534, 1198, 1149 cm^{-1}.

^{1}H NMR (300 MHz, $CDCl_3$, 25 °C): δ = 8.57 (d, J = 4.8 Hz, 1H, H_{Ar}), 7.92 (d, J = 7.8 Hz, 1H, H_{Ar}), 7.50 (d, J = 8.1 Hz, 1H, NH), 7.33 (dd, J = 7.8, 4.8 Hz, 1H, H_{Ar}), 5.46 (s, 2H, NH_2), 4.62 (dd, J = 8.1, 5.1 Hz, 1H, CHNH), 3.69 (s, 3H, OCH_3), 2.22 – 2.12 (m, 1H, CH), 0.94 (d, J = 6.9 Hz, 3H, CH_3), 0.91 (d, J = 6.9 Hz, 3H, CH_3).

^{13}C NMR (75 MHz, $CDCl_3$, 25 °C): δ = 172.9, 168.3, 151.4, 150.1, 147.2, 138.4, 131.9, 124.5, 58.8, 52.8, 31.9, 19.4, 18.7.

Anal. Calcd for $C_{13}H_{18}N_4O_4$: C, 53.05; H, 6.16; N, 19.04. Found: C, 52.92; H, 6.18; N, 18.98.

LCMS: MH^+, 295.

Methyl (2*S*)-2-({[2-(*N*'-hydroxycarbamimidoyl)pyridin-3-yl]carbonyl}amino)-4-methylpentanoate (7f)

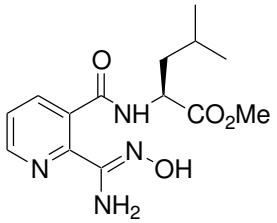

Purification by flash column chromatography (CH_2Cl_2/EtOH, 9:1) gave **7f** as a white solid; yield: 0.431 g (70%); mp 114-115 °C.

IR (KBr): 3479, 3377, 3236, 3076, 2955, 1746, 1638, 1581, 1547, 1248 cm^{-1}.

^{1}H NMR (300 MHz, $CDCl_3$, 25 °C): δ = 8.62 (d, J = 4.8 Hz, 1H, H_{Ar}), 7.95 (d, J = 7.8 Hz, 1H, H_{Ar}), 7.41 – 7.35 (m, 2H, NH+H_{Ar}), 5.46 (br s, 2H, NH_2), 4.84 – 4.76 (m, 1H, CH), 3.76 (s, 3H, OCH_3), 1.78 – 1.64 (m, 3H, CH_2+CH), 0.98 (d, J = 6.3 Hz, 3H, CH_3), 0.96 (d, J = 6.3 Hz, 3H, CH_3).

^{13}C NMR (75 MHz, $CDCl_3$, 25 °C): δ = 174.1, 168.3, 151.4, 150.1, 147.0, 138.4, 131.9, 124.5, 53.0, 52.2, 42.1, 25.5, 23.4, 22.7.

Anal. Calcd for $C_{14}H_{20}N_4O_4$: C, 54.54; H, 6.54; N, 18.17. Found: C, 54.36; H, 6.55; N, 18.10.

LCMS: MH^+, 309.

Methyl (2*S*)-2-({[2-(*N*'-hydroxycarbamimidoyl)pyridin-3-yl]carbonyl}amino)-3-(1*H*-indol-3-yl)propanoate (7g)

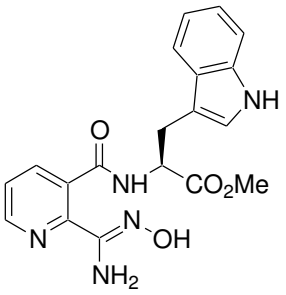

Purification by flash column chromatography (CH_2Cl_2/MeOH, 94:6) gave **7g** as a white solid; yield: 0.507 g (67%); mp 129-130 °C.

IR (KBr): 3331, 3043, 1730, 1641, 1582, 1214 cm^{-1}.

^1H NMR (300 MHz, $CDCl_3$, 25 °C): δ = 8.90 (s, 1H, NH), 8.46 (d, J = 4.8 Hz, 1H, H_{Ar}), 7.72 (dd, J = 4.8, 1.2 Hz, 1H, H_{Ar}), 7.50 (d, J = 7.5 Hz, 1H, NH), 7.33 – 7.24 and 7.18 – 7.02 (2×m, 6H, 5×H_{Ar}), 5.49 (s, 2H, NH_2), 5.07 (dd, J = 12.9, 6.0 Hz, 1H, CH), 3.62 (s, 3H, OCH_3), 3.32 (m, 2H, CH_2).

^{13}C NMR (75 MHz, $CDCl_3$, 25 °C): δ = 173.1, 168.6, 151.5, 150.1, 147.0, 137.9, 136.8, 131.7, 128.1, 124.5, 122.4, 119.9, 119.0, 112.1, 109.9, 54.1, 53.1, 28.0.

Anal. Calcd for $C_{19}H_{19}N_5O_4$: C, 59.84; H, 5.02; N, 18.36. Found: C, 59.65; H, 5.04; N, 18.29.

LCMS: MH^+, 382.

Methyl (2*S*)-2-[({2-[amino(hydroxyimino)methyl]pyridin-3-yl}carbonyl)amino]-3-(tritylsulfanyl)propanoate (7h)

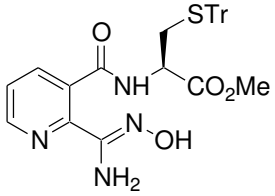

Purification by flash column chromatography (CH_2Cl_2/MeOH, 94:6) gave **7h** as a light-yellow solid; yield: 1.015 g (94%); mp 76-80 °C.

^{1}H NMR (300 MHz, $CDCl_3$): δ = 8.46 (d, *J* = 3.6 Hz, 1H, H_{Ar}), 7.76 (dd, *J* = 7.7, 1.2 Hz, 1H, H_{Ar}), 7.43 (d, *J* = 7.4 Hz, 1H, NH), 7.35 – 7.00 (m, 16H, 16×H_{Ar}), 5.36 (s, 2H, NH_2), 4.67 (dd, *J* = 12.4, 5.4 Hz, 1H, CH), 3.58 (s, 3H, OCH_3), 2.69 (ddd, *J* = 27.4, 12.3, 5.4 Hz, 2H, CH_2).

^{13}C NMR (75 MHz, $CDCl_3$): δ = 171.32, 168.09, 150.86, 149.90, 146.69, 144.85, 138.15, 131.41, 130.00, 128.53, 127.41, 124.24, 67.37, 53.18, 52.72, 34.16.

Pyrrolo[3,4-b]pyridine-5,7-dione 7-oxime (III)

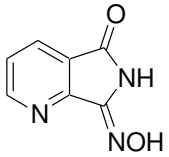

^{1}H NMR (300 MHz, DMSO): δ = 11.63 (s, 1H, OH), 11.36 (s, 1H, NH), 8.84 (d, *J* = 4.9 Hz, 1H, H_{Ar}), 8.19 (dd, *J* = 7.8, 1.1 Hz, 1H, H_{Ar}), 7.61 (dd, *J* = 7.7, 4.9 Hz, 1H, H_{Ar}).

^{13}C NMR (75 MHz, DMSO): δ = 165.39, 154.16, 153.16, 143.98, 131.65, 125.52, 125.06.

Synthesis of Compounds 5', 6' (a-c); General Procedure:

To a solution of 3-cyanopyrazine-2-carboxylic acid (3) (0.740 g, 5 mmol) in THF (30 mL) were added: Et_3N (1.39 mL, 10 mmol), the corresponding methyl ester of an amino acid hydrochloride (5 mmol) and HOBt (0.675 g, 5 mmol). The mixture was stirred at 0 °C and EDCI (0.967 g, 5.05 mmol) was added. Then, the mixture was stirred at r.t. overnight. The precipitate was filtered and the filtrate was evaporated under *vacuo*. The residue was diluted with CH_2Cl_2 (50mL), washed with a solution of 0,1M HCl (3×15 mL), brine (20 mL), then dried with MgSO4 and concentrated *in vacuo*.

Methyl (2S)-2-{[(3-cyanopyrazin-2-yl)carbonyl]amino}propanoate (5'a)

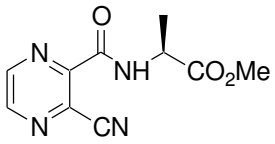

Purification by flash column chromatography (AcOEt/CH_2Cl_2, 1:1) gave **5'a** as a pale-yellow solid (0.161 g, 23%); mp 71-72 °C.

IR: ν_{max} = 3367, 3047, 2994, 2954, 2240 (CN), 1736, 1678, 1517, 1203, 1150 cm^{-1}.

^1H NMR (300 MHz, $CDCl_3$, 25 °C): δ = 8.89 (d, *J* = 2.3 Hz, 1H, H_{Ar}), 8.79 (d, *J* = 2.3 Hz, 1H, H_{Ar}), 8.26 (d, *J* = 7.4 Hz, 1H, NH), 4.71 (pseudo-p, *J* = 7.3 Hz, 1H, CH), 3.72 (s, 3H, OCH_3), 1.49 (d, *J* = 7.2 Hz, 3H, CH_3).

^{13}C NMR (75 MHz, $CDCl_3$, 25 °C): δ = 173.0, 160.5, 147.9, 146.7, 145.6, 129.5, 115.4, 53.2, 48.8, 18.6.

ESI calculated for $C_{10}H_{10}N_4NaO_3$ $[M+Na]^+$ *m/z* = 257.0654, found 257.0645.

Methyl (2S)-2-[(5E)-5-imino-7-oxo-5,7-dihydro-6H-pyrrolo[3,4-b]pyrazin-6-yl]propanoate (6'a)

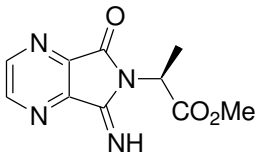

Purification by flash column chromatography (AcOEt/CH_2Cl_2, 1:1) gave **6'a** as a yellow oil (0.197 g, 28%).

IR: ν_{max} = 3272, 3001, 2953, 1733, 1666, 1518, 1372, 1220, 1157 cm^{-1}.

^1H NMR (300 MHz, $CDCl_3$): δ = 9.51 (s, 1H, NH), 8.91 (d, *J* = 2.6 Hz, 1H, H_{Ar}), 8.84 (d, *J* = 2.6 Hz, 1H, H_{Ar}), 5.36 – 5.29 (m, 1H, CH), 3.74 (s, 3H, OCH_3), 1.77 (d, *J* = 7.3 Hz, 3H, CH_3).

^{13}C NMR (75 MHz, $CDCl_3$): δ = 170.6, 163.6, 157.1, 149.2, 148.7, 144.7, 144.7, 53.4, 48.8, 15.6.

ESI calculated for $C_{10}H_{11}N_4O_3$ $[M+H]^+$ m/z = 235.0838, found 235.0826.

Methyl (2S)-2-{[(3-cyanopyrazin-2-yl)carbonyl]amino}-3-phenylpropanoate (5'b)

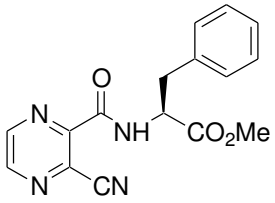

Purification by flash column chromatography (AcOEt/petroleum ether, 7:3) gave **5'b** as a light-yellow solid (0.047 g, 3%); mp 97-99 °C.

IR: ν_{max} = 3402, 3389, 3059, 3031, 2954, 2853, 2237 (CN), 1736, 1686, 1508, 1374, 1261cm^{-1}.

^{1}H NMR (300 MHz, $CDCl_3$): δ = 8.89 (d, *J* = 2.3 Hz, 1H, H_{Ar}), 8.74 (d, *J* = 2.3 Hz, 1H, H_{Ar}), 8.20 (d, *J* = 7.9 Hz, 1H, NH), 7.29 – 7.13 (m, 5H, 5×H_{Ar}), 5.11 (dt, *J* = 8.0, 6.0 Hz, 1H, CH), 3.77 (s, 3H, OCH_3), 3.28 (2×dd, *J* = 8.1, 5.8 Hz, 2H, CH_2).

^{13}C NMR (75 MHz, $CDCl_3$): δ = 171.9, 160.7, 147.8, 146.9, 145.4, 136.1, 129.8, 129.4, 128.0, 115.5, 54.2, 53.2, 38.6.

ESI calculated for $C_{16}H_{14}N_4NaO_3$ $[M+Na]^+$ m/z = 333.0954, found 333.0958.

Methyl (2S)-2-[(5E)-5-imino-7-oxo-5,7-dihydro-6H-pyrrolo[3,4-b]pyrazin-6-yl]-3-phenylpropanoate (6'b)

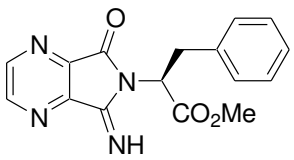

Purification by flash column chromatography (AcOEt/petroleum ether, 7:3) gave **6'b** as a yellow oil (1.007 g, 65%).

IR: ν_{max} = 3279, 3062, 3029, 2953, 2847, 1737, 1666, 1413, 1374, 1244, 1123 cm^{-1}.

^{1}H NMR (300 MHz, $CDCl_3$): δ = 9.46 (s, 1H, NH), 8.82 (d, *J* = 2.6 Hz, 1H, H_{Ar}), 8.75 (d, *J* = 2.6 Hz, 1H, H_{Ar}), 7.19 – 7.07 (m, 5H, 5×H_{Ar}), 5.55 (dd, *J* = 10.9, 5.6 Hz, 1H, CH), 3.77 (s, 3H, OCH_3), 3.74 – 3.61 (m, 2H, CH_2).

^{13}C NMR (75 MHz, $CDCl_3$): δ = 169.7, 163.7, 157.2, 149.1, 148.7, 144.3, 144.2, 137.2, 129.4, 129.0, 127.3, 54.4, 53.4, 35.0.

ESI calculated for $C_{16}H_{14}N_4NaO_3$ $[M+Na]^+$ *m/z* = 333.0961, found 333.0958.

Methyl (2S)-1-[1-(3-cyanopyrazin-2-yl)ethenyl]pyrrolidine-2-carboxylate (5'c)

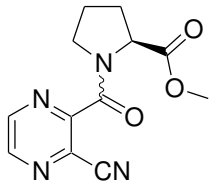

Purification by flash column chromatography (AcOEt/CH_2Cl_2, 1:1) gave **5'c** as a light-yellow oil (0.382 g, 49%).

IR: ν_{max} = 2955, 2887, 2239 (CN), 1738, 1637, 1455, 1373, 1171 cm^{-1}.

^{1}H NMR (300 MHz, $CDCl_3$): δ = 8.74 (s, 1H, H_{Ar}), 8.71 and 8.61 (2×d, *J* = 2.3 Hz, 1H, H_{Ar}), 4.80 and 4.64 (2×dd, *J* = 8.4, 3.2 Hz, 1H, CH), 3.76 – 3.64 (m, 2H, CH_2N), 3.68 and 3.53 (2×s, 3H, OCH_3), 2.30 – 1.90 (m, 4H, CH_2CH_2).

^{13}C NMR (75 MHz, $CDCl_3$): δ = 172.0 (172.6), 162.3 (162.2), 152.2 (151.7), 146.1 (145.9), 145.6 (144.6), 130.0 (130.8), 114.9 (115.2), 60.2 (61.2), 52.9 (52.8), 49.5 (48.4), 29.4 (31.8), 25.6 (22.6).

ESI calculated for $C_{12}H_{12}KN_4O_3$ $[M+K]^+$ *m/z* = 299.0551, found 299.0541.

Boc-Pro-Phe-OMe

Compound is commercially available, but was prepared according to the general procedure for the synthesis of compounds **5,6(a-f)**. It was prepared by coupling of Boc-Pro-OH

hydrochloride (1.08 g, 5 mmol) and H-Phe-OMe (1.08 g, 5 mmol) using EDC (0.97 g, 5.05 mmol), HOBt (0.77 g, 5 mmol) and triethylamine (1.4 mL, 10 mmol) in CH_2Cl_2 (30 mL). The mixture was stirred at room temperature overnight and then washed with a solution of 0.1M HCl (3×15 mL), brine (20 mL), dried with $MgSO_4$ and then the solvent was removed *in vacuo*. The product was purified by flash chromatography, eluting with AcOEt/Petroleum ether, 2/1; yield: 92% (1.73 g).

^{1}H NMR (300 MHz, $CDCl_3$, 25 °C): δ = 7.32 – 7.07 (m, 5H, H_{Ph}), 6.46 (s, 1H, NH), 4.97 - 4.77 (m, J = 1.4 Hz, 1H, CH_{Phe}), 4.37 - 4.10 (s, 1H, CH^{α}_{Pro}), 3.72 (s, 3H, OCH_3), 3.47 -3.21 (m, 2H, $CH_2{}^{\delta}_{Pro}$), 3.10 (ddd, J = 20.8, 13.9, 6.3 Hz, 2H, CH_{2Phe}), 2.33 -1.67 (m, 4H, $CH_2CH_2{}^{\beta,\gamma}_{Pro}$), 1.43 (s, 9H, $(CH_3)_3$).

^{13}C NMR (75 MHz, $CDCl_3$, 25 °C): δ = 172.4, 172.7, 136.6, 129.9, 129.2, 127.7, 81.4, 61.8 (60.5), 53.3 (53.9), 52.9, 47.6, 38.8, 30.3 (31.2), 28.9, 25.1 (24.1).

H-Pro-Phe-OMe TFA salt

Compound is commertially available, but was synthesized from Boc-Pro-Phe-OMe (0.752 g, 2 mmol) by treatment with 30% trifluoroacetic acid – dichlorometham (10 mL) during one hour. The solvent was then evaporated in high *vacuo*. A beige solid (0.772 g, 99%) was obtained.

^{1}H NMR (300 MHz, MeOD, 25 °C): δ = 7.32 - 7.18 (m, 5H, H_{Ph}), 4.67 (t, J = 6.8 Hz, 1H, CH), 4.52 (dd, J = 8.5, 3.9 Hz, 1H, CH), 3.82 – 3.72 (m, 2H, CH_2), 3.70, 3.66 (2×s, 3H, $OCH_3{}^{cis/trans}$), 3.24 – 2.91 (m, 2H, CH_2), 2.32 – 1.67 (m, 4H, CH_2CH_2).

^{13}C NMR (75 MHz, MeOD, 25 °C): δ = 173.0 (173.3), 138.0 (138.3), 130.5 (130.2), 129.6, 128.0, 119.8 (116.0), 62.7 (61.8), 55.5 (55.2), 52.7 (52.9), 38.4 (38.1), 30.2 (33.4), 26.0 (22.2).

Methyl (2*S*)-2-[({(2*S*)-1-[(3-cyanopyrazin-2-yl)carbonyl]pyrrolidin-2-yl}carbonyl)amino]-3-phenylpropanoate (5'd)

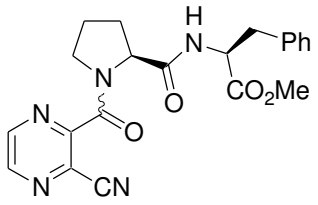

To a solution of dipeptide Boc-Pro-Phe-OMe (0.390 g, 1 mmol), acide **4'** (0.149 g, 1 mmol) and HOBt (0.168 g, 1.1 mmol) in THF (5 mL) at 0° C, HATU (0.380 g, 1 mmol) and DIEA (0.4 mL, 2.1 mmol) were added. After 15 min at 0° C and 10 hours at room tempereture, the solvent was evaporated and the crude product was purified by flash column chromatography (AcOEt/CH_2Cl_2, 7:3) to give **5'd** as a light-yellow oil (0.830 g, 68%).

^{1}H NMR (300 MHz, $CDCl_3$, 25 °C, $K_{t/c}$ = 1.73): δ = 8.77 (s, 4H, $H^{trans}{}_{Ar}$), 8.62 (d, *J* = 2.3 Hz, 1H, $H^{cis}{}_{Ar}$), 8.35 (d, *J* = 2.2 Hz, 1H, $H^{cis}{}_{Ar}$), 7.31 – 7.05 (m, 18H, $H^{trans/cis}{}_{Ph}$), 6.58 (d, *J* = 7.8 Hz, 1H, NH), 4.87 – 4.74 and 4.68 (m, ddd, *J* = 13.8, 7.4, 4.8 Hz, 6H, $CH^{trans/cis}$ Phe, CH-$\alpha^{trans/cis}$ Pro), 3.71, 3.69 and 3.85 – 3.51 (s, s, m, 16H, $OCH_3{}^{trans}$, $OCH_3{}^{cis}$, CH_2-$\delta^{trans/cis}$ Pro), 3.23 – 3.05 and 2.96 - 2.88 (2×m, 6H, $CH_2{}^{trans}$, $CH_2{}^{cis}$ Phe), 2.32 – 1.78 and 1.67 – 1.50 (2×m, 16H, CH_2CH_2-$\beta,\gamma^{trans/cis}$ Pro).

^{13}C NMR (75 MHz, $CDCl_3$, 25 °C): *δ* = 172.3 (172.2), 170.6 (171.8), 163.4 (163.1), 152.5 (151.5), 146.2 (145.9), 145.6 (144.6), 136.6, 130.4 (131.1), 130.0 (129.5), 129.0 (129.3), 127.4 (127.8), 115.2 (115.5), 61.5 (63.1), 54.2 (53.8), 52.9 (53.0), 49.9 (48.6), 38.3 (37.9), 28.3 (32.3), 25.8 (22.4).

ESI calculated for $C_{21}H_{21}KN_5O_4$ $[M+K]^+$ *m/z* = 446.1232, found 446.1225.

Synthesis of Compounds 7'a-d; General Procedure:

To a solution of (2*S*)-*N*-(3-cyanopyrazin-2-yl)carbonyl-substituted amino acids **5'** and/or methyl esters of methyl (2*S*)-2-[(5*E*)-5-imino-7-oxo-5,7-dihydro-6*H*-pyrrolo[3,4-*b*]pyrazin-6-yl]alkanoic acids **6'** (2 mmol) in MeOH (15 mL) was added Et_3N (0.56 mL, 4 mmol) followed by hydroxylamine hydrochloride (0.278 g, 4 mmol) and the reaction was stirred at r.t. overnight. The mixture was then evaporated to dryness. The residue was dissolved in ethyl acetate (100 mL) and washed with H_2O (20 mL). The organic layer was dried with $MgSO_4$ and the solvent was removed *in vacuo*. The residue was purified by column chromatography.

Methyl (2*S*)-2-({[3-(*N′*-hydroxycarbamimidoyl)pyrazin-2-yl]carbonyl}amino)propanoate (7'a)

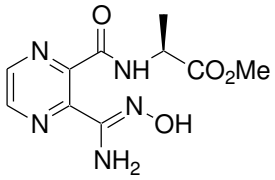

Purification by flash column chromatography (CH_2Cl_2/MeOH, 95:5) gave **7'a** as a pale-yellow oil (0.449 g, 84%).

IR: ν_{max} = 3462, 3328, 3066, 2995, 2954, 2847, 1733, 1646, 1537, 1454, 1435, 1340, 1215, 1161 cm^{-1}.

^1H NMR (300 MHz, $CDCl_3$): δ = 8.57 (d, *J* = 2.3 Hz, 1H, H_{Ar}), 8.49 (d, *J* = 2.3 Hz, 1H, H_{Ar}), 7.71 (d, *J* = 7.5 Hz, 1H, NH), 5.45 (br s, 2H, NH_2), 4.70 (*pseudo-p*, *J* = 7.2 Hz, 1H, CH), 3.70 (s, 3H, OCH_3), 1.45 (d, *J* = 7.2 Hz, 3H, CH_3).

^{13}C NMR (75 MHz, $CDCl_3$): δ = 173.8, 165.5, 150.4, 146.7, 145.0, 145.0, 143.5, 53.2, 49.2, 18.5.

ESI calculated for $C_{10}H_{13}KN_5O_4$ $[M+K]^+$ *m/z* = 306.0603, found 306.0599.

Methyl (2*S*)-2-({[3-(*N′*-hydroxycarbamimidoyl)pyrazin-2-yl]carbonyl}amino)-3-phenylpropanoate (7'b)

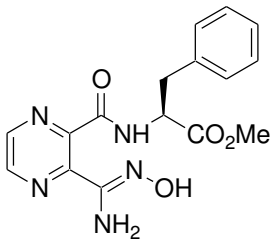

Purification by flash column chromatography (CH_2Cl_2/MeOH, 93:7) gave **7'b** as a light-yellow solid (0.432 g, 63%); mp 154-157 °C.

IR: ν_{max} = 3474, 3350, 3060, 2926, 1717, 1675, 1645, 1547, 1435, 1161, 971 cm^{-1}.

^{1}H NMR (300 MHz, DMSO-d_6): δ = 9.97 (s, 1H, OH), 8.79 (d, J = 7.5 Hz, 1H, NH), 8.71 (d, J = 2.3 Hz, 1H, H_{Ar}), 8.64 (d, J = 2.3 Hz, 1H, H_{Ar}), 7.32-7.20 (m, 5H, 5×H_{Ar}), 5.82 (s, 2H, NH_2), 4.70 (dt, J = 7.2, 6.8 Hz, 1H, CH), 3.57 (s, 3H, OCH_3), 3.19 – 2.99 (m, 2H, CH_2).

^{13}C NMR (75 MHz, DMSO-d_6): δ = 171.3, 165.5, 148.6, 147.5, 143.9, 143.5, 142.6, 136.9, 129.1, 128.2, 126.5, 53.8, 51.7, 37.1.

ESI calculated for $C_{16}H_{18}N_5O_4$ $[M+H]^+$ m/z = 344.1353, found 344.1353.

Methyl (2*S*)-1-{[3-(*N′*-hydroxycarbamimidoyl)pyrazin-2-yl]carbonyl}pyrrolidine-2-carboxylate (7'c)

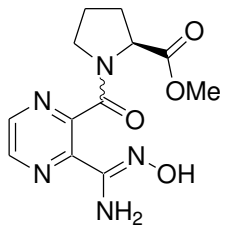

Purification by flash column chromatography (CH_2Cl_2/MeOH, 93:7) gave **7'c** as a white solid (0.545 g, 93%); mp 135-138 °C.

IR: ν_{max} = 3479, 3369, 2983, 2959, 2919, 2871, 2850, 1733, 1651, 1620, 1557, 1453, 1416, 1282, 1156, 936 cm^{-1}.

^{1}H NMR (300 MHz, $CDCl_3$): δ = 8.57 and 8.54 (2×d, J = 2.4 Hz, 1H, H_{Ar}), 8.54 and 8.51 (2×d, J = 2.2 Hz, 1H, H_{Ar}), 5.48 and 5.38 (2×s, 2H, NH_2), 4.74 and 4.11 (2×dd, J = 8.5, 3.8 Hz, 1H, CH), 3.77 and 3.55 (2×s, 3H, OCH_3), 3.39 – 3.36 and 3.29 – 3.23 (2×m, 2H, CH_2N), 2.37 – 2.22 (m, 2H, CH_2), 2.05 – 1.87 (m, 2H, CH_2).

^{13}C NMR (75 MHz, $CDCl_3$): δ = 173.3 (172.9), 167.1, 148.9 (149.2), 148.6, 143.9, 143.4 (143.7), 142.7 (142.5), 59.3 (61.1), 53.0 (52.8), 48.3 (47.3), 30.2 (31.5), 25.2 (23.5).

ESI calculated for $C_{12}H_{16}N_5O_4$ $[M+H]^+$ m/z = 294.1210, found 294.1197.

Methyl (2*S*)-2-({[(2*S*)-1-({3-[(*Z*)-(hydroxyamino)(imino)methyl]pyrazin-2-yl}carbonyl)pyrrolidin-2-yl]carbonyl}amino)-3-phenylpropanoate (7'd)

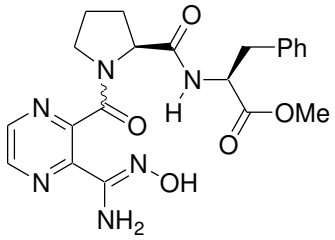

Purification by flash column chromatography (CH_2Cl_2/MeOH, 95:5) gave **7'd** as a light-yellow solid (0.669 g, 76%); mp 59-62 °C.

IR (ATR): ν_{max} = 3517, 3402, 3319 (NH, OH), 1743, 1722, 1679, 1670, 1656, 1653 (C=O, C=N) cm^{-1}.

IR: ν_{max} = 3483, 3311, 3064, 2960, 2924, 2853, 1739, 1642, 1528, 1454, 1409, 1259, 1066, 798, 700 cm^{-1}.

^{1}H NMR (300 MHz, $CDCl_3$, 25 °C, $K_{t/c}$ = 13.30): δ = 9.42 (s, 1H, OH), 8.55 and 8.49 (d, *J* = 2.4 Hz, 1H, $H^{trans/cis}{}_{Ar}$), 8.52 and 8.41 (d, *J* = 2.4 Hz, 1H, $H^{trans/cis}{}_{Ar}$), 7.78 (d, *J* = 9.2 Hz, 1H, NH), 7.27 – 6.97 (m, 5H, 5×$H^{trans/cis}{}_{Ph}$), 5.68 and 5.42 (2×s, 2H, $NH_2{}^{trans}$, $NH_2{}^{cis}$), 5.10 and 4.69 (td, m, *J* = 9.4, 6.5 Hz, 1H, CH^{trans}, CH^{cis} Phe), 4.77 and 4.43 (m, 1H, CH^{trans}, CH^{cis} Pro), 3.69 and 3.52 (s, 3H, $OCH_3{}^{trans}$, $OCH_3{}^{cis}$), 3.21 – 2.84 (m, 4H, $CH_2{}^{trans/cis}$ Phe, CH_2-δ $^{trans/cis}$ Pro), 2.06 - 1.87 (m, 2H, CH_2-β$^{trans/cis}$ Pro), 1.61 - 1.52 and 1.11 – 0.96 (2×m, 2H, CH_2-γ$^{trans/cis}$ Pro).

^{13}C NMR (75 MHz, $CDCl_3$, 25 °C): *δ* = 175.8, 171.9 (171.6), 167.1 (167.7), 150.3 (150.0), 148.4, 144.2, 143.7, 141.6, 136.6 (137.4), 129.8, 129.2, 127.7, 60.7 (63.0), 53.6 (52.9), 48.2 (47.1), 39.1 (37.9), 30.1 (31.1), 24.0 (22.8).

ESI calculated for $C_{21}H_{24}KN_6O_5$ $[M+K]^+$ *m/z* = 479.1448, found 479.1440.

Synthesis of Compounds 8, 8' (a-c); General Procedure:

Amidoxime **7**, **7'** (**a-c**; 1 mmol) was dissolved in anhydrous acetonitrile (20 mL). After addition of N-*t*-butoxycarbonyl-L-valine(phenylalanine) (1.3 mmol), 4-DMAP (0.011 g, 0.09

mmol) and DCC (0.268 g, 1.3 mmol) the solution was stirred for 24h at r.t.. The solvent was evaporated under reduced pressure and the crude product was purified by column chromatography.

Methyl (2*S*)-2-[({2-[(*Z*,5*S*)-1-amino-5-isopropyl-9,9-dimethyl-4,7-dioxo-3,8-dioxa-2,6-diazadec-1-en-1-yl]pyridin-3-yl}carbonyl)amino]propanoate (8a)

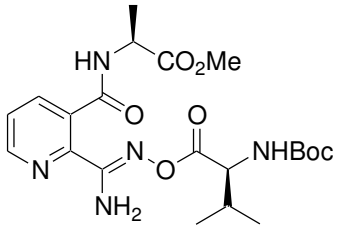

Purification by flash column chromatography (CH_2Cl_2/AcOEt, 3:7) gave **8a** as a white solid (0.298 g, 64%); mp 139 – 141 °C;

IR ($CHCl_3$): ν_{max} = 3438, 3408, 1767, 1741, 1712, 1670, 1651 cm^{-1}.

^{1}H NMR (300 MHz, $CDCl_3$): δ = 8.64 (dd, *J* = 4.7, 1.5 Hz, 1H, H_{Ar}), 8.00 (dd, *J* = 7.8, 1.5 Hz, 1H, H_{Ar}), 7.58 (d, *J* = 6.8 Hz, 1H, NH), 7.44 (dd, *J* = 7.8, 4.8 Hz, 1H, H_{Ar}), 5.85 (s, 2H, NH_2), 5.08 (d, *J* = 8.6 Hz, 1H, N*H*Boc), 4.79 (p, *J* = 7.1 Hz, 1H, C*H*CH_3), 4.26 (dd, *J* = 8.3, 6.1 Hz, 1H, C*H*$CH(CH_3)_2$), 3.74 (s, 3H, OCH_3), 2.14 (dq, *J* = 13.4, 6.7 Hz, 1H, C*H*$(CH_3)_2$), 1.52 (d, *J* = 7.2 Hz, 3H, CH_3), 1.44 (s, 9H, $(CH_3)_3$), 0.99 (dd, *J* = 11.5, 6.8 Hz, 6H, $(CH_3)_2$).

^{13}C NMR (75 MHz, $CDCl_3$): δ = 173.9, 170.2, 167.3, 156.5, 156.0, 150.3, 145.6, 138.64, 133.1, 125.7, 80.8, 58.7, 53.0, 49.8, 31.8, 29.0, 19.7, 18.6, 18.5.

ESI calculated for $C_{21}H_{32}N_5O_7$ $[M+H]^+$ *m/z* = 466.2293, found 466.2296.

Methyl (2*S*)-2-[({2-[(*Z*,5*S*)-1-amino-5-isopropyl-9,9-dimethyl-4,7-dioxo-3,8-dioxa-2,6-diazadec-1-en-1-yl]pyridin-3-yl}carbonyl)amino]-3-phenylpropanoate (8b)

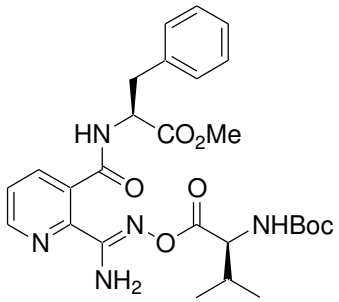

Purification by flash column chromatography (CH_2Cl_2/AcOEt, 3:7) gave **8b** as a light-yellow solid (0.492 g, 91%); mp 149 – 151 °C;

IR ($CHCl_3$): ν_{max} = 3435, 3408, 1766, 1743, 1711, 1670, 1648 cm^{-1}.

^1H NMR (300 MHz, $CDCl_3$): δ = 8.64 (d, *J* = 4.0 Hz, 1H, H_{Ar}), 7.88 (d, *J* = 7.0 Hz, 1H, H_{Ar}), 7.43 (dd, *J* = 7.8, 4.8 Hz, 1H, H_{Ar}), 7.34 (d, *J* = 6.3 Hz, 1H, NH), 7.30 – 7.18 (m, 5H, C_6H_5), 5.83 (s, 2H, NH_2), 5.13 - 5.07 (m, 2H, N*H*Boc + C*H*CH_2), 4.29 (dd, *J* = 8.4, 5.9 Hz, 1H, C*H*CH$(CH_3)_2$), 3.71 (s, 3H, OCH_3), 3.39 – 3.22 (m, 2H, CH_2), 2.14 (dq, *J* = 13.4, 6.8 Hz, 1H, C*H*$(CH_3)_2$), 1.46 (s, 9H, $(CH_3)_3$), 0.98 (dd, *J* = 13.2, 6.8 Hz, 6H, $(CH_3)_2$).

^{13}C NMR (75 MHz, $CDCl_3$): δ = 172.5, 170.1, 167.5, 156.4, 155.6, 150.2, 145.6, 138.3, 137.2, 133.0, 130.1, 129.1, 127.5, 125.6, 80.7, 58.6, 55.1, 52.8, 38.2, 31.9, 29.0, 19.7, 18.5.

ESI calculated for $C_{27}H_{35}N_5NaO_7$ $[M+Na]^+$ *m/z* = 564.2434, found 564.2429.

Methyl (2*S*)-1-({2-[(*Z*,5*S*)-1-amino-5-benzyl-9,9-dimethyl-4,7-dioxo-3,8-dioxa-2,6-diazadec-1-en-1-yl]pyridin-3-yl}carbonyl)pyrrolidine-2-carboxylate (8c)

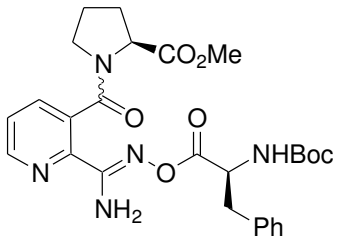

Purification by flash column chromatography (CH_2Cl_2/MeOH, 95:5) gave **8c** as a light-yellow solid (0.523 g, 97%); mp 84 – 87 °C;

IR ($CHCl_3$): ν_{max} = 3437, 3396, 1768, 1743, 1708, 1650, 1634 cm^{-1}.

^{1}H NMR (300 MHz, $CDCl_3$): δ = 8.58 – 8.56 (m, 1H, H_{Ar}), 7.78 and 7.65 (2×dd, *J* = 7.8, 1.4 Hz, 1H, H_{Ar}), 7.45 and 7.34 (dd, *J* = 7.7, 4.8 Hz, 1H, H_{Ar}), 7.40 – 7.11 (m, 5H, C_6H_5), 5.50 (d, *J* = 25.0 Hz, 2H, NH_2), 5.11 (d, *J* = 6.1 Hz, 1H,NHBoc), 4.80 and 4.29 (dd, *J* = 8.2, 3.8 Hz, 1H, CH-α of Pro), 4.73 – 4.47 (m, 1H, CH of Phe), 3.80 and 3.54 (2×s, 3H, OCH_3), 3.96 – 3.66 and 3.60 – 3.20 (2×m, 2H, CH_2-δ of Pro), 3.33 – 2.99 (m, 2H, CH_2 of Phe), 2.57 – 2.30 and 2.15 – 1.60 (m, 4H, CH2CH2-β,γ of Pro), 1.45 and 1.44 (2×s, 9H, $(CH_3)_3$).

^{13}C NMR (75 MHz, $CDCl_3$): δ = 174.0, 169.3, 169.2, 168.5, 168.1, 155.9, 154.7, 154.32, 149.3, 149.2, 143.9, 143.6, 137.3, 137.0, 136.8, 136.7, 133.5, 133.1, 130.1, 130.0, 129.4, 127.7, 125.9, 125.4, 80.8, 78.1, 77.7, 77.3, 61.5, 59.3, 54.6, 52.8, 52.7, 49.3, 48.8, 47.3, 39.5, 39.3, 31.5, 30.3, 29.0, 26.3, 25.6, 25.4, 23.8.

ESI calculated for $C_{27}H_{33}N_5NaO_7$ $[M+Na]^+$ *m/z* = 562.2275, found 562.2272.

Methyl (2*S*)-2-[({3-[(*Z*,5*S*)-1-amino-5-isopropyl-9,9-dimethyl-4,7-dioxo-3,8-dioxa-2,6-diazadec-1-en-1-yl]pyrazin-2-yl}carbonyl)amino]propanoate (8'a)

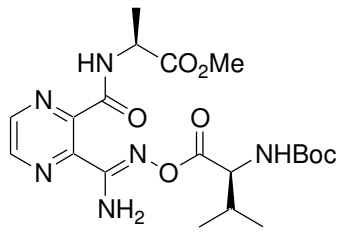

Purification by flash column chromatography (CH_2Cl_2/AcOEt, 3:7) gave **8'a** as a white solid (0.391 g, 84%); mp 91-94 °C.

IR: ν_{max} = 3424, 3311, 3193, 2970, 2934, 2878, 1738, 1681, 1644, 1514, 1366, 1172, 893, 670 cm^{-1}.

IR ($CHCl_3$): ν_{max} = 3436, 3410, 1764, 1743, 1711, 1688, 1645 cm^{-1}.

^{1}H NMR (300 MHz, $CDCl_3$): δ = 8.68 (s, 1H, H_{Ar}), 8.61 (s, 1H, H_{Ar}), 7.82 (d, J = 6.7 Hz, 1H, NH), 5.78 (br s, 2H, NH_2), 5.17 (d, J = 8.5 Hz, 1H, NH), 4.83 – 4.61 (m, 1H, CH), 4.36 – 4.15 (m, 1H, CH), 3.77 (s, 3H, OCH_3), 2.23 – 2.08 (m, 1H, CH), 1.53 (d, J = 6.9 Hz, 3H, CH_3), 1.43 (s, 9H, $(CH_3)_3$), 1.01 (3H, d, *J* 7.1 Hz, $(C\underline{H}_3)_2$), 0.97 (3H, d, *J* 7.0 Hz, $(C\underline{H}_3)_2$).

^{13}C NMR (75 MHz, $CDCl_3$): δ = 173.6, 170.2, 164.0, 156.4, 155.7, 147.0, 145.5, 144.9, 144.4, 80.6, 58.6, 53.2, 49.2, 31.9, 28.9, 19.7, 18.7, 18.5.

ESI calculated for $C_{20}H_{31}N_6O_7$ $[M+H]^+$ m/z = 467.2244, found 467.2249.

Methyl (2*S*)-2-[({3-[(*Z*,5*S*)-1-amino-5-isopropyl-9,9-dimethyl-4,7-dioxo-3,8-dioxa-2,6-diazadec-1-en-1-yl]pyrazin-2-yl}carbonyl)amino]-3-phenylpropanoate (8'b)

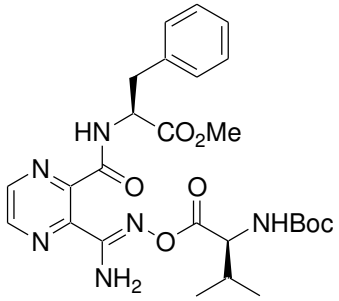

Purification by flash column chromatography (CH_2Cl_2/AcOEt, 3:7) gave **8'b** as a white solid (0.363 g, 67%); mp 86-89 °C.

IR: ν_{max} = 3326, 2969, 2877, 2856, 1738, 1688, 1681, 1643, 1514, 1367, 1171, 898, 670 cm^{-1}.

IR ($CHCl_3$): ν_{max} = 3438, 3408, 1766, 1745, 1712, 1686, 1645 cm^{-1}.

^{1}H NMR (300 MHz, $CDCl_3$): δ = 8.70 (d, J = 2.0 Hz, 1H, H_{Ar}), 8.61 (d, J = 2.0 Hz, 1H, H_{Ar}), 7.72 (d, J = 7.4 Hz, 1H, NH), 7.30 – 7.18 (m, 5H, 5×H_{Ar}), 5.70 (s, 2H, NH_2), 5.15 (d, J = 8.7 Hz, 1H, NH), 5.05 (m, 1H, CH), 4.38 – 4.25 (m, 1H, CH), 3.73 (s, 3H, OCH_3), 3.26 (d, J = 5.6 Hz, 2H, CH_2), 2.16 (m, 1H, CH), 1.45 (s, 9H, $(CH_3)_3$), 1.01 and 0.97 (2×d, J = 6.8 Hz, 6H, $(CH_3)_2$).

^{13}C NMR (75 MHz, $CDCl_3$): δ = 172.0, 170.1, 163.9, 156.4, 155.7, 146.9, 145.6, 145.0, 144.5, 136.4, 130.1, 129.2, 127.7, 80.7, 58.6, 54.5, 53.0, 38.5, 32.0, 29.0, 19.7, 18.5.

ESI calculated for $C_{26}H_{34}KN_6O_7$ $[M+K]^+$ m/z = 581.2117, found 581.2121.

Methyl (2*S*)-1-({3-[(*Z*,5*S*)-1-amino-5-benzyl-9,9-dimethyl-4,7-dioxo-3,8-dioxa-2,6-diazadec-1-en-1-yl]pyrazin-2-yl}carbonyl)pyrrolidine-2-carboxylate (8'c)

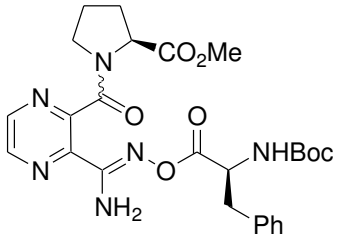

Purification by flash column chromatography (CH_2Cl_2/AcOEt, 3:7) gave **8'c** as a light-yellow solid (0.540 g, 100%); mp 96-98 °C.

IR: ν_{max} = 3444, 3330, 2977, 2935, 2878, 1742, 1711, 1644, 1498, 1455, 1365, 1163, 701 cm^{-1}.

IR ($CHCl_3$): ν_{max} = 3437, 3404, 1771, 1745, 1707, 1686, 1649 cm^{-1}.

^1H NMR (300 MHz, $CDCl_3$): δ = 8.67 (d, J = 2.3 Hz, 1H, H_{Ar}), 8.61 – 8.49 (m, 1H, H_{Ar}), 7.43 – 7.11 (m, 5H, 5×H_{Ar}), 5.58 (br s, 2H, NH_2), 5.15 (d, J = 7.8 Hz, 1H, NH), 4.84 – 4.72 and 4.30 – 4.27 (2×m, 1H, CH), 4.65 (m, 1H, CH), 3.79 and 3.62 (2×s, 3H, OCH_3), 3.46 (m, 2H, CH_2N), 3.11 (m, 2H, CH_2), 2.40, 2.02 and 1.82 – 1.52 (3×m, 4H, CH_2CH_2), 1.44 (m, 9H, $(CH_3)_3$).

^{13}C NMR (75 MHz, $CDCl_3$): δ = 173.4, 169.2, 166.3, 155.9, 153.1, 150.6, 145.6 (145.1), 143.4 (143.5), 141.1, 136.7 (136.9), 130.0, 129.4, 127.7, 80.8, 59.4 (61.4), 54.5, 52.9 (52.8), 48.7 (47.2), 39.2, 30.2 (31.5), 28.9, 25.4 (23.5).

ESI calculated for $C_{26}H_{32}KN_6O_7$ $[M+K]^+$ m/z = 579.1984, found 579.1964.

Synthesis of Compounds 9, 9' (a-c); General Procedure:

A 5 mL CEM microwave process vessel was charged with **8**, **8'** (**a-c**; 0.2 mmol) in CH_2Cl_2 (5 mL) and the vessel was capped. The mixture was stirred and heated under microwave conditions (300 W) at 150 °C for 25 min. The solution was then concentrated under vacuum and chromatographed on silica gel to give 1,2,4-oxadiazoles **9**, **9'** (**a-c**).

Methyl (2*S*)-2-({[2-(5-{(1*S*)-1-[(*tert*-butoxycarbonyl)amino]-2-methylpropyl}-1,2,4-oxadiazol-3-yl)pyridin-3-yl]carbonyl}amino)propanoate (9a)

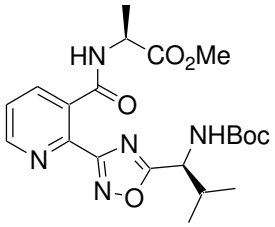

Purification by preparative HPLC (cyclohexane/AcOEt) gave **9a** as light-yellow oil (0.056 g, 63%).

IR ($CHCl_3$): ν_{max} = 3436, 3411, 1738, 1715, 1673 cm^{-1}.

^1H NMR (300 MHz, $CDCl_3$): δ = 8.84 (d, *J* = 3.8 Hz, 1H, H_{Ar}), 7.98 (d, *J* = 6.9 Hz, 1H, H_{Ar}), 7.49 (dd, *J* = 7.8, 4.8 Hz, 1H, H_{Ar}), 6.78 (d, *J* = 7.1 Hz, 1H, NH), 5.39 (d, *J* = 9.3 Hz, 1H, NHBoc), 5.03 (dd, *J* = 8.3, 6.2 Hz, 1H, C*H*CH$(CH_3)_2$), 4.76 (p, *J* = 7.1 Hz, 1H, C*H*CH_3), 3.77 (s, 3H, OCH_3), 2.34 – 2.21 (m, 1H, C*H*$(CH_3)_2$), 1.49 (d, *J* = 7.1 Hz, 3H, CH_3), 1.43 (s, 9H, $(CH_3)_3$), 0.97 (d, *J* = 6.7 Hz, 6H, $(CH_3)_2$).

^{13}C NMR (75 MHz, $CDCl_3$): δ = 180.4, 173.8, 167.7, 166.8, 155.8, 151.7, 143.6, 137.5, 133.9, 125.6, 81.0, 54.2, 53.3, 49.5, 33.7, 28.9, 19.4, 18.8, 18.5.

ESI calculated for $C_{21}H_{30}N_5O_6$ $[M+H]^+$ *m/z* = 448.2190, found 448.2191.

LC/MS: m/z = 470 $[M+Na]^+$.

Methyl (2*S*)-2-({[2-(5-{(1*S*)-1-[(*tert*-butoxycarbonyl)amino]-2-methylpropyl}-1,2,4-oxadiazol-3-yl)pyridin-3-yl]carbonyl}amino)-3-phenylpropanoate (9b)

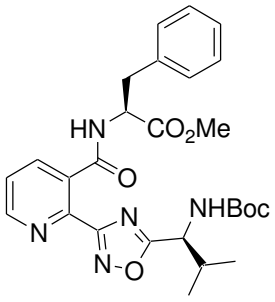

Purification by flash column chromatography (CH_2Cl_2/AcOEt, 6:4) gave **9b** as light-brown oil (0.085 g, 63%).

IR ($CHCl_3$): ν_{max} = 3438, 3413, 1741, 1714, 1674 cm^{-1}.

^1H NMR (300 MHz, $CDCl_3$): δ = 8.78 (dd, *J* = 4.5, 1.1 Hz, 1H, H_{Ar}), 7.81 (dd, *J* = 7.7, 1.1 Hz, 1H, H_{Ar}), 7.43 (dd, *J* = 7.8, 4.8 Hz, 1H, H_{Ar}), 7.29 – 7.09 (m, 5H, C_6H_5), 6.81 (d, *J* = 7.6 Hz, 1H, NH), 5.44 (d, *J* = 9.1 Hz, 1H, NHBoc), 4.98 - 5.07 (m, 2H, 2×CH), 3.72 (s, 3H, OCH_3), 3.31 – 3.13 (m, 2H, CH_2), 2.24 (dd, *J* = 12.6, 6.3 Hz, 1H, C*H*$(CH_3)_2$), 1.40 (s, 9H, $(CH_3)_3$), 0.95 (d, *J* = 6.7 Hz, 6H, $(CH_3)_2$).

^{13}C NMR (75 MHz, $CDCl_3$): δ = 180.2, 172.2, 167.5, 166.8, 155.8, 151.6, 143.7, 137.1, 136.3, 133.6, 129.9, 129.2, 127.7, 125.5, 80.8, 54.4, 54.0, 53.0, 38.3, 33.5, 28.8, 19.3, 18.4.

ESI calculated for $C_{27}H_{33}N_5NaO_6$ $[M+Na]^+$ *m/z* = 546.2323, found 546.2323.

LC/MS: m/z = 524 $[M+H]^+$.

Methyl (2*S*)-1-{[2-(5-{(1*S*)-1-[(*tert*-butoxycarbonyl)amino]-2-phenylethyl}-1,2,4-oxadiazol-3-yl)pyridin-3-yl]carbonyl}pyrrolidine-2-carboxylate (9c)

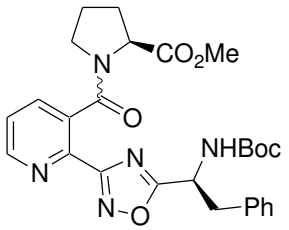

Purification by flash column chromatography (CH_2Cl_2/AcOEt, 1:1) gave **9c** as light-yellow oil (0.060 g, 58%).

IR ($CHCl_3$): ν_{max} = 3436, 3358, 1743, 1714, 1640 cm^{-1}.

^1H NMR (300 MHz, $CDCl_3$): δ = 8.88 – 8.77 (m, 1H, H_{Ar}), 7.84 and 7.75 (2×dd, *J* = 7.7, 1.1 Hz, 1H, H_{Ar}), 7.51 and 7.44 (2×dd, *J* = 7.8, 4.8 Hz, 1H, H_{Ar}), 7.31 – 7.04 (m, 5H, C_6H_5), 5.62 – 5.47 and 5.32 -5.22 (2×m, 1H, NH), 5.47 -5.32 (m, 1H, CH of Phe), 4.66 and 4.06 -3.95 (dd, m, *J* = 8.5, 4.4 Hz, 1H, CH-α of Pro), 3.79 and 3.53 (2×s, 3H, OCH_3), 3.39 – 3.75, 3.37 -3.13

(2×m, 2H, CH_2-δ of Pro), 3.37 – 3.05 (m, 2H, CH_2 of Phe), 2.36 – 1.79 (m, 4H, CH2CH2-β,γ of Pro), 1.39 (s, 9H, $(CH_3)_3$).

^{13}C NMR (75 MHz, $CDCl_3$): δ = 180.4, 173.0, 167.7, 167.3, 155.4, 151.2, 142.2, 141.8, 137.0, 136.6, 135.9, 135.5, 134.2, 134.1, 129.9, 129.4, 129.3, 128.0, 127.8, 126.0, 125.6, 81.1, 81.0, 61.4, 59.3, 53.0, 52.9, 50.1, 49.3, 47.2, 40.8, 40.7, 31.6, 30.3, 30.2, 28.8, 25.4, 23.5.

ESI calculated for $C_{27}H_{31}N_5NaO_6$ $[M+Na]^+$ *m/z* = 544.2186, found 544.2167.

LC/MS: m/z = 544 $[M+Na]^+$.

Methyl (2*S*)-2-({[3-(5-{(1*S*)-1-[(tert-butoxycarbonyl)amino]-2-methylpropyl}-1,2,4-oxadiazol-3-yl)pyrazin-2-yl]carbonyl}amino)propanoate (9'a)

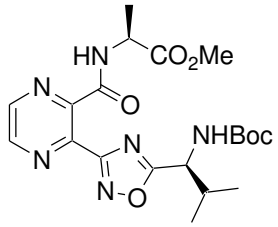

Purification by flash column chromatography (CH_2Cl_2/AcOEt, 4:6) gave **9'a** as a colorless oil (0.068 g, 75%).

IR: ν_{max} = 3424, 3311, 3193, 2970, 2934, 2878, 1738, 1681, 1644, 1514, 1366, 1172, 893, 670 cm^{-1}.

IR ($CHCl_3$): ν_{max} = 3442, 3397, 1740, 1716, 1688 cm^{-1}.

^{1}H NMR (300 MHz, $CDCl_3$): δ = 8.79 (s, 1H, H_{Ar}), 8.66 (s, 1H, H_{Ar}), 8.05 (d, *J* = 7.3 Hz, 1H, NH), 5.20 (d, *J* = 9.0 Hz, 1H, NH), 5.10 – 4.90 (m, 1H, CH), 4.64 (*pseudo-p, J* = 7.3 Hz, 1H, CH), 3.71 (s, 3H, OCH_3), 2.32 – 2.15 (m, 1H, CH), 1.44 (d, *J* = 7.1 Hz, 3H, CH_3), 1.38 (s, 9H, $(CH_3)_3$), 0.96 (d, *J* = 6.8 Hz, 6H, $(CH_3)_2$).

^{13}C NMR (75 MHz, $CDCl_3$): δ = 179.7, 173.5, 167.1, 162.4, 155.8, 146.6, 145.8, 144.5, 143.3, 81.0, 54.2, 53.3, 48.9, 33.8, 28.9, 19.2, 19.1, 18.5.

ESI calculated for $C_{20}H_{28}KN_6O_6$ $[M+K]^+$ *m/z* = 487.1705, found 487.1702. LC/MS: m/z = 471 $[M+Na]^+$.

Methyl (2*S*)-2-({[3-(5-{(1*S*)-1-[(tert-butoxycarbonyl)amino]-2-methylpropyl}-1,2,4-oxadiazol-3-yl)pyrazin-2-yl]carbonyl}amino)-3-phenylpropanoate (9'b)

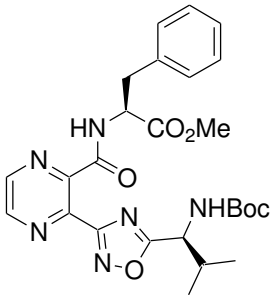

Purification by flash column chromatography (CH_2Cl_2/AcOEt, 4:6) gave **9'b** as a colorless oil (0.100 g, 95%).

IR: ν_{max} = 3424, 3311, 3193, 2970, 2934, 2878, 1738, 1681, 1644, 1514, 1366, 1172, 893, 670 cm^{-1}.

IR ($CHCl_3$): ν_{max} = 3442, 3395, 1742, 1715, 1689 cm^{-1}.

^1H NMR (300 MHz, $CDCl_3$): δ = 8.77 (s, 1H, H_{Ar}), 8.60 (s, 1H, H_{Ar}), 7.95 (d, *J* = 7.4 Hz, 1H, NH), 7.23 – 7.03 (m, 5H, 5×H_{Ar}), 5.19 (d, *J* = 9.2 Hz, 1H, NH), 5.02 (m, 1H, CH), 4.90 (m, 1H, CH), 3.65 (s, 3H, OCH_3), 3.15 (d, *J* = 5.3 Hz, 2H, CH_2), 2.32 – 2.15 (m, 1H, CH), 1.37 (s, 9H, $(CH_3)_3$), 0.95 (d, *J* = 6.3 Hz, 6H, $(CH_3)_2$).

^{13}C NMR (75 MHz, $CDCl_3$): δ = 179.7, 172.0, 167.1, 162.5, 155.8, 146.6, 145.8, 144.5, 143.3, 136.3, 130.0, 129.3, 127.8, 80.9, 54.2, 53.1, 38.5, 33.8, 28.9, 19.2, 18.4.

ESI calculated for $C_{26}H_{32}N_6NaO_6$ $[M+Na]^+$ *m/z* = 547.2278, found 547.2276. LC/MS: m/z = 547 $[M+Na]^+$.

Methyl (2*S*)-1-{[3-(5-{(1*S*)-1-[(tert-butoxycarbonyl)amino]-2-phenylethyl}-1,2,4-oxadiazol-3-yl)pyrazin-2-yl]carbonyl}pyrrolidine-2-carboxylate (9'c)

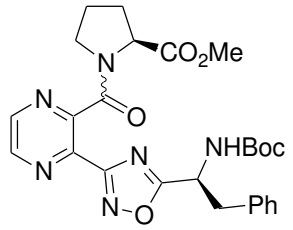

Purification by flash column chromatography (CH_2Cl_2/AcOEt, 4:6) gave **9'c** as a light-yellow oil (0.079 g, 76%).

IR: ν_{max} = 3424, 3311, 3193, 2970, 2934, 2878, 1738, 1681, 1644, 1514, 1366, 1172, 893, 670 cm^{-1}.

IR ($CHCl_3$): ν_{max} = 3438, 3362, 1746, 1714, 1650, 1615 cm^{-1}

^{1}H NMR (300 MHz, $CDCl_3$): δ = 8.72 (d, *J* = 2.2 Hz, 1H, H_{Ar}), 8.65 and 8.56 (2×d, *J* = 2.2 Hz, *J* = 2.3 Hz, 1H, H_{Ar}), 7.26 – 6.97 (m, 5H, 5×H_{Ar}), 5.62 and 5.17 (2×d, *J* = 8.1 Hz, 1H, NH), 5.35 – 5.37 (m, 1H, CH), 4.60 and 4.26 (2×dd, *J* = 8.5, 4.0 Hz, 1H, CH), 3.71 and 3.50 (2×s, 3H, OCH_3), 3.40 – 3.05 (2×m, 4H, 2×CH_2), 2.34 – 1.79 (m, 4H, CH_2CH_2), 1.24 (m, 9H, $(CH_3)_3$).

^{13}C NMR (75 MHz, $CDCl_3$): δ = 180.8 (180.6), 172.8 (172.7), 166.4, 165.4, 155.4, 150.8, 145.7, 145.3 (145.1), 139.9, 135.9 (135.5), 130.0, 129.4, 127.9, 81.0, 59.5 (61.2), 53.1 (52.9), 49.9, 48.8 (47.4), 40.9, 30.1 (31.7), 28.9, 25.5 (23.3).

ESI calculated for $C_{26}H_{30}KN_6O_6$ $[M+K]^+$ *m/z* = 561.1864, found 561.1858. LC/MS: m/z = 545 $[M+Na]^+$.

Boc-(*S*)Phe-OMe

To a solution of H-Phe-OMe hydrochloride (3.23 g, 15 mmol) in saturated aqueous $NaHCO_3$ (150 mL), Di-*tert*-butyl dicarbonate (3.43 g, 15.75 mmol) was added. The reaction mixture was stirred for two days. The organic phase was extracted with EtOAc (3×50 mL) and washed with HCl 10% (2×50 mL), $NaHCO_3$ 10% (50 mL) and finally with brine (50 mL). The

resulting solution was dried with $MgSO_4$ and concentrated under vacuum. The colorless solid was obtained in quantitative yield (4.2 g); mp 46 °C.

^{1}H NMR (300 MHz, $CDCl_3$): δ = 7.27 – 7.00 (m, 5H, H_{Ph}), 4.90 (d, *J* = 6.3 Hz, 1H, NH), 4.58 -4.42 (m, 1H, CH), 3.64 (s, 3H, OCH_3), 3.11 – 2.90 (m, 2H, CH_2), 1.34 (s, 9H, $(CH_3)_3$).

^{13}C NMR (75 MHz, $CDCl_3$): δ = 174.6, 156.1, 137.3, 130.0, 129.5, 127.7, 80.7, 55.4, 52.9, 36.8, 29.0.

Boc-(*S*)Phe-NHNH$_2$

To a solution of Boc-Phe-OMe (4.03 g, 14.4 mmol) in MeOH (50 mL), hydrazine monohydrate (2.79 mL, 57.6 mmol) was added. The resulting solution was vigorously stirred until completion (monitored by TLC) and co-evaporated several times with CH_2Cl_2 at reduced pressure until complete elimination of the hydrazine monohydrate. The colorless solid was obtained in quantitative yield (4.0 g); mp 128 °C.

^{1}H NMR (300 MHz, $CDCl_3$): δ = 7.52 (s, 1H, N*H*NH_2), 7.32 – 7.16 (m, 5H, H_{Ph}), 5.19 (d, 1H, *J* = 8.1 Hz, NHBoc), 4.32 (dd, 1H, *J* = 15.0, 7.3 Hz, CH), 3.65 (br, 2H, NH_2), 3.10 – 2.97 (m, 2H, CH_2), 1.34 (s, 9H, $(CH_3)_3$).

^{13}C NMR (75 MHz, $CDCl_3$): δ = 172.6, 156.8, 137.1, 129.9, 129.4, 127.8, 81.2, 55.4, 39.2, 29.0.

Synthesis of Compounds 10, **10'** (**a**,**b**)**; General Procedure:**

Methanolic (25 mL) suspension of the methyl ester of a (2*S*)-2-(imino-oxo-dihydro-6*H*-pyrrolo[3,4-*b*] (hetero)aryl)alkanoic acid **6**, **6'** (**a**,**b**; 1 mmol) and Boc-(*S*)Phe-NHNH$_2$ (1.1 mmol) was stirred overnight at r.t. Then, the precipitate was filtered off, washed with cold methanol (10 mL) and dried *in vacuo*.

Methyl (2*S*)-2-[({2-[amino((*Z*)-2-{(2*S*)-2-[(*tert*-butoxycarbonyl)amino]-3-phenylpropanoyl}hydrazono)methyl]pyridin-3-yl}carbonyl)amino]propanoate (10a)

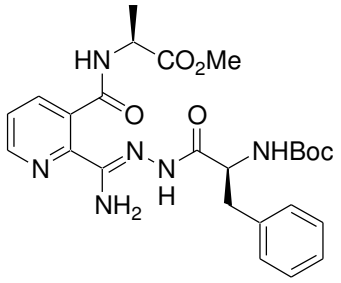

White solid; yield: 0.420 g (82%); mp 188-189 °C.

IR: ν_{max} = 3435, 3318, 3062, 3027, 2982, 1738, 1688, 1660, 1634, 1590, 1526, 1455, 1390, 1294, 645 cm^{-1}.

^{1}H NMR (300 MHz, DMSO): δ = 9.86 and 9.75 (2×s, 1H, NH-N=), 8.77 and 8.54 (2×d, *J* = 6.0, 7.0 Hz, 1H, NH), 8.68 – 8.59 (m, 1H, H_{Ar}), 7.87 and 7.78 (dd, *J* = 7.7, 1.5 Hz, 1H, H_{Ar}), 7.57 and 7.54 (2×dd, *J* = 7.8, 4.9 Hz, 1H, H_{Ar}), 7.33 - 7.08 (m, 5H, 5×H_{Ar}), 7.01 and 6.21 (2×d, *J* = 8.4 Hz, 1H, NHBoc), 6.58 and 6.53 (2×s, 2H, NH_2), 4.90 – 4.78 and 4.30 – 4.19 (2×m, 1H, C<u>H</u>NHBoc), 4.69 – 4.59 and 4.59 – 4.48 (2×m, 1H, C<u>H</u>CH_3), 3.63 and 3.60 (2×s, 3H, OCH_3), 2.99 – 2.70 (m, 2H, CH_2), 1.38 – 1.17 (m, 12H, $(CH_3)_3$ and CH_3).

^{13}C NMR (75 MHz, DMSO): δ = 173.4 (172.0), 167.6, 167.3, 167.1, 155.3 (154.8), 148.5 (148.7), 148.5 (149.5), 147.3 (144.1), 138.1 (137.8), 136.8 (136.6), 132.0, 129.2 (129.5), 128.0 (127.8), 126.2 (126.0), 123.8 (123.7), 77.9 (77.8), 54.9 (52.3), 51.7 (51.8), 48.3 (47.9), 37.8 (36.2), 28.1, 16.7 (16.7).

Methyl (2*S*)-2-[({2-[amino((*Z*)-2-{(2*S*)-2-[(*tert*-butoxycarbonyl)amino]-3-phenylpropanoyl}hydrazono)methyl]pyridin-3-yl}carbonyl)amino]-3-phenylpropanoate (10b)

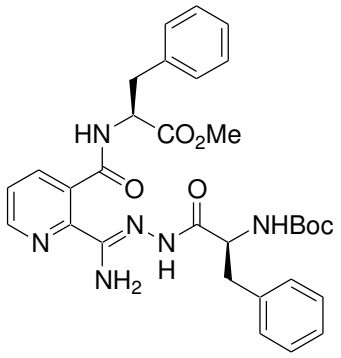

White solid; yield: 0.570 g (97%); mp 183-185 °C.

IR: ν_{max} = 3449, 3320, 3063, 3024, 2971, 2930, 1737, 1690, 1662, 1631, 1563, 1524, 1454, 1392, 1267, 1250, 1201, 699, 651 cm^{-1}.

^{1}H NMR (300 MHz, DMSO): δ = 9.91 and 9.87 (2×s, 1H, NH-N=), 9.03 (d, *J* = 6.6 Hz, 1H, NH), 8.67 – 8.58 (m, 1H, H_{Ar}), 7.74 and 7.66 (2×d, *J* = 6.6, 7.5 Hz, 1H, H_{Ar}), 7.56 – 7.46 (m, 1H, H_{Ar}), 7.33 – 7.08 (m, 10H, 10×H_{Ar}), 7.00 and 6.11 (2×d, *J* = 8.5 Hz, 1H, NHBoc), 6.62 and 6.55 (2×s, 2H, NH_2), 4.85 – 4.68 (m, 1H, CH), 4.79 – 4.68 and 4.32 – 4.28 (2,×m, 1H, CH), 3.52 and 3.45 (2×s, 3H, OCH_3), 3.20 – 2.71 (m, 4H, 2×CH_2), 1.30 and 1.27 (2×s, 9H, $(CH_3)_3$).

^{13}C NMR (75 MHz, DMSO): δ = 171.9 (171.8), 167.5, 167.3, 167.0, 155.2 (154.7), 149.1, 148.7, 148.0, 144.3, 138.1 (137.8), 137.4 (136.9), 137.1 (136.6), 131.7, 129.6, 129.2, 128.1, 128.0, 127.7, 126.4, 126.2, 126.2, 125.9, 123.8 (123.7), 77.9 (77.7), 54.5 (54.7), 53.8 (52.4), 51.4, 37.9 (37.1), 36.7 (36.1), 28.0.

Methyl (2*S*)-2-[({3-[amino((*Z*)-2-{(2*S*)-2-[(*tert*-butoxycarbonyl)amino]-3-phenylpropanoyl}hydrazono)methyl]pyrazin-2-yl}carbonyl)amino]propanoate (10'a)

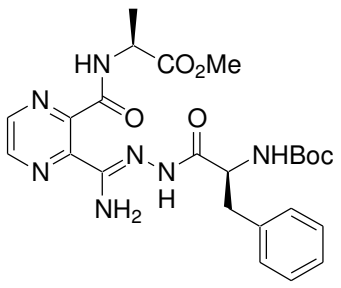

White solid; yield: 0.257 g (50%); mp 191-192 °C.

IR: ν_{max} = 3440, 3319, 3066, 2982, 2931, 1737, 1687, 1666, 1635, 1596, 1543, 1525, 1453, 1295, 1165, 648 cm^{-1}.

^1H NMR (300 MHz, DMSO): δ = 9.91 and 9.80 (2×s, 1H, NH-N=), 8.86 – 8.65 (m, 3H, H_{Ar} and NH), 7.35 – 7.08 (m, 5H, 5×H_{Ar}), 7.03 and 6.38 (2×d, *J* = 8.0 Hz, 1H, NHBoc), 6.61 (s, 2H, NH_2), 4.88 – 4.75 and 4.32 – 4.16 (2×m, 1H, C<u>H</u>NHBoc), 4.68 – 4.52 (m, 1H, C<u>H</u>CH_3), 3.64 and 3.57 (2×s, 3H, OCH_3), 2.99 – 2.61 (m, 2H, CH_2), 1.39 – 1.20 (m, 12H, $(CH_3)_3$ and CH_3).

^{13}C NMR (75 MHz, DMSO): δ = 173.2, 172.9, 172.3, 167.3, 165.4, 164.9, 155.3 (154.9), 148.3, 147.3, 146.6, 145.6, 145.0, 143.2 (143.8), 143.8 (143.0), 138.1, 129.2 (129.4), 128.0 (127.8), 126.2 (125.9), 77.9 (77.7), 54.8 (52.5), 51.7, 48.1 (47.7), 37.8 (36.2), 28.1, 16.9.

Methyl (2*S*)-2-[({3-[amino((*Z*)-2-{(2*S*)-2-[(*tert*-butoxycarbonyl)amino]-3-phenylpropanoyl}hydrazono)methyl]pyrazin-2-yl}carbonyl)amino]-3-phenylpropanoate (10'b)

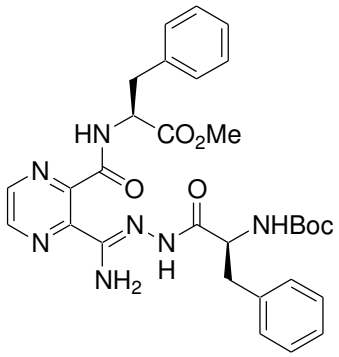

White solid; yield: 0.483 g (82%); mp 171-174 °C.

IR: ν_{max} = 3488, 3432, 3320, 3062, 3028, 2980, 1747, 1687, 1664, 1634, 1601, 1538, 1519, 1449, 1385, 1163, 698 cm^{-1}.

^1H NMR (300 MHz, DMSO): δ = 9.93 and 9.32 (2×s, 1H, NH-N=), 8.83 – 8.71 (m, 2H, H_{Ar} and 0.4H, NH), 8.69 (d, *J* = 2.3 Hz, 0.6H, NH), 7.34 – 7.08 (m, 10H, 10×H_{Ar}), 7.02 and 6.32 (d, *J* = 8.4 Hz, 1H, NHBoc), 6.63 (s, 2H, NH_2), 4.79 (dd, *J* = 13.2, 6.3 Hz, 1H, CH), 4.82 – 4.74 and 4.35 – 4.22 (2×m, 1H, C<u>H</u>NHBoc), 3.52 and 3.44 (2×s, 3H, OCH_3), 3.25 – 2.63 (m, 4H, 2×CH_2), 1.28 and 1.26 (2×s, 9H, $(CH_3)_3$).

^{13}C NMR (75 MHz, DMSO): δ = 172.1, 171.7, 171.3, 167.3, 165.3, 164.6, 155.3 (154.9), 147.7, 146.5, 146.1, 145.3, 144.1, 143.6, 143.5, 143.1, 138.1 (138.2), 137.1 (136.6), 129.4, 129.2, 128.1, 128.0, 127.7, 126.5, 126.3, 126.2, 125.9, 77.9 (77.7), 54.3 (54.7), 53.6 (52.6), 51.45 (51.6), 37.9, 36.8, 36.1, 28.0.

Synthesis of Compounds 11'a,b; General Procedure:

A 5 mL CEM microwave process vessel was charged with **10'a**,**b** (0.2 mmol) in CH_3CN (5 mL) with addition of cat.HOAc (2%) and the vessel was capped. The mixture was stirred and heated under microwave conditions (150 W) at 110 °C for 20 min. The solution was then concentrated under vacuum and purified by NP-HPLC with a gradient of MeOH (1-5% v/v) in $CHCl_3$ to yield 1,2,4-triazoles **11'a**,**b**.

Methyl (2*S*)-2-({[3-(5-{(1*S*)-1-[(*tert*-butoxycarbonyl)amino]-2-phenylethyl}-1*H*-1,2,4-triazol-3-yl)pyrazin-2-yl]carbonyl}amino)propanoate (11'a)

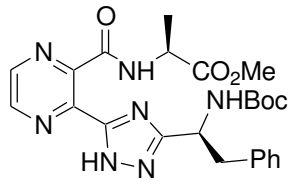

Light-yellow solid; yield: 0.084 g (85%); mp 177-180 °C.

^{1}H NMR (300 MHz, $CDCl_3$): δ = 9.04 (s, 1H, H_{Ar}), 8.76 (d, *J* = 6.3 Hz, 1H, NH_{amide}), 8.69 (s, 1H, H_{Ar}), 7.25 – 7.09 (m, 5H, 5×H_{Ar}), 5.66 (d, *J* = 6.4 Hz, 1H, NHBoc), 5.42 – 5.27 (m, 1H, C<u>H</u>NHBoc), 4.79 (*pseudo*-p, *J* = 7.2 Hz, 1H, C<u>H</u>CH_3), 3.82 (s, 3H, OCH_3), 3.45 – 3.23 (m, 2H,), 1.59 (d, *J* = 7.1 Hz, 3H, CH_3), 1.37 (s, 9H, $(CH_3)_3$).

^{13}C NMR (75 MHz, $CDCl_3$): δ = 173.20, 164.67, 164.44, 155.91, 152.90, 147.87, 143.22, 142.55, 141.52, 137.61, 130.26, 128.95, 127.20, 80.24, 53.50, 50.78, 49.59, 41.66, 28.98, 18.74.

LC/MS: m/z = 496 $[M+H]^+$.

Methyl (2*S*)-2-({[3-(5-{(1*S*)-1-[(*tert*-butoxycarbonyl)amino]-2-phenylethyl}-1*H*-1,2,4-triazol-3-yl)pyrazin-2-yl]carbonyl}amino)-3-phenylpropanoate (11'b)

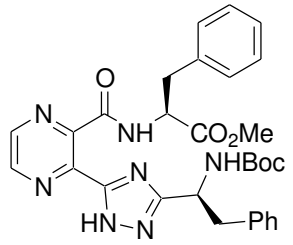

Yellow solid; yield: 0.099 g (87%); mp 152-154 °C.

^{1}H NMR (300 MHz, $CDCl_3$): δ = 8.96 (d, *J* = 1.4 Hz, 1H, H_{Ar}), 8.71 – 8.49 (m, 2H, NH_{amide} and H_{Ar}), 7.33 – 7.04 (m, 10H, 10×H_{Ar}), 5.49 (d, *J* = 8.5 Hz, 1H, NHBoc), 5.40 – 5.19 (m, 1H, C<u>H</u>NHBoc), 5.06 (dd, *J* = 13.9, 6.2 Hz, 1H, C<u>H</u>COOCH$_3$), 3.77 (s, 3H, OCH_3), 3.41 – 3.14 (m, 4H, 2×CH_2), 1.37 (s, 9H, $(CH_3)_3$).

^{13}C NMR (75 MHz, $CDCl_3$): δ = 171.79, 164.82, 155.80, 153.55, 147.54, 142.89, 142.66, 142.21, 137.71, 136.05, 130.19, 129.83, 129.30, 128.82, 127.96, 127.05, 80.04, 54.69, 53.22, 50.79, 41.71, 38.54, 28.91.

LC/MS: m/z = 572 $[M+H]^+$.

Synthesis of Compounds 12, 12' (a,b); General Procedure:

The corresponding amidoxime **7**, **7'** (**a**,**b**; 0.8 mmol, 1 eq.) was added to triphosgene (0.4 mmol, 0.5 eq.) in CH_2Cl_2 (10 mL) at 0 °C and the mixture was warmed to r.t. and stirred for 2.5 h. To the above mixture a solution of Boc-(*S*)Phe-$NHNH_2$ (1.08 mmol, 1.5 eq.) and DIEA (2.16 mmol, 3 eq.) in CH_2Cl_2 (10 mL) at 0 °C was added. The reaction was allowed to warm to r.t. and stirred overnight. The reaction mixture was washed with water (2×15 mL), brine (20 mL) and concentrated to give a crude which was purified by preparative NP-HPLC, using $CHCl_3$ and MeOH as eluents.

Methyl (2*R*)-2-[({2-[(*Z*,8*R*)-1-amino-8-benzyl-12,12-dimethyl-4,7,10-trioxo-3,11-dioxa-2,5,6,9-tetraazatridec-1-en-1-yl]pyridin-3-yl}carbonyl)amino]propanoate (12a)

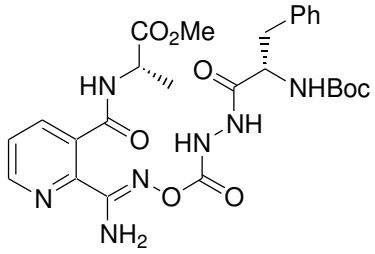

Purification by preparative NP-HPLC ($CHCl_3$/MeOH, 95:5) gave **12a** as a white solid (0.183 g, 44%); mp 71-74 °C.

^{1}H NMR (300 MHz, $CDCl_3$): δ = 8.72 – 8.63 (m, 1H, H_{Ar}), 8.36 (s, 1H, NH-NH), 8.05 (s, 1H, NH-NH), 7.90 (d, *J* = 6.3 Hz, 1H, H_{Ar}), 7.56 – 7.45 (m, 1H, H_{Ar}), 7.33 – 7.15 (m, 5H, 5×H_{Ar}), 6.82 (br s, 1H, NH), 6.09 (s, 2H, NH_2), 5.14 (d, *J* = 5.8 Hz, 1H, NHBoc), 4.87 – 4.71 (m, 1H, $CHCH_3$), 4.54 – 4.39 (m, 1H, CHNHBoc), 3.77 (s, 3H, OCH_3), 3.11 (ddd, *J* = 39.5, 13.7, 6.7 Hz, 2H, CH_2), 1.51 (d, *J* = 7.0 Hz, 3H, CH_3), 1.39 (s, 9H, $(CH_3)_3$).

^{13}C NMR (75 MHz, $CDCl_3$): δ = 174.0, 171.5, 168.7, 155.6, 152.0, 149.8, 144.1, 137.9, 137.1, 132.7, 130.2, 129.4, 127.6, 126.0, 81.1, 54.9, 53.4, 49.5, 38.7, 29.0, 18.7.

Methyl (2*R*)-2-[({2-[(*Z*,8*R*)-1-amino-8-benzyl-12,12-dimethyl-4,7,10-trioxo-3,11-dioxa-2,5,6,9-tetraazatridec-1-en-1-yl]pyridin-3-yl}carbonyl)amino]-3-phenylpropanoate (12b)

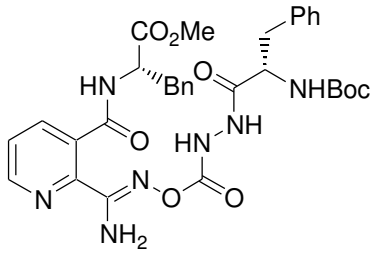

Purification by preparative NP-HPLC ($CHCl_3$/MeOH, 95:5) gave **12b** as a white solid (0.311 g, 60%); mp 102-105 °C.

^{1}H NMR (300 MHz, $CDCl_3$): δ = 8.68 – 8.58 (d, *J* = 3.5 Hz, 1H, H_{Ar}), 8.32 (s, 1H, NH-NH), 7.92 (s, 1H, NH-NH), 7.64 (d, *J* = 6.6 Hz, 1H, H_{Ar}) 7.45 – 7.37 (m, 1H, H_{Ar}), 7.35 – 7.08 (m, 10H, 10×H_{Ar}), 6.34 (br s, 1H, NH), 6.00 (s, 2H, NH_2), 5.28 – 5.00 (m, 2H, NHBoc and CH),

4.48 (d, *J* = 6.9 Hz, 1H, CH), 3.76 (s, 3H, OCH_3), 3.40 – 2.99 (m, 4H, 2×CH_2), 1.40 (s, 9H, $(CH_3)_3$).

^{13}C NMR (75 MHz, $CDCl_3$): δ = 172.6, 172.2, 171.3, 169.0, 156.2, 155.7, 150.1, 144.2, 137.2, 137.1, 136.4, 132.4, 130.1, 129.3, 127.9, 127.7, 125.7, 81.1, 54.8, 54.2, 53.3, 38.8, 38.2, 29.0.

Methyl (2*R*)-2-[({3-[(*Z*,8*R*)-1-amino-8-benzyl-12,12-dimethyl-4,7,10-trioxo-3,11-dioxa-2,5,6,9-tetraazatridec-1-en-1-yl]pyrazin-2-yl}carbonyl)amino]propanoate (12'a)

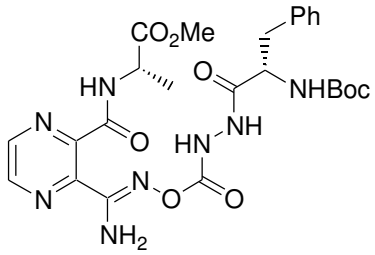

Purification by preparative NP-HPLC ($CHCl_3$/MeOH, 95:5) gave **12'a** as a white solid (0.201 g, 44%); mp 96-98 °C.

^{1}H NMR (300 MHz, $CDCl_3$): δ = 8.68 (d, *J* = 12.6 Hz, 2H, H_{Ar}), 8.32 (s, 1H, NH-NH), 8.14 (s, 1H, NH-NH), 7.53 (d, *J* = 5.5 Hz, 1H, NH), 7.36 – 7.16 (m, 5H, 5×H_{Ar}), 5.94 (s, 2H), 5.12 (d, *J* = 9.4 Hz, 1H, NHBoc), 4.86 – 4.69 (m, 1H, $CHCH_3$), 4.52 – 4.41 (m, 1H, CHNHBoc), 3.77 (s, 3H, OCH_3), 3.10 (ddd, *J* = 19.7, 14.0, 6.7 Hz, 4H, 2×CH_2), 1.54 (d, *J* = 7.3 Hz, 3H, CH_3), 1.38 (s, 9H, $(CH_3)_3$).

^{13}C NMR (75 MHz, $CDCl_3$): δ = 173.7, 171.3, 165.3, 155.5, 153.0, 147.3, 145.2, 144.7, 143.3, 137.0, 130.2, 129.4, 127.6, 81.2, 54.9, 53.4, 49.3, 38.7, 28.9, 18.9.

Methyl (2*R*)-2-[({3-[(*Z*,8*R*)-1-amino-8-benzyl-12,12-dimethyl-4,7,10-trioxo-3,11-dioxa-2,5,6,9-tetraazatridec-1-en-1-yl]pyrazin-2-yl}carbonyl)amino]-3-phenylpropanoate (12'b)

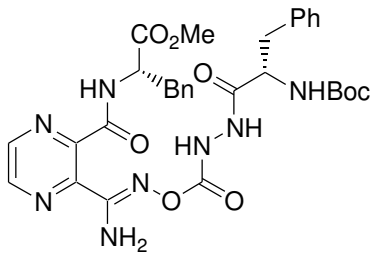

Purification by preparative NP-HPLC ($CHCl_3$/MeOH, 95:5) gave **12'b** as a colorless solid (0.358 g, 69%); mp 107-110 °C.

^{1}H NMR (300 MHz, $CDCl_3$): δ = 8.65 (d, 1.8 Hz, 2H, H_{Ar}), 8.60 (d, 1.8 Hz, 2H, H_{Ar}), 8.33, 8.28 (2×s, 2H, NH-NH), 7.45 (d, *J* = 7.8 Hz, 1H, NH), 7.33 – 7.10 (m, 10H, 10×H_{Ar}), 5.97 (s, 2H, NH_2), 5.20 (d, *J* = 7.5 Hz, 1H, NHBoc), 5.10 (dd, *J* = 13.1, 5.6 Hz, 1H, CH), 4.48 (m, 1H, CHNHBoc), 3.71 (s, 3H, OCH_3), 3.31 – 3.20 (m, 2H, CH_2), 3.08 (ddd, *J* = 21.3, 13.9, 6.8 Hz, 2H, CH_2CHNHBoc), 1.37 (s, 9H, $(CH_3)_3$).

^{13}C NMR (75 MHz, $CDCl_3$): δ = 172.2, 171.4, 165.4, 156.2, 155.6, 153.2, 147.1, 145.2, 144.7, 143.3, 137.1, 136.3, 130.2, 129.3, 127.8, 127.5, 81.2, 54.8, 54.3, 53.2, 38.8, 38.4, 28.9.

X-Ray Diffraction Study of Compounds 6d and 7b

Intensities of reflections were measured on an automatic «Xcalibur 3» diffractometer (graphite monochromated $Mo_{K\alpha}$ radiation, CCD-detector ω scanning). All structures were solved by direct method using SHELX97 package.[151] Positions of the hydrogen atoms were located from electron density difference maps and refined by "riding" model with Uiso = nUeq of carrier non-hydrogen atom (n = 1.5 for methyl group and n = 1.2 for other hydrogen atoms). Full-matrix least-squares refinement against F^2 was performed for non-hydrogen atoms within anisotropic approximation. Final atomic coordinates, geometrical parameters and crystallographic data have been deposited with the Cambridge Crystallographic Data Centre, 12 Union Road, Cambridge, CB2 1EZ, UK (fax: +44 1223 336033; e-mail: deposit@ccdc.cam.ac.uk). CCDC dep. numbers for structures **6d** and **7b** are 991411 and 991412 respectively. These data can be obtained free of charge from the Cambridge Crystallographic Data Centre *via* www.ccdc.cam.ac.uk/products/csd/request/.

Crystal data for **6d** at 293K: ($C_{10}H_9N_3O_3$, M = 219.20), ***a*** = 5.0866(4) Å, ***b*** = 9.0455(7) Å, ***c*** = 21.7603(13) Å, ***β*** = 92.030(7)°, *V* = 1000.58(13) Å^3, space group $P2_1/n$, Z = 4, D_c = 1.455

g/sm^{-3}, μ(MoKα) = 0.111 mm^{-1}, F(000) = 456. 10110 reflections measured up to $2\theta_{max}$= 64.4°, 3209 unique (R_{int} = 0.0218) which were used in all calculations. Refinement was converged at wR_2=0.1334 (all data), R_1=0.0473 (2332 reflections with I>2σ(I)), GoF=1.03.

Crystal data for **7b** at 293K: ($C_{17}H_{18}N_4O_4$, M = 342.35), ***a*** = 8.5563(3) Å, ***b*** = 10.2899(3) Å, ***c*** = 10.1182(3) Å, ***β*** = 104.315(3)°, V = 863.19(5) Å^3, space group $P2_1$, Z = 2, D_c = 1.317 g/sm^{-3}, μ(MoKα) = 0.096 mm^{-1}, F(000) = 360. 9410 reflections measured up to $2\theta_{max}$= 64.3°, 4673 unique (R_{int} = 0.0129) which were used in all calculations. Refinement was converged at wR_2=0.0957 (all data), R_1=0.0354 (4279 reflections with I>2σ(I)), GoF=1.02.

X-ray Diffraction Study of 7'b

The structure was solved by direct method using OLEX2 software. Visualization and analysis of crystal structure was done in Mercury 3.8.[152] Positions of the hydrogen atoms were located from electron density difference maps and refined by "riding" model with Uiso = nUeq of the carrier atom (n = 1.5 for methyl and OH groups, n = 1.2 for other hydrogen atoms). Full-matrix least-squares refinement of the structure against F^2 in anisotropic approximation for non-hydrogen atoms was converged to wR_2 = 0.104 (R_1 = 0.0390 for 3341 reflections with I>2σ(I), S = 1.033). The final atomic coordinates and crystallographic data have been deposited with the Cambridge Crystallographic Data Centre, 12 Union Road, Cambridge, CB2 1EZ, UK (fax: +44 1223 336033; e-mail: deposit@ccdc.cam.ac.uk) and are available on request quoting the deposition number CCDC 1475179 for **7'b**.

Compound **7'b** ($C_{16}H_{17}N_5O_4$): monoclinic crystals; at 110 K, ***a*** = 8.6226(2) Å, ***b*** = 10.4629(2) Å, ***c*** = 9.5228(2) Å, ***β*** = 105.842(2)°, V = 826.49(3) Å3, M_r = 343.34, Z = 2, space group $P2_1$, D_c = 1.3795 g/sm-3, μ(CuKα) = 0.854 mm-1, F(000) = 361.274. Intensities of 15088 reflections (3341 independent, R_{int} = 0.0340) were measured on a SuperNova Agilent diffractometer equipped with a copper microsource (Cu Kα radiation with mirror optics, Atlas CCD detector, ω-scanning, 2θmax= 76.43°). The frames were integrated with the Agilent CrysAlisPro software package.

X-ray Diffraction Study of (7*Z*)-7-(hydroxyimino)-6,7-dihydro-5H-pyrrolo[3,4-b]pyrazin-5-one (IV)

The structure was solved by direct method using OLEX2 software. Positions of the hydrogen atoms were located from electron density difference maps and refined by "riding" model with

*U*iso = n*U*eq of the carrier atom (n = 1.5 for methyl and OH groups, n = 1.2 for other hydrogen atoms). Full-matrix least-squares refinement of the structure against F^2 in anisotropic approximation for non-hydrogen atoms was converged to wR_2 = 0.1181 (R_1 = 0.0452 for 681 reflections with I>2σ(I), S = 1.0918).

Compound **IV** ($C_6H_4N_4O_2$): orthorhombic crystals; at 111 K, $\boldsymbol{a}$ = 7.9831(5) Å, $\boldsymbol{b}$ = 6.1619(4) Å, $\boldsymbol{c}$ = 13.0089(10) Å, $\boldsymbol{\beta}$ = 90°, V = 639.93(8) $Å^3$, M_r = 328.25, Z = 2, space group *P*nma, D_{calc} = 1.7034 g/sm^{-3}, μ(CuKα) = 1.151 mm^{-1}, F(000) = 337.2908. Intensities of 6071 reflections (681 independent, R_{int} = 0.0517) were measured on a SuperNova diffractometer (Cu Kα radiation with mirror optics, Atlas CCD detector, ω-scanning, $2\theta_{max}$= 76.20°).

References:

(1) Kiuru, P.; Yli-Kauhaluoma, J. In *Heterocycles in Natural Product Synthesis*; Wiley-VCH Verlag GmbH & Co. KGaA: 2011, p 267.

(2) Baumann, M.; Baxendale, I. R. *Beilstein J. Org. Chem.* **2013**, *9*, 2265.

(3) Eloy, F.; Lenaers, R. *Chem. Rev.* **1962**, *62*, 155.

(4) Nicolaides, D. N.; Varella, E. A. In *Acid Derivatives (1992)*; John Wiley & Sons, Inc.: 1992, p 875.

(5) Fylaktakidou, K. C.; Hadjipavlou-Litina, D. J.; Litinas, K. E.; Varella, E. A.; Nicolaides, D. N. *Curr. Pharm. Design* **2008**, *14*, 1001.

(6) Peterlin-Mašič, L.; Kikelj, D. *Tetrahedron* **2001**, *57*, 7073.

(7) Peterlin-Masic, L.; Cesar, J.; Zega, A. *Curr. Pharm. Design* **2006**, *12*, 73.

(8) Masic, L. P. *Curr. Med. Chem.* **2006**, *13*, 3627.

(9) Clement, B. *Drug Metab. Rev.* **2002**, *34*, 565.

(10) Rautio, J.; Kumpulainen, H.; Heimbach, T.; Oliyai, R.; Oh, D.; Jarvinen, T.; Savolainen, J. *Nat. Rev. Drug Discov.* **2008**, *7*, 255.

(11) Ettmayer, P.; Amidon, G. L.; Clement, B.; Testa, B. *J. Med. Chem.* **2004**, *47*, 2393.

(12) Ott, G.; Havemeyer, A.; Clement, B. *J. Biol. Inorg. Chem.* **2015**, *20*, 265.

(13) Jakobs, H. H.; Froriep, D.; Havemeyer, A.; Mendel, R. R.; Bittner, F.; Clement, B. *ChemMedChem* **2014**, *9*, 2381.

(14) Clement, B.; Raether, W. *Arzneimittel-Forschung/Drug Research* **1985**, *35-2*, 1009.

(15) Clement, B.; Immel, M.; Terlinden, R.; Wingen, F.-J. *Arch. Pharm.* **1992**, *325*, 61.

(16) Clement, B.; Bürenheide, A.; Rieckert, W.; Schwarz, J. *ChemMedChem* **2006**, *1*, 1260.

(17) Kotthaus, J.; Schade, D.; Schwering, U.; Hungeling, H.; Muller-Fielitz, H.; Raasch, W.; Clement, B. *ChemMedChem* **2011**, *6*, 2233.

(18) Kotthaus, J.; Hungeling, H.; Reeh, C.; Schade, D.; Wein, S.; Wolffram, S.; Clement, B. *Bioorg. Med. Chem.* **2011**, *19*, 1907.

(19) Clement, B.; Kotthaus, J.; Schade, D. WO Patent 2013014059, 2013; *Chem. Abstr.* **2014**, *158*, 253720.

(20) Antonsson, T.; Gustafsson, D.; Hoffmann, K. J.; Nyström, J. E.; Sörensen, H.; Sellén, M. WO Patent 9723499, 1997; *Chem. Abstr.* **1997**, *127*, 136080.

(21) Gustafsson, D.; Elg, M. *Thromb. Res.* **2003**, *109*, S9.

(22) Clement, B.; Lopian, K. *Drug Metab. Dispos.* **2003**, *31*, 645.

(23) van Ryn, J.; Stangier, J.; Haertter, S.; Liesenfeld, K. H.; Wienen, W.; Feuring, M.; Clemens, A. *Thromb. Haemost.* **2010**, *103*, 1116.

(24) Clement, B.; Kotthaus, J.; Schade, D. EP Patent 2550966, 2013; *Chem. Abstr.* **2013**, *158*, 253723.

(25) Froriep, D.; Clement, B.; Bittner, F.; Mendel, R. R.; Reichmann, D.; Schmalix, W.; Havemeyer, A. *Xenobiotica* **2013**, *43*, 780.

(26) Meyer, J. E.; Brocks, C.; Graefe, H.; Mala, C.; Thans, N.; Burgle, M.; Rempel, A.; Rotter, N.; Wollenberg, B.; Lang, S. *Breast Care* **2008**, *3*, 20.

(27) Schade, D.; Kotthaus, J.; Riebling, L.; Kotthaus, J.; Müller-Fielitz, H.; Raasch, W.; Koch, O.; Seidel, N.; Schmidtke, M.; Clement, B. *J. Med. Chem.* **2014**, *57*, 759.

(28) Schwarz, L.; Girreser, U.; Clement, B. *Eur. J. Org. Chem.* **2014**, *9*, 1961.

(29) Kitamura, S.; Fukushi, H.; Miyawaki, T.; Kawamura, M.; Terashita, Z.-i.; Naka, T. *Chem. Pharm. Bull.* **2001**, *49*, 268.

(30) Ouattara, M.; Wein, S.; Calas, M.; Hoang, Y. V.; Vial, H.; Escale, R. *Bioorg. Med. Chem. Lett.* **2007**, *17*, 593.

(31) Kode, N.; Vanden Eynde, J.; Mayence, A.; Wang, G.; Huang, T. *Molecules* **2013**, *18*, 11250.

(32) Wang, P. G.; Xian, M.; Tang, X.; Wu, X.; Wen, Z.; Cai, T.; Janczuk, A. J. *Chem. Rev.* **2002**, *102*, 1091.

(33) Serafim, R. A. M.; Primi, M. C.; Trossini, G. H. G.; Ferreira, E. I. *Curr. Med. Chem.* **2012**, *19*, 386.

(34) Boucher, J.-L.; Genet, A.; Vadon, S.; Delaforge, M.; Henry, Y.; Mansuy, D. *Biochem. Biophys. Res. Commun.* **1992**, *187*, 880.

(35) Andronik-Lion, V.; Boucher, J. L.; Delaforge, M.; Henry, Y.; Mansuy, D. *Biochem. Biophys. Res. Commun.* **1992**, *185*, 452.

(36) Clement, B.; Jung, F. *Drug Metab. Dispos.* **1994**, *22*, 486.

(37) Jousserandot, A.; Boucher, J.-L.; Desseaux, C.; Delaforge, M.; Mansuy, D. *Bioorg. Med. Chem. Lett.* **1995**, *5*, 423.

(38) Jousserandot, A.; Boucher, J.-L.; Henry, Y.; Niklaus, B.; Clement, B.; Mansuy, D. *Biochemistry* **1998**, *37*, 17179.

(39) Rehse, K.; Bade, S.; Harsdorf, A.; Clement, B. *Arch. Pharm.* **1997**, *330*, 392.

(40) Koikov, L. N.; Alexeeva, N. V.; Lisitza, E. A.; Krichevsky, E. S.; Grigoryev, N. B.; Danilov, A. V.; Severina, I. S.; Pyatakova, N. V.; Granik, V. G. *Mendeleev Commun.* **1998**, *8*, 165.

(41) Vetrovsky, P.; Boucher, J.-L.; Schott, C.; Beranova, P.; Chalupsky, K.; Callizot, N.; Muller, B.; Entlicher, G.; Mansuy, D.; Stoclet, J.-C. *J. Pharmacol. Exp. Ther.* **2002**, *303*, 823.

(42) Chalupsky, K.; Lobysheva, I.; Nepveu, F.; Gadea, I.; Beranova, P.; Entlicher, G.; Stoclet, J.-C.; Muller, B. *Biochem. Pharmacol.* **2004**, *67*, 1203.

(43) Jaroš, F.; Straka, T.; Dobešová, Z.; Pintérová, M.; Chalupský, K.; Kuneš, J.; Entlicher, G.; Zicha, J. *Eur. J. Pharmacol.* **2007**, *575*, 122.

(44) Oresmaa, L.; Kotikoski, H.; Haukka, M.; Oksala, O.; Pohjala, E.; Vapaatalo, H.; Moilanen, E.; Vainiotalo, P.; Aulaskari, P. *Eur. J. Med. Chem.* **2006**, *41*, 1073.

(45) Ispikoudi, M.; Amvrazis, M.; Kontogiorgis, C.; Koumbis, A. E.; Litinas, K. E.; Hadjipavlou-Litina, D.; Fylaktakidou, K. C. *Eur. J. Med. Chem.* **2010**, *45*, 5635.

(46) Chapman, E.; Stephen, H. *J. Chem. Soc.* **1925**, *127*, 1791.

(47) Sauers, C. K.; Cotter, R. J. *J. Org. Chem.* **1961**, *26*, 6.

(48) Spiessens, L. I. M.; Anteunis, M. J. O. *Bull. Soc. Chim. Belg.* **1980**, *89*, 205.

(49) Holenz, J.; Karlström, S.; Kihlström, J.; Kolmodin, K.; Lindström, J.; Rakos, L.; Rotticci, D.; Swahn, B. M.; Von, B. S. WO Patent 2011002409, 2011; *Chem Abstr.* **2011**, *154*, 109655.

(50) Rice, K. D.; Nuss, J. M. *Bioorg. Med. Chem. Lett.* **2001**, *11*, 753.

(51) Hébert, N.; Hannah, A. L.; Sutton, S. C. *Tetrahedron Lett.* **1999**, *40*, 8547.

(52) Duchet, L.; Legeay, J. C.; Carrié, D.; Paquin, L.; Vanden Eynde, J. J.; Bazureau, J. P. *Tetrahedron* **2010**, *66*, 986.

(53) Dunn, A. D. *J. Heterocyclic Chem.***1984**, *21*, 965.

(54) Devillers, I.; Arrault, A.; Olive, G.; Marchand-Brynaert, J. *Tetrahedron Lett.* **2002**, *43*, 3161.

(55) Dunn, A. D. *J. Heterocyclic Chem.* **1984**, *21*, 961.

(56) Ovdiichuk, O.; Hordiyenko, O.; Voitenko, Z.; Arrault, A.; Medviediev, V. *Acta Cryst. E* **2013**, *69*, o1810.

(57) Grathwohl, C.; Wuthrich, K. *Biopolymers* **1981**, *20*, 2623.

(58) Zimmerman, S. S.; Scheraga, H. A. *Macromolecules* **1976**, *9*, 408.

(59) Elvidge, J. A.; Linstead, R. P. *J. Chem. Soc.* **1952**, 5000.

(60) Naredla, R. R.; Dash, B. P.; Klumpp, D. A. *Org. Lett.* **2013**, *15*, 4806.

(61) Ovdiichuk, O. V.; Hordiyenko, O. V.; Medviediev, V. V.; Shishkin, O. V.; Arrault, A. *Synthesis* **2015**, *47*, 2285.

(62) Dautrey, S.; Bodiguel, J.; Arrault, A.; Jamart-Grégoire, B. *Tetrahedron* **2012**, *68*, 4362.

(63) Jiménez, A. I.; Cativiela, C.; Gómez-Catalán, J.; Pérez, J. J.; Aubry, A.; París, M.; Marraud, M. *J. Am. Chem. Soc.* **2000**, *122*, 5811.

(64) Ovdiichuk, O. V.; Hordiyenko, O. V.; Arrault, A. *Tetrahedron* **2016**, *72*, 3427.

(65) Jochims, J. C. In *Comprehensive Heterocyclic Chemistry II*; Rees, C. W., Scriven, E. F. V., Eds.; Pergamon: Oxford, 1996, p 179.

(66) Pace, A.; Pierro, P. *Org. Biomol. Chem.* **2009**, *7*, 4337.

(67) Diana, G. D.; Volkots, D. L.; Nitz, T. J.; Bailey, T. R.; Long, M. A.; Vescio, N.; Aldous, S.; Pevear, D. C.; Dutko, F. J. *J. Med. Chem.* **1994**, *37*, 2421.

(68) Andersen, K. E.; Lundt, B. F.; Jørgensen, A. S.; Braestrup, C. *Eur. J. Med. Chem.* **1996**, *31*, 417.

(69) Jakopin, Ž.; Roškar, R.; Dolenc, M. S. *Tetrahedron Lett.* **2007**, *48*, 1465.

(70) Sureshbabu, V. V.; Hemantha, H. P.; Naik, S. A. *Tetrahedron Lett.* **2008**, *49*, 5133.

(71) Borg, S.; Estenne-Bouhtou, G.; Luthman, K.; Csoeregh, I.; Hesselink, W.; Hacksell, U. *J. Org. Chem.* **1995**, *60*, 3112.

(72) Borg, S.; Vollinga, R. C.; Labarre, M.; Payza, K.; Terenius, L.; Luthman, K. *J. Med. Chem.* **1999**, *42*, 4331.

(73) Jakopin, Ž. *Tetrahedron Lett.* **2015**, *56*, 504.

(74) Nordhoff, S.; Bulat, S.; Cerezo-Gálvez, S.; Hill, O.; Hoffmann-Enger, B.; López-Canet, M.; Rosenbaum, C.; Rummey, C.; Thiemann, M.; Matassa, V. G.; Edwards, P. J.; Feurer, A. *Bioorg. Med. Chem. Lett.* **2009**, *19*, 6340.

(75) Buchanan, J. L.; Vu, C. B.; Merry, T. J.; Corpuz, E. G.; Pradeepan, S. G.; Mani, U. N.; Yang, M.; Plake, H. R.; Varkhedkar, V. M.; Lynch, B. A.; MacNeil, I. A.; Loiacono, K. A.; Tiong, C. L.; Holt, D. A. *Bioorg. Med. Chem. Lett.* **1999**, *9*, 2359.

(76) Vu, C. B.; Corpuz, E. G.; Merry, T. J.; Pradeepan, S. G.; Bartlett, C.; Bohacek, R. S.; Botfield, M. C.; Eyermann, C. J.; Lynch, B. A.; MacNeil, I. A.; Ram, M. K.; van Schravendijk, M. R.; Violette, S.; Sawyer, T. K. *J. Med. Chem.* **1999**, *42*, 4088.

(77) Mathews, T. P.; Kennedy, A. J.; Kharel, Y.; Kennedy, P. C.; Nicoara, O.; Sunkara, M.; Morris, A. J.; Wamhoff, B. R.; Lynch, K. R.; Macdonald, T. L. *J. Med. Chem.* **2010**, *53*, 2766.

(78) Santos, W. L.; Lynch, K. R.; Macdonald, T. L.; Kennedy, A.; Kharel, Y.; Raje, M. R.; Houck, J. WO Patent 2013119946, 2013; *Chem. Abstr.* **2013**, *159*, 371277.

(79) Sasikumar, P. G. N.; Ramachandra, M.; Naremaddepalli, S. S. S. WO Patent 2015033299, 2015; *Chem. Abstr.* **2015**, *162*, 413506.

(80) Kotthaus, J.; Hungeling, H.; Reeh, C.; Kotthaus, J.; Schade, D.; Wein, S.; Wolffram, S.; Clement, B. *Bioorg. Med. Chem.* **2011**, *19*, 1907.

(81) Kode, R. N.; Vanden Eynde, J. J.; Mayence, A.; Wang, G.; Huang, L. T. *Molecules* **2013**, *18*.

(82) Ziga, J.; Marija Sollner, D. *Curr. Org. Chem.* **2008**, *12*, 850.

(83) Hemming, K. In *Comprehensive Heterocyclic Chemistry III*; Ramsden, C. A., Scriven, E. F. V., Taylor, R. J. K., Eds.; Elsevier: Oxford, 2008, p 243.

(84) Deegan, T. L.; Nitz, T. J.; Cebzanov, D.; Pufko, D. E.; Porco Jr, J. A. *Bioorg. Med. Chem. Lett.* **1999**, *9*, 209.

(85) Hamzé, A.; Hernandez, J.-F.; Fulcrand, P.; Martinez, J. *J. Org. Chem.* **2003**, *68*, 7316.

(86) Braga, A. L.; Lüdtke, D. S.; Alberto, E. E.; Dornelles, L.; Severo Filho, W. A.; Corbellini, V. A.; Rosa, D. M.; Schwab, R. S. *Synthesis* **2004**, *10*, 1589.

(87) Katritzky, A. R.; Shestopalov, A. A.; Suzuki, K. *Arkivoc* **2005**, 36.

(88) Gangloff, A. R.; Litvak, J.; Shelton, E. J.; Sperandio, D.; Wang, V. R.; Rice, K. D. *Tetrahedron Lett.* **2001**, *42*, 1441.

(89) Koufaki, M.; Theodorou, E.; Alexi, X.; Alexis, M. N. *Bioorg. Med. Chem.* **2010**, *18*, 3898.

(90) Congdon, M. D.; Childress, E. S.; Patwardhan, N. N.; Gumkowski, J.; Morris, E. A.; Kharel, Y.; Lynch, K. R.; Santos, W. L. *Bioorg. Med. Chem. Lett.* **2015**, *25*, 4956.

(91) Otaka, H.; Ikeda, J.; Tanaka, D.; Tobe, M. *Tetrahedron Lett.s* **2014**, *55*, 979.

(92) Lukin, K.; Kishore, V. *J. Heterocyclic Chem.* **2014**, *51*, 256.

(93) Lloyd, J.; Finlay, H. J.; Vacarro, W.; Hyunh, T.; Kover, A.; Bhandaru, R.; Yan, L.; Atwal, K.; Conder, M. L.; Jenkins-West, T.; Shi, H.; Huang, C.; Li, D.; Sun, H.; Levesque, P. *Bioorg. Med. Chem. Lett.* **2010**, *20*, 1436.

(94) Amarasinghe, K. K. D.; Maier, M. B.; Srivastava, A.; Gray, J. L. *Tetrahedron Lett.* **2006**, *47*, 3629.

(95) Baykov, S.; Sharonova, T.; Osipyan, A.; Rozhkov, S.; Shetnev, A.; Smirnov, A. *Tetrahedron Lett.* **2016**, *57*, 2898.

(96) Oussaid, B.; Moeini, L.; Martin, B.; Villemin, D.; Garrigues, B. *Synth. Commun.* **1995**, *25*, 1451.

(97) Porcheddu, A.; Cadoni, R.; De Luca, L. *Org. Biomol. Chem.* **2011**, *9*, 7539.

(98) Muraglia, E.; Altamura, S.; Branca, D.; Cecchetti, O.; Ferrigno, F.; Orsale, M. V.; Palumbi, M. C.; Rowley, M.; Scarpelli, R.; Steinkühler, C.; Jones, P. *Bioorg. Med. Chem. Lett.* **2008**, *18*, 6083.

(99) Wang, Y.; Miller, R. L.; Sauer, D. R.; Djuric, S. W. *Org. Lett.* **2005**, *7*, 925.

(100) Bretanha, L. C.; Teixeira, V. E.; Ritter, M.; Siqueira, G. M.; Cunico, W.; Pereira, C. M. P.; Freitag, R. A. *Ultrason. Sonochem.* **2011**, *18*, 704.

(101) Lamb, J. P.; Engers, D. W.; Niswender, C. M.; Rodriguez, A. L.; Venable, D. F.; Conn, P. J.; Lindsley, C. W. *Bioorg. Med. Chem. Lett.* **2011**, *21*, 2711.

(102) Ackermann, J.; Bleicher, K.; Ceccarelli, G. S. M.; Chomienne, O.; Mattei, P.; Schulz-Gasch, T. WO Patent 2007063012, 2007; *Chem. Abstr.* **2007**, *147*, 52814.

(103) Bolli, M.; Boss, C.; Brotschi, C.; Gude, M.; Heidmann, B.; Sifferlen, T.; Williams, J. T. WO Patent 2014057435, 2014; *Chem. Abstr.* **2014***, 160,* 592500.

(104) Bogdan, A. R.; Wang, Y. *RSC Adv.* **2015**, *5*, 79264.

(105) Taylor, C. M.; Hardré, R.; Edwards, P. J. B.; Park, J. H. *Org. Lett.* **2003**, *5*, 4413.

(106) Hitotsuyanagi, Y.; Motegi, S.; Fukaya, H.; Takeya, K. *J. Org. Chem.* **2002**, *67*, 3266.

(107) Thompson, S. K.; Eppley, A. M.; Frazee, J. S.; Darcy, M. G.; Lum, R. T.; Tomaszek Jr, T. A.; Ivanoff, L. A.; Morris, J. F.; Sternberg, E. J.; Lambert, D. M.; Fernandez, A. V.; Petteway Jr, S. R.; Meek, T. D.; Metcalf, B. W.; Gleason, J. G. *Bioorg. Med. Chem. Lett.* **1994**, *4*, 2441.

(108) Burrell, G.; Evans, J. M.; Hadley, M. S.; Hicks, F.; Stemp, G. *Bioorg. Med. Chem. Lett.* **1994**, *4*, 1285.

(109) Demange, L.; Boeglin, D.; Moulin, A.; Mousseaux, D.; Ryan, J.; Bergé, G.; Gagne, D.; Heitz, A.; Perrissoud, D.; Locatelli, V.; Torsello, A.; Galleyrand, J.-C.; Fehrentz, J.-A.; Martinez, J. *J. Med. Chem.* **2007**, *50*, 1939.

(110) Manku, S.; Allan, M.; Nguyen, N.; Ajamian, A.; Rodrigue, J.; Therrien, E.; Wang, J.; Guo, T.; Rahil, J.; Petschner, A. J.; Nicolescu, A.; Lefebvre, S.; Li, Z.; Fournel, M.; Besterman, J. M.; Déziel, R.; Wahhab, A. *Bioorg. Med. Chem. Lett.* **2009**, *19*, 1866.

(111) Hirai, K.; Fujishita, T.; Ishiba, T.; Sugimoto, H.; Matsutani, S.; Tsukinoki, Y.; Hirose, K. *J. Med. Chem.* **1982**, *25*, 1466.

(112) Moulin, A.; Bibian, M.; Blayo, A.-L.; El Habnouni, S.; Martinez, J.; Fehrentz, J.-A. *Chem. Rev.* **2010**, *110*, 1809.

(113) Mydlak, M.; Yang, C.-H.; Polo, F.; Galstyan, A.; Daniliuc, C. G.; Felicetti, M.; Leonhardt, J.; Strassert, C. A.; De Cola, L. *Chem. Eur. J.* **2015**, *21*, 5161.

(114) Naziruddin, A. R.; Galstyan, A.; Iordache, A.; Daniliuc, C. G.; Strassert, C. A.; De Cola, L. *Dalton Trans.* **2015**, *44*, 8467.

(115) Dumur, F.; Lepeltier, M.; Graff, B.; Contal, E.; Wantz, G.; Lalevée, J.; Mayer, C. R.; Bertin, D.; Gigmes, D. *Synth. Met.* **2013**, *182*, 13.

(116) Mydlak, M.; Mauro, M.; Polo, F.; Felicetti, M.; Leonhardt, J.; Diener, G.; De Cola, L.; Strassert, C. A. *Chem. Mater.* **2011**, *23*, 3659.

(117) Sanning, J.; Ewen, P. R.; Stegemann, L.; Schmidt, J.; Daniliuc, C. G.; Koch, T.; Doltsinis, N. L.; Wegner, D.; Strassert, C. A. *Angew. Chem. Int. Ed.* **2015**, *54*, 786.

(118) Bumagin, N.; Petkevich, S.; Kletskov, A.; Livantsov, M.; Golantsov, N.; Potkin, V. *Chem. Heterocycl. Compd.* **2014**, *49*, 1515.

(119) Ghazvini Zadeh, E. H.; El-Gendy, B. E.-D. M.; Pop, A. G.; Katritzky, A. R. *MedChemComm* **2012**, *3*, 52.

(120) Bokor, É.; Docsa, T.; Gergely, P.; Somsák, L. *ACS Med. Chem. Lett.* **2013**, *4*, 612.

(121) Bokor, É.; Fekete, A.; Varga, G.; Szőcs, B.; Czifrák, K.; Komáromi, I.; Somsák, L. *Tetrahedron* **2013**, *69*, 10391.

(122) Rocha, A.; Bacelar, A. H.; Fernandes, J.; Proenca, M. F.; Carvalho, M. A. *Synlett* **2014**, *25*, 343.

(123) Menteşe, E.; Yılmaz, F. *Synth. Commun.* **2014**, *44*, 2348.

(124) Liu, X.; Sun, L.; Zhou, H.; Cen, P.; Jin, X.; Xie, G.; Chen, S.; Hu, Q. *Inorg. Chem.* **2015**, *54*, 8884.

(125) Drover, M. W.; Tandon, S. S.; Anwar, M. U.; Shuvaev, K. V.; Dawe, L. N.; Collins, J. L.; Thompson, L. K. *Polyhedron* **2014**, *68*, 94.

(126) Hurtaud, D.; Baudy-Floc'h, M.; Gougeon, P.; Gall, P.; Le Grel, P. *Synthesis* **2001**, 2435.

(127) Bhuniya, D.; Umrani, D.; Dave, B.; Salunke, D.; Kukreja, G.; Gundu, J.; Naykodi, M.; Shaikh, N. S.; Shitole, P.; Kurhade, S.; De, S.; Majumdar, S.; Reddy, S. B.; Tambe, S.; Shejul, Y.; Chugh, A.; Palle, V. P.; Mookhtiar, K. A.; Cully, D.; Vacca, J.;

Chakravarty, P. K.; Nargund, R. P.; Wright, S. D.; Graziano, M. P.; Singh, S. B.; Roy, S.; Cai, T.-Q. *Bioorg. Med. Chem. Lett.* **2011**, *21*, 3596.

(128) Balo, C.; Lopez, C.; Manuel Brea, J.; Fernandez, F.; Caamano, O. *Chem. Pharm. Bull.* **2007**, *55*, 372.

(129) Francis, J. E.; Gorczyca, L. A.; Mazzenga, G. C.; Meckler, H. *Tetrahedron Letters* **1987**, *28*, 5133.

(130) Biitseva, A. V.; Rudenko, I. V.; Hordiyenko, O. V.; Jamart-Grégoire, B.; Arrault, A. *Eur. J. Org. Chem.* **2012**, *23*, 4387.

(131) Biitseva, A. V.; Rudenko, I. V.; Hordiyenko, O. V.; Omelchenko, I. V.; Arrault, A. *Synthesis* **2015**, *47*, 3733.

(132) Proulx, C.; Sabatino, D.; Hopewell, R.; Spiegel, J.; García Ramos, Y.; Lubell, W. D. *Future Med. Chem.* **2011**, *3*, 1139.

(133) Chang, X.-W.; Han, Q.-C.; Jiao, Z.-G.; Weng, L.-H.; Zhang, D.-W. *Tetrahedron* **2010**, *66*, 9733.

(134) Li, X.; Yang, D. *Chem. Commun.* **2006**, 3367.

(135) Fischer, L.; Didierjean, C.; Jolibois, F.; Semetey, V.; Manuel Lozano, J.; Briand, J.-P.; Marraud, M.; Poteau, R.; Guichard, G. *Org. Biomol. Chem.* **2008**, *6*, 2596.

(136) Zhou, Z.; Deng, C.; Abbas, C.; Didierjean, C.; Averlant-Petit, M.-C.; Bodiguel, J.; Vanderesse, R.; Jamart-Grégoire, B. *Eur. J. Org. Chem.* **2014**, 7643.

(137) Humbert-Voss, E.; Arrault, A.; Jamart-Grégoire, B. *Tetrahedron* **2014**, *70*, 363.

(138) Dorman, D. E.; Bovey, F. A. *J. Org. Chem.* **1973**, *38*, 2379.

(139) Dorman, D. E.; Bovey, F. A. *J. Org. Chem.* **1973**, *38*, 1719.

(140) Beausoleil, E.; Lubell, W. D. *J. Am. Chem. Soc.* **1996**, *118*, 12902.

(141) Mikhailov, D.; Daragan, V. A.; Mayo, K. H. *Biophys. J.* **1995**, *68*, 1540.

(142) DeRider, M. L.; Wilkens, S. J.; Waddell, M. J.; Bretscher, L. E.; Weinhold, F.; Raines, R. T.; Markley, J. L. *J. Am. Chem. Soc.* **2002**, *124*, 2497.

(143) Hinderaker, M. P.; Raines, R. T. *Protein Sci.* **2003**, *12*, 1188.

(144) Wiberg, K. B.; Hadad, C. M.; Rablen, P. R.; Cioslowski, J. *J. Am. Chem. Soc.* **1992**, *114*, 8644.

(145) MacArthur, M. W.; Thornton, J. M. *J. Mol. Biol.***1991**, *218*, 397.

(146) Fischer, S.; Dunbrack, R. L.; Karplus, M. *J. Am. Chem. Soc.* **1994**, *116*, 11931.

(147) Kishore, R.; Raghothama, S.; Balaram, P. *Biopolymers* **1987**, *26*, 873.

(148) Ianelli, S.; Pelosi, G.; Ponticelli, G.; Cocco, M. T.; Onnis, V. *J. Chem. Crystallogr.* **2001**, *31*, 149.

(149) Griess, P. *Ber. Dtsch. Chem. Ges.* **1879**, *12*, 426.

(150) Case, D. A.; Cheatham, III, T. E.; Simmerling, C. L.; Wang, J.; Duke, R. E.; Luo, R.; Crowley, M.; Walker, R. C.; Zhang, W.; Merz, K. M.; Wang, B.; Hayik, S.; Roitberg, A.; Seabra, G.; Kolossváry, I.; Wong, K. F.; Paesani, F.; Vanicek, J.; Wu, X.; Brozell, S. R.; Steinbrecher, T.; Gohlke, H.; Yang, L.; Tan, C.; Mongan, J.; Hornak, V.; Cui, G.; Mathews, D. H.; Seetin, M. G.; Sagui, C.; Babin, V.; Kollman, P. A. University of California, S. F., Ed. **2008**.

(151) Sheldrick, G. *Acta Cryst. A* **2008**, *64*, 112.

(152) Macrae, C. F.; Edgington, P. R.; McCabe, P.; Pidcock, E.; Shields, G. P.; Taylor, R.; Towler, M.; van de Streek, J. *J. Appl. Crystallogr.* **2006**, *39*, 453.

Appendix

Figure 1: NOESY NMR spectrum of **5c**

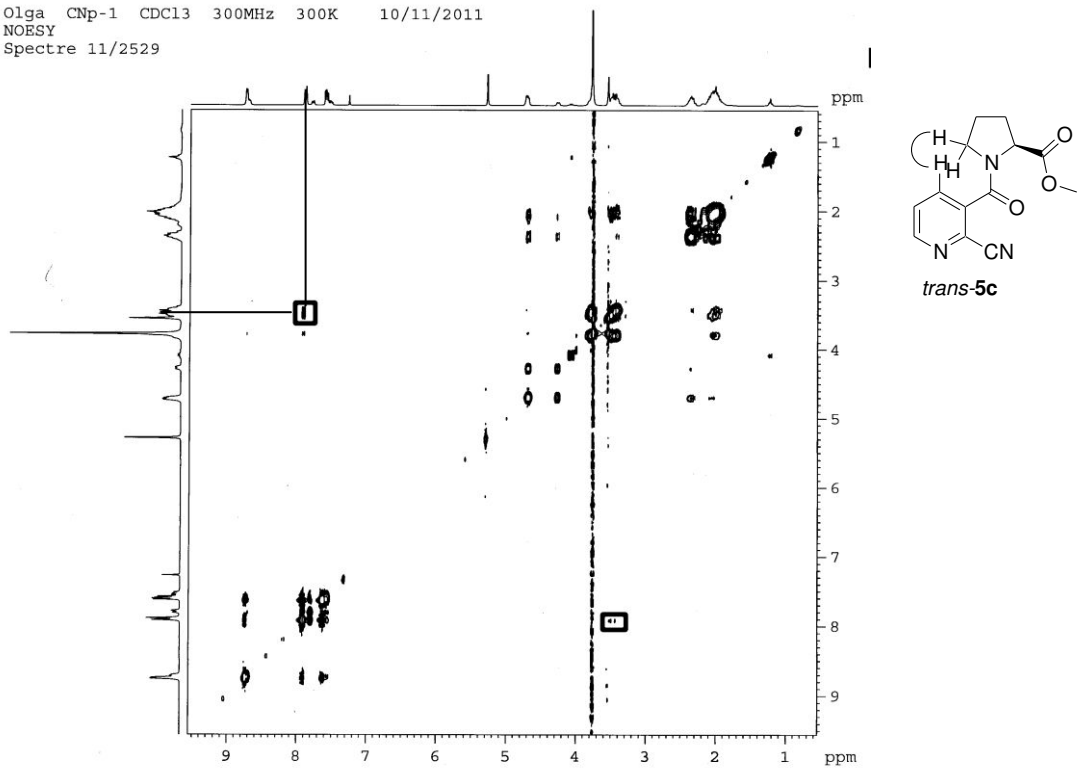

Figure 2: NOESY NMR spectrum of **8c**

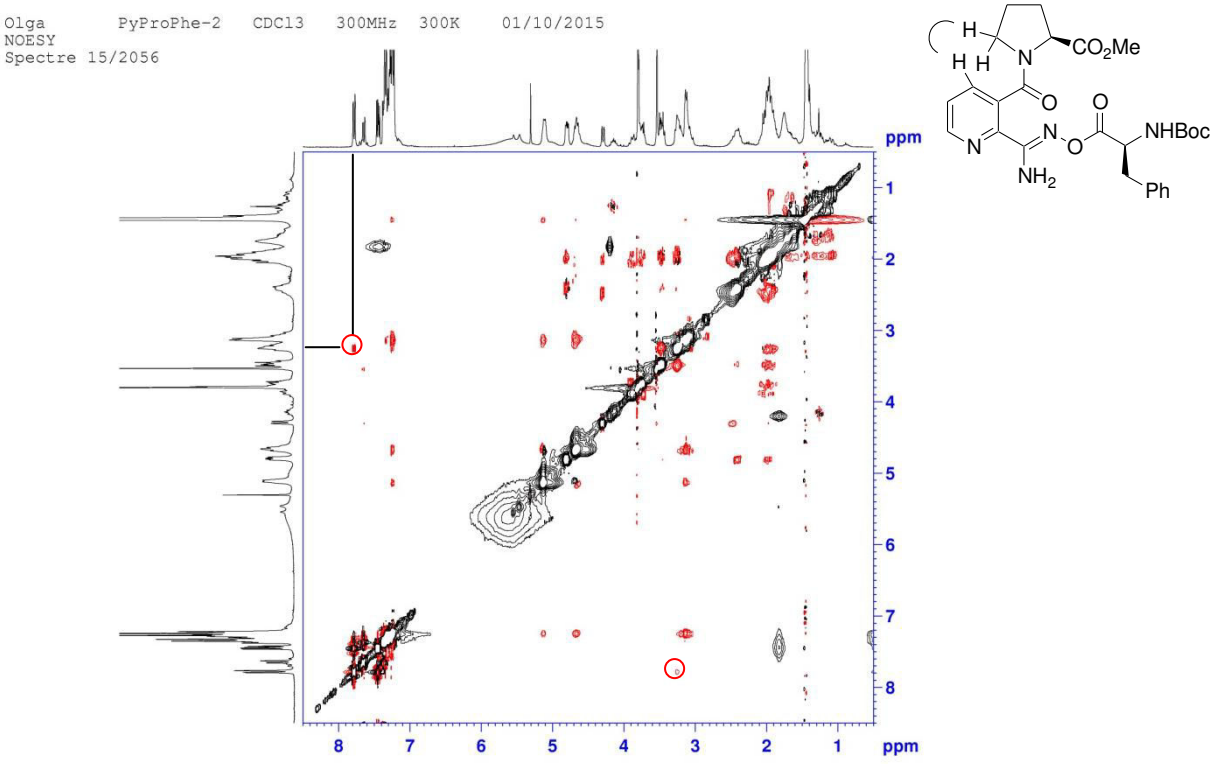

Figure 3: NOESY NMR spectrum of **9c**

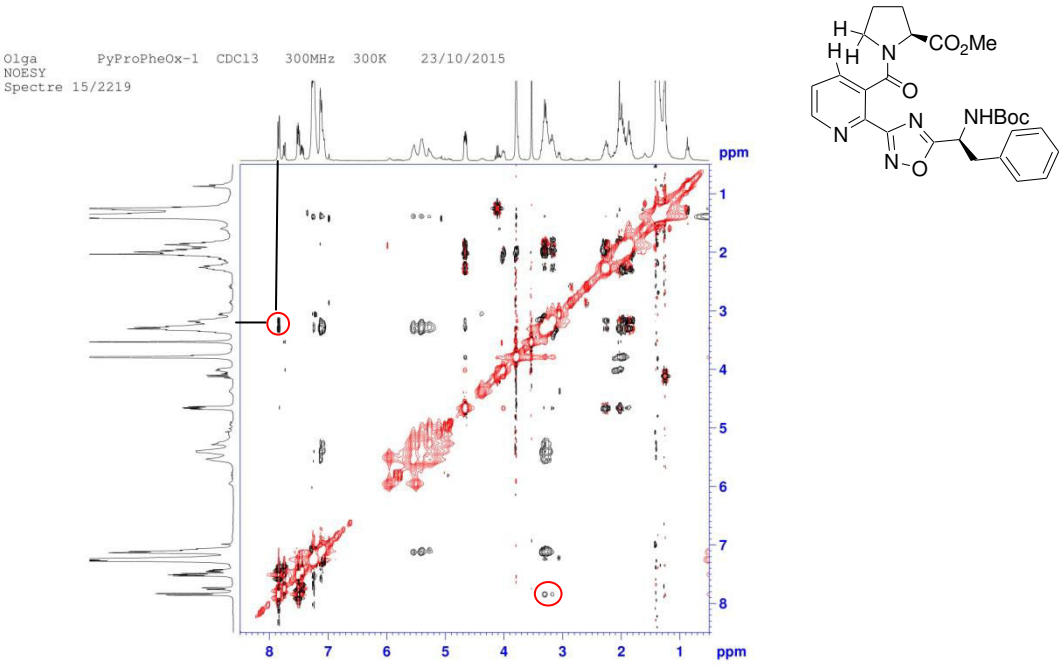

Superpositions of AOPzPro (7'c), AOPzPhe (7'b) and AOPzProPhe (7'd)

Figure 4: Superposition of AOPzProPhe (in blue) and AOPzPhe (in green) on backbone atoms from H of amidoxime to C of carbonyl next to the pyrazine ring. The rmsd on these 6 atoms is 0.262 Å.

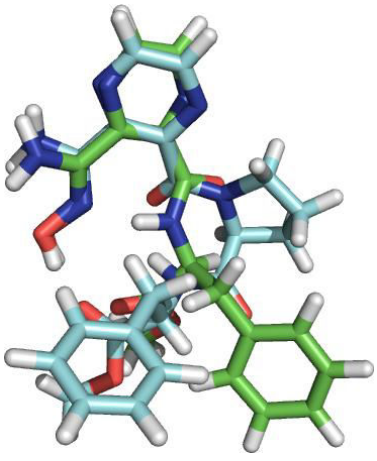

Figure 5: Superposition of AOPzProPhe (in blue) and AOPzPro (in pink) on backbone atoms from H of amidoxime to N of proline residue next to the pyrazine ring. The rmsd on these 7 atoms is 0.411 Å.

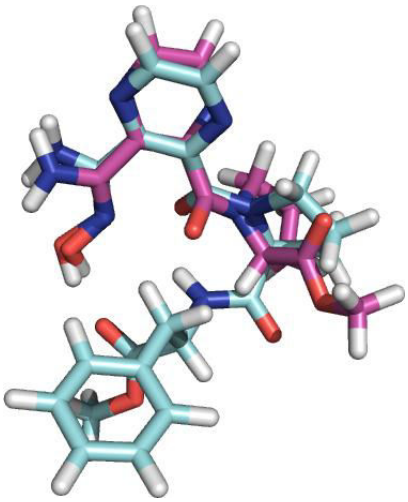

Figure 6: Superposition of AOPzPhe (in green) and AOPzPro (in pink) on backbone atoms from H of amidoxime to C of carbonyl next to the pyrazine ring. The rmsd on these 6 atoms is 0.209 Å.

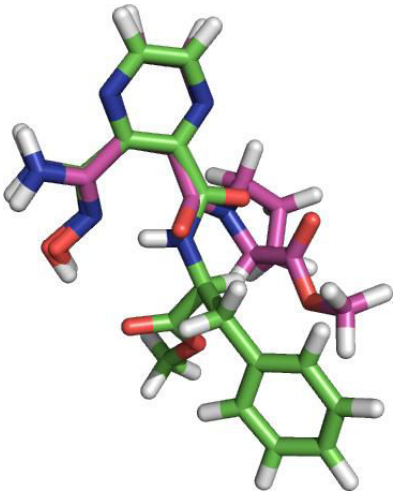

Figure 7: Structure of AOPzPro obtained from molecular dynamics simulationin explicit solvent boxes $CHCl_3$ (a) and DMSO (b)

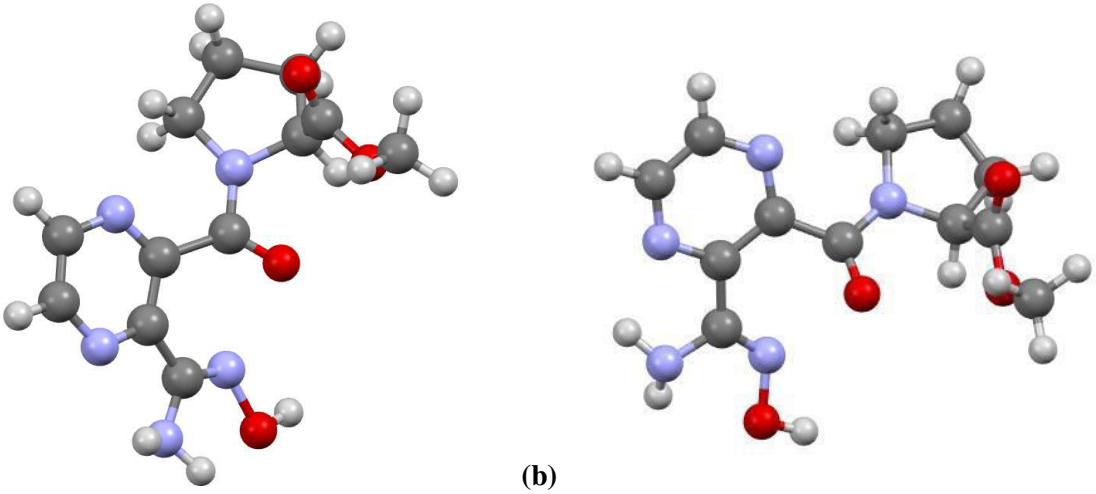

(a) **(b)**

LIST OF COMPOUNDS

Starting compounds

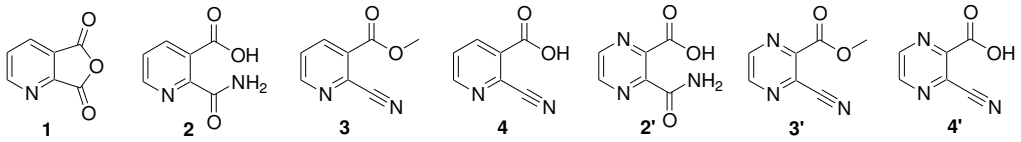

Nitriles and pyrrolopyridines(pyrazines)

Pyridine series

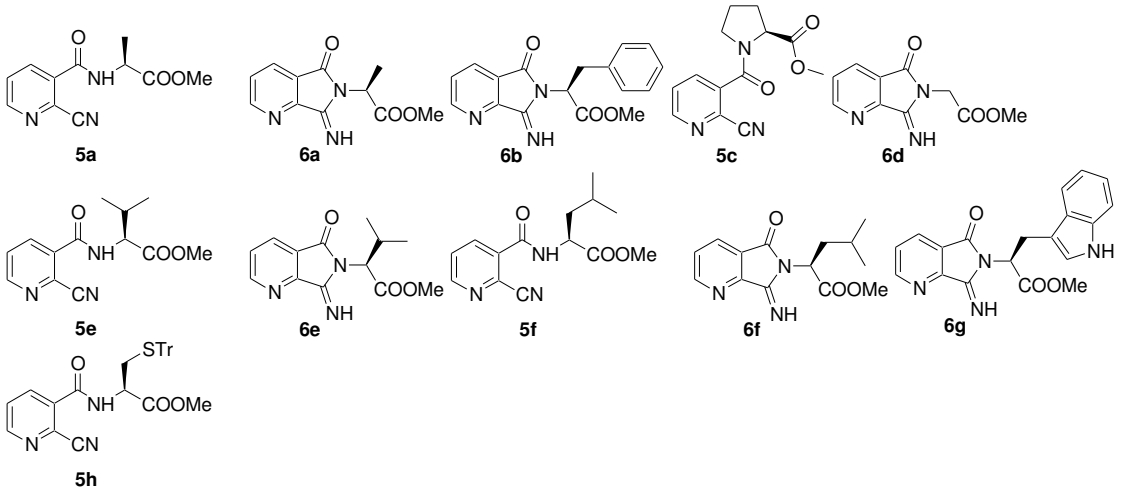

Pyrazine series

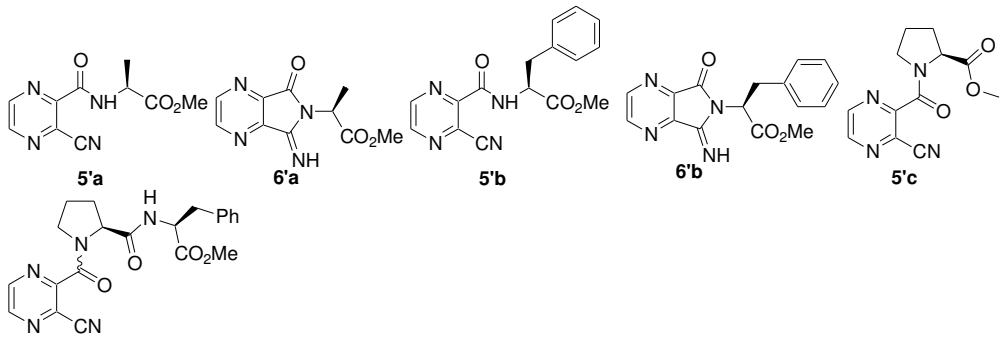

5'a **6'a** **5'b** **6'b** **5'c** **5'd**

Amidoximes: *Pyridine series*

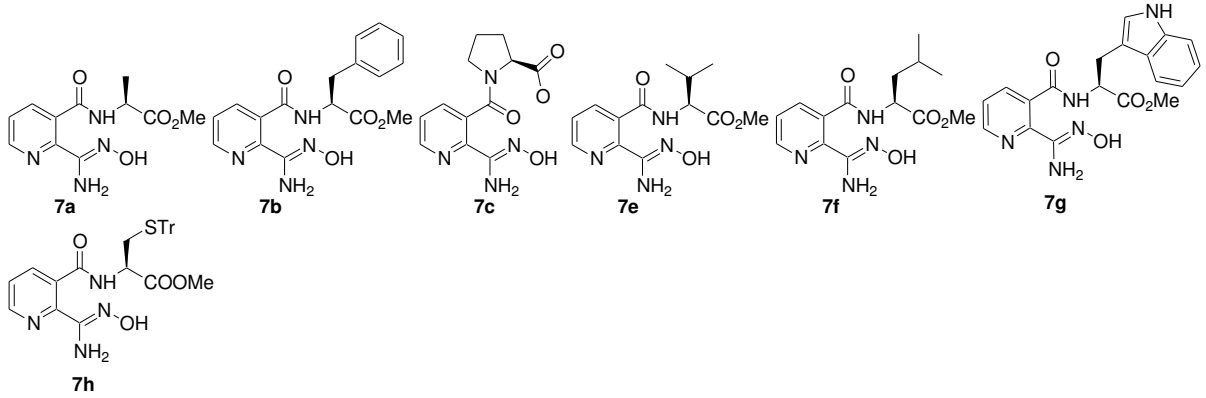

7a **7b** **7c** **7e** **7f** **7g** **7h**

Pyrazine series

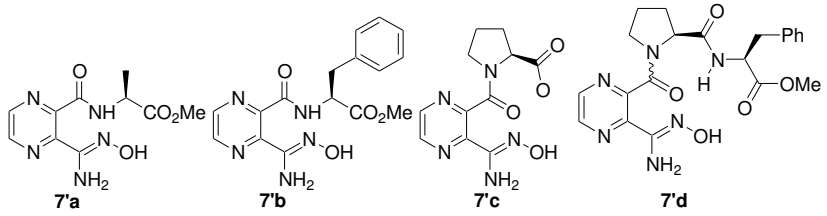

7'a **7'b** **7'c** **7'd**

Amidoxime esters

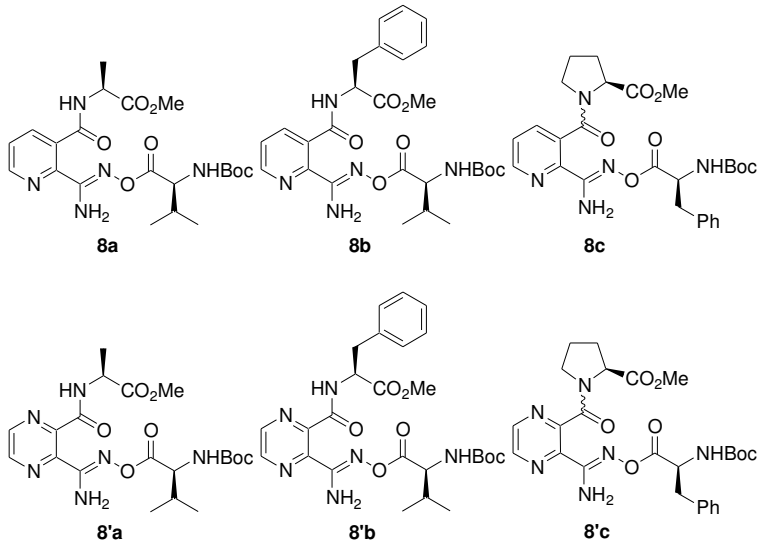

8a **8b** **8c** **8'a** **8'b** **8'c**

1,2,4-Oxadiazoles

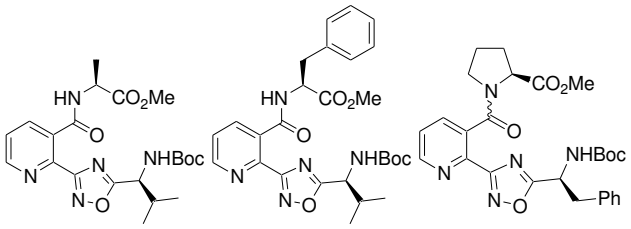

9a **9b** **9c**

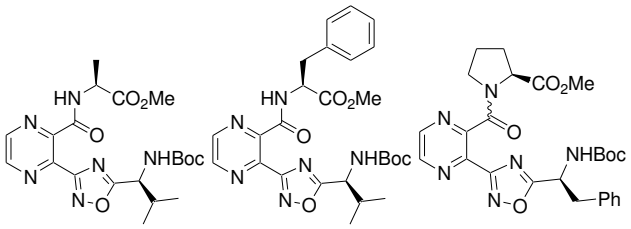

9'a **9'b** **9'c**

N-acylamidrazones

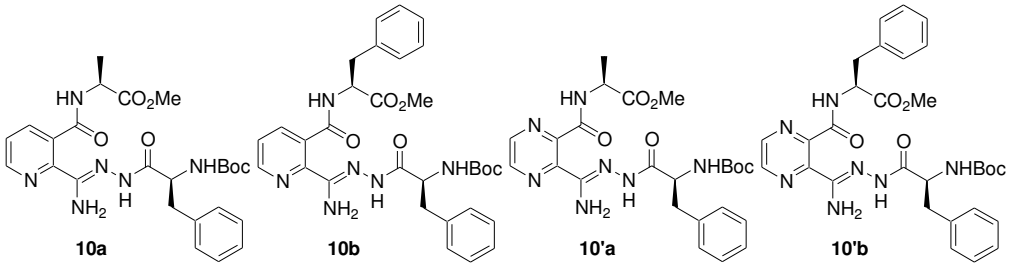

10a **10b** **10'a** **10'b**

1,2,4-triazoles

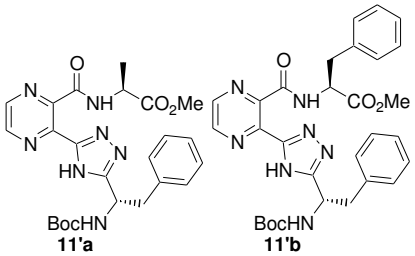

11'a **11'b**

Hydrazide modified turn mimics

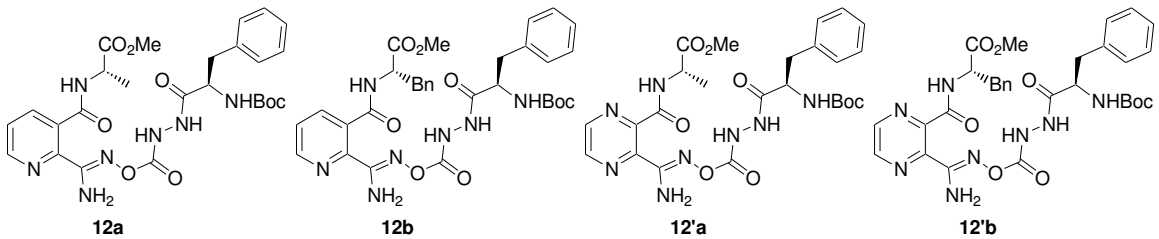

12a **12b** **12'a** **12'b**

LIST OF PUBLICATIONS

1. Ovdiichuk O.V.; Hordiyenko O.V.; Voitenko Z.V.; Arrault A., Methyl *N*-(3-cyanopicolinoyl)-l-tryptophanate, *Acta Crystallogr. E* **2013**, *69*, o1810.

2. Ovdiichuk, O.V.; Hordiyenko, O.V.; Medviediev, V.V.; Shishkin, O.V.; Arrault, A., Efficient Synthesis of Nicotinic Acid Based Pseudopeptides Bearing an Amidoxime Function*, Synthesis* **2015**, *47*, 2285-2293.

3. Ovdiichuk O.V.; Hordiyenko O.V., Amidoximes and their masked derivatives as prodrugs of amidines - arginine mimetics, *J. Org. Pharm. Chem.* (*Kharkiv, Ukraine*) **2016**, *14 (1)*, 36-45.

4. Ovdiichuk O.V.; Hordiyenko O.V.; Arrault A., Synthesis and conformational study of novel pyrazine-based pseudopeptides bearing amidoxime, amidoxime ester and 1,2,4-oxadiazole units, *Tetrahedron* **2016**, *72 (24),* 3427-3435.

5. Ovdiichuk O.; Hordiyenko O.; Fotou E.; Gaucher C.; Arrault A.; Averlant-Petit M.-C. Conformational studies of new pseudotripeptide with pyrazine amidoxime motif and simplified analogues using IR, NMR spectroscopy and Molecular Dynamics Simulations, *Struct. Chem.* **2016**, DOI: 10.1007/s11224-016-0870-2.

Résumé de thèse

L'objectif de ce projet est la synthèse de peptidomimétiques possédant un hétérocycle de type pyridine ou pyrazine substitué en ortho qui aurait l'intérêt de pouvoir favoriser une structure coudée, assurant ainsi une rigidité conformationnelle supplémentaire. Afin d'atteindre cet objectif, la synthèse et l'étude structurale de composés portant un substituant de type aminoacide et une fonction amidoxime en remplacement de l'amidine ont été réalisées. L'étude a été élargie afin d'introduire cet acide aminé supplémentaire par une liaison différente telle que l'hydrazide, l'ester ou une petite unité hétérocyclique (1,2,4-oxadiazole, 1,2,4-triazole).

Introduction

Un composé peptidomimétique est une molécule dont la structure de base est non peptidique, mais dont les motifs structuraux miment les propriétés tridimensionnelles et fonctionnelles des structurespeptidiques. Ces composés ont l'intérêt de conserver les caractéristiques avantageuses reliées aux peptides tout en s'affranchissant de certains inconvénients. Effectivement, elles sont plus lentement dégradées par les protéases, augmentant ainsi considérablement leur stabilité et leur biodisponibilité.

Une des stratégies possibles pour l'élaboration de peptidomimétiques est d'associer des noyaux aromatiques ou hétérocycliques avec un motif peptidique. Les acides aminés combinés à des hétérocycles sont devenus des précurseurs importants dans la conception de peptidomimétiques. Dans cette thèse, nous décrivons l'étude des nouveaux peptidomimétiques possédant un motif de type pyridine ou pyrazine. Les noyaux pyridiniques et pyraziniques se caractérisent par un large éventail d'activités biologiques. A titre d'exemples, le motif pyridine est naturellement présent dans les vitamines, l'acide nicotinique (vitamine B3 / niacine) et la pyridoxine (vitamine B6) et un certain nombre d'alcaloïdes comme la nicotine. De plus, la niacine et le nicotinamide sont des précurseurs des coenzymes nicotinamide adénine dinucléotide (NAD) et nicotinamide adénine dinucléotide phosphate (NADP) *in vivo*.

Un certain nombre de composés contenant un fragment pyrazine sont en phase finale d'essais cliniques (VE-821 - un inhibiteur de l'ATR) ou sont déjà commercialisés (bortezomib - le premier inhibiteur protéasome thérapeutique, eszopiclone - un sédatif hypnotique non benzodiazépine, etc…).

Pourquoi y intégrer une fonction amidoxime? Les amidines sont souvent utilisées comme mimes de la chaîne latérale guanidine de l'arginine, responsable des effets pharmacologiques. Une variété de médicaments et de candidats médicaments possèdent la fonction amidine, comme les inhibiteurs de thrombine, les inhibiteurs de facteur Xa et VIIa, les antagonistes des récepteurs aux glycoprotéines IIb / IIIa, etc…. Cependant, en raison de leur grande hydrophilie, ils sont aisément protonés au niveau de l'atome d'azote sp^2, formant un cation fortement stabilisé dans des conditions physiologiques qui empêche une absorption du tractus gastro-intestinal. Ce problème peut justement être contourné en utilisant des amidoximes comme prodrogues qui seront alors administrées par voie orale. Un groupe amidoxime introduit dans la structure ne sera pas protoné dans ces mêmes conditions physiologiques et peut donc être utilisé pour remplacer une amidine. Cette approche d'utilisation des amidoximes comme prodrogues des amidines présente un intérêt croissant en raison de l'amélioration notable des propriétés physico-chimiques et de biodisponibilité orale. Récemment, il a été montré que le système enzymatique *N*-réducteur est responsable de l'activation des prodrogues amidoxime dans les mitochondries. Une autre stratégie pour imaginer de nouvellespro drogues est l'utilisation d'amidoximes estérifiées et de 1,2,4-oxadiazol-5-ones ou 1,2,4-oxadiazoles avec la fonctionnalité amidine masquée afin de réduire le caractère basique et d'améliorer la biodisponibilité.

La seconde raison qui a orienté le choix de cette fonction amidoxime est sa transformation par diverses enzymes en fonction amide accompagnée d'une libération ultérieure d'une molécule de NO.

L'oxyde nitrique (NO) est un médiateur endogène gazeux et radicalaire impliqué dans de nombreux processus physiologiques et joue un rôle clé dans de nombreux systèmes de bio-régulation du tonus cardiovasculaire: relaxation vasculaire, inhibition de l'agrégation plaquettaire et également dans d'autres fonctions biologiques essentielles : neurotransmission, réponse immunitaire, processus inflammatoires, le choc septique et enfin l'érection.

En raison de ces nombreuses propriétés, il y a un grand intérêt à élaborer de nouveaux composés - donneurs d'oxyde nitrique (donneurs de NO). La première oxydation des amidoximes a été décrite par Andronik-Lion *et al.*en 1992 (Schéma 1) sur la *p*-hexyloxy-benzamidoxime qui est transformée en présence d'oxygène en arylamide correspondante a libéré de l'oxyde nitrique en présence de cytochromes P450 et de NADPH (forme réduit du nicotinamide adénine dinucléotide phosphate).

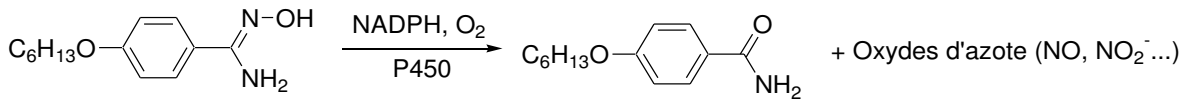

Schéma 1 Oxydation d'amidoxime en présence de cytochromes P450 de microsomes de foie

Résultats

Plan de synthèse

La voie de synthèse envisagée pour accéder aux différents peptidomimétiques en série pyridine et pyrazine est décrite dans le Schéma 2.

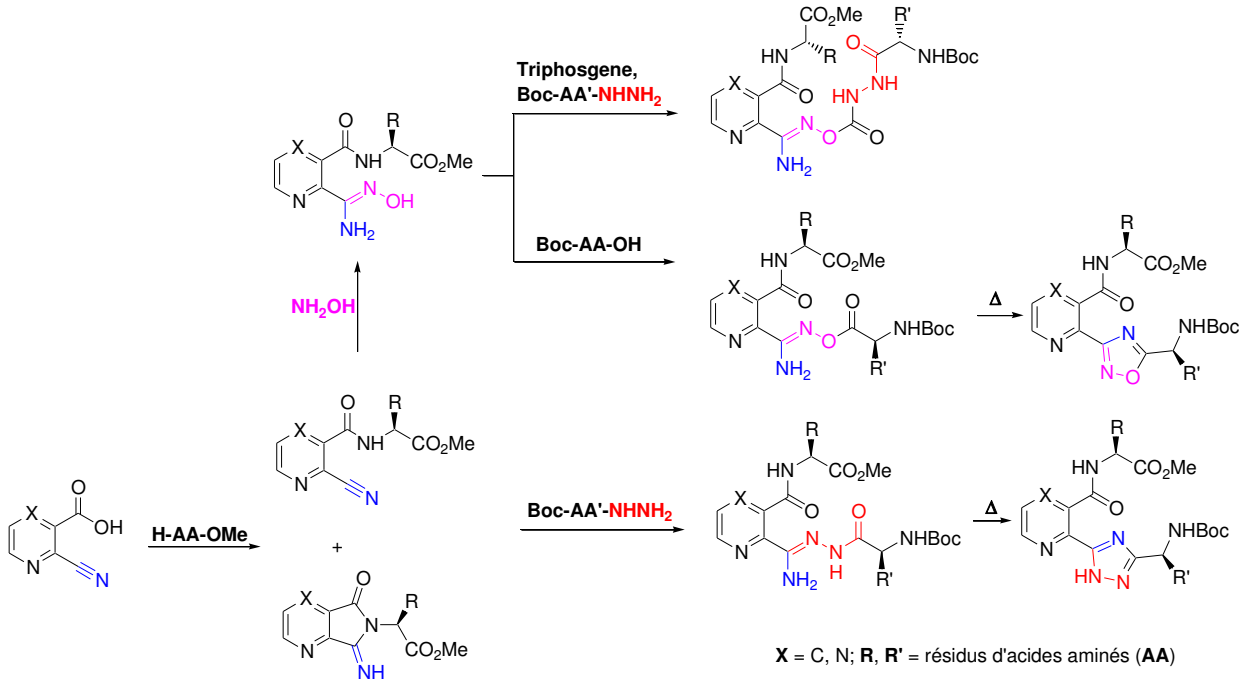

Schéma 2 Stratégie de synthèse des peptidomimetiques ciblés

Suivant la série étudiée, cette stratégie utilise les acides 2-cyanonicotinique et 3-cyanopyrazine-2-carboxylique comme produits de départ. La substitution en positions 2,3 de ces cycles azotes présente l'avantage de fournir une rigidité conformationnelle supplémentaire, donc d'induire une structure préférentielle. Plus particulièrement, la présence de la fonction amidoxime en position ortho permet de mimer un β-turn rigide se retrouvant habituellement dans la structure de l'arginine, précurseur physiologique de NO.

Les amidoximes correspondantes sont alors synthétisées en deux étapes pour générer ensuite les différents pseudodipeptides dans les deux séries.

De plus, dans un premier temps, les composés intermédiaires générés peuvent être utilisés pour réagir avec des hydrazides d'acides aminés afin d'obtenir des *N*-acylamidrazones, précurseurs, dans un second temps, des squelettes de type 1,2,4-triazole.

L'estérification des amidoximes, réalisée soit avec un acide aminé ou soit avec un hydrazide d'acide aminé, permet l'accès à de nouveaux pseudotripeptides ou «doubles pro drogues» d'amidines. Enfin, une étape de cyclisation de ces pseudotripeptides permettra de générer des dérivés 1,2,4-oxadiazole, reconnus pour leur intérêt biologique.

L'intérêt de ce travail synthétique est clairement l'obtention de structures peptidomimétiques variées à partir d'un seul et même précurseur.

Synthèse des composés de départ: les acides 2-cyanonicotinique et 3-cyanopyrazine-2-carboxyliques

La préparation de l'acide carboxylique de départ **4** a été effectuée suivant un protocole décrit dans la littérature. Pour cela, l'anhydride quinoléique **1**, commercialement accessible, a d'abord été hydrolysé rapidement par une solution d'ammoniaque aqueuse (28%), pour donner l'acide 2-carbamoylnicotinique (**2**) (Schéma 3). Cette réaction permet la formation sélective du produit **2** en s'affranchissant totalement de l'éventuel isomère: l'acide 3-carbamoylpicolinique. Ceci peut être expliqué par l'effet électronégatif de l'atome d'azote qui améliore ainsi le caractère électrophile du carbone du groupement carbonyle le plus proche, favorisant ainsi l'attaque sur cet atome de carbone. Il est aussi possible qu'une liaison hydrogène créée entre le proton de la molécule d'ammoniaque et le doublet non liant de l'atome d'azote de la pyridine puisse orienter l'attaque à l'origine de la formation exclusive de l'acide **2**. Ensuite, l'ester **3** a été obtenu par traitement de l'acide **2** avec du chloroformiate de méthyle, suivi d'une hydrolyse avec une solution aqueuse de soude (1M) pour donner l'acide 2-cyanonicotinique correspondant **4** avec un rendement global de 28%.

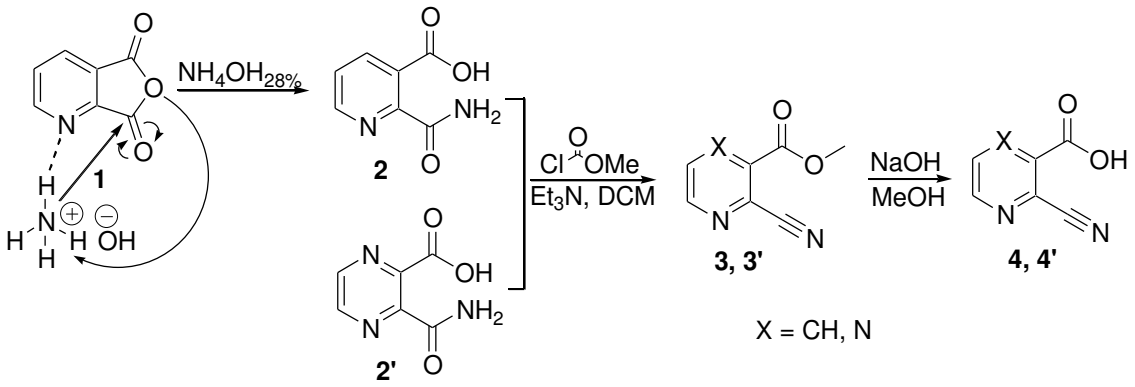

Schéma 3 Synthèse des acides 2-cyanonicotinique et 3-cyanopyrazine-2-carboxylique

Concernant la série pyrazine, le composé de départ, à savoir l'acide 3-cyanopyrazine-2-carboxylique **4'** a été synthétisé à partir de l'acide 3-carbamoylpyrazine-2-carboxylique **2'** commercial. Après traitement par du chloroformiate de méthyle et hydrolyse sélective de la fonction ester par une solution aqueuse de soude 1M, l'acide désiré **4'** est généré avec un bon rendement global (71%).

Synthèse des amidoximes

Lors de nos tentatives de développement de nouvelles variétés de peptidomimétiques d'arginine possédant un motif amidinohétéroaroyle dans une chaîne peptidique, nous avons élaboré une voie de synthèse de molécules pseudopeptidiques (acide nicotinique couplé à un acide aminé) et où la fonction amidoxime est portée par le cycle pyridinique et ceci en tant que précurseurs des pseudopeptides correspondants contenant de l'amidine.

Cette stratégie permet d'accéder aux peptidomimétiques en série pyridinique et a été envisagée de la façon suivante: en premier lieu, par couplage de l'acide 2-cyanonicotinique **4** avec des esters méthyliques d'acides L-α-aminés puis, par conversion du résidu cyano en groupement amidoxime. Pour étudier la portée de cette nouvelle stratégie, le couplage de l'acide 2-cyanonicotinique **4** a été testé avec plusieurs esters méthyliques d'acides L-*α*-aminés (tels que Ala, Phe, Pro, Gly, Val, Leu, Trp et CysTr) commerciaux (Schéma 4). Le chlorhydrate de *N*-éthyl-*N'*-(3-diméthylaminopropyl)carbodiimide (EDCI) a été utilisé comme agent d'activation en présence de 1-hydroxybenzotriazole (HOBt) et de triéthylamine.

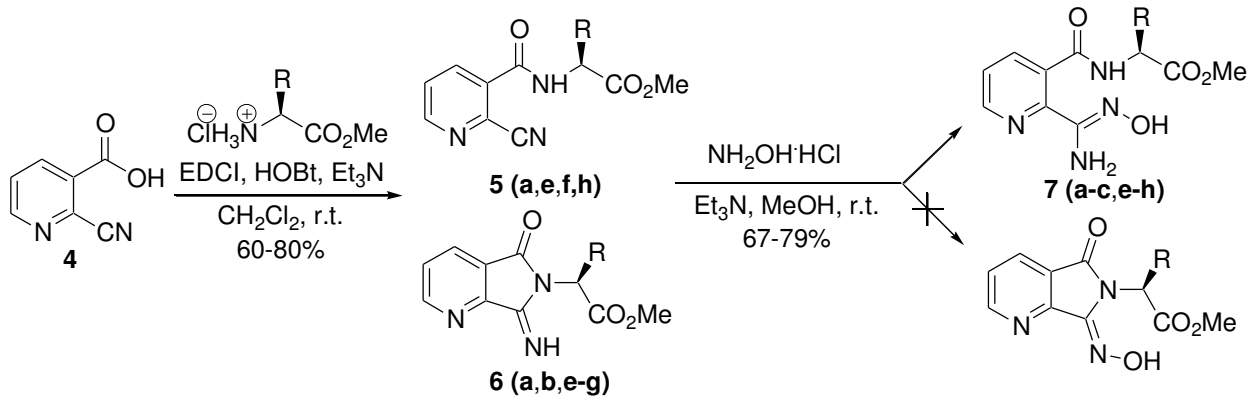

Schéma 4 Synthèse des esters méthyliques des (2*S*)-*N*-[2-(*N'*-hydroxycarbamimidoyl)pyridin-3-yl]carbonyles substitués par des aminoacides **7a-c, e-h**

L'analyse des produits de réaction effectuée par spectroscopie RMN ^{1}H confirme, dans la majorité des cas, que la formation des esters méthyliques **5** des (2*S*)-*N*-(2-cyanopyridin-3-yl)carbonyles substitués a été suivie par une réaction de cyclisation intramoléculaire à l'origine d'un cycle pyrrolidinique, générant les pyrrolopyridines tautomères **6**.

Dans le cas d'utilisation des esters méthyliques de l'alanine, de la valine et de la leucine, la formation des deux produits **5** et**6** est observée avec des ratios différents, alors qu'au contraire dans le cas de la phénylalanine, de la glycine et du tryptophane, les esters cycliques **6b**,**d**,**g** sont isolés exclusivement (Tableau 1). Le rendement global d'obtention des dérivés **5** et **6** est de l'ordre de 60-80% après purification par colonne chromatographique.

Tableau 1 Rendements de la réaction de formation des composés **5**, **6** et**7**

R		**5 (rendement %)**	**6 (rendement %)**	**7 (rendement %)**
Me (Ala)	**a**	15	58	68
Bn(Phe)	**b**	-	76	76
Pro-résidu	**c**	87	-	70
H(Gly)	**d**	-	58	-
i-Pr (Val)	**e**	37	34	79
i-Bu (Leu)	**f**	9	76	70
Trp-résidu	**g**	-	83	67

CH_2STr (CysTr)	**h**	60	-	94

La séparation des composés sous forme ouverte **5** et cyclique **6** a été réalisée par colonne chromatographique flash (cas des dérivés de la valine et de la leucine). La caractérisation des composes de structures ouvertes ou fermées ont été possible par comparaison entre les valeurs des déplacements chimiques des protons (RMN) et les données obtenues par radiocristallographie.

L'étape suivante pour la synthèse de prodrogues d'amidines consiste en la transformation du groupement cyano en fonction amidoxime. Les amidoximes **7** sont alors obtenues à partir des esters méthyliques**5a**,**e**,**f**,**h** et/ou des esters méthyliques **6a**,**b**,**e-g** avec de bons rendements (67-79%) par simple traitement avec le chlorhydrate de l'hydroxylamine dans le méthanol (Schéma 4, Table 1).

En effet, que ce soit à partir d'un dérivé d'acide aminé de structure ouverte **5** ou de sa forme correspondante cyclique **6** un unique produit de type amidoxime **7** est obtenu.

Aucune amidoxime cyclique n'a été reportée (sa formation aurait pu être attendue selon la condensation précédemment rapportée de l'analogue de benzène 3-imino-1-oxoisoindoline avec l'hydroxylamine).

Le seul produit formé à partir de la réaction du glycinate de méthyle avec l'acide **4** a été analysé par diffraction des rayons X du monocristal. Les résultats montrent que ce produit adopte la structure **6d** (Figure 1).

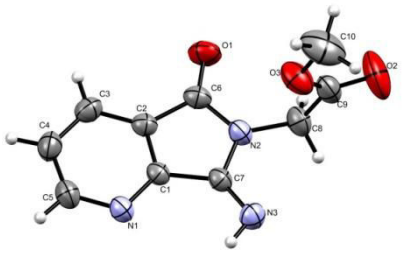

Figure 1 Structure moléculaire du compose **6d** (radiocristallographie)

A partir des données de radiocristallographie, il s'avère que le composé **6d** adopte la configuration E de la liaison C=N avec de plus une orientation *syn* du proton du cycle aromatique NH, et ceci pour des raisons stériques évidentes.

Dans le cas du dérivé du tryptophane **6g**, une très petite quantité de cristaux d'une substance inattendue **6g'** a été isolée du mélange réactionnel (Figure 2). Contrairement au produit cyclique majeur **6g**, ce composé inattendu présente une structure ouverte, régioisomère de la forme ouverte non isolée de **6g**. Bien que l'acide cyanonicotinique de départ ait été obtenu en tant que composé individuel de pureté à 100% (selon les données LC/MS), la présence de cet ester isomère **6g'** pourrait résulter d'une impureté d'acide 3-cyanopicolinique présente et non détectée avec l'acide 2-cyanonicotinique **4**.

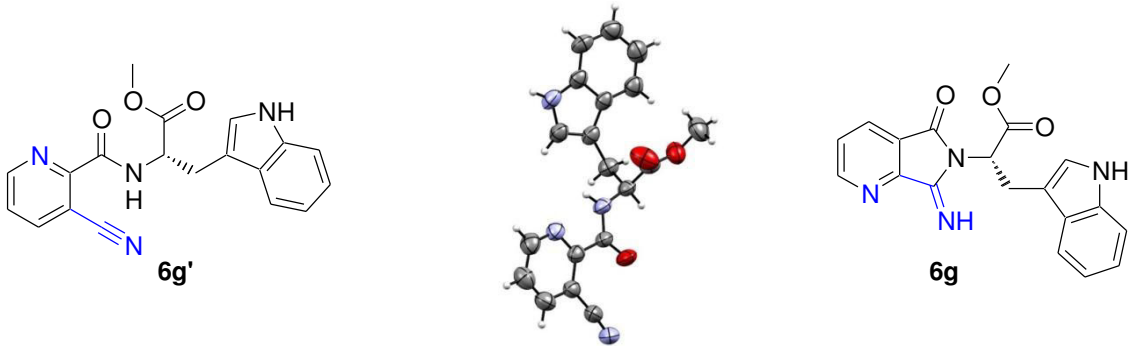

Figure 2 Structures des composés **6g'** et **6g**

L'analyse par RMN et diffraction des rayons X du pseudopeptide **7b** représenté ci-dessous ont confirmé la présence d'un seul et unique isomère structural à chaîne ouverte de l'acide nicotinique (Figure 3). Ainsi, la réaction des esters de pyrrrolopyridine avec l'hydroxylamine s'est poursuivie avec une ouverture sélective et inattendue du cycle au niveau du lien C-N le plus proche de la fraction du groupe imino. La même régiochimie est observée pour tous les autres produits **7a**,**b**,**e-h** formés à partir de cette réaction.

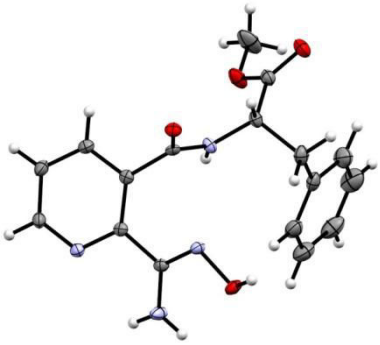

Figure 3 Structures moléculaires des composés **7b** (étude par diffraction des rayons X)

La synthèse d'amidoximes en série pyrazine a été réalisée en deux étapes selon la stratégie élaborée précédemment en série pyridine: couplage de l'acide 3-cyanopyrazine-2-

carboxylique **4'** avec différents esters méthyliques d'acides L-α-aminés (Ala, Phe et Pro) puis réaction des nitriles obtenus avec le chlorhydrate d'hydroxylamine (Schéma 5). Comme en série pyridine, l'EDCI en présence de HOBt a été utilisé comme agent de couplage. Par contre pour des raisons de solubilité du produit de départ, le tétrahydrofurane a été utilisé comme solvant au lieu du dichlorométhane.

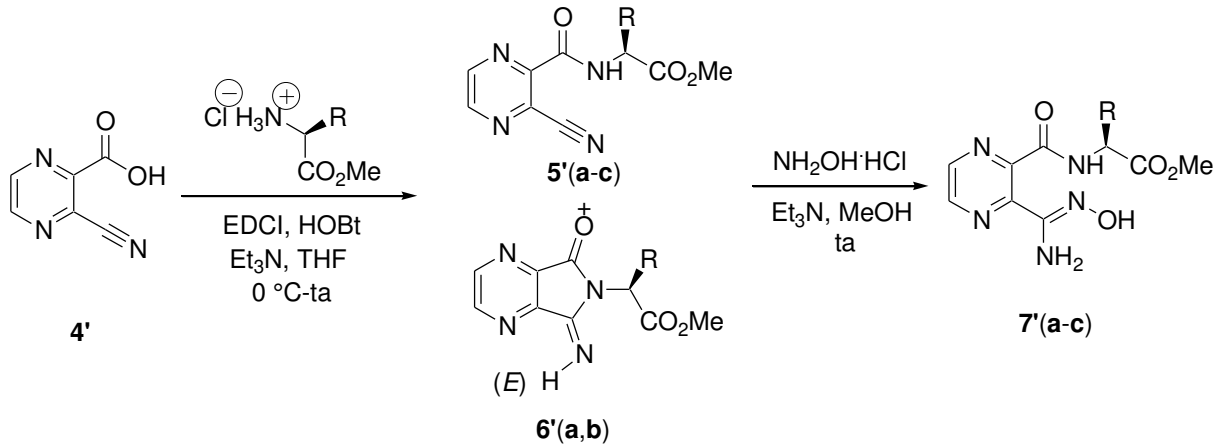

Schéma 5 Synthèse des pseudodipeptides **5'-7'**(Ala, Phe, Pro)

Lors de cette réaction les pseudodipeptides **5'a**,**b** ont été obtenus en mélange avec les produits cycliques pyrrolopyraziniques tautomères **6'a**,**b**. La séparation et la purification des dérivés **5'**et **6**' ont été réalisées par chromatographie sur colonne et ont permis d'isoler les produits ouverts **5'a**,**b** et cycliques **6'a**,**b** (Tableau 2). Lorsque l'alanine a été utilisée, les deux produits **5'a** et **6'a** ont été obtenus dans des proportions assez similaires alors que dans le cas de la phénylalanine, la forme cyclique **6'b** était très largement prédominante.

Tableau 2 Rendements d'obtention des composes **5'**, **6'** et**7'**

R		**5' (rendement %)**	**6' (rendement %)**	**7' (rendement %)**
Me (Ala)	a	23	28	84
Bn (Phe)	b	3	65	63
Pro-résidu	c	49	-	94

Comme en série pyridine, les amidoximes de la famille **7'** peuvent être préparées efficacement soit à partir du composé à chaîne ouverte ou cyclique **5'** ou **6'** ou soit à partir du mélange des deux composés **5'** et **6'** par réaction avec le chlorhydrate d'hydroxylamine (Schéma 5, Tableau 2).

L'analyse par diffraction des rayons X de l'amidoxime **7'b** (Figure 4) a révélé que la liaison C=N de la fonction amidoxime était de configuration *Z*, au même titre que son analogue de la série pyridine **7b**. Cependant, contrairement au dérivé pyridinique **7b**, le groupe NH du composé de pyrazine **7'b** est projeté plus vers l'intérieur du plan formé par la chaîne principale (distance NH...N est 3,14 Å, angle NH...N 78°).

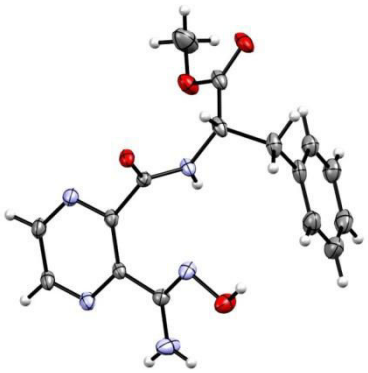

Figure 4 Structure moléculaire du (2*S*)-2-({[3-(*N'*-hydroxycarbamimidoyl)pyrazin-2-yl]carbonyl}amino)-3-phénylpropanoate de méthyle **7'b** (étude par diffraction des rayons X)

La formation des pseudopeptides **7**, **7'** a été réalisée à partir des esters **6**, **6'** par ouverture du cycle pyrrolidine par l'hydroxylamine pour donner les mêmes composés amidoxime à chaîne ouverte que celles obtenues à partir des cyanoesters correspondants **5**, **5'** (Schéma 6). Cependant, une petite quantité d'un produit secondaire, l'hydroxyiminopyrrolopyridinone **I** ou **II** a été isolée après traitement et/ou purification des amidoximes correspondantes sur colonne chromatographique.

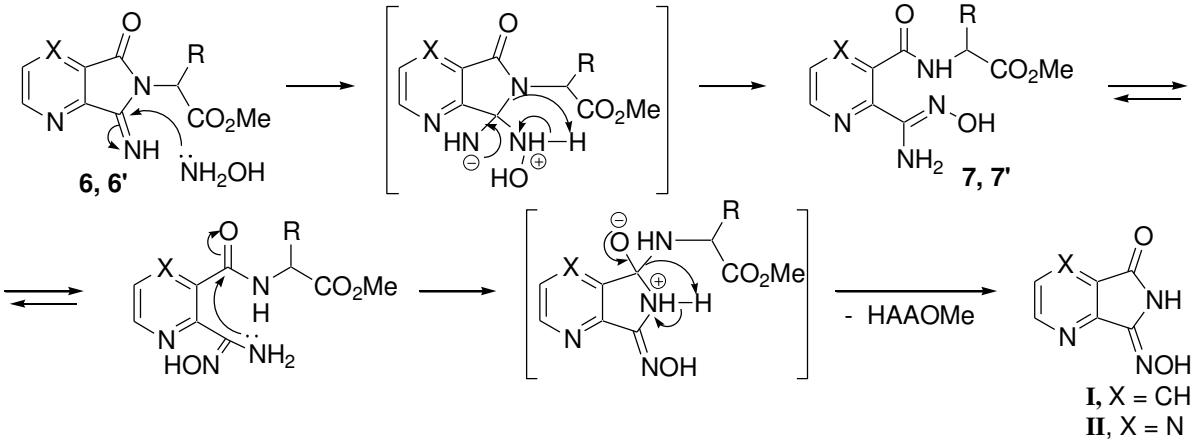

Schéma 6 Mécanisme proposé pour la formation des amidoximes **7**, **7'**et des oximes **I**, **II** *via* l'ouverture de la pyrrolidine par l'hydroxylamine

Après une période prolongée de stockage ou de chauffage de l'amidoxime, un précipité correspondant au composé **I** a été observé. Lors de l'analyse par LC/MS, l'ion de l'oxime **I** a été détecté comme impureté dans certains cas (**7e**,**f**) ou comme un métabolite de l'ion principal qui est supposé être dû à la dégradation de la molécule étudiée dans les conditionsd'analyse par LC/MS.

La formation d'hydroxyiminopyrrolopyrazinone **II** en tant que produit secondaire n'a été observée qu'après un long stockage des amidoximes de pyrazine **7'**. De plus, dans nos tentatives de cristallisation du dérivé d'alanine, il a été possible d'obtenir le cristal de l'oxime correspondante **II** comme sous-produit (Figure 5).

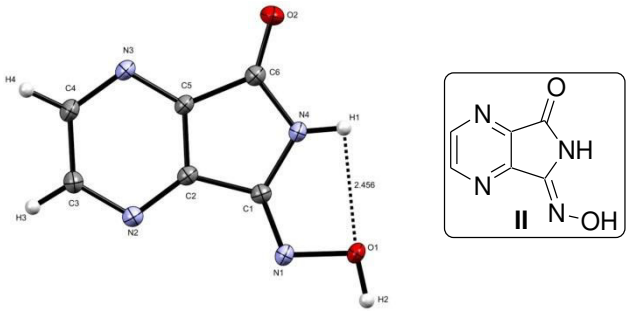

Figure 5 Structure moléculaire de la (7*Z*)-7-(hydroxyimino)-6,7-dihydro-5*H*-pyrrolo[3,4-*b*]pyrazin-5-one**II** (en accord avec les résultats par diffraction des rayons X)

Comme il en ressort des données de radiocristallographie, la liaison C=N du composé **II** adopte la configuration *Z*. La molécule présente une interaction entre H1-O1 de 2,43 Å (plus court que la somme des rayons de Van der Waals des atomes d'hydrogène et d'oxygène qui est de 2,72 Å).

Le couplage avec l'ester méthylique de la proline génère nécessairement le dérivé à chaîne ouverte **5c**, **5'c** avec des rendements respectifs de 87 et 49%. Les amidoximes de proline **7c**, **7'c** correspondantes ont été synthétisées, comme décrit précédemment, par traitement avec du chlorhydrate d'hydroxylamine dans du méthanol avec des rendements de 70 et 93%.

Les spectres RMN de ces composés couplés à la proline ont révélé deux jeux de signaux dans le $CDCl_3$ à température ambiante: ils correspondent aux rotamères des liaisons amide *cis* et *trans* qui sont énergiquement proches dans le cas de la proline à la différence de la majorité des acides aminés naturels pour lesquels adoptent préférentiellement une configuration *trans* de la liaison peptidique. A partir des spectres RMN ^{1}H, RMN ^{13}C et

NOESY des dérivés **5c, 5'c, 7c, 7'c**, il a été possible d'attribuer et d'estimer le rapport approximatif de ces rotamères. Les pics de corrélation observés dans les spectres NOESY de **5c** correspondent à l'interaction spatiale entre le proton en position C4 du cycle pyridine et les protons en position C5 du résidu pyrrolidine et, de ce fait, indiquent que le produit majoritaire est l'isomère *trans* (en conséquence, le produit minoritaire est l'isomère *cis*) (Figure 6).

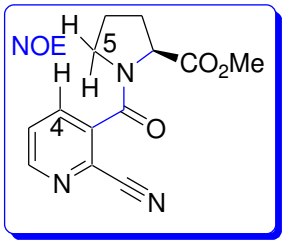

Figure6 Corrélation observée par effet NOE dans le dérivépyridinique**5c**

Les attributions des dérivés de pyrazine couplés à la proline **5'c**, **7'c** ont été réalisés après étude des déplacements chimiques des spectres RMN ^{13}C (effectués dans le $CDCl_3$) des atomes de carbones α et δ. En effet dans les dérivés de la proline, le signal correspondant au carbone α du rotamère *trans* est blindé par rapport à celui du rotamère *cis* en raison de la position *syn* par rapport à l'atome d'oxygène du carbonyle des amides. Le signal du carbone δ, devrait être cependant plus blindé dans l'isomère *cis*. En effet, dans les conformères *trans* de **5'c**, **7'c**, les déplacements chimiques du carbone α se situent entre 59,3 et 60,2 ppm tandis que dans la forme *cis*, ils se retrouvent de 61,1 à 61,4 ppm.

Les populations des deux isomères *cis* et *trans* de la liaison amide ont été mesurées grâce au spectre RMN ^{1}H par intégration des signaux bien résolus. Les contributions majoritaires de ce mélange ont été clairement déterminées par spectroscopie RMN comme étant les conformères *trans* (Tableau 3).

Tableau 3 Population *cis/trans* du lien amide des isomères **5c**, **5'c**, **7c-9c**, **7'c-9'c** mesurée à partir du spectre RMN ^{1}H effectué dans le $CDCl_3$

X		**Ratio pour 5 (*trans/cis* %)**	**Ratio pour 7 (*trans/cis* %)**
CH	c	77/23	68/32
N	'c	54/46	74/26

Nous avons également décidé d'étendre ce protocole afin de synthétiser de nouveaux pseudotripeptides avec le motif «pyrazineamidoxime» en position *N*-terminale dans le squelette. Le dipeptide proline-phénylalanine a été sélectionné afin de pouvoir étudier les effets stériques de la substitution C-terminale de la proline sur l'équilibre d'isomère amide du substitut simplement substitué par la proline (modèle). De même, la substitution ortho sur un fragment non peptidique par un dipeptide doit permettre d'augmenter la rigidité conformationnelle.

Le couplage peptidique de l'acide **4'**avec le dipeptide H-Pro-Phe-OMe a été réalisé en présence de HATU/HOBt et a permis d'isoler le nitrile correspondant **5'd** avec un rendement de 68%. Le traitement de ce dernier avec du chlorhydrate d'hydroxylamine en présence de triéthylamine a permis d'obtenir la molécule cible **7'd** avec un bon rendement (Schéma 7).

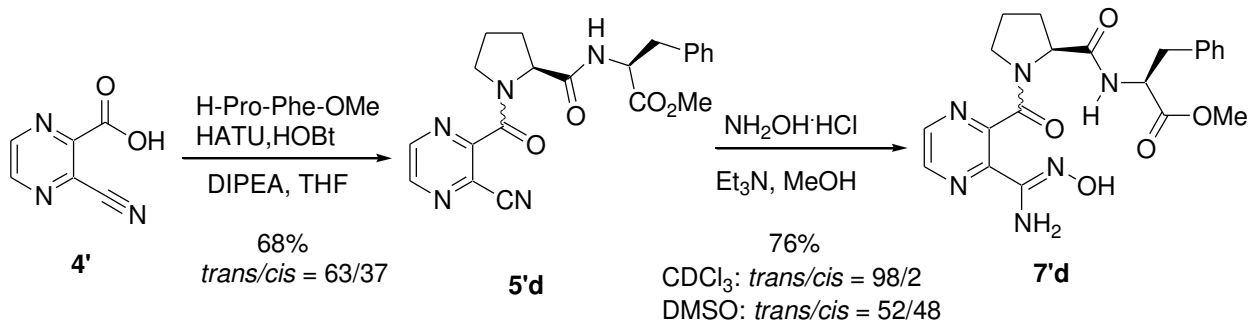

4' **5'd** **7'd**

Schéma 7 Synthèse des pseudotripeptides **7'd**

L'analyse des propriétés structurales du motif pyridine amidoxime ajouté en *N*-terminal du pseudo peptide a été faite afin de déterminer son utilisation pour de futures applications. La spectroscopie infrarouge (FT-IR) combinée à la RMN du proton ont permis d'apporter des réponses quant à la conformation adoptée par **7'd** en solution. Les expériences FT-IR de **7'd** à 25°C montrent une bande large à 3319 cm^{-1} synonyme qu'au moins proton NH et/ou OH est impliqué dans une liaison hydrogène. Dans la région de carbonyle six bandes sont présentes (Tableau4).

Tableau 4 Région d'adsorption des C=O de AOPzPhe (**7'b**), AOPzPro (**7'c**) et AOPzProPhe (**7'd**) dans le chloroforme à température ambiante (10 mM)

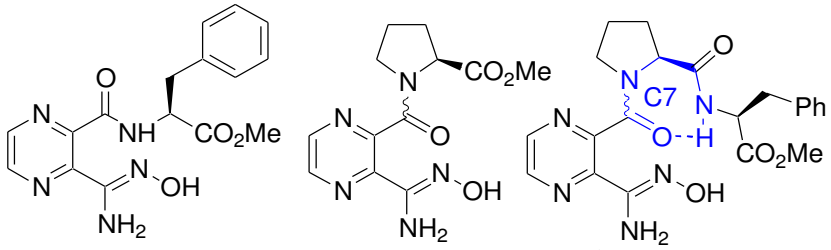

Produit	ν, cm^{-1} (C=O ester)	ν, cm^{-1} (C=O amide)	ν, cm^{-1} (C=N)
AOPzPhe	1743/1691	1680	1659
AOPzPro	1743	1655	1642
AOPzProPhe	1743/1722	1679 1670/1656	1653

Le nombre de bandes dans les spectres infrarouge indique qu'au moins deux ou trois groupes carbonyle sont impliqués dans des liaisons hydrogène: ils ont été attribués en fonction de leur longueur d'onde: les deux bandes à 1743 cm^{-1} et 1722 cm^{-1} correspondent au C=O du groupe ester, respectivement libre et impliqué dans une liaison hydrogène. Les quatre bandes suivantes ont été attribuée à partir des spectres infrarouge des peptides plus petits **7'b** et **7'c**, comprenant un acide aminé et un motif pyrazineamidoxime (Tableau 4).

Donc la vibration d'élongation d'un CO amide à 1679 cm^{-1} correspond au groupe carbonyle de la proline et est proche des valeurs obtenues pour AOPzPhe (**7'b**). Les bandes à 1670 cm^{-1} et 1656 cm^{-1} ont été attribuées au carbonyle amide entre le groupe pyrazine et le dipeptide proline-phenylalanine sous les formes liée et libre.

Les résultats obtenus à partir des analyses infrarouge ont ensuite été corroborés par des expériences 1D RMN dans des mélanges de solvants qui montrent que dans les conditions de la RMN à chaque instant deux jeux de signaux sont présents pour chaque point.

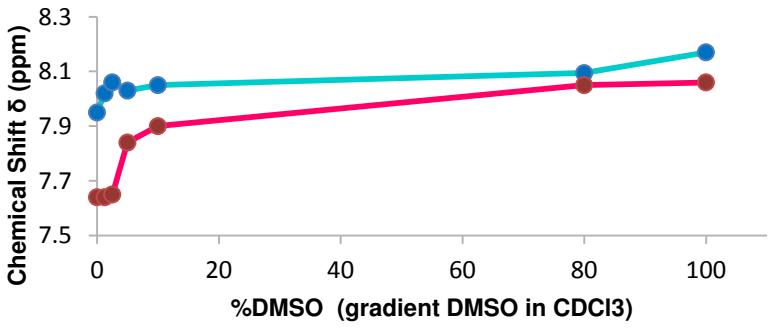

Figure 7 Variation des déplacements chimiques du proton NH de **7'd** en fonction du ratio $CDCl_3$/DMSO-d_6 (3 mM)

Ces résultats sont en adéquation avec une isomérie *cis/trans* autour du lien peptidique de la proline. De plus, pour les deux conformères le proton amide de la phénylalanine de présente une différence très important ($\Delta\delta$ = +0,22 et +0,42 ppm), ce qui signifie que dans les deux conformations le proton NH est impliqué dans une liaison hydrogène intra-moléculaire. Ce résultat est en accord avec la bande large observée à une longueur d'onde inférieure à 3400 cm^{-1} en spectroscopie infrarouge. De fait, le NH amide de la phénylalanine est impliqué dans une liaison hydrogène avec le groupe carbonyle de la pyrazine (1656 cm^{-1}); ils forment un coude – γ en C7.

Afin de confirmer ces observations nous avons effectué des calculs de dynamique moléculaire en solvant explicite sans contraintes. Ces simulations confirment les résultats expérimentaux de l'IR et de la RMN: deux liaisons hydrogène sont possibles - la première entre le carbonyle du groupe ester terminal et l'hydrogène de la fonction alcool du de l'amidoxime et la seconde entre le groupe carbonyle proche de noyau pyrazine et le proton amide de la phénylalanine qui forme un coude γ (Figure 8).

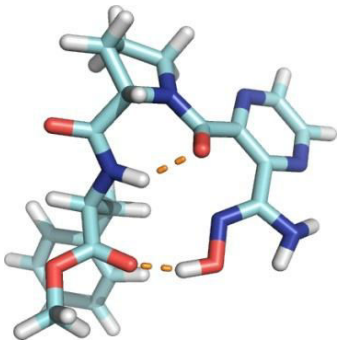

Figure 8 Conformation de pseudopeptide **7'd** issue de calculs de dynamique moléculaire en solvant explicite; les liaisons hydrogène sont représentées en orange

Les simulations menées dans le DMSO montrent que la liaison hydrogène entre le groupe OH et le carbonyle, et une augmentation drastique du rotamère *trans* (jusqu'à 98%) dans un solvants non polaire comme le chloroforme.

La superposition des structures issues de la simulation dans $CHCl_3$ du pseudotripeptide **7'd** et de ses analogues plus courts **7'b** et **7'c** montre que le motif amidoxime-pyrazine induit de la rigidité dans les molécules (Figures 4, 5 dans l'Annexe).

L'étape suivante a été la mesure des angles dièdres φ, ψ et ω des trois molécules AOPzPhe **7'b**, AOPzPro **7'c** et AOPzProPhe **7'd**. Les résultats montrent sur toute la trajectoire de la dynamique moléculaire que les angles ω sont consistants avec une conformation *trans* de la liaison peptidique (Tableau 5).

Tableau 5 Valeurs moyennes des angles dièdres provenant des 25000 structures obtenues par calculs de dynamique moléculaire

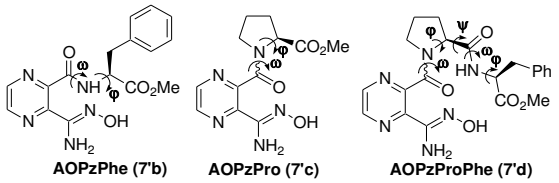

	φPro	φPhe	ψ	ωPro	ωPhe
AOPzProPhe (**7'd**)	-71±9	-139±18	|19±14|	|171±6|	|169±7|
AOPzPro (**7'c**)	|169±7|	-	-	|168±7|	-
AOPzPhe (**7'b**)	-	|94±57|	-	-	|156±21|

Toutes les valeurs des angles φ et ψ de la proline du pseudopeptide **7'd** sont reportées dans le diagramme de Ramachandran (Figure 9). Ce diagramme montre que ces valeurs restent dans les zones permises pour les peptides naturels (φ, ψ = -61°, -35°).

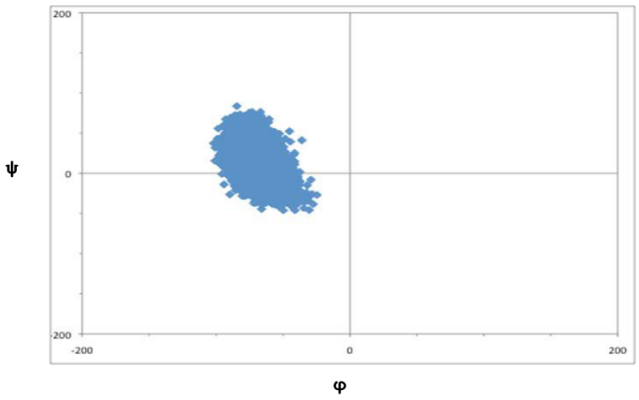

Figure 9 Diagramme de Ramachandran du résidupseudotripeptide **7'd**

Enfin, une étude concernant la toxicité cellulaire des composés a été réalisée afin de vérifier leur potentielle utilisation comme agents thérapeutiques (Figure 10).

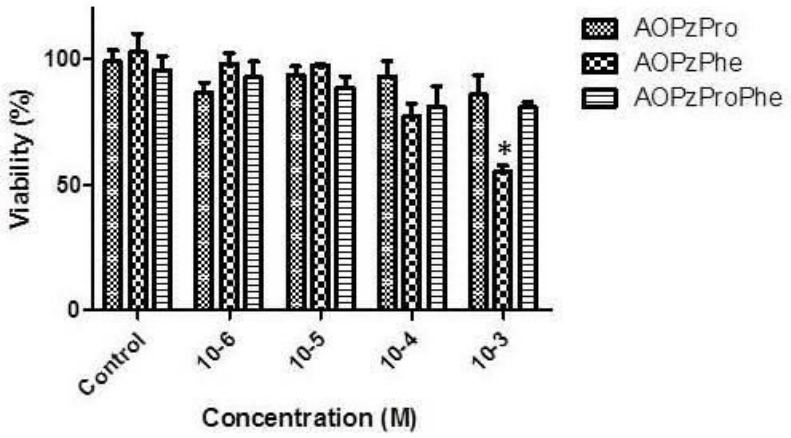

Figure 10 Etude de cytocompatibilité des trois dérivés pyrazineamidoxime (AOPzPhe (**7'b**), AOPzPro (**7'c**) et AOPzProPhe (**7'd**)) réalisée *in vitro* sur la lignée cellulaire de muscle lisse (A-10) par rapport aux cellules témoins (culture moyen). Les cellules A-10 ont été traitées avec les concentrations indiquées de dérivés **7** pendant 24 h à 37° C. La viabilité a été estimée par le test MTT.

Les cellules portant une activité mitochondriale comprise entre 100 et 80% sont considérées comme viables. Les molécules AOPzPro (**7'c**) et AOPzProPhe (**7'd**) ne présentent aucune toxicité quelle que soit la concentration étudiée. Par contre, la molécule AOPzPhe (**7'b**) affiche une toxicité au-dessus d'une concentration de 10^{-3} M. Ce résultat renforce l'idée de pouvoir utiliser le squelette pyrazine-amidoxime couplé à la proline en thérapeutique. Cependant, il ne faut pas totalement exclure la troisième molécule ne possédant pas de proline puisqu'au cours d'un traitement médical la concentration très élevée de 10^{-3} M ne sera probablement jamais atteinte.

Réaction d'estérification des peptidomimétiques amidoximes et formation du cycle 1,2,4-oxadiazole

L'estérification d'amidoximes par des acides aminés et la condensation en oxadiazoles permettent d'envisager l'accès à des composés de type double pro-drogue créant des dérivés d'amidines (disponibilité orale améliorée et meilleure solubilité dans l'eau). De plus, le cycle 1,2,4-oxadiazole est utilisé depuis longtemps comme isostére du groupe amide et/ou ester en raison de sa haute résistance à la dégradation métabolique. Des molécules contenant ce cycle 1,2,4-oxadiazoles dérivés d'α-aminoacides ont déjà été employées comme blocs de construction de peptidomimétiques, inhibiteurs de la dipeptidyl peptidase IV (DPP-4),

inhibiteurs du domaine SH2 de Src (régulateur de cascades de signalisation intracellulaire), inhibiteurs de la sphingosine kinase (pour ralentir la croissance tumorale ainsi que sensibiliser les cellules cancéreuses à des agents chimiothérapeutiques) et immunomodulateurs.

Tout ceci montre l'intérêt de la synthèse et caractérisation de nouvelles amidoximes estérifiées en série pyridine (ou pyrazine) et de peptidomimétiques possédant ce cycle 1,2,4-oxadiazole obtenus après transformation de la fonction amidoxime. La réaction s'effectue en deux étapes distinctes et a permis d'accéder aux 1,2,4-oxadiazoles désirées **9**, **9'** (Tableau 6).

Tout d'abord, la L-valine protégée par un groupement Boc est estérifiée avec les amidoximes correspondantes portant des résidus Ala et Phe. Cette étape a été réalisée après utilisation du couple DCC/DMAP dans de l'acétonitrile anhydre et a permis de générer les *O*-acylamidoximes **8**, **8'**(**a**,**b**).

Tableau 6 Synthèse des pseudopeptides possédant le motif 1,2,4-oxadiazole **9**, **9'** (**a**,**b**)

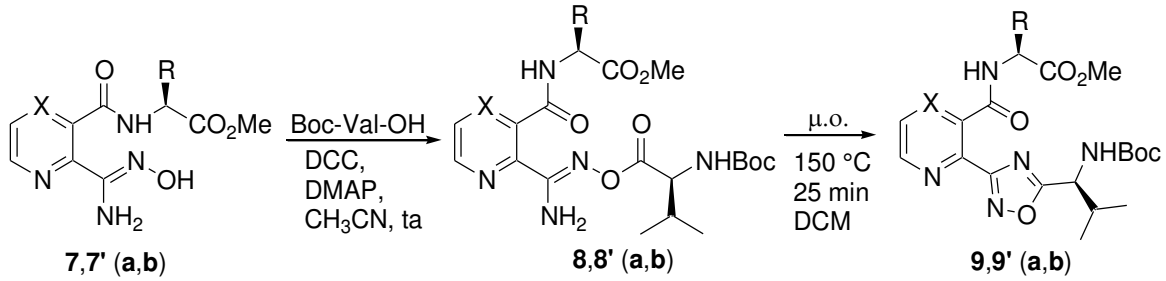

X	R		8, 8' (rendement, %)[a]	9, 9' (rendement, %)[a] (conversion, %)[b]
CH	Me (Ala)	**a**	64	63 (66)
CH	Bn (Phe)	**b**	91	81 (83)
N	Me (Ala)	**a**	84	75 (77)
N	Bn (Phe)	**b**	67	94 (96)

[a]Rendement après purification.
[b]Conversion déterminée par analyse LC/MS.

Les esters **8**, **8'** ont été chauffés sous irradiation par micro-ondes pour donner les 1,2,4-oxadiazoles **9**, **9'**. Différents solvants, températures et temps de réaction ont été explorés afin de trouver les conditions permettant la meilleure conversion. Par cette technologie, la réaction effectuée dans le dichlorométhane à 150 °C pendant 25 minutes a permis d'observer la meilleure conversion (déterminée par analyse par LC/MS) en un temps optimal et d'obtenir

les *O*-acylamidoximes **8**, **8'** (**a**,**b**) avec des rendements de 64-91%. La cyclodéshydratation assistée par micro-ondes, a quant à elle, donné les 1,2,4-oxadiazoles **9**, **9'** avec des rendements de 63-94%. Les rendements sont meilleurs en ce qui concerne les 1,2,4-oxadiazoles en série pyrazine et ceci peut être expliqué par l'effet stabilisant d'une interaction NH...N seulement envisageable sur ces dérivés de la pyrazine. En série pyridine, une réduction du rendement de l'ordre de 10% a été observée suite à la formation et détection par analyse LC/MS d'un sous produit non désiré de réaction (pyrrolopyridine **6**, Tableau 6).

Ensuite, la L-phénylalanine a été introduite sur des amidoximes de proline **7c** et **7'c** afin d'étudier la propension de la liaison amide à être en conformation *cis* (qui est élevée dans le cas où la proline est précédée d'un résidu aromatique). Par conséquent, les amidoximes **7c**, **7'c** ont été mises en contact avec la phénylalanine *N*-protégée pour former les esters attendus **8c** et **8'c** avec des rendements quantitatifs (Tableau 6). Enfin, la condensation effectuée sous irradiation micro-ondes de la solution de **8c**, **8'c** dans du dichlorométhane (récipient fermé, 300W, 150 °C, 25 min) a fourni les dérivés de type 1,2,4-oxadiazole **9c** et **9'c** avec des rendements respectifs de 58% et 76%.

Tableau 7 Synthèse de pseudopeptides possédant le cycle 1,2,4-oxadiazole (résidu proline)

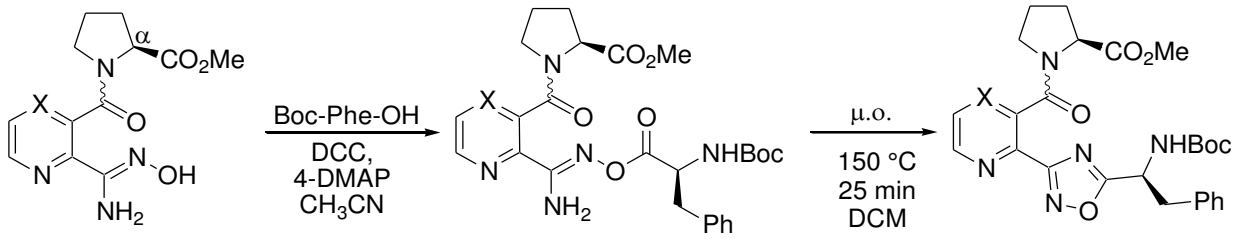

7,7' c **8,8' c** **9,9' c**

X		Rendement, %	Conversion, %
CH	**8c**	quantitatif	-
CH	**9c**	58	65
N	**8'c**	quantitatif	-
N	**9'c**	76	80

Le rapport entre les différents rotamères a été défini à partir des spectres RMN 1D ^{1}H et ^{13}C ainsi que des spectres 2D-NOESY. Dans les spectres NOESY de **8c** et **9c**, des pics de corrélation indiquent que l'isomère majoritaire est l'isomère *cis*. En ce qui concerne les dérivés proline pyrazine **8'c** et **9'c** l'attribution des déplacements chimiques des carbones α et δ des spectres enregistrés dans le $CDCl_3$ ont été définis par rapport à celles des dérivés **5'c** et

7'c précédemment réalisées.

Les spectres infrarouge des composés amidoxime estérifiés **8**, **8'** montrent que dans le chloroforme, à une concentration de 10 mM seulement des NH non investis dans des liaisons hydrogène sont visibles.

Les spectres infrarouge des dérivés pyrazine Ala- et Phe- **9a**,**b**, montrent que dans les mêmes conditions deux bandes correspondant à l'élongation des liaisons NH ont des valeurs au-dessus de 3400 cm^{-1}. Alors que pour les dérivés pyrazine 1,2,4-oxadiazoles les fréquences de vibrations observées sont 3398 cm^{-1} et 3395 cm^{-1} correspondant à des NH impliqués dans des liaisons hydrogène.

Dans les spectres infrarouge des dérivés pyrazine oxadiazole **9'c** on observe des bandes à 3438 cm^{-1} et 3363 cm^{-1} correspondant aux NH libres et liés dans une liaison hydrogène respectivement. Ces bandes sont présentes à 10 mM ainsi qu'à des concentrations diluées confirmant l'absente d'interaction intermoléculaires.

L'analyse de la région des vibrations d'élongation des CO, dans le $CHCl_3$ n'a pas permis l'attribution des bandes correspondant aux CO liés, probablement à cause de leur faible intensité et du recouvrement avec d'autres bandes. Nous avons également supposé qu'il pouvait exister une interaction faible entre le NH, lorsque le CO de l'ester est orienté vers l'extérieur pour former une interaction C=O...C=O n $\rightarrow\pi^*$ (Figure 11).

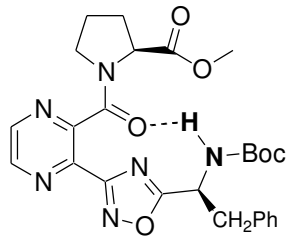

9'c

Figure 11 Interaction intramoléculaire supposée dans le dérivé oxadiazole **9'c**

Les expériences FT-IR ont été complétées par des données RMN qui montrent un déplacement des liaisons hydrogène vers les hauts champs du NH amide des dérivés pyridine **8a**,**b** et **9a**,**b** du au courant de cycle du noyau pyridine. Le shift vers les bas-champs de 0,23 ppm des déplacements chimiques des NH des dérivés esters pyrazine **8'a**,**b** et des oxadiazoles **9'a**,**b** et des déplacements chimiques de NH amide de +1,27 et +1,14 ppm par comparaison avec les déplacements chimiques des dérivés oxadiazoles (pyridine et pyrazyne) permet

d'affirmer la présence d'une liaison intramoléculaire NH…N (Figure 12).

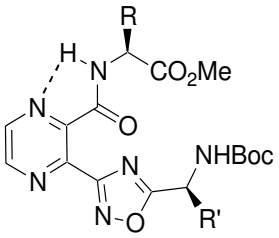

9'a,**b**

Figure 12 Interaction intramoléculaire supposée dans le dérivé oxadiazole **9'a**,**b**

On peut également noter un faible impact sur ces interactions par les effets de solvatation; pour **9'a**,**b** (à partir de 20% de DMSO) il existe une variation des déplacements chimiques des NH amide de +0,43 et +0.39 ppm.

Dans le cas des composés oxadiazolespyrazine **9'c**, les premières étapes de titration montrent un mouvement vers les bas-champs des déplacements chimiques ($\Delta\delta$ = 0,44/0,53 ppm – *trans/cis* dans 5% DMSO-d_6). Ces observations sont cohérentes avec l'implication du NHBoc dans une liaison hydrogène faible à faible concentration en DMSO-d_6 qui devient exposé au solvant à cause du changement conformationnel dans des solvants plus polaires.

Synthèse de 1,2,4-triazoles *via* les *N*-acylamidrazones

Le squelette 1,2,4-triazole se retrouve dans un grand nombre de composés possédant un large éventail d'activités biologiques et peut être également utilisé comme lien pseudopeptidique. Ainsi, divers 1,2,4-triazoles contenant des α-aminoacides chiraux ont été conçus et synthétisés. Avec un lien avec le L-Tryptophane, des composés ont été décrits comme ligands du récepteur de la ghréline (GHS-R1a) alors que lorsqu'il est lié avec la lysine d'autres molécules ont prouvé leur utilité en tant qu'inhibiteurs de l'histone désacétylase (HDAC) avec une stabilité métabolique élevée. De plus, lorsqu'il s'agit de dérivés de dipeptidiques incluant ce motif 1,2,4-triazole, un niveau élevé d'activité du système nerveux central (SNC) a été rapportée.

L'approche comprenant l'ouverture du cycle pyrrolidine des précurseurs cycliques **6, 6'** a été appliquée sur les amidoximes avec, cette fois, l'utilisation de l'hydrazide de l'acide aminé *N*-protégé afin d'obtenir des précurseurs de *N*-acylamidrazones. Tout d'abord, l'hydrazide de phénylalanine Boc-protégée a été synthétisé à partir de l'ester méthylique de la phénylalanine commercial. Après une première étape de protection par un groupement *tert*-

butyloxycarbonyle, le traitement avec de l'hydrazine monohydraté a permis de former l'hydrazide correspondant avec un rendement quantitatif (Schéma 8). Suite à cela, l'hydrazide formé est mis en contact avec une des pyrrolopyridines (ou pyrazines) **6**, **6'**(**a**,**b**) dans le méthanol à température ambiante, générant ainsi une famille de *N*-acylamidrazones. Dans ce cas précis, il n'a pas observé la formation de dérivés de pyrrolopyridines cycliques (ou pyrazines) attendus **10''**. En effet, ils auraient pu être formés selon une condensation précédemment rapportée de la 1-imino-1*H*-isoindol-3-amine et de son analogue de pyrazine avec des hydrazides d'acides aminés et qui a donné 1*H*-isoindol et le peptidomimétique possédant le motif 5*H*-pyrrolo[3,4-b]pyrazine **A** (Schéma 8).

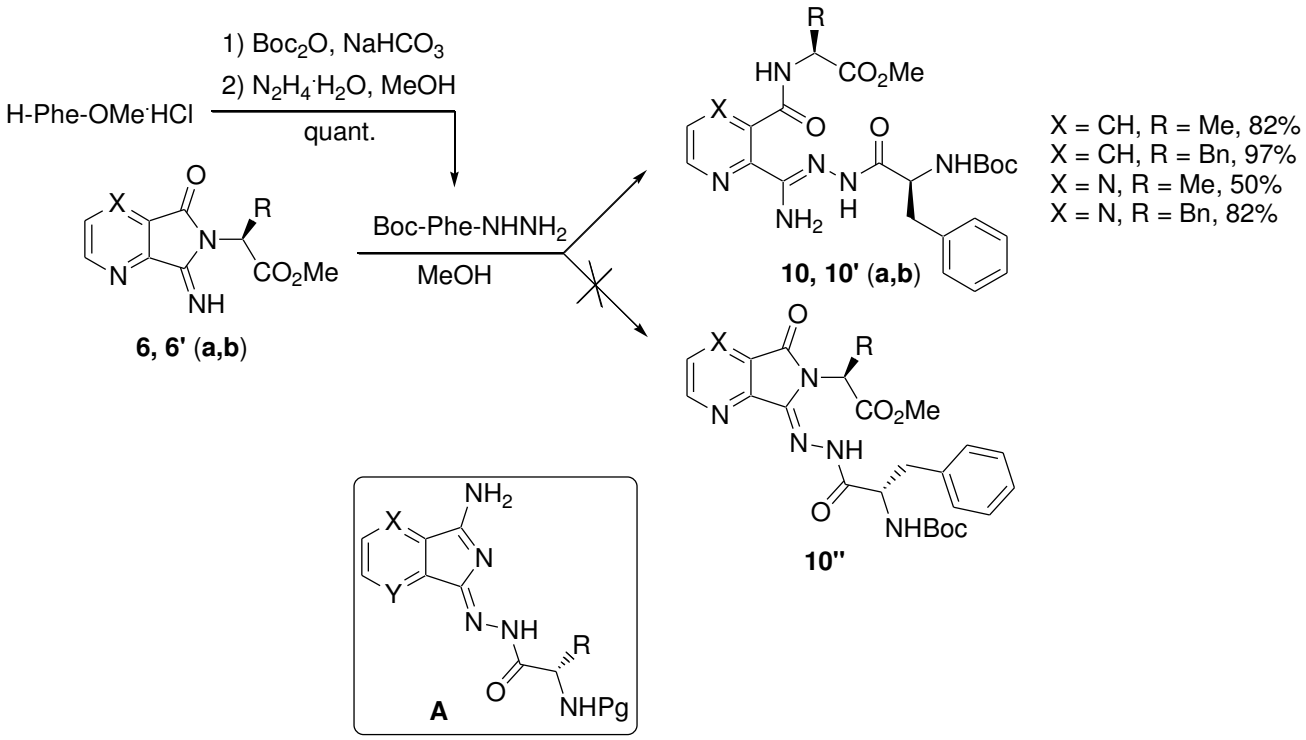

Schéma 8 Synthèse de dérivés de *N*-acylamidrazone **10**, **10'** (**a**,**b**)

La formation d'acylamidrazones **10**, **10'**, réalisée de manière analogue à la réaction impliquant l'hydroxylamine, s'est poursuivie par l'ouverture du cycle pyrrolidine par l'hydrazide d'acide aminé et a donné les produits **10a**,**b** et **10'b** avec de très bons rendements. Cependant, il ne fut pas possible d'améliorer le rendement de formation de l'acylamidrazone **10'a**, qui n'a pas pu dépasser 50%. La réactivité du composé de départ a pu être comparée à celle des précurseurs d'acylamidrazone décrits précédemment vis-à-vis des hydrazides (nucléophiles) et a permis de les comparer à des époxy imidates hautement réactifs, précurseurs d'époxy acylamidrazones.

Par conséquent, cette nouvelle approche se révèle être une synthèse simple et douce de *N*-acylamidrazones.

Deux jeux de signaux ont été observés dans les spectres RMN ^{1}H et ^{13}C de ces produits dans les DMSO-d_6. La duplication des bandes dans les spectres FT-IR sont clairement en faveur d'une isomérisation *Z/E* des composés. Nous avons trouvé dans la littérature que les composés acylamidrazones existent sous deux formes tautomères amide hydrazone (A) - hydrazide imine (B), à cause de l'isomérie *Z/E* d'une liaison C=N ou d'un lien amide (Schéma 9). A partir de ces observations l'attribution des signaux RMN est devenue plus claire.

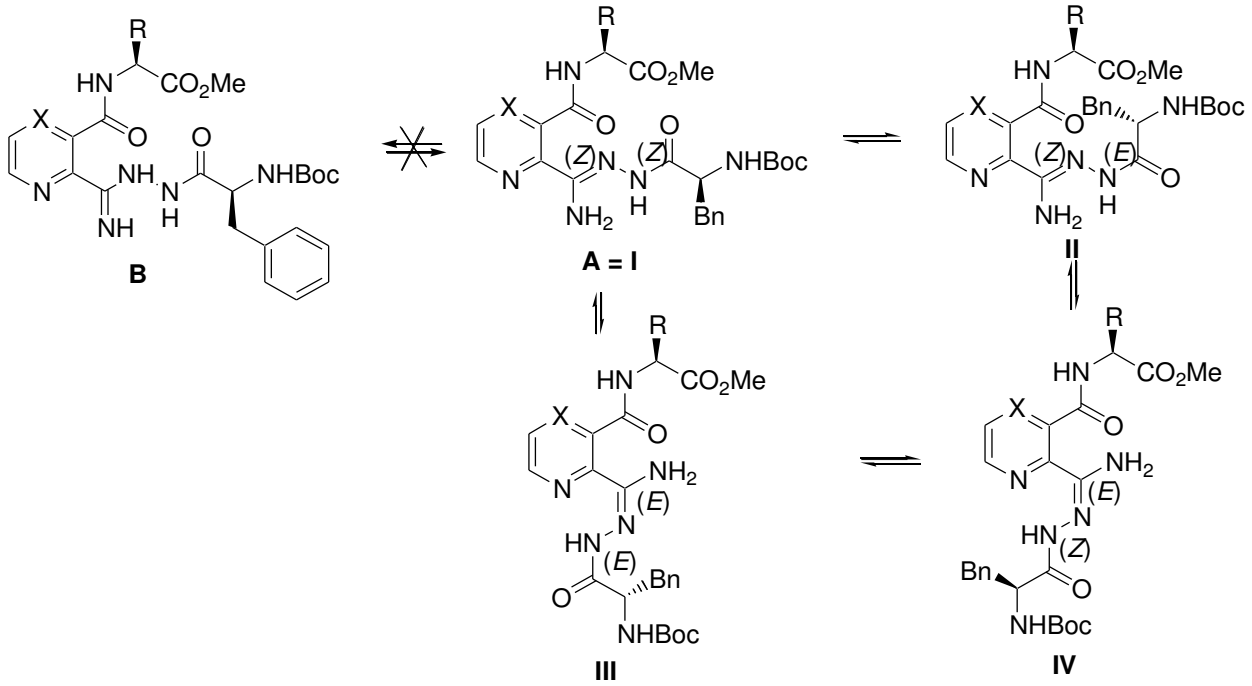

Schéma 9 Possibilité d'isomérisation des *N*-acylamidrazones **10** (X = CH) et **10'** (X = N)

Deux singulets correspondant aux signaux des NH_2 ont été notés dans les spectres RMN: nous avons donc abandonné l'hypothèse de deux formes tautomériques A et B. Pour réaliser l'attribution des deux populations, des expériences COSY et NOESY ont été réalisées. Un pic de corrélation NOE entre le groupe =N-NH et les protons NH_2 des dérivés pyridine **10b** a été observé pour chaque conformation: cela indique la présence des isomères *Z* autour de la de la double liaison C=N et confirme la possibilité de rotamères *Z* et *E* autour de la liaison amide (Figure 13).

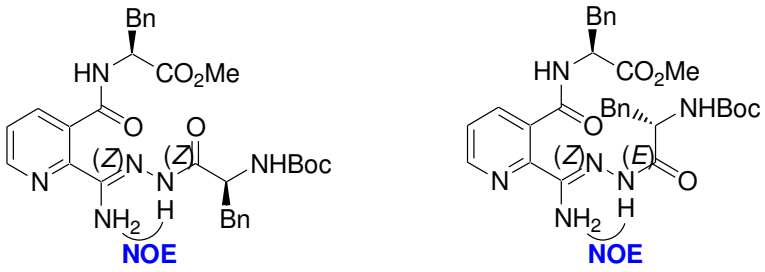

Figure 13 Effets NOE observés pour les différents isomères **10b**

Cependant, comme les protons =N-NH des analogues de la série (**10a**, **10'a**, **10'b**) ont les mêmes déplacements chimiques, nous sommes dans l'impossibilité de démontrer l'isomérisation pour ces composés. De plus, aucune corrélation qui aurait pu mettre en évidence l'un ou l'autre des isomères n'a été mis en évidence.

Afin de faire l'attribution des protons, les conformations les plus stables ont été recherchées par calcul des énergies relative et absolue pour les quatre isomères *N*-acylamidrazone (Tableau 8). Les formes I et II correspondant aux isomères amides *Z/E* ont les énergies les plus basses dans le cas des dérivés pyridine **10a**, **10b**, et donc sont les isomères les plus stables dans le vide et en accord avec les données expérimentales pour le composé **10b**. Pour les isomères III et IV les formes *E* autour de la liaison C=N ont les énergies les plus haute donc les plus défavorables. Les composés pyrazine **10'a** et **10'b** montrent une isomérisation autour de la liaison C=N, les énergies les plus basses correspondent aux conformères II et III. D'après les calculs précédents, l'isomère amide *E* possède l'énergie la plus basse dans toutes les séries. Les différences des énergies (ΔE) entre les conformères I et II **10a,b** pour les composés pyridine, et entre II et III **10'a,b** pour les analogues pyrazine étaient dans l'intervalle 2,49 à 4,91 kcal/mol et dépendent principalement de l'hétérocycle (le plus élevé pour les dérivés pyridine **10a,b** et les plus bas pour les dérivés pyrazine **10'a**,**b**).

Tableau 8 Energies absolues et relatives (unité atomiques et kcal/mol, respectivement) pour les isomères des *N*-acylamidrazones calculées (B3LYP , 6-31G(d,p))

X, **R**	**E_I [a.u.]**	**E_{II} [a.u.]**	**E_{III} [a.u.]**	**E_{IV} [a.u.]**	**ΔE [kcal/mol]**
CH, Me (**10a**)	-1751.286540	-1751.294366	-1751.280429	-1751.277908	4.91
CH, Bn (**10b**)	-1982.258785	-1982.265883	-1982.256207	-1982.252817	4.45

N, Me (**10'a**)	-1767.328071	-1767.335808	-1767.331841	-1767.326273	2.49
N, Bn (**10'b**)	-1998.299683	-1998.306963	-1998.300874	-1998.298101	3.82

Nous avons également recherché l'influence de la polarité du solvant sur le rapport des différents rotamères des acylamidrazones (Tableau 9). Nous avons alors noté une décomposition des composés pyridine **10a**,**b** après ajout du chloroforme. Les signaux RMN des protons des composés pyrrolopyridines **6** dans le mélange DMSO-d_6/$CDCl_3$ deviennent prédominants avec l'augmentation de ce rapport jusqu'à 1:3. La formation de pyrrolopyridine **6** a également été détectée par LCMS.

Tableau 9 Influence de la polarité du solvant sur le rapport *E*/Z dans les composés **10**, **10'**

	Rapport *E/Z*		
DMSO-d_6/$CDCl_3$	**1:0**	**1:1**	**1:3**
10a	1/0.63	-[a]	-[b]
10b	1/0.56	-[c]	-[d]
	Rapport *Z/E*		
10'a	1/0.70	1/0.66	1/0.50
10'b	1/0.67	1/0.69	1/0.55

[a]Mélange de **10a** et **6a** (≈ 45% de **6a**);
[b]Mélange de **10a** et **6a** (≈ 65% de **6a**);
[c]Mélange de **10b** et **6b** (≈ 35% de **6a**);
[d]Mélange de **10b** et **6b** (≈ 55% de **6a**).

Dans ce cas, il est possible de suggérer un mécanisme différent de celui proposé lors de la décomposition de l'amidoxime par l'attaque nucléophile du NH_2 sur le carbone du groupement carbonyle de l'amide. En effet, le mécanisme proposé ici considérerait, cette fois, en l'attaque nucléophile du NH sur le carbone de la double liaison C=N de l'acylamidrazone suivie par une étape de cyclisation intramoléculaire (Schéma 10).

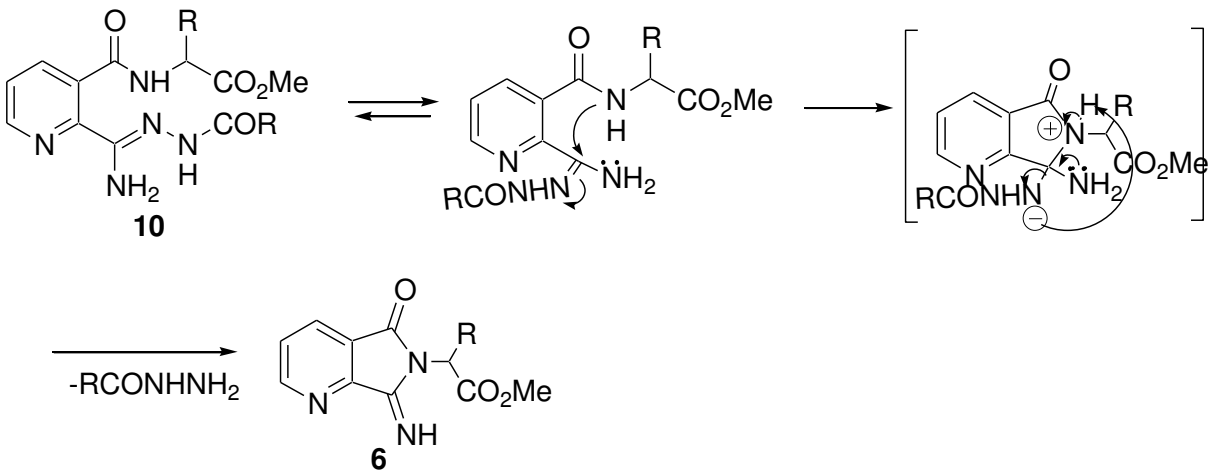

Schéma 10 Mécanisme suggéré de cyclisation intramoléculaire des composés en série pyridine **10a**, **b** dans des solvants non donneurs de liaison hydrogène

Cette cyclisation intramoléculaire est observée dans moins de 5% des analogues pyrazine **10'** et l'occurrence du conformère *Z* diminue lorsque la polarité du solvant augmente.

L'analyse de ces résultats montre clairement que dans les solvants polaires tels que le DMSO, tous les composés présentent une structure stabilisée par une liaison hydrogène. Ceci suggère qu'une liaison hydrogène entre le NH amide et l'atome d'azote du noyau pyrazine pourrait stabiliser les dérivés pyrazine et peut exister également dans des solvants non favorables à l'établissement des liaisons hydrogène, favorisant la cyclisation intramoleculaire en précurseur **6'**. Si l'on considère les conformations de plus basses énergies pour les composés acylamidrazones **10'**, calculées à partir de la fonction densité en chimie quantique, on remarque que dans **10'a** et **10'b**, une liaison hydrogène NH…N est possible avec des distances interatomiques de 2,41 Å et 2,39 Å et des angles NH…N de 99° et 100° respectivement (Figure 14).

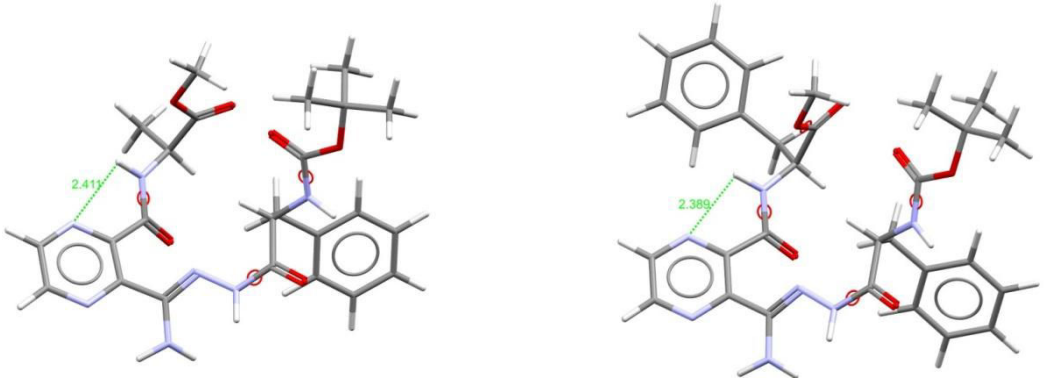

10'a **10'b**

Figure 14 Formation de la liaison hydrogène dans les conformations de plus basses énergies **10'a,b**

Dans les la littérature, plusieurs exemples de cyclisation des *N*-acylamidrazones **10**,**10'** (**a**,**b**) en 1,2,4-triazoles correspondant ont été tentés dans différents solvants (toluène, CH_3CN,THF, 1,4-doixane, MeOH) à hautes températures (60-150 °C). Cependant, dans le cas présent, seuls les composés pyrazine-acyclamidrazones **10'a**,**b** ont été convertis, alors que pour les composés analogues à base de pyridine les réactions ont invariablement conduits aux pyrrolopyridines **6** et la conversion visée en 1,2,4-triazoles n'a pas excédé un rendement de 10%, quelques soient les conditions testées (Schéma 11). Les réactions conventionnelles de cyclisation des acylamidraones **10'a**,**b** dans le toluène à 110 °C pour 18 h on conduit à des composés pyrazine-triazole**11'a**,**b** avec des rendements de 45 et 64% respectivement. L'alternative qui consiste à utiliser la synthèse sous micro-ondes a apporté plusieurs avantages: une diminution du temps de réaction de 20 minutes et une augmentation des rendements jusqu'à 87%.

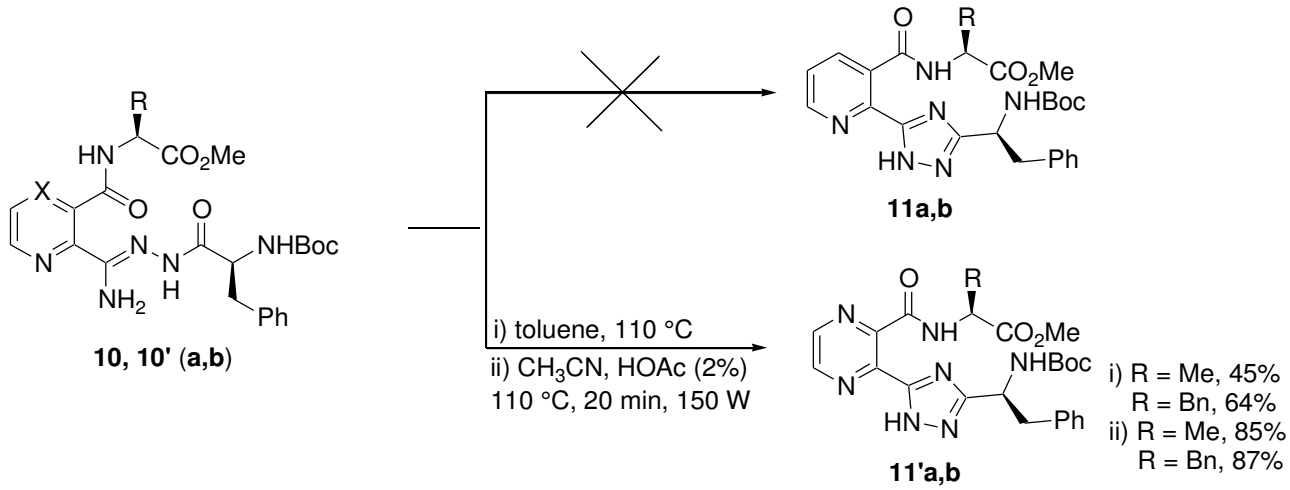

Schéma 11 Schéma de synthèse des 1,2,4-triazoles

La formation des composés pyrrolopyridines **6a**,**b** est probablement le résultat d'une décomposition thermique suivie d'une cyclisation intramoléculaire du cycle pyrrolidine.

Synthèse et étude structurale de peptidomimétiques possédant un lien hydrazide

Au cours du développement de peptidomimétiques contraints, la synthèse et l'étude structurale des composés hydrazides dérivés des amidoximes **7** et **7'** ont été envisagées. Ces

peptidomimétiques **12** et **12'** sont des composés de structure hybride d'azapeptides et d'aminoxypeptides (Figure 15).

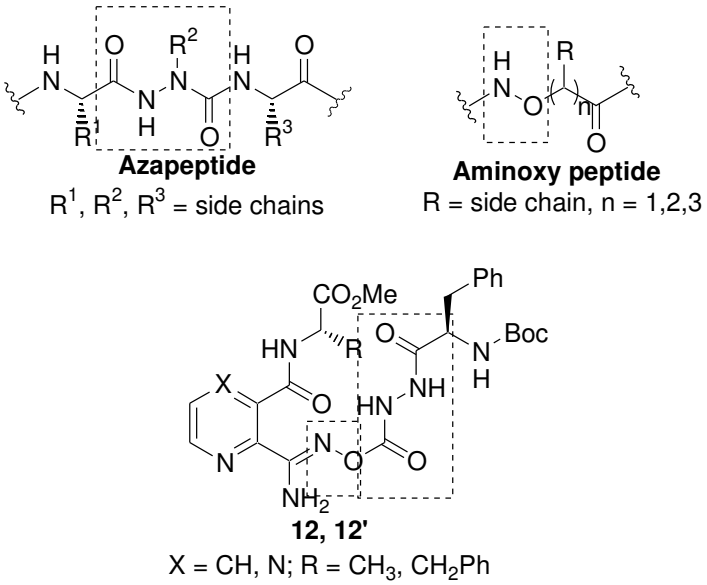

Figure 15 Structure des peptidomimétiques **12** et **12'**

La synthèse de ces molécules a été réalisée par condensation de la fonction amidoxime avec l'hydrazide de la phénylalanine par ajout d'une liaison carbonyle supplémentaire. Ce couplage a été réalisé à partir des amidoximes **7, 7'** (**a**,**b**) en série pyridine ou pyrazine traitées par du triphosgène et l'hydrazide de la phénylalanine préalablement obtenu en présence de diisopropyléthylamine dans le dichlorométhane (Schéma 12). Les dérivés de la phéylalanine **12b** et **12'b** ont été isolés après purification par CLHP préparative avec des rendements de 60 et 69% de rendements. Dans le cas des dérivés d'alanine **12a** et **12'a**, les rendements de réaction n'ont pas dépasser 44%: la réactivité plus faible de l'amidoxime correspondante vis-à-vis du triphosgène en est la cause et a conduit à une quantité accrue de produit secondaire dérivé de la condensation de l'hydrazide de la phénylalanine avec le triphosgène.

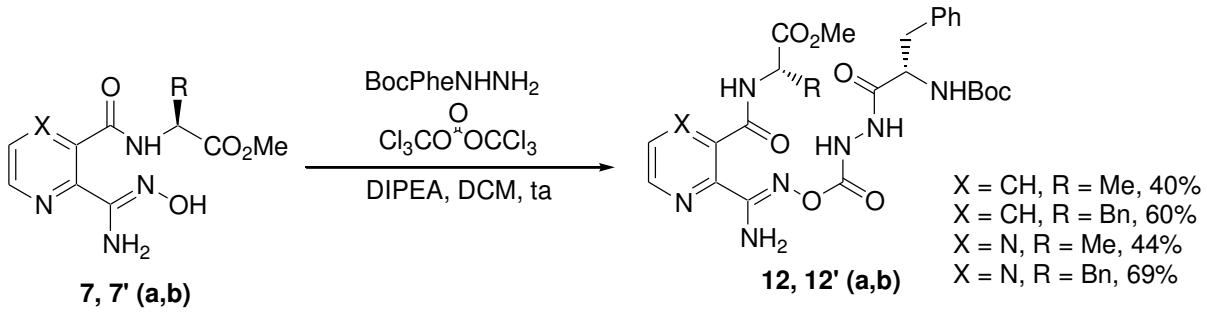

Schéma 12 Synthèse des peptidomimétiques **12** et **12'**(**a**,**b**)

L'étude en solution des conformations de mimes peptidiques **12** et **12'** a été réalisée en utilisant les spectroscopies FT-IR et ^{1}H-RMN permettant de mettre en évidence les liaisons hydrogène. Premièrement, les expériences de FT-IR des dérivés pyridine **12a**,**b** à 25 °C montrent qu'il existe une bande large en dessous 3400 cm^{-1} correspondant aux deux NH des fragments hydrazide. Malheureusement, il n'a pas été possible de distinguer les différents NH impliqués dans cette bande. Dans la région caractéristique des vibrations des carbonyles plusieurs bandes sont mises en évidences après déconvolution. Les nombres de bandes indiquent qu'au moins un groupe CO dans ces molécules est impliqué dans une liaison hyrogène (Tableau 10).

Tableau 10 Vibrations d'élongation des groupes CO dans les mimes peptidiques à base de pyridine **12a,b**

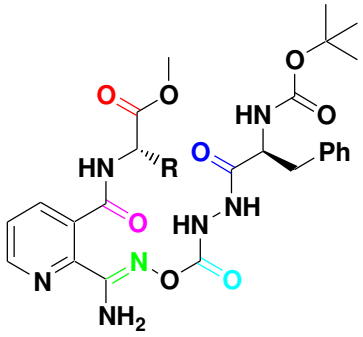

	v, cm^{-1}						
	C=O	C=O	C=O	C=O	C=O libre	C=O liée	C=N
12a (R = Me)	1755	1742	1708	1703	1693	1668	1661
12b (R = Bn)	1754	1745	1713	1705	1699	1669	1657

Suite à l'attribution des bandes de vibrations en fonction de leurs longueurs d'onde, deux bandes (1693 cm^{-1} et 1699 cm^{-1}) ont été considérées comme celles des carbonyle amide libres, et deux bandes (1668 cm^{-1} et 1669 cm^{-1}) ont été considérées comme reflétant l'état des groupes CO impliqués dans des liaisons hydrogène.

Les spectres FT-IR des analogues pyrazine présentent également un épaulement large en dessous de 3400 cm^{-1}, cependant nous n'avons pas réussi dans la déconvolution spectrale à attribuer les bandes de vibrations de la région des CO.

Ces résultats ont alors été complétés par des analyses dans des mélanges de solvants à différentes concentrations ($CDCl_3$/DMSO-d_6) (Tableau 11). Les déplacements chimiques des NH ont été déterminés et leur évolution en fonction des concentrations a été suivie pour mettre en évidence les NH impliqués dans des liaisons hydrogène. Seul un NH-hydrazide (en bleu) présente une valeur faible de $\Delta\delta$ (dans un intervalle de 0,18-0,48 ppm) ce qui reflète son implication dans une liaison hydrogène. Les protons amide des dérivés pyrazine **12'a,b** montrent également une faible évolution de leur déplacement chimiques vers les champs faibles ($\Delta\delta$ = 077 et 0.62 ppm respectivement à 10% de DMSO-d_6) ce qui pourrait traduire une faible implication des atomes d'azote du noyau pyrazine.

Tableau 11 Influence de la polarité du solvant sur les déplacements chimiques des protons NH de **12a**,**b** et **12'a**,**b**

Produit	$\Delta\delta$ (ppm) = δ (DMSO-d_6) - δ ($CDCl_3$)			
	NHBoc	**NH-amide**	**NH-hydrazide**	**NH-hydrazide**
12a	2.09	2.6	2.82	0.35
12b	1.92	2.47	2.3	0.18
12'a	2.12	1.76	2.33	0.4
12'b	1.98	1.88	2.35	0.48

De plus amples informations sur la conformation de ces composés en solution ont été obtenues grâce à des expériences NOESY dans le chloroforme. En particulier, deux corrélations NOE ont été trouvées dans les spectres du composé **12b** montrant une proximité spatiale entre le NH hydrazide (Figure 16, en rouge) et le CH de la partie *N*-terminale de la phénylalanine, et le NH hydrazide (Figure 16, en bleu) et le CH de la partie C-terminale de la phénylalanine. Ces empreintes NOE du composé **12b** sont clairement en faveur d'une structuration en coude de ce composé.

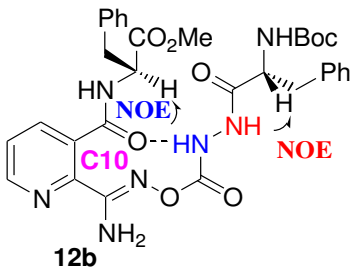

12b

Figure 16 Représentation des interactions NOE observées pour le composé **12b** dans $CDCl_3$

Par conséquent, les mimes peptidiques modifiés avec un motif hydrazide **12**,**12'** adoptent un coude stabilisé par une liaison hydrogène entre le C=O amide et le NH hydrazide formant ainsi un pseudocycle-C10. Un autre argument en faveur d'une liaison hydrogène faible NH…N est la faible accessibilité au solvant décrite dans les expériences de mélange de solvant à différentes concentration (10% DMSO-d_6) (Figure 17).

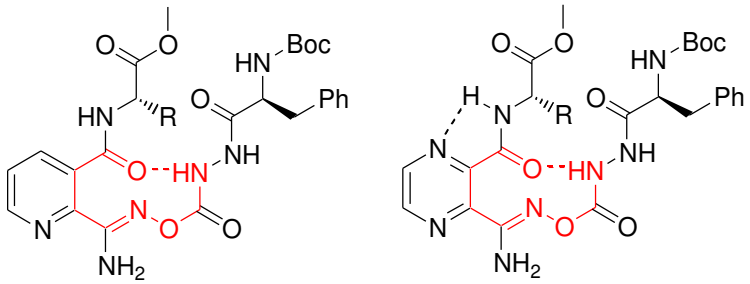

Figure 17 Structures des mimes peptidiques - hydrazides **12**, **12'**

Evaluation biologique préliminaire des amidoxymes en tant que donneurs de NO

Un moyen d'étudier la formation d'oxyde nitrique consiste à mesurer la concentration de l'ion nitrite [NO^{2-}], qui est l'un des deux produits de décomposition primaire de NO et qui présente l'avantage d'être stable et non volatile. (Schéma 13).

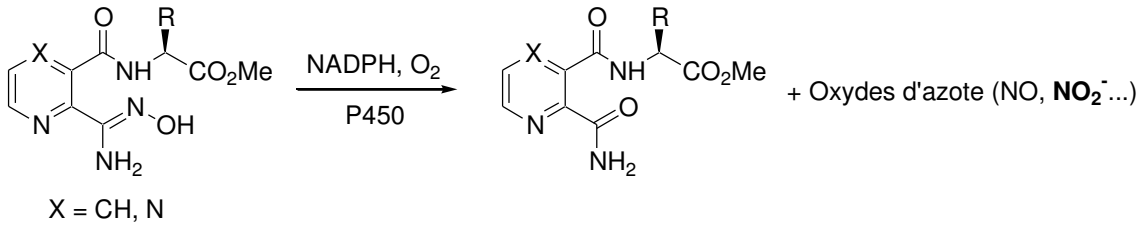

Schéma 13 Oxydation des amidoxymes en présence de microsomes

Les mesures correspondantes de l'essai de libération de NO sur les amidoxymes ont été effectuées et les données collectées sont énumérées dans le tableau 12.

Tableau 12 Résultats préliminaires de la libération de NO par les amidoxymes

Amidoxymes	**$[NO_2^-]_1$ µM**	**$[NO_2^-]_2$ µM**	**$[NO_2^-]_3$ µM**	**Valeur moyenne (µM)**	**Déviation standard**

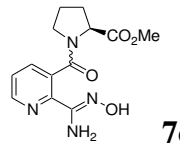 **7c**	1.34	2.62	1.22	**1.73**	0.776
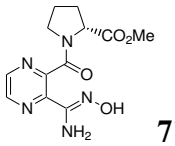 **7'c**	1.95	0.98	0.53	**1.15**	0.726
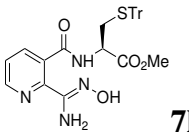 **7h**	3.81	0.99	1.15	**1.98**	1,584
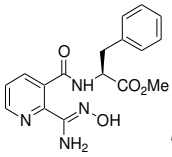 **7b**	1.50	2.62	-	**2.06**	0.792
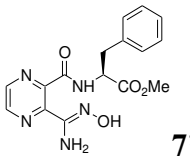 **7'b**	0.98	-	-	**0.98**	-
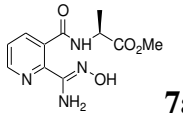 **7a**	0.83	-	-	**0.83**	-
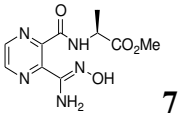 **7'a**	1.95	1.81	-	**1.88**	0.099
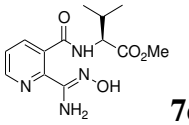 **7e**	1.60	2.42	-	**2.01**	0.580
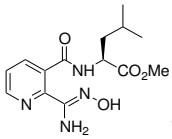 **7f**	1.45	1.40	-	**1.43**	0.035
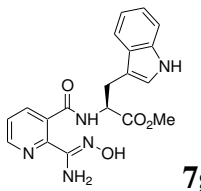 **7g**	1.10	-	-	**1.10**	-
4-	2.40	3.39	1.26	**2.35**	1.066

chlorobenzamidoxime

Pour des questions d'optimisation de la quantité de cytochromes P450 issus de microsomes de foie mis à notre disposition, les composés présentant la plus forte libération de NO ont été testés trois fois (**7c**, **7'c**, **7h**), ceux avec des valeurs plus modérées ont été testés deux fois (**7b**, **7'a**, **7e**, **7f**) et les produits possédant la capacité de libération de NO la plus faible seulement qu'une seule fois (**7'b**, **7a**, **7g**). La comparaison de l'effet attendu a pu être effectuée avec la molécule modèle décrite dans la littérature (4-chlorobenzamidoxime), connue pour sa bonne capacité de libération de NO.

Une corrélation provisoire entre les valeurs des analogues en série pyridine et pyrazine (**7**,**7'**(**a**)**- 7**, **7'**(**c**)) permet de conclure que le meilleur effet de libération de NO est observé pour les composés en série pyridine (résidus Phe et Pro). Par contre, concernant les amidoximes avec un résidu Ala, le produit au noyau pyrazinique semble être plus efficace que son homologue pyridinique.

La corrélation entre les chaînes latérales d'acides aminés et la concentration en nitrite des dérivés pyridine permet un classement: Phe>Val>Cys(Tr)>Pro>Leu>Trp>Ala.

Il est cependant à noter que dans le cas des composés en série pyrazine, il est observé une capacité opposée à la libération de NO: Ala>Pro>Phe.

Conclusion

Les différentes études menées dans ce travail de thèse ont permis la synthèse de nouvelles familles de peptidomimétiques ciblés, avec pour objectif de promouvoir des structures coudées stables afin de donner de la rigidité par rapport à leurs équivalents peptidiques. Différentes amidoximes à motif pyridinique (ou pyrazinique) disubstitué ont, dans un premier temps, été synthétisées. Dans un second temps, cette fonction amidoxime qui a été estérifiée par des acides aminés et des hydrazides a permis ensuite diverses transformations: en *N*-acylamidrazones, 1,2,4-oxadiazoles et 1,2,4-triazoles (liens pseudopeptidiques).

L'intérêt de ce travail est clairement l'obtention d'un large éventail de nouvelles structures peptidomimétiques à partir d'un même précurseur.

Il a été mis en évidence que l'acide 2(3)-cyanohétéroaromatique réagit avec des esters méthyliques de différents acides aminés naturels pour donner deux types d'esters d'acides aminés, un sous sa forme ouverte (dérivé cyano) et un sous sa forme fermée, pyrrolo-pyridine (ou pyrazine) qui génèrent des amidoximes à chaîne ouverte par action de l'hydroxylamine. De plus, on a trouvé que ces mêmes précurseurs cycliques présentaient un intérêt majeur dans la synthèse directe et douce de *N*-acylamidrazones *via* l'ouverture du cycle pyrrolidine par l'hydrazide d'un acide aminé.

La fermeture en un cycle 1,2,4-oxadiazole ou 1,2,4-triazole a été réalisée sous irradiation par micro-ondes avec des conditions optimisées et des temps de réaction réduits.

Une première condensation d'amidoximes avec de l'hydrazide d'un acide aminé a permis d'obtenir des composés coudés hybrides avec une liaison de type amidoxime-carbonyle-hydrazide. L'étude structurale a prouvé que ces peptidomimétiques modifiés par cet hydrazide adoptaient la structure d'un coude stabilisé par une liaison hydrogène formée entre le C=O de l'amide et le NH de l'hydrazide formant ainsi un pseudocycle en C_{10}.

L'analyse conformationnelle réalisée sur les dérivés contenant la proline a démontré la tendance générale qu'a cet acide aminé particulier à augmenter la proportion en isomère *trans*. L'amidoxime obtenue en série pyrazine et couplée au dipeptide Pro-Phe semble attrayant afin de l'utiliser comme pseudotripeptide modèle pour l'étude conformationnelle de l'isomérisation *cis*/*trans* de la liaison prolylamide.

De plus, les études conformationnelles des composés synthétisés ont confirmé que les motifs hétérocycliques pyridine et pyrazine présentent l'intérêt d'augmenter la rigidité et pus particulièrement le noyau pyrazine qui pourrait avoir un effet plus fort sur la stabilisation de la conformation.

Les amidoximes synthétisées ont ensuite été testés afin de mesurer leur capacité de libération d'oxyde nitrique démontrant ainsi la libération de NO en concentration suffisante pour des effets pharmacologiques (≥ 1 μM). En comparaison avec la molécule de référence, la 4-chlorobenzamidoxime, certains composés présentent une capacité de relargage de NO assez intéressante. Cependant, aucune rationalisation satisfaisante en terme de relation structure-activité n'a pu être encore établie avec ces premiers résultats.

En perspective, les composés les plus prometteurs seront soumis à d'autres tests *in vivo*. Les amidoximes pourraient également être testées pour leur capacité à être réduites *in vitro/in vivo* en amidines pharmacologiquement actives, mîmes de l'arginine.

NEW VARIETY OF PYRIDINE AND PYRAZINE-BASED ARGININE MIMICS: SYNTHESIS, STRUCTURAL STUDY AND PRELIMINARY BIOLOGICAL EVALUATION

Amino acids, mimetics, synthesis, structural study, NO donors

This work describes the synthesis, structural study and preliminary biological evaluation of new variety of pyridine and pyrazine-based arginine mimics.

Initially, we have developed a convenient synthesis of new peptidomimetics with amidoxime function as a replacement of amidine one. The latter can imitate arginine residue in biological structures. Chemical functionalization of these scaffolds led to novel 2,3-disubstituted pyridine(pyrazine) turn structures bearing amidoximes esterified with amino acid or modified with amino acid hydrazides, *N*-acylamidrazones, 1,2,4-oxadiazole and 1,2,4-triazole residues. Additionally, all structures were analyzed by NMR, IR, molecular modelling and XRD. Conformational studies confirmed that pyridine and pyrazine heterocycles can be used to increase rigidity and the pyrazine core has stronger effect on conformation stabilization. Examination of a new ProPhe pyrazine-based pseudotripeptide revealed the hydrogen bond formation between the proton of the OH and the carbonyl oxygen of the *C*-terminal phenylalanine. This hydrogen bond adopts a seven-membered γ-turn conformation. Therefore, a dramatic increase of the *trans* rotamer up to 98% was observed in weakly polar solvent, which is $CHCl_3$.

Finally, preliminary results of the NO release assay on amidoximes demonstrated sufficient values for pharmacological effect.

NOUVEAUX MIMES D'ARGININE A MOTIF PYRIDINIQUE OU PYRAZINIQUE: SYNTHESE, ETUDE STRUCTURALE ET EVALUATION BIOLOGIQUE PRELIMINAIRE

Acides aminés, mimes, synthèse, étude structurale, donneurs de NO

Ce travail décrit la synthèse, l'étude structurale et une première évaluation des propriétés biologiques d'une nouvelle famille de mimes de l'arginine issus de motifs pyridine et pyrazine.

Pour cela, nous avons mis au point la synthèse de nouveaux peptidomimétiques dans lequels la fonction amidine est remplacée par une amidoxime mime potentiel du résidu arginine. La fonctionnalisation chimique de ces motifs a permis à partir de la pyridine (ou pyrazine) 2,3-disubstituée l'obtention de nouveaux coudes non-peptidiques possédant des motifs amidoximes estérifiés par des acides aminés ou modifiés par des hydrazides d'acides aminés, des N-acylamidrazones et des résidus de 1,2,4-oxadiazole et de 1,2,4-triazole. L'analyse structurale réalisée par RMN, IR, modélisation moléculaire et par XRD a confirmé les propriétés des hétérocycles pyridine et pyrazine, en particulier dans la stabilisation des conformations et le noyau pyrazine qui semble jouer un rôle essentiel sur la stabilisation de la conformation. L'étude d'un nouveau pseudotripeptide à base de pyrazine-ProlylPhenylalanine a révélé la formation d'une liaison hydrogène entre le proton du groupe OH et l'oxygène du carbonyle de la phénylalanine C-terminale. La liaison hydrogène, ferme un pseudocycle à 7 atomes (C7). De plus, une augmentation considérable du rotamère *trans* (jusqu'à 98%) dans un solvant faiblement polaire ($CHCl_3$) a été observée.

Enfin, les premières amidoximes testées ont permis de révéler la libération de NO en concentration suffisante pour produire un effet pharmacologique.